# Development of an In-Situ Faecal Sludge Solar Dryer at Pilot-Scale

Report to the
**Water Research Commission**

by

**Santiago SEPTIEN STRINGEL[1], Pareshin NAIDOO[1], Akhil RAMLUCKEN[2], Freddie INAMBAO[2], Craig MCGREGOR[3], Jon POCOCK[4], Anusha SINGH[4]**

[1] WASH R&D Centre, University of KwaZulu-Natal, Durban, South Africa
[2] Mechanical Engineering, University of KwaZulu-Natal, Durban, South Africa
[3] Solar Thermal Energy Research Group, University of Stellenbosch, Stellenbosch, South Africa
[4] Chemical Engineering, University of KwaZulu-Natal, Durban, South Africa

**WRC Report No. 2897/1/22**
**ISBN 978-0-6392-0506-9**

**January 2023**

WATER
RESEARCH
COMMISSION

**Obtainable from**
Water Research Commission
Bloukrans Building
4 Daventry Road
Lynnwood Manor
PRETORIA

orders@wrc.org.za or download from www.wrc.org.za

# EXECUTIVE SUMMARY

Thermal drying is an efficient treatment method for sludge treatment for volume reduction and disinfection, but it requires a high input of energy. The use of solar thermal energy for drying proposes could reduce drastically the energy consumption, leading to a significant cost reduction. Even though an important number of solar drying technologies have been deployed in the food and agriculture sectors and some applications of solar thermal drying exist for sewage sludge treatment, this option has not been enough exploited for faecal sludge treatment, with only a few cases greenhouse drying beds reported in literature.

The present project (K5/2897) was about the development, testing and evaluation of two prototype solar thermal drying technologies for the treatment of faecal sludge, namely a greenhouse-type solar dryer and a screw conveyer, and it included a pre-feasibility study. The present project is the continuation of a previous WRC project (K5/2582) that demonstrated the great potential of the application of solar thermal energy for faecal sludge drying. The expected outcome from this project is to develop solar thermal drying technologies that will provide a cost-effective, decentralized and sustainable solution to sanitation practitioners and stakeholders for faecal sludge drying.

A preliminary study was carried out prior to the development of the solar dryers through a solar assessment in the location of the study (i.e. Durban, South Africa) and experiments in a bench-scale solar drier developed at the end of the project (K5/2582). The solar assessment showed that the evaporation rate would vary between 4.3 to 7.5 kg/d/m$^2$ along the year in Durban, with an average value of 5.8 kg/d/m$^2$. Based on these figures, the theoretical capacity of a solar plant to reduce the sludge moisture content from 80 to 20% would be 2.8 ton/y/m$^2$. The tests in the bench-scale solar drier confirmed that solar drying in a thermal system was more efficient than open-air drying as in conventional drying beds and brought valuable information for the design of the solar drying prototypes.

Thereafter, two solar thermal drying technologies were developed, namely a greenhouse-type solar dryer and a screw conveyer. The greenhouse-type solar dryer (2 m length x 1.5 m wide x 2 m height) consists in a batch system where the sludge is placed as a bed of a given thickness in a suspended grid. This system incorporates a ventilation system (below and above the bed), circulation fans, a scraping system to mix the sludge and an absorber wall. The screw conveyer is composed of a transparent tube (1000 mm length x 200 mm diameter), inside which the sludge is dried in continuous mode as it moves forward from the inlet to the outlet. The system includes a ventilation system, a solar air heater, and an air dehumidification unit and solar reflectors. The prototypes were tested by placing instrumentation at different locations of the systems to monitor and record the key parameters from the process, namely temperature and relative humidity. Functionality tests were firstly conducted to characterize and evaluate the operation of the prototypes without material to dry. Thereafter, tests with a few kg of wet soil and synthetic sludge were carried out by monitoring the evolution of the moisture content of the material as a function of time during the daytime (without considering the nights).

The prototype testing showed that, temperatures between 35 and 45°C could be obtained with peaks up to 50°C, as well as relative humidities lower than 40%, leading to favourable conditions for drying. The prototypes were capable to handle material from viscoelastic consistency (paste-like aspect) to granular solids, but they were not adapted to a too watery feedstock. The optimal operating conditions identified for the greenhouse solar drier were as follow: no need of dehumidifier, low ventilation rates. The solar air heater and reflectors did not bring any gain in performance, but it is deemed that they can improve the process after optimization of their use. In the case of the greenhouse, the prototype performed the best at low ventilation and air circulation rates and using the rake system.

Under the most favourable weather and operating conditions, the feedstock could be dried in the prototypes at drying rates around 1-2 kg/h/$m^2$, efficiencies up to 30-70% and a specific energy consumption of 100-400 kWh/ton, which is lower than the typical values found in conventional thermal driers (800 and 1000 kWh/ton). The drying rate drastically slowed down at the last phase of drying and the specific energy consumption increased to values superior than 800 kWh/ton, which was presumed to be due to remaining moisture being tightly bounded to the solid matrix. The screw conveyer solar drier shown a higher performance than the greenhouse, but it experienced serious stickiness issues that can compromise the long-term operation of the prototype. This stickiness issues were attempted to be mitigated by mixing the sludge with additives. So far, lime addition to the sludge was observed to diminish the stickiness problem but not yet in a significant way.

Based on a techno-economic analysis, it was estimated that the cost to treat one tonne of sludge would be approximately ZAR600 and ZAR150 for the greenhouse and screw conveyor solar thermal drying prototypes, respectively. The estimated capital cost to treat the sludge at municipal level would be prohibitive in the current state of the solar thermal drying systems (higher than R100 million), with the screw conveyor solar drier incurring the highest cost. Nonetheless, this result is normal since the solar driers are still in the prototype level, so a drastic decrease of their construction cost would result after their optimization, upscaling and mass scale production.

Some potential technical challenges and areas of improvement were identified after the testing of the prototypes. The operation of the prototypes can be further optimised, which will lead to a further decrease of specific energy consumption, as well as the design specification for the reduction of the construction costs.

This study confirmed that solar thermal drying is an interesting cost-effect alternative for faecal sludge treatment. In the developed solar driers, the drying of faecal sludge is expected to occur at the optimal time and at low energy consumption when the weather conditions are favourable, and with the correct operating conditions. The process could be stopped at low moisture content before reaching a high level of moisture boundness where drying progresses very slowly and the process becomes inefficient. The continuation of this project will consist in tests with real faecal sludge, optimize and improve the systems, and prepare its deployment in the field and future commercialisation.

# ACKNOWLEDGEMENTS

The project team wishes to thank the following people for their contributions to the project.

| Persons | Affiliation |
|---|---|
| Susan MERCER | WASH R&D Centre, University of KwaZulu-Natal, Durban, South Africa |
| Kerry L. PHILP | |
| Poovalingum GOVENDER | |

In addition, we would like to thank the Reference Group for Water Research Commission (WRC) Research Project K5/2897:

| | |
|---|---|
| Dr. Sudhir Pillay | Water Research Commission (Chairperson) |
| Mr. Benny Mokgonyana | Water Research Commission |
| Prof. Freddie Inambao | University of KwaZulu-Natal |
| Mr. Arun Kumar RS | University of KwaZulu-Natal |
| Dr. Jaap Hoffman | University of Stellenbosch |
| Ms. Lungi Zuma | eThekwini Water & Sanitation |
| Mr. Sabelo Mathenjwa | eThekwini Water & Sanitation |
| Mr. Melvin Pillay | eThekwini Water & Sanitation |
| Mr. Doran Shoeman | E3 Energy |
| Mr. Nick Alcock | Khanyisa Projects |
| Dr. Chris Brouckaert | University of KwaZulu-Natal |
| Prof. Babatunde Bakare | Mangosuthu University of Technology |
| Dr. Tumisang Seodigeng | Vaal University of Technology |
| Ms. Ruth Cottingham | Khanyisa Projects |
| Mr. Karlin Naidoo | Khanyisa Projects |
| Mr. Kaverajen (Melvin) Pillay | eThekwini municipality |
| Dr. Ian Mabbett | Swansea University |

*In memory to our dear Pr. Chris Buckley for his dedication and hard work in the WASH sector, becoming a legend who will continue to enlighten us through his legacy and inspire us for a future with better sanitation and water management*

This page was intentionally left blank

# TABLE OF CONTENTS

# LIST OF FIGURES

# LIST OF TABLES

# ACRONYMS & ABBREVIATIONS

| | |
|---|---|
| ac | Alternative current |
| CFD | Computational fluid dynamics |
| DC | Drying chamber |
| dc | Direct current |
| PMMA | Polymethyl methacrylate |
| PV | Photovoltaic |
| SAH | Solar air heater |
| SASTeP | South Africa Sanitation Technology Platform |
| SD | Secure Card |
| SEC | Specific energy consumption |
| STERG | Solar Thermal Energy Research Group |
| UDDT | Urine Diversion Dry Toilets |
| UKZN | University of KwaZulu-Natal |
| VIP | Ventilated improved pit |
| WASH | Water, Sanitation& Hygiene |
| WRC | Water Research Commission |

# 1 INTRODUCTION

## 1.1 MOTIVATION

Many regions in the world rely on onsite sanitation, particularly in developing countries due to the lack of infrastructure and low affordability to connect all the population to a sewage system. Onsite sanitation is also the most viable option to provide sanitation to the poor communities where this basic service is lacking. It can also serve in developed areas and cities to change the paradigm of sewage sanitation into a more water-sensitive and sustainable model, particularly in places where the sewage system requires critical maintenance, the wastewater treatment plants are not operating adequately, and the water resources are in course of depletion.

One of the main challenges of onsite sanitation is the accumulation of the faecal waste in the site of generation. Methods have to be therefore developed for its in-situ treatment, or its collection and transportation to a faecal sludge treatment plant for its disposal and eventual resource recovery. The removal of the moisture from the faecal sludge is an essential operation for the minimization of the mass and volume of the waste. Thermal drying is the most efficient method to remove completely the moisture or into very low levels, and to ensure the destruction of pathogen organisms, in comparison to mechanical dewatering methods and drying beds. However, thermal drying requires a high input of energy for moisture evaporation, due to the high latent heat of water vaporization (2 260 kJ per L of evaporated water), leading to high operating costs difficult to afford.
The use of solar thermal energy for drying proposes could reduce drastically the energy consumption, leading to a significant cost reduction. This should involve the setup of a thermal system to harness in an efficient way the solar energy for its conversion into heat. Most of the solar drying applications are found in the agriculture and food industry sectors, for the preservation of grains and dehydration of food products. Solar thermal energy has also been widely applied for sewage sludge drying. Seginer and Bux (2006) identified approximately 70 solar driers in operation in European countries, the United States and Australia. This number has probably increased along the years in the developed countries and solar drying has also gained interest in further countries, such as Greece, Turkey, Algeria, Morocco and China.

The largest sewage sludge solar drying plant worldwide is located in Mallorca, Spain, with a surface of 17 260 $m^2$ and a capacity of 30 000 tonnes of sludge per year (Socias, 2011). Two other examples of large capacity are: (i) the plant from Oldenburg, Germany, with a surface of 6 500 $m^2$ and able to treat 30 000 tonnes of sludge per year (Thermo-System, no date); (ii) the plant from Managua, Nicaragua, with a total surface of 8 760 $m^2$ and a capacity of treatment of 26 000 tonnes per year (Meyer-Scharenberg and Pöppke, 2010). These plants enable to increase the solid content of the sludge from 20-30% to 60-80%. In addition, an important number of Research & Development activities have been conducted in order to improve the process (Seginer, Ioslovich and Bux, 2007; Horn *et al.*, 2008; Zhao, Chen and Xie, 2009), as well as for the development and testing of new pilot plants (Mathioudakis *et al.*, 2013; Kurt, 2014; Kurt, Aksoy and Sanin, 2015). Sewage sludge solar thermal drying is mostly done in greenhouses, but the use of other types of solar driers are under investigation (Khanlari et al., 2020; Wang et al., 2019; Ameri et al., 2018). Bennamoun (2012) presents a comprehensive review of the research conducted about sewage sludge solar drying and the different technologies that have been developed.

Solar thermal energy has been rarely employed so far for on-site sanitation applications. Only a few cases have been reported, such as the testing of greenhouse drying beds in Rwanda, Uganda, Ghana and Senegal (Meyer-Scharenberg and Pöppke, 2010; Seck *et al.*, 2015; Pivot, 2016), or the development of toilet technologies with in-situ solar drying of the faecal waste (3P-Technik-Sanitation, 2016; RaVikas, 2016). The use of solar thermal energy has a great potential for faecal sludge drying, as most of the countries relying on

on-site sanitation are located in tropical areas with abundant solar energy source along the year. Solar thermal drying seems like the compromise between the conventional drying beds that are inexpensive but inefficient, and the thermal driers that show a good performance but at usual high costs. However, this option has not been enough exploited, probably because of the lack of awareness, knowledge and data.

## 1.2 AIM AND OBJECTIVES

The present project, funded by the Water Research Commission (WRC) through K5/2897, is about the development of pilot-scale solar thermal drying technologies for the treatment of faecal sludge from onsite sanitation facilities. It is expected that the developed technologies will provide a cost-effective solution to sanitation practitioners and stakeholders for faecal sludge drying. It should have the versatility to be implemented near the site of waste generation for its in-situ treatment or in a faecal sludge treatment plant.
The specific objectives of the project are:

- Design, build and test solar drying technologies.
- Study the technical-economic feasibility of the implementation of the technologies.
- Disseminate the generated knowledge, learnt lessons and developed products.

## 1.3 SCOPE

The present project is the continuation of a previous WRC project (K5/2582) to explore the use of solar thermal energy using a custom-design experimental rig. The WRC project (K5/2582) demonstrated the great potential of the application of solar thermal energy for faecal sludge drying, allowed to obtain kinetic data to characterize better the process and led to a better understanding of faecal sludge behaviour as it was exposed to solar radiation and dried. The final report of this project can be found in the Supporting Document A. The dissertation of a MSc research project that followed this project can be consulted in Supporting Document B. In addition to this, an expertise about the fundamental of faecal sludge drying has been developed at the University of KwaZulu-Natal (UKZN) WASH R&D Centre from previous investigations. The knowledge, data, findings and lessons learnt from the WRC project (K5/2582) and previous investigations of faecal sludge drying was the base on the development of the solar thermal drying prototypes.

The pilot-scale solar drying technologies were designed, built and tested at the WASH R&D Centre at the UKZN. Two technologies were developed: a greenhouse-type solar drier and a screw conveyor solar drier. The greenhouse prototype was developed and tested through a MSc research project. The screw conveyer started to be built by a final year project from undergraduate Mechanical Engineering students, and its development was achieved through a second MSc research project, that also included its testing.

The tests were carried out at the roof from the Chemical Engineering building, at Howard College campus, UKZN (Durban, South Africa). The first testing phase was done to verify the functionality of the individual components of the prototype and the fully integrated system. After this, tests were done without feedstock to characterize the system, and with water and wet soil as feedstock to identify the optimum operating conditions (particularly in terms of ventilation rate). Finally, tests were done to measure the performance of the system with a simulant of faecal sludge. For each test, the temperature and relative humidity were measured at different locations in the prototype, the ambient conditions were determined (including temperature, relative humidity and irradiance), the moisture content of the material (wet soil or synthetic sludge) was monitored during the process and the performance metric were calculated (drying curves, drying rate, process efficiency, specific power consumption). Note that tests with real faecal sludge could not be carried out because this would require high amount of sludge required and the roof at the Chemical Engineering building did not have the health and safety protocols for this. The summary of the results was used to evaluate the potential of application of the developed technologies in the field.

## 1.4 DELIVERABLES

During the duration of this project, five deliverables have been submitted, including:

- Deliverable 1, where a preliminary study was carried out through a solar assessment of the experimental site and experiments in a bench-scale solar drier (developed during the project K5/2582), and the concepts of the solar drying prototypes are presented.
- Deliverable 2, which described the design of the solar drying prototypes.
- Deliverable 3, which presented the progress in the prototypes manufacturing and the testing plan.
- Deliverable 4, which reported the final phases in the prototypes manufacturing and the results from the first tests,
- Deliverable 5, corresponding to the final report (present document), which contains the description of the tests, the discussion of the results and the final outcomes from this project.

The previous Deliverables from this project can be found in the Supporting Documents C.

## 1.5 OUTLINE

This report is organized as follow:

- Chapter 1 (present one), which describes the motivation to conduct the project, as well as the aim, specific objectives, background and scope.
- Chapter 2, which presents a preliminary study carried out in this project, consisting in a solar assessment of the experimental site and results from the tests of a bench-scale solar drier, developed in the WRC project (K5/2582).
- Chapter 3, which describes the greenhouse solar drier prototype, the testing procedure, the results and their analysis.
- Chapter 4, which focuses on the screw conveyor solar drier prototype, its testing, results and data analysis.
- Chapter 5, which provides the outcomes of this project, in terms of developed product, knowledge creation and dissemination, and capacity building.
- Chapter 6, which gives a description of the wat forward and next steps after this project to carry on with the solar thermal drying prototypes for their maturation, implementation in the field and commercialisation.
- Chapter 7, which presents the information and data supporting the previous paragraphs as appendices.

## 1.6 REFERENCES

3P-Technik-Sanitation (2016) The product – SANI SOLAR. Available at: http://3psanitation.de/the-product-sani-solar/?lang=en (Accessed: 1 March 2018).

Ameri, B., Hanini, S., Benhamou, A. & Chibane, D. (2018). Comparative approach to the performance of direct and indirect solar drying of sludge from sewage plants, experimental and theoretical evaluation. Solar Energy, 159, 722-732.

Bennamoun, L. (2012) 'Solar drying of wastewater sludge: A review', Renewable and Sustainable Energy Reviews. Elsevier, 16(1), pp. 1061-1073.

Horn, S. et al. (2008) 'Accelerated air drying of sewage sludge using a climate controlled solar drying hall'.

Kurt, M. (2014) EVALUATION OF SOLAR SLUDGE DRYING ALTERNATIVES ON COSTS AND AREA REQUIREMENTS. Master thesis, Middle East Technical University (Turkey).
Kurt, M., Aksoy, A. and Sanin, F. D. (2015) 'Evaluation of solar sludge drying alternatives by costs and area requirements', Water research. Elsevier, 82, pp. 47-57.
Khanlari, A., Tuncer, A. D., Sözen, A., Şirin, C., & Gungor, A. (2020). Energetic, environmental and economic analysis of drying municipal sewage sludge with a modified sustainable solar drying system. Solar Energy, 208, 787-799.
Mathioudakis, V. L. et al. (2013) 'Sewage sludge solar drying: Experiences from the first pilot-scale application in Greece', Drying technology. Taylor & Francis, 31(5), pp. 519-526.
Meyer-Scharenberg, U. and Pöppke, M. (2010) 'Large-scale Solar Sludge Drying in Managua/Nicaragua', Wasser und Abfall, 12(3), p. 26.
Pivot (2016) PIVOT WORKS OVERVIEW. Available at: http://thesff.com/system/wp-content/uploads/2016/11/2016-Pivot-Works-overview.pdf (Accessed: 20 July 2008).
RaVikas (2016) RaVikas 'MAITRI' Zero Odor / Zero Flush Composter. Available at: http://swachhsolartoilet.com/ (Accessed: 1 March 2018).
Seck, A. et al. (2015) 'Faecal sludge drying beds: increasing drying rates for fuel resource recovery in Sub-Saharan Africa', Journal of Water Sanitation and Hygiene for Development. IWA Publishing, 5(1), pp. 72-80.
Seginer, I. and Bux, M. (2006) 'Modeling solar drying rate of wastewater sludge', Drying Technology. Taylor & Francis, 24(11), pp. 1353-1363.
Seginer, I., Ioslovich, I. and Bux, M. (2007) 'Optimal control of solar sludge dryers', Drying Technology. Taylor & Francis, 25(2), pp. 401-415.
Socias, I. (2011) 'The solar drying plant in Mallorca: the drying process in waste management', in European Drying Conference. Palma de Mallorca, Spain.
Thermo-System (no date) Case study Oldenburg. Available at: https://www.parkson.com/sites/default/files/documents/document-oldenburg-case-study-1073.pdf (Accessed: 11 January 2018).
Wang, P., Mohammed, D., Zhou, P., Lou, Z., Qian, P., & Zhou, Q. (2019). Roof solar drying processes for sewage sludge within sandwich-like chamber bed. Renewable Energy, 136, 1071-1081.
Zhao, L., Chen, D. and Xie, J. (2009) 'Sewage sludge solar drying practise and characteristics study', in Power and Energy Engineering Conference, 2009. APPEEC 2009. Asia-Pacific. IEEE, pp. 1-5.

# 2 PRELIMINARY STUDY

## 2.1 INTRODUCTION

A preliminary study was carried out prior to start with the design of the solar dryers. In one hand, a solar assessment and thermodynamic calculations were performed in order to evaluate the potential of solar thermal energy for drying applications at the proximity of the experimental site. In the other hand, a bench-scale solar drier, developed through a Mechanical Engineering student project under the previous WRC project (K5/2582), was tested using a faecal sludge simulant and real sludge collected from on-site sanitation facilities in the eThekwini municipality.

## 2.2 SOLAR ASSESSMENT

A solar assessment was conducted in Durban during 2014-2018 in order to evaluate the potential of solar energy resource. The irradiance values were obtained from an online database, SAURAN (Southern African Universities Radiometric Network), which is available at the following website: http://sauran.ac.za. SAURAN is an initiative from various South African institutions (including UKZN and Stellenbosch University) to record weather and solar irradiance data through radiometric stations installed in different locations in South Africa, Namibia and Botswana, and make it available to the public (Brooks, 2015). The data used in this study was measured from a radiometric station located at the roof of Mechanical Engineering building, at the University of KwaZulu-Natal, Durban, South Africa (latitude: 29°52'15.5" S; longitude: 30°58'37.0"E), which is at a close distance from the Chemical Engineering building (experimental site). The measured data includes the solar irradiance, air temperature, relative humidity, wind speed and barometric pressure measured each hour from the 1st of April 2013 to the 31st August 2018. From the average irradiance data, thermodynamic calculations were done to determine the theoretical amount of water that could be evaporated using solar energy. The GHI (global horizontal irradiance) was selected as the irradiance reference parameter in this study.

**Table 2.1 compiles the monthly sum and average of the GHIs during the period of the study, and**

Table 2.2 summarizes the monthly average values for the other weather parameters.

**Table 2.1. Monthly sum and average of the GHIs from 2014 to 2018**

| | 2014 | 2015 | 2016 | 2017 | 2018 | |
|---|---|---|---|---|---|---|
| Month | GHI Month sum (kW/m²) | | | | | 5 years average (kW/m²) |
| January | 171.44 | 151.59 | 163.93 | 165.30 | 181.61 | 167.01 |
| February | 144.77 | 126.42 | 153.72 | 136.87 | 151.53 | 142.66 |
| March | 90.26 | 154.35 | 146.10 | 135.20 | 133.38 | 142.10 |
| April | 109.23 | 123.45 | 113.69 | 116.32 | 130.77 | 118.69 |
| May | 57.41 | 100.58 | 107.75 | 109.47 | 104.46 | 105.25 |
| June | 94.40 | 75.87 | 89.53 | 93.25 | 93.90 | 92.48 |
| July | 103.40 | 92.71 | 91.00 | 86.71 | 104.47 | 95.66 |
| August | 102.76 | 112.22 | 122.87 | 111.38 | 112.47 | 112.34 |
| September | 119.33 | 112.48 | 87.46 | 109.02 | 134.22 | 116.51 |
| October | 151.81 | 132.54 | 8.78 | 153.14 | 127.39 | 138.50 |
| November | 151.50 | 140.76 | 118.75 | 143.58 | 123.07 | 135.53 |
| December | 145.49 | 147.01 | 167.45 | 153.83 | 149.17 | 152.59 |
| Average | 120.15 | 122.50 | 114.25 | 126.17 | 128.87 | 126.61 |

**Table 2.2. Average values of the weather conditions from 2014 to 2018**

| Month | Temp average (°C) | BP average (mbar) | RH average (%) | WS average (m/s) |
|---|---|---|---|---|
| January | 25.29 | 974.40 | 77.57 | 2.98 |
| February | 25.47 | 975.99 | 76.47 | 3.00 |
| March | 25.31 | 987.24 | 77.04 | 2.07 |
| April | 23.47 | 1000.07 | 73.03 | 2.70 |
| Mai | 22.35 | 1001.97 | 68.51 | 2.19 |
| June | 20.74 | 1002.83 | 59.98 | 2.19 |
| July | 19.64 | 1005.10 | 62.79 | 2.24 |
| August | 20.44 | 1002.39 | 66.51 | 2.65 |
| September | 20.90 | 998.32 | 75.47 | 2.80 |
| October | 21.30 | 990.92 | 75.05 | 3.20 |
| November | 22.06 | 987.22 | 76.78 | 3.18 |
| December | 24.12 | 983.14 | 78.87 | 3.16 |

As it could be expected, the lowest irradiances are obtained during the autumnal and hibernal period. Depending on the year, the month with lowest irradiance fell in May, June or July. On the opposite, the highest irradiances were observed during summer in December or January. A similar trend could be observed for the air temperature, pressure, relative humidity and wind speed: the winter recorded the lowest values while the summer presented the highest ones.

From the average GIH values in Table 2.1, the theoretical moisture evaporation rate was calculated by dividing the solar irradiance to the latent heat of water vaporization (2 260 kJ/kg). According to these calculations, the evaporation rate varied from 4.3 to 7.5 kg/d/m$^2$ along the year, with an average of 5.8 kg/d/m$^2$. Taking into account the typical moisture content of 80% for faecal sludge from Ventilated Improved Pit (VIP) latrines in the eThekwini municipality (Zuma, Velkushanova and Buckley, 2015), the theoretical annual capacity of a solar drying plant to reduce the moisture content to 20% would be 2.8 tonnes of sludge per m$^2$. Assuming that approximately 30 000 VIP latrines are served in a cycle of years (6 000 latrines/year) and that a pit can store up to 2 000 kg of sludge, a solar plant covering the area of four Olympic pools (around 5 000 m$^2$) would be required to treat all the VIP sludge generated within a year. Solar drying represents therefore an interesting option for faecal sludge treatment, with low running costs and a reasonable land footprint.

## 2.3 TESTS IN THE BENCH-SCALE SOLAR DRIER

### 2.3.1 Description of the device

Figure 2.1 depicts a photograph of the bench-scale solar drier through a Mechanical Engineering student project under the previous WRC project (K5/2582). The solar dryer is composed of two main parts: a solar collector for air heating and a transparent cabinet where the sludge is introduced for drying.

The cabinet was made from a stainless-steel frame and acrylic walls. The sludge can be introduced inside the cabinet through sliding drawers that can be opened and closed from one of the front faces of the box. The sludge was spread as a bed above a suspended fine mesh grid. A computer fan was placed on the roof of the cabinet to induce air circulation inside the drying zone, to avoid the saturation of air in humidity that can stop the process, and to enhance the mass transfer for moisture evaporation. The air introduced in the dryer was pre-heated in a solar collector that was connected to the cabinet through thermal insulated pipes. The heated air was introduced by the top and bottom of the grid, to expose both the bottom and top faces of the sludge to

the heated air stream for a more homogenous drying. A manual rake system was installed in the cabinet to scrape the top surface of the sludge at selected intervals of time. This operation should avoid the formation of a crust and enhance a better drying of the internal layers of the sludge in the bed.

The temperature and relative humidity were measured inside the drying chamber (DC) and at the outlet of the collector, through sensors introduced inside these devices through specific ports. The sensors were connected to a computer that recorded the data. The air flowrate was deduced from the measurement of the air velocity through a hot-wire anemometer probe placed inside the pipe at the outlet of the collector.

The solar collector was composed of a wood box with double glassing window in his top face. The absorber inside the wood box consisted in a black metallic surface with baffles, separated from the walls of the box through a thick layer of insulating material. The solar collector was placed on a tilting support to orient the absorber at the most optimum angle.

The surface area available to spread the sludge in the drier was about 1.3 $m^2$, whereas the surface area of the collector to absorb the solar energy was about 0.44 $m^2$. The air flowrate induced by the computer fan was around 1 $m^3/h$.

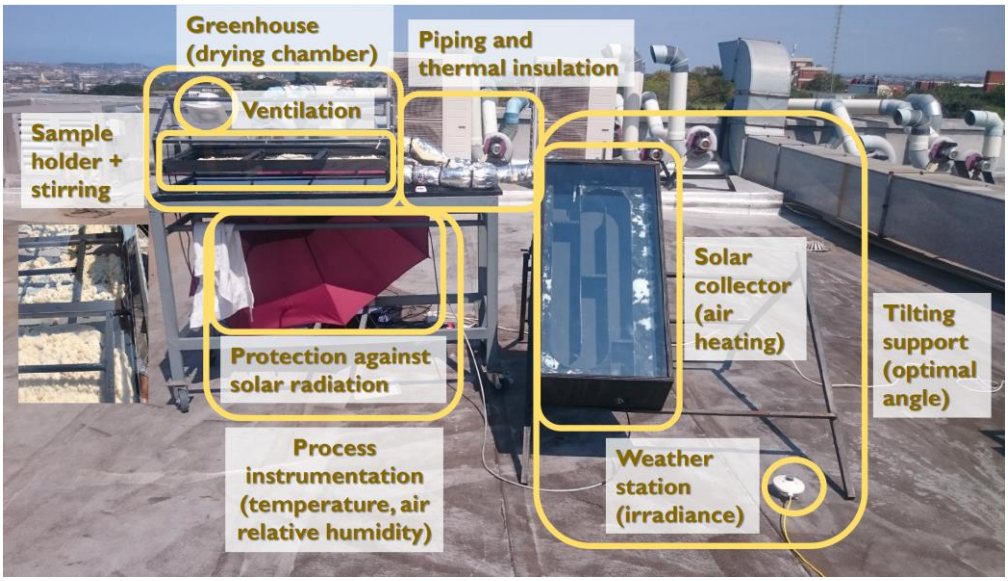


**Figure 2.1. Photograph of the bench-scale solar drier**

### 2.3.2 Experimental procedure

Experiments were performed in the solar drier using a simulant of faecal sludge and real faecal waste collected from Urine Diversion Dry Toilets (UDDT) from the eThekwini municipality, in Durban. The trials were conducted at the roof of the Chemical Engineering building, at UKZN (latitude: 29°52'08.1" S; longitude: 30°58'46.6"E). The duration of one experiment was approximately of one week, including the initial preparation of the setup and the final cleaning. After introducing the sample in the cabinet, it was let there for solar drying during 3-4 days from 10:00 AM to 4:30 PM. Outside these hours, the equipment was stored inside a shed, without removing the sludge from the cabinet if the experiment had not ended. The testing period was done between June to August 2019. At the beginning and end of each day of experimentation, a small amount of sludge was taken from the drier for the analysis of its moisture content and water activity. The moisture content measurement was based on a Standard Method for the Examination of Water and Wastewater (APHA, 2012). The water activity was analysed in an *AquaLab TDL* instrument.

The solar drier was aligned in the East-West axis and was positioned to face the North direction, to maximize the amount of received solar irradiance. It was verified that, in the selected position, the shades of the nearby objects did not obstruct the exposure to direct sunlight of the equipment along the day. The solar collector was titled at the most optimum angle for winter, i.e. 45°.

The parameters varied during the experiments were the mass of sample in the bed and the frequency of scrapping. The experiments included a control, consisting in a similar amount of sludge placed in a tray at the open air.

### 2.3.3 Results and data analysis

#### 2.3.3.1 *General observations*

During the solar drier tests, the sample changed from an initial wet look with a pasty-like consistency to a final dried granular solid aspect as drying proceeded, as it can be observed in Figure 2.2 for the synthetic sludge and Figure 2.3 for the UDDT sludge. It can be also noted an important shrinkage of the material and a fastest drying of the edges of the bed.


**Figure 2.2. Photographs of the faecal sludge simulant inside the solar dryer at different days of experiment**


**Figure 2.3. Photographs of the UDDT faecal sludge inside the solar dryer at different days of experiment**

### 2.3.3.2 *Effect of the mass sample*

Figure 2.4 presents the drying curves, i.e. the moisture content (in wet basis) as a function of time, for the simulant of faecal sludge placed inside the solar dryer at different mass loads: 1.8 and 4.4 kg. Thymol blue (TB) was added into one of the 1.8 kg sludge batch to stop the growth of fungi, as this phenomenon tended to occur in the synthetic sludge.

It was observed that the batch of 1.8 kg dried at a faster rate than the batch of 4.4 kg. This result could be related to the thicker bed of sludge resulting from a higher load of mass, leading to lower transfer rates and consequently reducing the drying rate. The incorporation of thymol did not have any significant effect on drying.

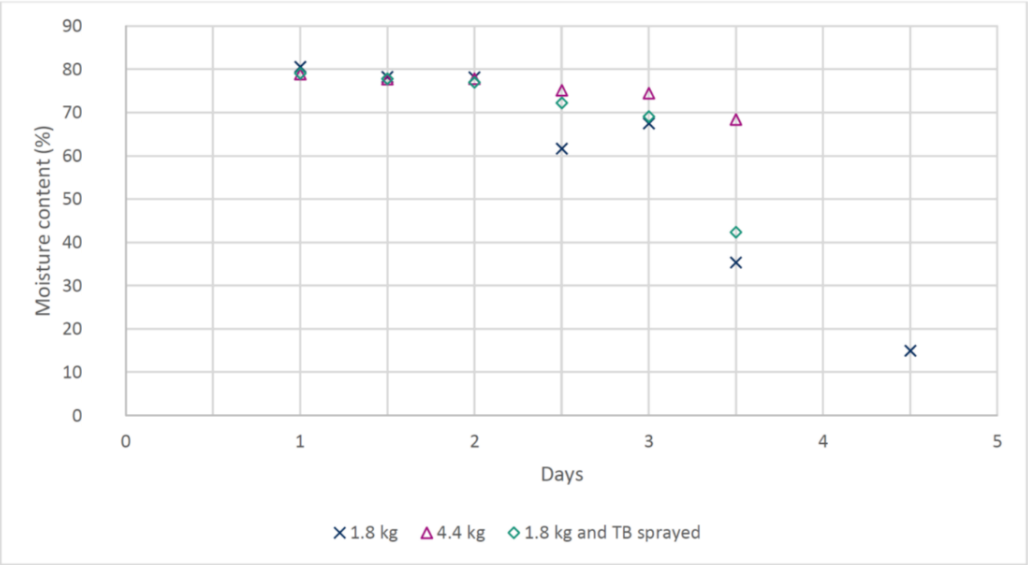


**Figure 2.4. Drying curves for different mass of synthetic faecal sludge samples during the tests of the solar drier**

### 2.3.3.3 *Effect of stirring*

Figure 2.5 shows the drying rate of synthetic sludge at different time intervals of scrapping (2 and 3 h). It can be clearly seen how a more frequent scrapping improved the drying of the sludge, probably because this operation homogenised better the drying of the sludge among the different layers in the bed and minimized the formation of a crust that can limit the transfer of moisture from the core of the material to the environment.

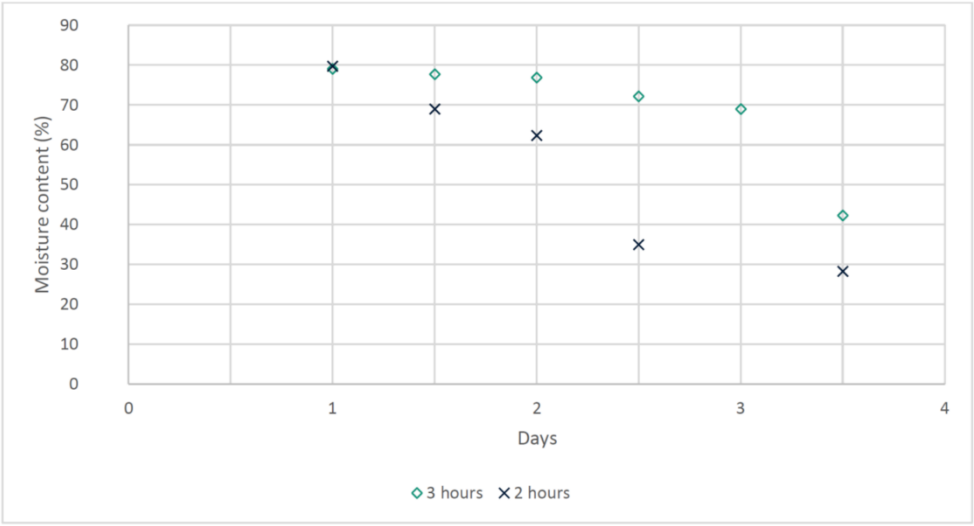

**Figure 2.5. Drying curves for different scrapping time intervals during the tests of the solar drier using synthetic faecal sludge**

#### 2.3.3.4 *Comparison with open-air drying*

Figure 2.6 compares the average moisture evaporation rate (equivalent to the drying rate) and final moisture content of the synthetic sludge between the samples placed inside the solar dryer and at the open-air (corresponding to the control), for the different experiments. Note that the results cannot be compared between weeks, because the operating and weather conditions were different.

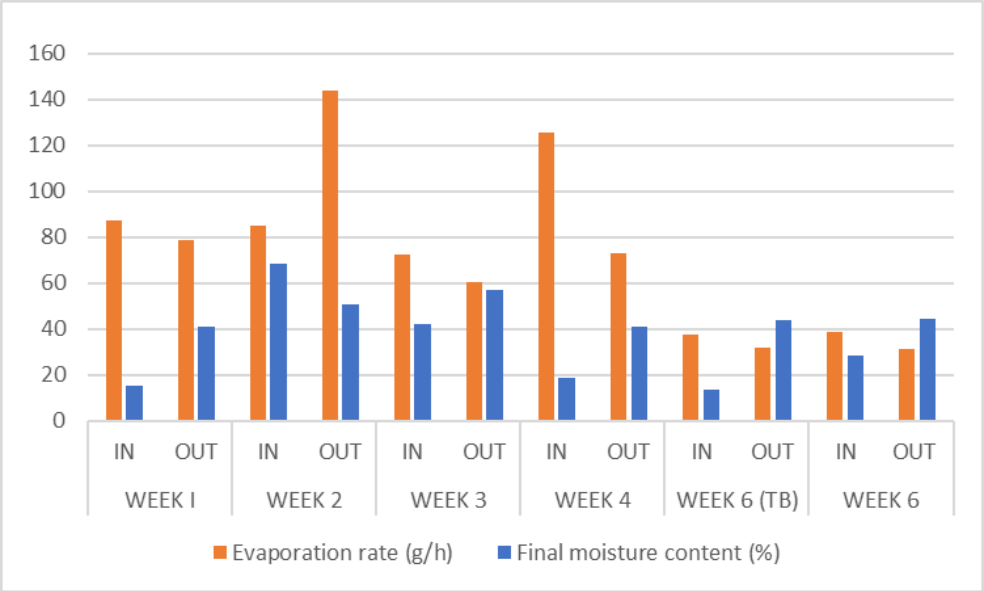


**Figure 2.6. Average moisture evaporation rate and final moisture content after the tests in the solar drier and at the open-air (control) with synthetic faecal sludge**

It can be observed that drying inside the solar drier usually led to a faster drying rate and a consequent lower moisture content at the end of the experiment, except for week 2. This result demonstrates that solar drying inside a thermal system is generally more efficient than drying at the open-air. Indeed, a thermal system allows to better harness the solar thermal energy by creating a greenhouse effect, which traps the radiation remitted by the bodies inside the enclosure. Besides, a thermal system avoids heat losses to the environment and enables to dry at more controlled conditions, leading to results that are more consistent. In addition to this, the air solar collector should bring a positive influence on the system for the drying of the sludge, by rising the air temperature and decreasing consequently its relative humidity. This allows increasing the heat input in the system for moisture evaporation and the thermodynamic capacity of air to hold further humidity.

The outlier from the aforementioned trend, corresponding to the results obtained during week 2, could be due to an experimental error, or could suggest that solar thermal drying may not lead to better results than open-air solar drying all the time. In fact, it could be that, under certain conditions, drying at the open-air leads to faster rates, for example during sunny conditions with strong hot winds. This assumption has to be verified with further experimentation.

#### 2.3.3.5 *Performance of the system*

Table 2.3 summarizes the computed efficiency of the solar dryer and collector. The efficiency of the solar dryer was calculated by dividing the measured amount of evaporated moisture with respect to what could be expected from the solar irradiance. For this calculation, the heat of drying was assimilated to the latent heat of

vaporization of pure water. The efficiency of the collector was calculated by dividing the measured amount of sensible heat at the outlet of the collector to what could be expected from the solar irradiance.

**Table 2.3. Efficiency of the system**

| Week | 1 | 2 | 3 | 4 | 5 | 6 (TB) | 6 |
|---|---|---|---|---|---|---|---|
| Dryer efficiency (%) | 27% | 26% | 21% | 36% | 19% | 19% | 12% |
| Efficiency collector (%) | 25% | 31% | 26% | 27% | 25% | 16% | 20% |
| Irradiance (W/m²) | 442 | 452 | 482 | 479 | 513 | 428 | |

The efficiencies of the solar dryer and collector varied mostly between 20 and 30% depending on the operating conditions, with a minimum value of 12% and maximum of 36%. The highest efficiency of the system was obtained during week 4, where the frequency of scrapping was increased, highlighting the importance of this operation on the process.

The efficiency of the system is within the range of values reported in literature for solar driers. Nonetheless, the theoretical maximum efficiency of the whole system, considering the inevitable radiation losses by absorbance and reflectance, would be around 75-80%, so there are still margins of improvement.

#### 2.3.3.6 *Water activity*

Figure 2.7 displays the water activity measured for the samples at different moments during their drying. The water activity is a thermodynamic value that reflects the level of boundedness of moisture in a solution, slurry or solid. If the activity is equal to 1, the water molecules interact only among them and thus they behave as they were pure water. In contrast, an activity lower than 1 means that the water molecules are bounded to other substances by interactions of variable strength intensity. As the water activity lowers, the boundedness of water with the other substances becomes stronger.

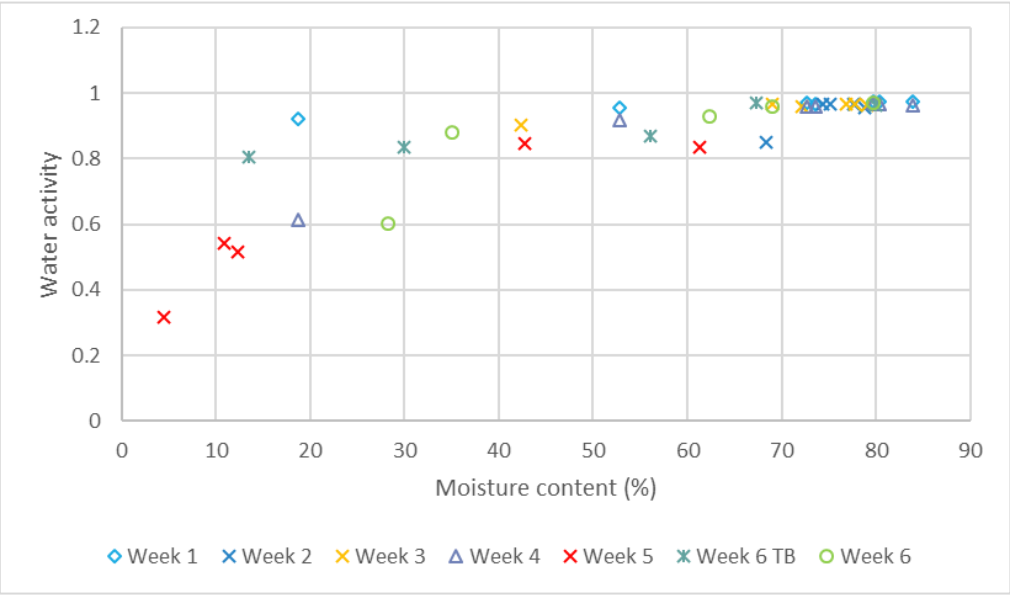


**Figure 2.7. Water activity versus moisture content for the synthetic faecal sludge samples during the tests in the solar drier**

From 85 to 70% moisture content, the water activity was close to 1. Below 70% moisture content, the activity slightly decreased to around 0.9 and was maintained at this value until reaching 30% moisture content. Below

30% moisture content, the activity dropped as the moisture content decreased. These results suggest that the moisture was completely or almost unbounded above a content of 70%, then it became weakly bounded at contents between 30 and 70%, and finally its boundedness strengthened considerably below 30% moisture content, suggesting that drying became more difficult to carry on from this point.

#### 2.3.3.7 *Tests with UDDT faecal sludge*

The final experiment from this study involved the use of real faecal sludge as feedstock (faecal sludge from UDDT). Figure 2.8 shows the drying curve from the UDDT sludge and compares it with one of the plots obtained for the simulant under similar conditions.

After 4 days of tests in the solar drier, the UDDT sludge was dried from 70 to 10% moisture content. The final moisture content was reached along the second day, and it did not vary further until the end of the experiment, indicating that the equilibrium moisture content was attained. Indeed, when this state is reached, the concentrations of the moisture in the sludge and the humidity in the air are in thermodynamic equilibrium, so the system does not evolve further.

Drying occurred at a faster rate for the UDDT sludge compared to the simulant. This result proposes that the UDDT sludge dried better than the simulant.

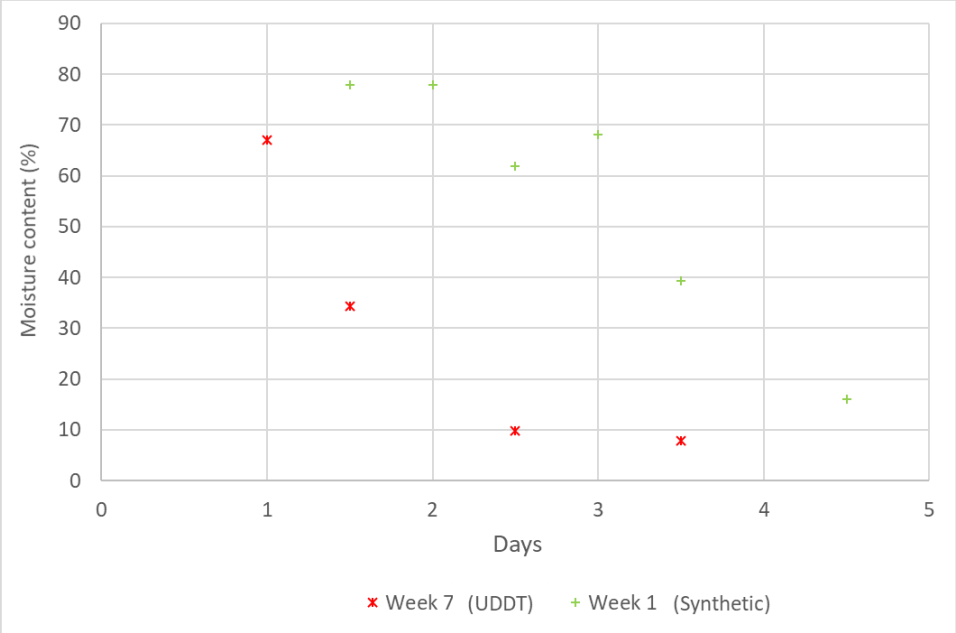


**Figure 2.8. Drying curves during the tests in the solar drier using the simulant and UDDT faecal sludge**

## 2.4 CONCLUSION

This preliminary study confirmed that solar drying in a thermal system is more efficient than in conventional drying beds, and brought valuable information for the design of the future pilot solar dryer.

It could be seen that the decrease of the initial mass of sample and the increase of the scrapping frequency improved the drying process. Therefore, important focus should be brought in the design of an efficient system for faecal sludge scrapping. This system should be able to avoid the crust formation at the top of the sludge and lead to a mixing effect between the different layers of the bed for a homogenized drying. With respect to

the amount of mass to load, the optimum value should be determined so as to lead to the fastest drying rates without affecting the productivity of the plant or requiring an increase of the surface area.
Based on this study, drying of faecal sludge in the developed prototypes could be expected to occur within a few days, if the weather conditions are favourable, and with the correct design of the ventilation and scrapping systems. The drying process could become significantly more difficult to carry on in the last stage of drying, as the moisture boundedness should strengthen as drying will proceed. If the moisture content is already low before the increase of the moisture boundedness, the process could be stopped at this point in order to lead to a higher performance.

If the theoretical calculations from section 2.2 are reconsidered by assuming an average efficiency of 25% for the solar drying plant (based on the outcomes from the solar drier tests), a total of 20 000 $m^2$ would be required to treat all the VIP sludge generated during a year in the eThekwini municipality. This land footprint equals to the area covered by 16 Olympic swimming pools or 3 standard soccer pitches, which is still acceptable. Therefore, solar thermal drying remains as an attractive and potential cost-effective option to deal with the treatment of faecal sludge.

## 2.5 REFERENCES

Brooks, M. J. (2015) 'SAURAN: A new resource for solar radiometric data in Southern Africa', Journal of Energy in Southern Africa, 26(1), pp. 2-10.
Zuma, L., Velkushanova, K. and Buckley, C. A. (2015) 'Chemical and thermal properties of dry VIP latrine sludge', Water S.A., 41(4), pp. 534-540.

# 3 GREENHOUSE-TYPE SOLAR DRIER PROTOTYPE

This section presents the greenhouse solar drier prototype, the testing plan, the discussion of the obtained results and the main outcomes from this part of the project. The information from this section was derived from the MSc of Pareshin Naidoo. In order to have a more detailed view of the results from this Chapter with a deeper level, the MSc dissertation from Pareshin Naidoo can be consulted (available in the Supporting Documents D from mid-2023).

## 3.1 MATERIALS & METHODS

### 3.1.1 Concept of the technology

The greenhouse prototype consists in a solar dryer where faecal sludge is placed in a bed and dried using solar thermal energy. The prototype offers an enclosed space where the solar thermal energy can be collected through greenhouse effect and the presence of an absorber wall. It includes a ventilation system and sludge rake system to boost the drying process. The sludge bed stands on a suspended grid, which allows the drying of the sludge from the bottom.

The greenhouse-type solar dryer is composed of the following components:

- A transparent enclosure in acrylic allowing the solar radiation penetration and creating a greenhouse effect by trapping the long-wave infrared radiation emitted by the bodies absorbing the solar thermal energy and protecting the process from the weather elements (in particular the rain from which the sludge can gain moisture) and preventing heat losses.
- A ventilation system (driven by ventilations fans) allowing to renew the air inside the enclosure and evacuate the evaporated moisture to avoid its accumulation, as a wet atmosphere could slow down or stop the drying process, and cause condensation in the walls and remoistening of the sludge.
- An air circulation system (driven by circulation fans) inside the enclosure in order to lead to a more homogeneous distribution of the evaporated moisture inside the volume of the dryer, avoiding the formation of high humidity layer at the surface of the sludge, which will affect negatively the process. Moreover, the circulation system creates movement of air at the surface of the sludge, which should enhance the mass transfer of the evaporated moisture from the sludge to the environment and consequently improve the drying process.
- A support where sludge will be placed as a layer of a given thickness to form a bed. The sludge bed stands on a fine mesh that will be elevated with respect to the ground level to allow air circulation underneath it and the drying of the sludge from the bottom.
- A rake system moving periodically back and forward along the bed to avoid crust formation and mixing the different layers of the sludge bed to lead to a more homogenous drying. The rake system consists in rotating bands with a series of blades orientated in alternate directions.
- A solar collector wall that increases the amount of solar radiation collected by the system. The wall is placed in the solar dryer between the air inlet and the bed. The bottom of the wall presents various holes from which the air stream is introduced to the drying zone. The wall should be placed facing south to collect the solar radiation entering the enclosure whose direction is not oriented to the sludge.
- Instrumentation to measure the temperature and relative humidity at different points inside the dryer, as well as the ambient conditions in the testing site (ambient temperature, ambient relative humidity, solar irradiance).
- An electronic system to log the data from the sensors and the rake system, and controllers for the motors from the ventilation and air circulation systems.

### 3.1.2 Components of the prototype

A greenhouse solar dryer was developed to dry faecal sludge. The dryer includes an enclosure, ventilation system, circulation fans, a sludge hanging bed (drying tray), a rake system, an absorber wall, and temperature and humidity sensors. The greenhouse solar dryer conforms to the specifications listed in Table 3.1.

**Table 3.1. Design specifications**

| Component | Specification | Explanation |
|---|---|---|
| Enclosure | Transparent dryer walls and roof (PMMA) | PMMA plastic allows sunlight to pass into the dryer |
| | Metal frame (Aluminium) | Ensure transparent walls are stable |
| | Ensure materials are corrosion resistant | Due to moisture material must be corrosion resistant |
| | Materials to have excellent UV stability (PMMA) | To prevent the decomposition of transparent material due to daily radiation exposure |
| | Dimensions are to be limited to 2m x 2m x 2m | To allow enough space to enter the dryer and allow a high volume of FS to be dried. |
| Absorber wall | Metal absorber wall (Aluminium) | High thermal conductivity to heat the air passing through the absorber wall and drying chamber |
| | Must have a black or dark surface (Matt paint) | To prevent long-wavelength radiation from escaping |
| | Will have inlets for extractor fans | To allow air to pass from the collector into the drying chamber |
| Rake system | Timed operation (Arduino) | To limit shade and minimize power usage. Unnecessary to constantly operate |
| | Linear actuator equipped with a NEMA 24 motor. | The rake was moved linearly across faecal sludge to reach the maximum area. Takes approximately 1 minute to move across the drying tray |
| | Blades rotating at approximately 60 rpm for mixing of FS (Aluminium) | To bring bound moisture onto the top surface of FS to improve drying time. |
| Drying tray | The tray is composed of a finely perforated steel mesh with 1mm diameter holes | Allow sludge to be dried from the bottom through the holes in the mesh and allow loose water to pass through |
| | The tray frame is to be composed of corrosion-resistant material | Exposed to wet surfaces of faecal sludge over long periods. |
| Ventilation system | Fans positioned on the front and rear of the dryer | Allow dry air to enter and expel moist air on the rear side of the dryer |
| | 4 fans positioned on the rear side of the dryer | To expel air from the top and bottom chambers of the dryer |
| | 4 Fans with a flow rate of 1000 $m^3$/h were chosen<br>2 Fans of flow rate 750 $m^3$/h were chosen for ventilation below the tray | Calculations determined a required flow rate of approximately 2000 $m^3$/h volume flow rate to dry faecal sludge in a 2m x 2m dryer |
| Circulation fans | 2 fans are positioned inside the sides of the dryer above the drying tray | Circulation fans ensure air is circulated throughout the dryer |
| | Adjustable fan speeds | A variable speed switch was used to change fan speeds accordingly |
| Temperature & humidity control system | 6 x DHT 22 temperature sensors, positioned connected to the temperature control system. | Mounted in various positions to determine temperature and humidity at determined points in the dryer |
| | Data is stored on a micro-SD card and can be transferred to a computer | Temperatures and humidity values are stored according to the time of the day and record readings are every 10 seconds |

These specifications were applied to the greenhouse solar dryer. Each subsystem will address a certain aspect of the drying of faecal sludge. A *CMP3* flat class C pyranometer was used to determine solar irradiance. The pyranometer was connected to a separate control unit in a plastic box. The control unit was made up of an

Arduino board, date and time sensor, micro secure digital (SD) adapter and direct current (dc) power supply. The control unit reads and stores the date, time and irradiance. Figure 3.1 shows the completed prototype.

**Figure 3.1. Greenhouse Solar Thermal Dryer**

#### 3.1.2.1 *Enclosure*

The enclosure (2m x 1.5m x 2m) was built using an aluminium angle iron frame and polymethyl methacrylate (PMMA) acrylic plastic sheets. The enclosure is the first sub-system that was developed as it houses all the other components of the greenhouse solar dryer. Two rectangular bases were constructed by welding 1.5 m x 2 m lengths of aluminium angle (2 mm thickness). Four vertical braces were developed to connect the top and bottom bases at each corner. The aluminium angle was TIG welded using tungsten welding rods. Thereafter the weld was ground to form a smooth finish. The vertical braces and base frame together with PMMA were assembled using M12x20 self-tapping galvanized set screws. The door frame was constructed using 25mm x 25mm square tubing. The PMMA door was fastened onto the frame using M12 self-tapping screws. The frame was important to reinforce PMMA as the plastic was very flexible. Hinges were fastened onto the door and enclosure frame. A lock was installed to pull the door tight against the aluminium angle. Figure 3.2 shows a picture of the final assembly of the enclosure.

**Figure 3.2. Greenhouse solar dryer enclosure**

#### 3.1.2.2 *Absorber Wall*

Aluminium sheet metal 3 mm thick was used as an absorber wall inside the greenhouse (1.5m x 2m). The sheet was painted black to retain heat within the dryer. Holes of 10 mm were drilled on the bottom of the absorber wall to allow airflow into the dryer to pass into the drying chamber (DC) where faecal sludge is to be dried. For this, 25 holes were drilled from the bottom of the absorber wall to a height of 600 mm. The absorber wall was mounted nearest to the back of the dryer using self-tapping set screws. Dry air from the greenhouse inlet would flow over the absorber wall, which should thereby heat the air stream through convection. Air passed then through the 10 mm holes into the DC. Figure 3.3 shows the black absorber wall developed.

**Figure 3.3. Absorber wall**

#### 3.1.2.3 *Ventilation & Circulation system*

Four *RS PRO* alternative current (A 220V axial fans with an effective diameter of 204 mm with a flow rate of 1002.4 $m^3$/ h were used within the greenhouse dryer. Two fans were mounted near the top back wall of the dryer to bring air into the dryer and two fans on the exit were mounted towards the front of the dryer to remove moist air in the DC.

Below the later ones, less powerful ManTech 220 V fans of 750 $m^3$/h with an effective diameter of 195 mm (2 fans) were also placed at the air stream exit near the bottom of the dryer. The air outlet fans (4 in total) are expected to create air flow in the top and bottom of the sludge bed.

Two *Ebm-Papst* axial S series, 230 V axial circulation fans with an effective diameter of 300 mm were mounted across each other on the side walls of the DC above the drying tray. These fans are capable of providing a 2034 $m^3$/ h volumetric air flow rate.

The optimal fan positions were determined by computation fluid dynamics simulations. The connections for the ventilation and circulation fans were similar. Circulation fans and ventilation fans were connected separately to two *Ebm-Papst*, 230V, ac fan speed controllers. Figure 3.4 shows an illustration of the parallel connections for the ventilation system.

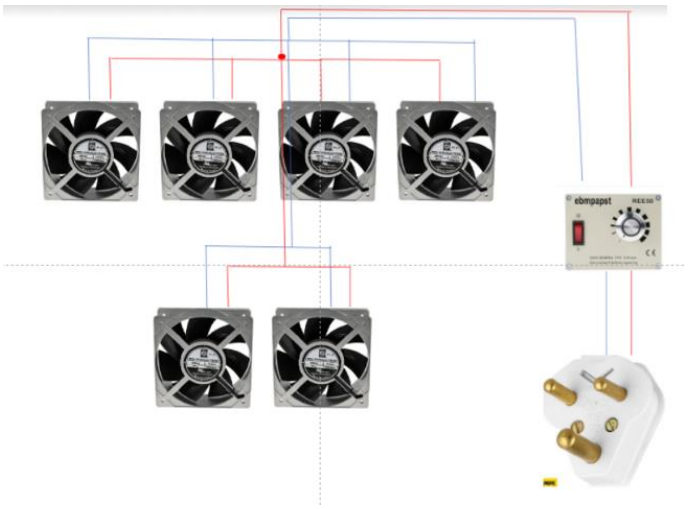

**Figure 3.4. Fan electrical connections**

### 3.1.2.4 *Rake System*

The rake system was made up of 5 major components. These components were rotating blades, linear actuator, guide rail, blade motor and rake control system. The rotating blades were used to mix and move the sludge to avoid crust formation. Indeed, the blade moved across the drying tray and rotated as it moves. Pillow block 20 mm inside diameter bearings were connected to both ends of the blade shaft and onto the guide rail and linear actuator. The linear actuator and guide rail were connected with a bracket to brace and join the two components together. The linear actuator moved the rotating blade across the drying tray. A mounting and *NEMA 3*4 stepper motor were connected on the linear actuator side of the blade shaft. It is a 48 V high torque stepper motor capable of operating at 12 N.m of torque. The motor drove the rotation of the blade that was supported by two bearings on either side and mix the sludge product. The linear actuator enabled the rake to move across the drying tray in both directions. The operation of the rake was controlled by the rake control system (Arduino board).

The rake system was mounted onto a frame and thereafter mounted to the drying table with two hinges on one side of the table and frame. This frame allows for the rake system to pick up on one side to allow the drying tray to slide in with no obstruction or collisions with the blade. The drying table and rake system were thereafter placed and connected to the dryer enclosure. The electronics were mounted in a box outside the dryer. The drying tray was constructed using aluminium angle iron and perforated fine steel mesh with a hole diameter of 1 mm. The tray mesh and frame were riveted together. The rake system and drying tray are shown in Figure 3.5.

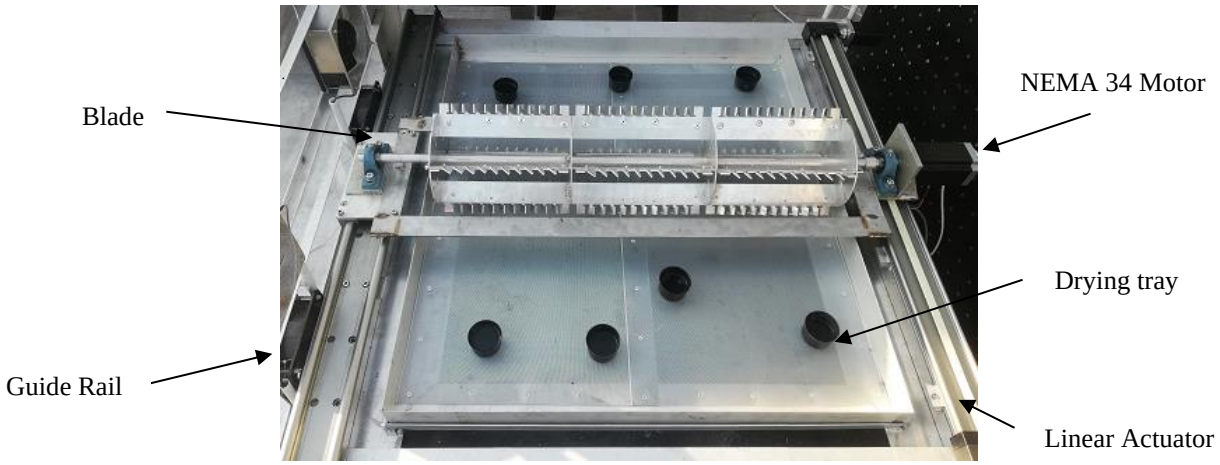


**Figure 3.5. Rake system and table support**

#### 3.1.2.5 *Instrumentation*

Temperature and humidity sensors were used to measure temperature and humidity at different points in the dryer. The temperature sensors were placed in different positions in the greenhouse. An ambient inlet sensor was positioned outside the dryer next to the inlet fans to determine the temperature and humidity entering the greenhouse dryer. A sensor was positioned on the absorber wall in the air inlet side to determine the air temperature of the air in the collector. Four sensors were positioned inside the DC: (i) under the drying tray; (ii) at the absorber wall air inlet above the tray; (iii) near the fans outlet above the drying tray; (iv) an elevated sensor hanging on the roof of the dryer. The different sensors in the dryer are allocated the numbers following their position: (i) T/H 1 for the collector; (ii) T/H 2 for the elevated area in the DC; (ii) T/H 3 for the air entering into the DC from the collector; (iv) T/H 4 for the DC floor; T/H 5 for the DC outlet or exit temperature; (v) T/H 6 for the ambient conditions. The positions of the sensors are shown in Figure 3.6.

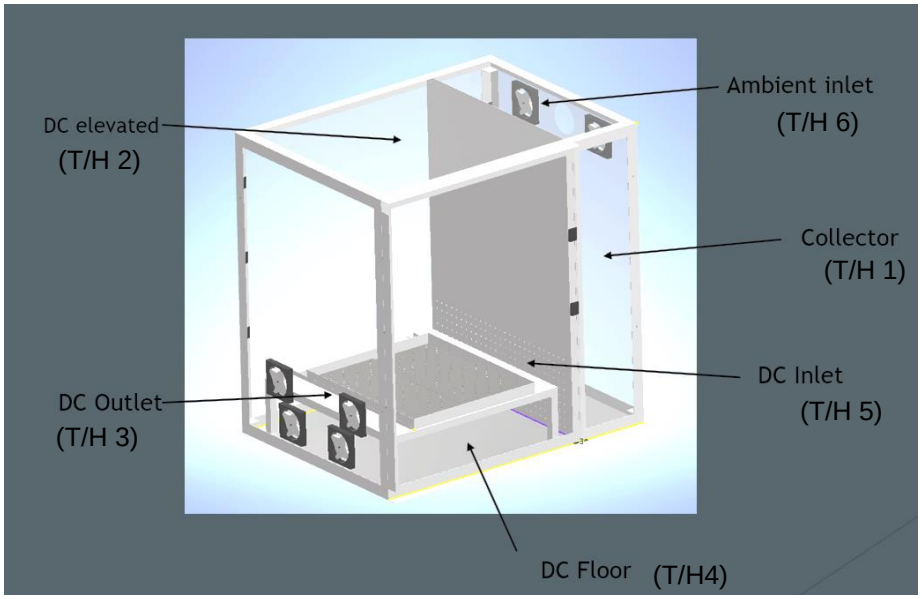


**Figure 3.6. Temperature sensor positioning**

Two electrical boxes housed the electronics for the fans, temperature sensors, motor drivers and power supplies. The ventilation and circulation fan potentiometers were housed in a separate box from the motor drivers and temperature and humidity control system. The potentiometers had 10-speed settings and were used to control the volumetric flow rate of fans. The complete assembly of the dryer from start to finish can be consulted in the previous Deliverables. The two electrical boxes are shown in Figure 3.7.

**Figure 3.7. Electrical control boxes**

## 3.2 EXPERIMENTS

Testing was conducted to validate the prototype functionality, evaluate the drying performance, improve the operational environment, and identify opportunities for improvement. The greenhouse dryer utilized temperature and humidity sensors at different positions in the dryer to determine temperature and humidity fluctuations in and around the dryer during the tests. The temperature control system recorded the date, time, temperature and humidity every short interval (10 s) and saved this data as a text file on a memory card. A *CMP3* flat class C pyranometer from *Kipp & Zonen* was used to determine the solar irradiance. The pyranometer measures irradiances up to 2000 W/m$^2$ and sensitivity by less than 4%. An isolated control system fitted in a portable box was developed to measure and log irradiance readings on a memory card. The moisture content of the material to dry was measured during the testing in a *Radwag MA 50R.WH* moisture analyser.

The front of the dryer where the outlet fans are positioned was oriented facing north to maximise the amount of solar radiation penetrating the greenhouse. The greenhouse was located on the Chemical Engineering building roof at Howard College campus, University of KwaZulu-Natal (Durban, South Africa), coordinates 29.8671° South and 30.9831° East. Experiments were conducted in the winter periods during August, September and October between 9 AM and 3 PM during the day, with average ambient temperatures of between 25 and 30°C, average relative humidity between 40 to 60%, and average irradiances between 500 to 600 W/m$^2$. Before 9 AM and after 3 PM, the solar radiation intensity was rising and dropping respectively, therefore most of the testing was conducted in the time interval between 9 AM and 3 PM where the solar irradiance reached its peak and experiences slight variations. Data shows temperatures reach the highest in the greenhouse towards the afternoon. Testing was stopped if the wind picked up or in the case of too much cloud coverage, as the tests should be done in consistent weather conditions (sunny conditions without or with low cloud coverage).

Experiments were performed without feedstock, with containers filled with water, with wet soil and with synthetic faecal sludge. The experimental procedure of the tests is detailed in Appendix A.

### 3.2.1 Functionality tests

The functionality tests were conducted to characterize the individual sub-system components' performance (the enclosure, absorber wall, rake system mixing effect, and ventilation and circulation fan speeds).

#### 3.2.1.1 *Enclosure tests*

A thermocouple was used to determine the temperatures inside the dryer enclosure and the ambient air temperature outside the enclosure. The test was conducted on the date 13/10/2021. Temperatures outside the dryer, inside the dryer with fans off, set to full and set to half capacity. It was observed that the dryer reached the highest temperatures when the fans were off, but temperatures were still higher than outside temperatures.

#### 3.2.1.2 *Ventilation and Circulation fans tests*

Tests on the ventilation and circulation fans were conducted for their calibration. During the calibration tests, the air flow velocity induced by each fan was measured using a hot wire anemometer to determine the volumetric flow rate at different fan speed control settings (10-speed settings). The volumetric flowrates were deduced from the product of the airflow speed and the cross-section surface area of the fan.

The power consumption of the fans was measured by a wattmeter. The different fan speeds consumed different amounts of power. Higher fan speeds used more power than slower fan speeds.

The power consumption and the fan speeds for the various speed combinations can be found in Appendix B. The ventilation and circulation potentiometer speed settings and volumetric flow rate of air calculated are shown in Table 3.2.

**Table 3.2. Ventilation and Circulation flowrates**

| **Circulation fans** | |
|---|---|
| **Setting** | **Flow rate ($m^3$/h)** |
| C0 | 0 |
| C3 | 661.28 |
| C6 | 1271.70 |
| C10 | 2034.72 |
| **Ventilation fans (204 mm)** | |
| **Setting** | **Flow rate ($m^3$/h)** |
| V0 | 0 |
| V1 | 294.01 |
| V4 | 423.38 |
| V7 | 733.86 |
| V10 | 1011.41 |
| **Ventilation fans (195 mm)** | |
| **Setting** | **Flow rate ($m^3$/h)** |
| V0 | 0 |
| V1 | 0 |
| V4 | 0 |
| V7 | 100 |
| V10 | 400 |

#### 3.2.1.3 *Absorber wall temperature fluctuation tests*

Thermal imagining using a FLIR One infrared camera determined the temperature absorber wall reaches during the winter season. Pictures taken with a camera are shown in Appendix B.

#### 3.2.1.4 *Rake system and instrumentation*

Functionality tests of the rake system were conducted to verify the correct operation of the device and to determine mixing effects. Dry sand was initially used to ensure motors are powerful enough to mix and move through sand. Results discussing the functionality of the rake system are discussed in Appendix B.
Testing instrumentation functionality tests were conducted to ensure temperature sensors are calibrated and display correct temperature and humidity values.

#### 3.2.1.5 *Greenhouse dryer integrated functionality tests*

The subsystems were all installed in the greenhouse dryer and the dryer was tested as a whole. The rake system was tested to ensure all the components are working effectively together. Temperature and humidity sensors were calibrated to ensure correct values were recorded. The rake system worked efficiently during dry tests with no feedstock.

### 3.2.2 Feedstock tests

#### 3.2.2.1 *Water evaporation tests*

Water tests were conducted between the periods of 13th July 2022 to 5th August 2022. Water was used as a material to test the integrated greenhouse dryer prototype to determine the water evaporation rate, and the temperature and humidity inside the enclosure. Ventilation and circulation power were adjusted to determine the best speed setting for the optimal water evaporation rate. Temperature and humidity were measured at the different ventilation speeds to link these parameters to the evaporation performance of the greenhouse. During the tests, water was placed in 7 round metal containers and placed at different points in the dryer to determine how much water evaporated. The mass of both the metal containers and water weighed initially 100 g. Ventilation fans and circulation fan speeds were adjusted during testing to determine the most optimal fan speed for the evaporation of water. Circulation speeds were set at one speed for the day and ventilation speeds were adjusted every 30 minutes. The next day the circulation fan was changed, and the same procedure was repeated. The mass of the crucibles and water were measured after each change of ventilation speed. To prevent heat loss from the system after taking out the crucibles from the greenhouse for their weighing, only 2 containers' mass was measured at hourly intervals. **Error! Reference source not found.** summarizes the basic information from t the water evaporation tests. The testing setup is shown in

Figure 3.8.

**Table 3.3. Water evaporation tests conditions**

| Specifications | Amount | Description |
|---|---|---|
| Diameter | 55mm | Metal container diameter |
| Height | 40mm | Metal container Height |
| Ventilation speeds ($m^3$/hr) | 294, 423, 733, 1011 | Ventilation speed adjustments |
| Circulation speeds ($m^3$/hr) | 0, 660, 1271, 2024 | Circulation speed adjustments |
| The initial mass of the crucible and water | 100g | Starting weight |
| Drying time | 4-5 hours | 9:00-14:00 |

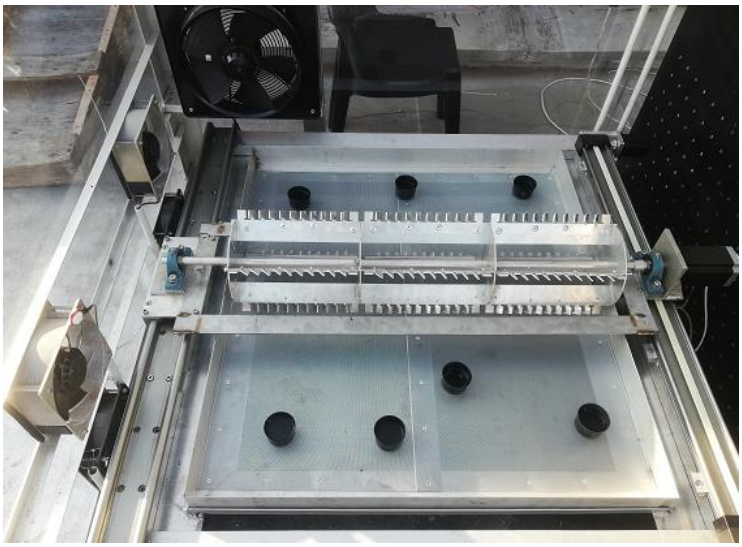

3.2.2.2 *Figure 3.8. Water evaporation tests setup Wet soil tests*

Wet soil was used as a drying product to determine the rake system's effectiveness and the drying performance of the greenhouse dryer. A first test was done with 1.4 kg of wet soil of around the drier handled 60% wet soil well without a large amount of water filtering through the drying tray into the drainage tray. Thereafter a higher moisture content sample of wet soil of around 65% was dried in the greenhouse dryer with the rake system in constant operation.

A second test was conducted at 15 kg mass of wet soil (70% moisture content). The wet soil was spread onto the drying tray and left to dry from 10:00 AM to 3 PM. To produce the wet soil, a certain amount of dry soil was mixed with water. Note that this feedstock presented a watery consistency, leading to some amount of water being drained into the tray below the drying tray when poured onto the drying tray. Results might display imprecise data due to the water being drained and not evaporated.

For each of the feedstock mass, the rake system was turned off for one first test and the rake system was used for the second test. Each test was conducted on separate days. For each test, a small amount of sample between 2-5 grams was taken at every 1-hour interval from the bottom of the drying bed closest to the center and placed in a moisture analyzer to determine the moisture content. The circulation and ventilation speeds were set to 1 on the potentiometer as it was determined lower fan speeds yield higher temperatures and more drying potential as determined from water evaporation tests. Table 3.4 lists the basic information from the soil tests. Figure 3.9 shows a picture of wet soil in the drying tray while the rake system is operating.

**Table 3.4. Wet soil tests information**

| Specifications | Amount | Description |
|---|---|---|
| Area | 0.5 $m^2$ | Centralized mass of wet soil |
| Thickness | 0.02 cm | Approximate thickness of soil |
| Ventilation speed | 294 $m^3$/hr | As determined from the water test |
| Circulation speeds | 508 $m^3$/hr | As determined from the water test |
| The initial mass of wet soil | 15 kg | Starting weight |
| The initial moisture content of wet soil | 70% | Starting moisture content |
| Drying time | 5 hours | 10:00-15:00 |

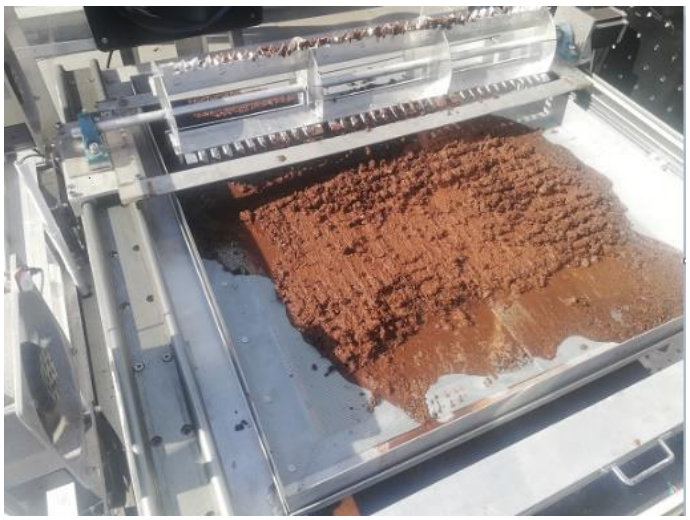

**Figure 3.9. Wet soil tests setup with rake system in operation**

#### 3.2.2.3 *Synthetic faecal sludge tests*

Synthetic sludge was used due to the restrictions of faecal sludge use on the Chemical Engineering building's roof at the UZKN campus, due to the hazards associated with the handling of faecal sludge outside from the laboratory of the WASH R&D Centre. A recipe for the production of synthetic sludge from the WASH R&D Centre was followed and was used to make a sample to be tested in the greenhouse dryer. Synthetic sludge was developed to test the performance of the dryer. The synthetic sludge preparation procedure is presented in Appendix C.

Drying time, temperature and humidity measurement mixing effect and system functionality were observed during the tests. For these tests, a mass of around 10 kg of synthetic sludge at 80% moisture content was dried within a period of a few days. Table 3.5 summarizes the basic information for the synthetic sludge tests. Figure 3.10 shows a picture of the initial sample of 10 Kg of synthetic sludge spread onto the drying tray.

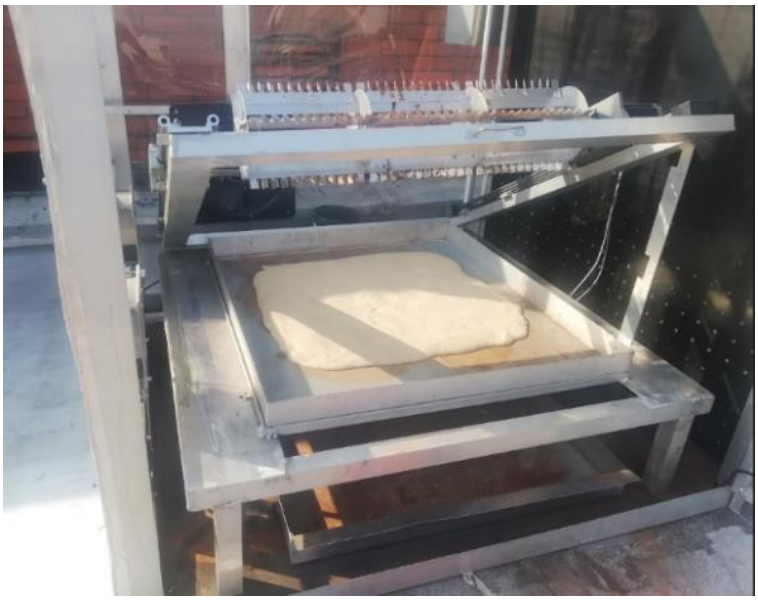

**Figure 3.10. Synthetic sludge tests setup**

**Table 3.5. Synthetic sludge tests conditions**

| Specifications | amount | description |
|---|---|---|
| **Area** | 0.8-0.9 $m^2$ | Centralized mass of sludge |
| **Thickness** | 10 mm | Thickness of sludge |
| **The initial mass of wet soil** | 10 kg | Starting weight |
| **The initial moisture content of wet soil** | 80% | Starting moisture content |
| **Ventilation speed** | 294 $m^3$/hr | As determined from the water test |
| **Circulation speeds** | 506 $m^3$/hr | As determined from the water test |
| **Drying time (1 day)** | 6 hours | 9:00-15:00 |
| **Duration** | 1 week (9AM-3PM) | 05/09/2022-09/09/2022 |

## 3.3 DATA ANALYSIS

### 3.3.1 Output parameters

The measured parameters during the tests can be summarized as follows:

- Temperature (°C)
- Humidity (%)
- Solar irradiance (I)
- Power consumption (W)
- Mass of drying product (kg)
- Moisture content (%)
- Drying time (h)

### 3.3.2 Performance parameters calculations

The measured parameters were used to calculate the performance parameters of the dryer, such as drying rate, moisture removal, solar dryer efficiency and specific energy consumption, using the following formulas:

- Moisture removal

$$\Delta \boldsymbol{m} = (\boldsymbol{Mi} \times \boldsymbol{m}_{\boldsymbol{i}}) - (\boldsymbol{Mf} \times \boldsymbol{m}_{\boldsymbol{f}}) \quad \textbf{Equation 3.1}$$

Where,
$\Delta m$: Mass of moisture removed (kg)
$m_i$: Initial mass of sample (kg)
$m_f$: Final mass of sample (kg)
$M_i$: Initial moisture content (Wet basis)
$M_f$: Final moisture content (Wet basis)

With,

$$\boldsymbol{m_f} = \frac{\boldsymbol{m_i}(\boldsymbol{1-M_i})}{\boldsymbol{1-M_f}} \quad \textbf{Equation 3.2}$$

- Drying Rate

$$\boldsymbol{DR} = \frac{\Delta \boldsymbol{m}}{\Delta \boldsymbol{t}\ \boldsymbol{x}\ \boldsymbol{A_{sludge}}} \quad \textbf{Equation 3.3}$$

Where,
*DR:* Drying rate (kg/h/m$^2$)
$A_{sludge}$: Surface area of the sludge (m$^2$)
$\Delta t$ : Drying time (h)

With,
$A_{sludge} \approx 1$ m$^2$ (as the dimensions of the sludge bed are 1m x 1m)

- Dryer efficiency

$$\eta = \frac{\boldsymbol{DR} * \Delta \boldsymbol{Hvap}}{\boldsymbol{I} * \boldsymbol{A_{absorber}}} \times \frac{\boldsymbol{1000}}{\boldsymbol{3600}} \quad \textbf{Equation 3.4}$$

Where,
*η:* efficiency

*I*: Solar irradiance (W/m$^2$)
$A_{absorber}$: Surface area of solar absorber (m$^2$)
$\Delta Hvap$: Latent heat of vaporisation of water (kJ/kg)

With,
$A_{absorber}$ as the sum of the surface area of the sludge (1 m$^2$) and that of the absorber wall (3 m$^2$)

Note that the efficiency values are a rough approximation and may be underestimated because the global horizontal irradiance was used to calculate the solar irradiance received by the absorber wall, whereas its position is vertical, so it may receive less irradiance than the one estimated by the calculation. Besides, the latent heat of pure water vaporization was used as an approximation for the heat of drying for faecal sludge. The real value of the heat required to dry faecal sludge should be higher than the value of pure water vaporization.

Because of the inaccurate values of the solar irradiance received by the absorber and heat of drying (as explained above), the efficiencies would be likely underestimated and might have to be used with precaution for the comparison of performance with other solar driers.

- Specific Energy Consumption

**SEC =** $\frac{Psystem}{DR} \times 1000$ **Equation 3.5**

Where,
*SEC*: Specific energy consumption (kWh/ton evaporated moisture)
$P_{system}$: Power consumed in the drying system by the fans, rake system and instrumentation (kW)

### 3.3.3 Statistics/uncertainties

Replicates (2 or more) were done of the same operating conditions for the tests without feedstock and water tests to ensure data reproducibility. Nonetheless, it has to be noted that the duplicates could not be reproduced in identical conditions due to the variable nature of the weather. The soil tests couldn't be performed in duplicates because of time constraints.

A couple of synthetic faecal sludge tests were conducted at the same operating conditions, but the duration of the tests was long (various days) and consequently the variability of the weather conditions was too high for the runs to be considered as duplicates.

The data presented for the tests without feedstock and water tests are the average from the replicates. The uncertainty bar was determined from the standard deviation from the measured data.

## 3.4 RESULTS & DISCUSSION

This section presents the results obtained during the different testing phases. A selection of data is shown and discussed in this section. The overall of the data can be found in Appendix B.

### 3.4.1 Functionality test results

The subsystems performed well during the functionality tests. The dryer's temperatures were significantly higher than the outside temperature inside the greenhouse. The dryer's humidity reflected much lower values than the surrounding environment (due to the higher temperatures inside the greenhouse), which may result

in better evaporation conditions and promote better drying. The collected data was processed and separated based on the date and type of test. Appendix B contains more results from the functionality tests.

During the tests of the integrated system, the temperature and humidity data were recorded at the 6 different points. The temperatures recorded in the dryer were higher than the ambient temperature entering the dryer. The elevated sensor in the DC reached the highest temperatures which could be expected since hot air rises. Lower humidity was recorded inside the dryer as compared to the ambient inlet humidity (again, due to the higher temperatures leading to the decrease of the relative humidity).

Circulation speeds and ventilation speeds were adjusted to determine the highest temperatures and humidity reached at the different points in the dryer without feedstock. The changing of the fan speeds was done in batches on different days to determine the effect fan speed had on the temperature and humidity. It was found that higher fan speeds (circulation and ventilation fans) resulted in a decrease in temperature and an increase in humidity. The lower fan speeds resulted in higher temperatures and lower humidity being recorded. Table 3.6 shows the average temperatures and humidity reached at the various points in the dryer.

**Table 3.6. Temperature and relative humidity data recorded during the functionality tests of the fully integrated system (DC: drying chamber)**

| | | Collector | | DC elevated | | DC outlet | | DC floor | | DC inlet | | Ambient inlet | | |
|---|---|---|---|---|---|---|---|---|---|---|---|---|---|---|
| **Circulation** | **Ventilation** | T1 | H1 | T2 | H2 | T3 | H3 | T4 | H4 | T5 | H5 | T6 | H6 | Solar irradiance |
| **C0** | **v1** | 27.8 ±0.4 | 37 ±3.5 | 36.8 ±3.8 | 32.9 ±11.7 | 31.1±0.5 | 32.5 ±1.7 | 28.6±2.9 | 36.8±5.4 | 31.8±0.3 | 35.9±11.2 | 22.8±0.7 | 49.8±12.2 | 421.1± 99.5 |
| | **V4** | 26.7 ±2.3 | 38.7 ±8.1 | 34.2 ±6.4 | 39 ±20.5 | 29.1±2.4 | 35.2 ±6.0 | 27.5±0.9 | 39.5±12 | 29.5±2.9 | 41.8±19.8 | 22.7±0.2 | 51.65±16.3 | 512.995±8.3 |
| | **V7** | 26.8 ±0.6 | 37.2 ±5.9 | 33.4 ±1.9 | 35.9 ±14.4 | 29±0.1 | 33.1 ±1.7 | 28.1±0.1 | 38±11 | 29±04 | 40.8±17.3 | 23.9±0.6 | 47.55±14.1 | 539.39±6.9 |
| | **V10** | 29. 7±4 | 33.9 ±0.6 | 34.8 ±1 | 33.4 ±10.1 | 31.3±3.7 | 32.1 ±0.3 | 29.5±2.1 | 35.8±7.8 | 30.4±2.7 | 35±8.1 | 27.5±6.3 | 43.1±6.4 | 556.01±11.1 |
| **C3** | **v1** | 29.8 ±3.7 | 50.6 ±9.3 | 36.3 ±4.7 | 36.9 ±7.7 | 34.1±4.7 | 44.2 ±9.6 | 33.1±4.7 | 37.7±6.4 | 34.0±3.4 | 40.2±5.9 | 24.1±1.3 | 65.1±5.7 | 561.9±19.4 |
| | **V4** | 29.4 ±0.6 | 50.9 ±2.2 | 36.2 ±1.2 | 36.1 ±2.3 | 33.0±1.7 | 45.3 ±3.5 | 31.9±1.2 | 38.8±2.1 | 33.0±1.4 | 40.7±3 | 23.8±0.6 | 66.4±2.1 | 532.5±2.8 |
| | **V7** | 26.9 ±0.6 | 57.0 ±2.5 | 32.7 ±0.6 | 40.3 ±2.1 | 29.8±0.7 | 52.8 ±2.9 | 28.8±1 | 43.3±2.1 | 29.8±1 | 46.2±3.2 | 23.4±0.7 | 68.4±4.4 | 516.9±33.2 |
| | **V10** | 27.2 ±0.8 | 57.2 ±4.5 | 32.6 ±0.4 | 41.1 ±1.8 | 30.2±1.3 | 53.3 ±4.6 | 28.6±0.6 | 43.8±2.3 | 29.8±1.8 | 47.3±4.8 | 23.7±0.8 | 66.8±4.9 | 499.3±74.7 |
| **C6** | **v1** | 29.4 ±1.2 | 47.6 ±8.8 | 34.9 ±3.3 | 36.0 ±9.3 | 32.6±1.8 | 42.0 ±11.7 | 32.3±2.2 | 36.3±6.6 | 32.8±2.1 | 37.0±9.9 | 25.2±1.1 | 64.1±8.1 | 539.4±201 |
| | **V4** | 28.3 ±0.2 | 49.8 ±2 | 33.7 ±0.5 | 37.5 ±2.3 | 31.5±0.4 | 46.5 ±1.8 | 30.5±0.2 | 38.4±1.9 | 31.4±0.9 | 41.0±2.1 | 25.0±0.1 | 66.5±4.5 | 569.7±13.8 |
| | **V7** | 27.9 ±0.4 | 52.4 ±0.2 | 31.8 ±0.3 | 41.0 ±0.4 | 30.4±0.3 | 51.0 ±1 | 29.1±0.4 | 41.4±0.9 | 30.1±0.4 | 44.4±0.4 | 25.0±0.4 | 71.1±10.5 | 499.9±83.6 |
| | **V10** | 28. 6±1 | 52.5 ±0.4 | 31.9 ±0.7 | 42.0 ±0.3 | 29.9±0.4 | 54.7 ±2 | 28.9±0.1 | 41.8±0.1 | 29.5±0.3 | 46.8±1.1 | 23.8±0.4 | 81.4±11.9 | 480.6±11.9 |
| **C10** | **v1** | 29.7 ±2.3 | 41.8 ± 2.9 | 34.4 ±0.2 | 38.9 ±3.3 | 31.2±0.4 | 46.3 ±3.5 | 32.0±1.9 | 37.9±4.1 | 33.2±1.5 | 40.1±5.5 | 23.8±0.4 | 61.3±5.1 | 564.8±6.9 |
| | **V4** | 26.4 ±1.8 | 42.7 ±13.3 | 31.2 ±3.3 | 43.3 ±7.1 | 29.8±3.6 | 47.9 ±1.8 | 29.2±3.2 | 42.7±6.8 | 30.0±4 | 42.7±4 | 22.8±0.4 | 66.5±7.1 | 554.0±24.9 |
| | **V7** | 26.0 ±0.6 | 46.3 ±21.1 | 31.4 ±0.9 | 45.6 ±0.7 | 29.0±0.1 | 50.8 ±9.2 | 28.1±0.1 | 44.8±1.4 | 28.8±0.1 | 50.9±3 | 23.3±1.4 | 67.9±11.2 | 579.2±112.9 |
| | **V10** | 29. 1±5 | 49.1 ±21.6 | 32.6 ±4.4 | 44.5 ±5.7 | 30.9±4.2 | 51.1 ±15 | 29.0±3 | 43.5±3.6 | 30.3±4 | 48.5±5.2 | 26.4±6.6 | 65.1±19.8 | 563.3±173.5 |

### 3.4.2 Water tests results

During water tests, temperature and humidity inside the greenhouse dryer and the ambient air entering the greenhouse were compared and analysed. The average greenhouse temperature for each ventilation and circulation rate can be compared in Figure 3.11. Note that the average greenhouse temperature was calculated as the mean value from T1, T2, T3, T4 and T5. The temperature and humidity raw data are shown in Appendix B.

From the graph, temperatures inside the dryer were significantly higher than the temperatures of air entering the dryer. It can also be seen that the highest temperatures tended to be achieved at lower ventilation speeds (V1). Concerning the circulation rate, the highest temperature values were obtained for C3, meaning that mild circulation rate led to the best conditions for drying compared to non-circulation or higher values.

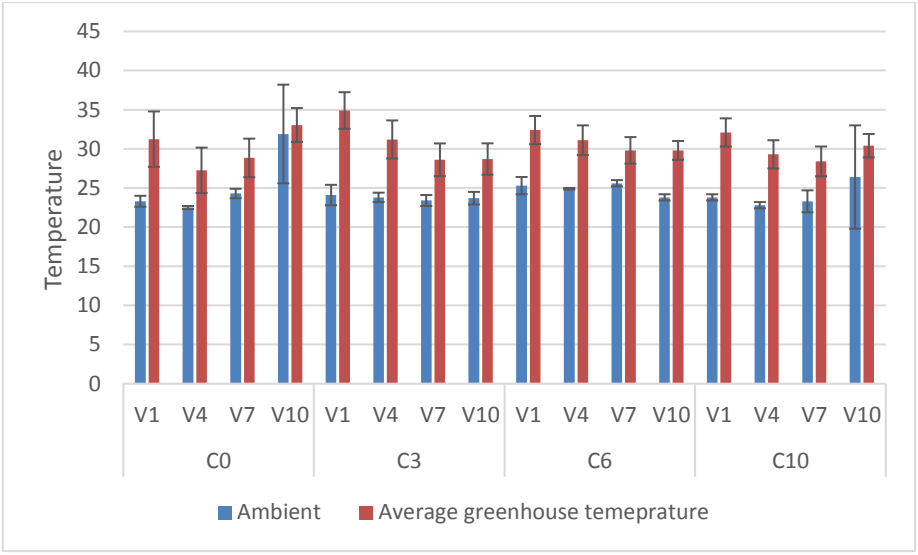


**Figure 3.11. Graph of temperature as a function of the circulation and ventilation rates**

Figure 3.12 shows the average humidity achieved in the dryer compared to relative humidity entering the dryer at different circulation and ventilation speeds. Humidity values inside the dryer at the different fan speeds varied between 30 to 50%. Consequently, humidity inside the dryer was much lower than that of the outside.

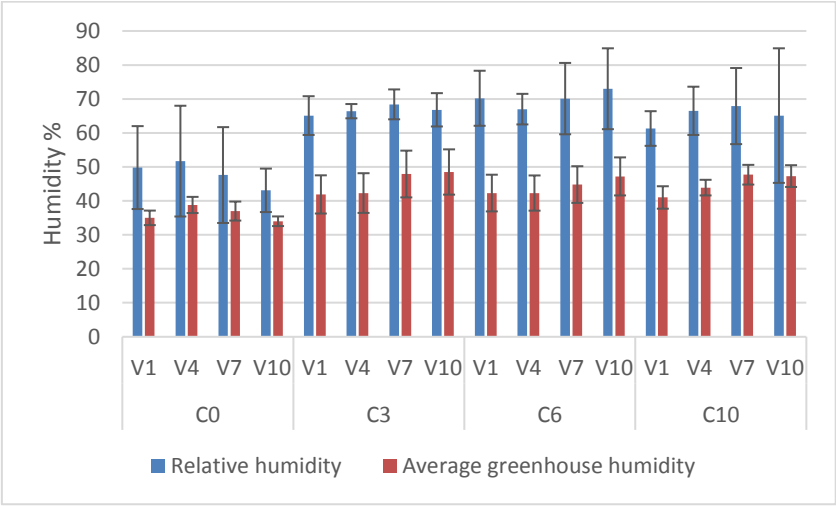


**Figure 3.12. Graph of temperature as a function of the circulation and ventilation rates**

The mass of water and the crucible were measured every 30-minute interval to determine how much water was evaporated in that space. The ventilation and circulation rates that achieved the most mass of water evaporated were evaluated. Performance parameters at varying ventilation rate and constant circulation rate (C3) are shown in Table 3.7. Performance parameters for the other circulation speeds are shown in Appendix B. Lower Ventilation fan speeds yielded higher efficiency and lower SEC, therefore V1 was selected as the best ventilation speed, and this value was used to determine which circulation speed yields higher efficiencies and better drying rates. Performance parameters for the various circulation speeds at set ventilation speeds are shown in Table 3.8.

**Table 3.7. Performance parameters at varying ventilation rate at fixed circulation rate (C3)**

| | V1 | V4 | V7 | V10 |
|---|---|---|---|---|
| **Average irradiance (W/m$^2$)** | 542 ± 19 | 532 ± 3 | 539 ± 33 | 499 ± 74 |
| **Average dryer temperature (°C)** | 33.5 ± 2.3 | 32.7 ± 5.84 | 29.6 ± 2.1 | 29.6±2 |
| **Average dryer humidity (%)** | 41.9 ± 5.62 | 42.3 ± 6.88 | 47.9 ± 6.88 | 48.5±6.6 |
| **Drying Rate (kg/h/m$^2$)** | 2.32 | 1.26 | 1.90 | 0.84 |
| **SEC (kWh/ton)** | 167 | 433 | 413 | 925.00 |
| **Efficiency (%)** | 21 | 13 | 20 | 2 |

**Table 3.8. Performance parameters at varying circulation rate at fixed circulation rate (V1)**

| | C0 | C3 | C6 | C10 |
|---|---|---|---|---|
| **Average irradiance (W/m$^2$)** | 522 ± 43 | 542 ± 19 | 548 ± 11 | 565 ± 3 |
| **Average dryer temperature (°C)** | 31.2 ± 3.5 | 33.5 ± 2.3 | 32.1 ±1 .8 | 32.1 ± 1.8 |
| **Average dryer humidity (%)** | 35 ± 2.1 | 41.9 ± 5.62 | 42.3 ± 5.4 | 41 ± 3.3 |
| **Drying Rate (kg/h/m$^2$)** | 1.26 | 2.94 | 2.73 | 2.74 |
| **SEC (kWh/ton)** | 330 | 167 | 285 | 49 |
| **Efficiency** | 9 | 27 | 20 | 23 |

The test where the circulation fans were set at fan speed 3 (C3) on the potentiometer and ventilation speed 1 (V1), resulted in the largest mass of water evaporated. The reason for these combinations of speeds being the best is that the lower fan speeds result in temperatures above 40°C and lower humidity as seen in Figure 3.11. These conditions promote better drying performance (higher drying rate, higher efficiency, lower SEC). At these fan speeds, a maximum of 4 grams of water is evaporated from one container in 30 minutes.

Figure 3.13 shows a surface chart of the SEC vs the fan speeds. In the chart it can be seen as fan speeds are increased so does the SEC value.

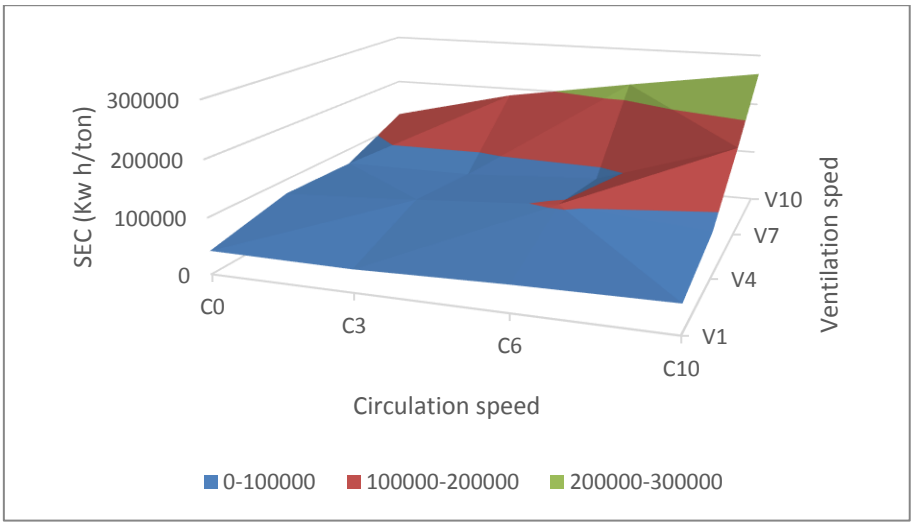


**Figure 3.13: Surface chart of SEC vs the fan speeds for selected data from water tests**

In summary, it was observed lower fan speed not only elevated temperatures and lowered humidity but also consumed less power and promoted more mass of water being evaporated. Temperatures above 30°C were achieved in the dryer as compared to ambient temperatures outside the dryer during water tests. Lower fan speeds resulted in lower SEC values due to less energy being consumed and higher drying rates being achieved. C3 yielded an SEC of 167 kWh/ton as compared to a SEC of 492 kWr/ton achieved at ventilation speed 10.

Nonetheless, circulation fans are necessary as lower performance (lower temperature inside the greenhouse, lower drying rate, lower efficiency, higher SEC) was observed when the circulations fans were not operating, but their rate should be kept low. Ventilation is also necessary to evacuate the evaporated moisture and avoid its accumulation, but it also needs to be kept at a low intensity.

### 3.4.3 Wet soil tests

Soil tests were conducted with 1.4 and 15 kg wet soil with and without the rake system.

#### 3.4.3.1 *1.4 kg wet soil drying test*

A sample of 1.4 kg of wet soil with around 60% moisture content was first dried without the use of the rake system. The drier handled 60% wet soil well without a large amount of water filtering through the drying tray into the drainage tray. Thereafter a higher moisture content sample of wet soil of around 65% was dried in the greenhouse dryer with the rake system in constant operation. The drying curve for both these tests is shown in Figure 3.14.

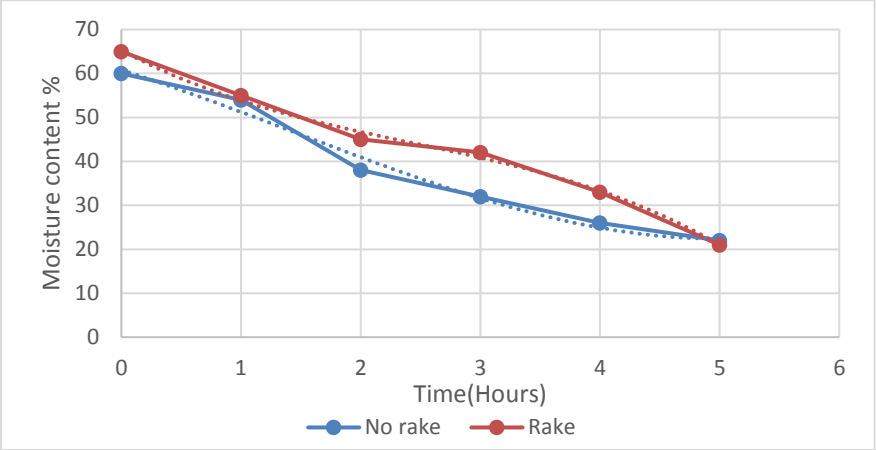


**Figure 3.14. Drying curve for 1.4 kg soil tests with and without the rake system**

The performance calculations determined for the two 1.4 kg soil tests are shown in Table 3.9.

**Table 3.9. Performance parameters for 1.4 kg soil tests**

| Quantity | No rake | Rake |
|---|---|---|
| **Drying time (h)** | 5 | 5 |
| **Average irradiance (W/m$^2$)** | 648 | 584 |
| **Average dryer temperature (°C)** | 40.6 | 38.1 |
| **Average dryer humidity (%)** | 32.9 | 39.0 |
| **Drying Rate (kg/h/m$^2$)** | 1.07 | 1.30 |
| **SEC (kWh/ton)** | 609 | 925 |
| **Efficiency** | 4 | 6 |

The use of the rake system led to a higher SEC but without achieving a considerably higher efficiency and drying rate. The use of the rake system consumed more energy even though it is expected to ensure homogenous drying of the wet soil sample by mixing and a more consistent moisture content of the final dry product. Nevertheless, the assumed positive effect of the rake system on the drying process could not been observed in these tests.

The dryer handles wet soil of 65% very well and thus it was decided to use higher moisture content wet soil in the 15 kg soil test with and without the rake system in operation.

#### 3.4.3.2 *15 kg wet soil drying test*

Wet soil tests were conducted to determine the rake system performance. The rake system is analysed by recording moisture content at hourly intervals during tests to determine how much of the soil is dried. The drying curve for the soil tests with 15 kg of 70% moisture content wet soil with and without the rake system in operation is shown in the drying curve graph shown in Figure 3.15. Within the space of 5 hours, the dryer was able to reduce 70% moisture content soil to 18%. From the drying curves, we can see that drying with the rake system leads to a considerably faster drying than without the rake in the initial stage (first 2 hours). After 5 hours of the experiment, both cases yielded approximately the same final moisture content.

The performance parameters from these tests are displayed in Table 3.10.

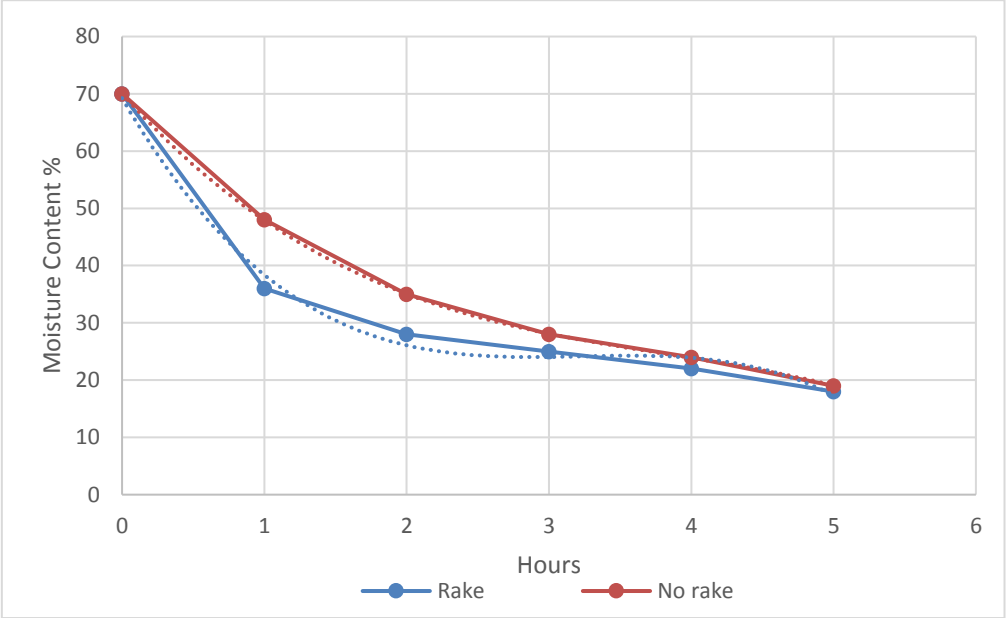


**Figure 3.15. Drying curve for 15 kg soil tests with and without rake system operating**

**Table 3.10. Performance data to dry wet soil with and without the use of the rake system**

| Quantity | No rake | Rake |
|---|---|---|
| **Drying time (h)** | 5 | 5 |
| **Average irradiance (W/m²)** | 619 | 582 |
| **Average dryer temperature (°C)** | 40 | 38 |
| **Average dryer humidity (%)** | 31 | 28 |
| **Drying Rate (kg/h/m²)** | 2.95 | 2.97 |
| **SEC (kWh/ton)** | 90 | 124 |
| **Efficiency (%)** | 51 | 73 |

Even though slightly better weather conditions were experienced with the test without the use of the rake system, better efficiency was achieved with the rake system in operation. Specific energy consumption with the rake system was slightly higher due to more power used. The specific energy consumption with the rake system operating was 124 kWh/ton whereas the SEC without the rake system was approximately 90 kWh/ton. Nonetheless, the rake system enabled the sludge to granulate more, and prevented a larger amount of sand from sticking to the bottom of the tray. Indeed, the rake system provided a better dispersed and granulated final product whereas without the rake system a large sample of soil remained on the bottom of the tray. In addition to these benefits, even though the rake system consumed more energy, a higher dryer efficiency was achieved, with higher drying rates during the first half of the process.

It can be then concluded that the rake system is a beneficial component for the prototype when enough quantities of material are placed on the tray, leading to the formation of a bed of a given thickness. Nonetheless, the use of the rake system is not optimal when a small amount of material is placed on the tray as a thin layer, or at the last stage of drying when the material has shrunk, and small quantity of material is remaining. In the later cases, the rake system will not improve drying, but it will increase the energy consumption of the prototype.

### 3.4.4 Synthetic sludge tests

Testing of synthetic sludge was conducted between the dates of 5-9f September 2022. A second test was done between the dates 14-15 September 2022. The initial moisture content of the synthetic sludge developed was 80% for both tests. The results and discussion for both tests are analysed individually.

#### 3.4.4.1 *Synthetic sludge Test 1*

Table 3.11 shows the evolution of synthetic sludge in the 4 days of testing. During the first day of tests, the greenhouse temperatures could not surpass 40°C but good amounts of sunshine were observed throughout the day. The synthetic sludge was dried until 70% moisture content despite experiencing frequent cloud cover and lots of wind throughout the day. Synthetic sludge was very sticky and thereby causing a lot of the sludge to stick on the blade of rake system. Testing for the first day of testing was stopped at 2 PM due to cloud cover and the roof becoming very windy.

The second day of testing was very cloudy and less windy than the first day. Clouds were present throughout the day with very little sunshine. A large reduction in mass was observed at the end of the second day of testing. Moisture content was reduced below 60% in the space of 5 hours. Testing was stopped at 2 PM due to high winds starting to pick up. The synthetic sludge being dried changed from a wet porridge texture to a silicon texture towards the end of the day. The rake system broke the synthetic sludge into smaller pieces and stuck less to the blade.

The third day of testing started very cloudy and less windy than the first two days. Clouds dispersed at around 10 AM. After this time, the skies became clear and important sunlight was observed. Temperatures of more than 40°C inside the greenhouse were observed at around noon. The synthetic sludge was reduced into smaller pebbles by the rake system during the day. The synthetic sludge texture became firmer and more compact as the day progressed. The sludge mass decreased throughout the day and synthetic sludge was reduced to 19% moisture content at the end of the day.

The fourth day of testing offered clear skies and good amounts of solar irradiation. Temperatures of more than 40°C inside the greenhouse were observed after 11 AM. The synthetic sludge texture became crispy and hard as the day progressed. The large wet porridge was reduced to tiny pebbles at the end of the day four of testing A reduction of moisture content from 18% to 6.5% moisture content was observed at the end of the day. The final sludge sample mass was drastically less at the end of testing.

On the 5$^{th}$ day, the dryer fans and temperature sensors were left to run but very little change in moisture content was observed.

The performance data for the four days of testing calculated from measured parameters are shown in Table 3.12. The drying curves for the 4 days of testing are shown in Figure 3.16.

**Table 3.11. Evolution of synthetic sludge during Test 1**

| Day 1 | Day 2 |
|---|---|
|  | 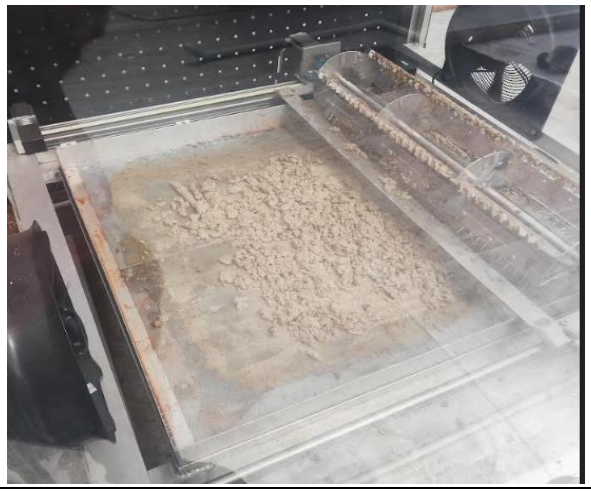 |
| **Day 3** | **Day 4** |
|  |  |

**Table 3.12. Performance data for synthetic sludge Test 1**

| | Day1 | Day2 | Day3 | Day4 |
|---|---|---|---|---|
| **Drying time (hour)** | 5 | 5 | 6 | 6 |
| **Average Solar irradiance (W/m$^2$)** | 663 | 365 | 704 | 798 |
| **Power (W)** | 238 | 238 | 238 | 238 |
| **Average dryer temperature (°C)** | 32.9 | 30.5 | 34.2 | 38 |
| **Average dryer humidity (%)** | 43 | 45 | 43 | 42 |
| **Drying Rate (kg/h/m$^2$)** | 1.12 | 0.55 | 0.51 | 0.10 |
| **SEC (kWh/ton)** | 328.15 | 668.27 | 723.19 | 3674.32 |
| **Efficiency (%)** | 20.45 | 18.28 | 9.65 | 1.64 |

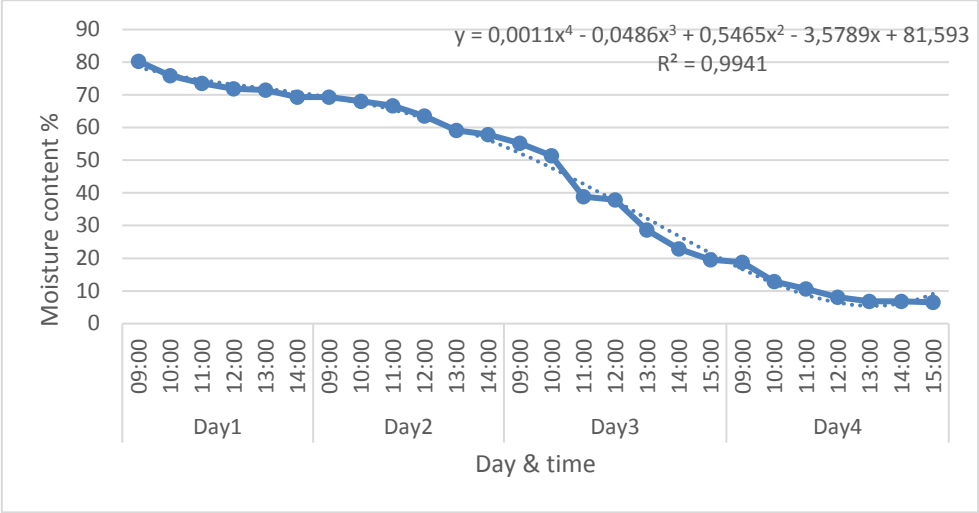


**Figure 3.16. Drying curve during Test 1**

As drying proceeded, the performance of the process decreased (lower drying rate and efficiency, higher SEC). After day 3, a drastic increase in SEC was observed due to a lower quantity of moisture in the sludge (less than 20% moisture content), making it more difficult to dry. This may be due to water becoming very bound to the sludge solid matrix at this level of moisture content.

#### 3.4.4.2 *Synthetic sludge test 2*

A second test was conducted the following week between the days 14/09/2022-15/09/2022. These two days offered clear skies and warm conditions throughout the day. Synthetic sludge of 80% moisture content was reduced to 12% moisture content in the space of 12 hours of testing (2 days). The performance data for the first day and second days of synthetic sludge duplicate tests are shown in Table 3.13. The drying curve of the test is depicted in Figure 3.17.

The solar irradiance was significantly higher during the first day of testing compared to all the other testing days. The dryer performed better due to very little cloud cover and winds. The dryer achieved more than 30% dryer efficiency during the first day with a large reduction in moisture content below 50%. The SEC was much lower, as well as the drying rate and efficiency were higher, than the previous tests due to more favorable weather conditions.

The second day of testing was very successful with a reduction of the moisture content from 50% to around 12%. It was also one of the hottest days of testing, with the dryer reaching temperatures up to 50°C. The great increase in temperature was due to load shedding between 12-2 PM, leading to the stop of the operation of the fans and a subsequent accumulation of the solar thermal energy collected by the dryer. The second day achieved an efficiency of 8.3% and SEC of around 922 kWh/ton.

**Table 3.13. Performance data for synthetic sludge Test 2**

| | Day 1 | Day 2 |
|---|---|---|
| **Drying time (h)** | 6 | 6 |
| **Average Solar irradiance (W/m$^2$)** | 660 | 693 |
| **Power (W)** | 238 | 238 |
| **Average dryer temperature (°C)** | 36.7 | 42.2 |
| **Average dryer humidity (%)** | 45.8 | 37.9 |
| **Drying Rate (Kg/hour m$^2$)** | 1.59 | 0.40 |
| **SEC (kWh/ton)** | 231.57 | 922.73 |
| **Efficiency (%)** | 34.14 | 8.36 |

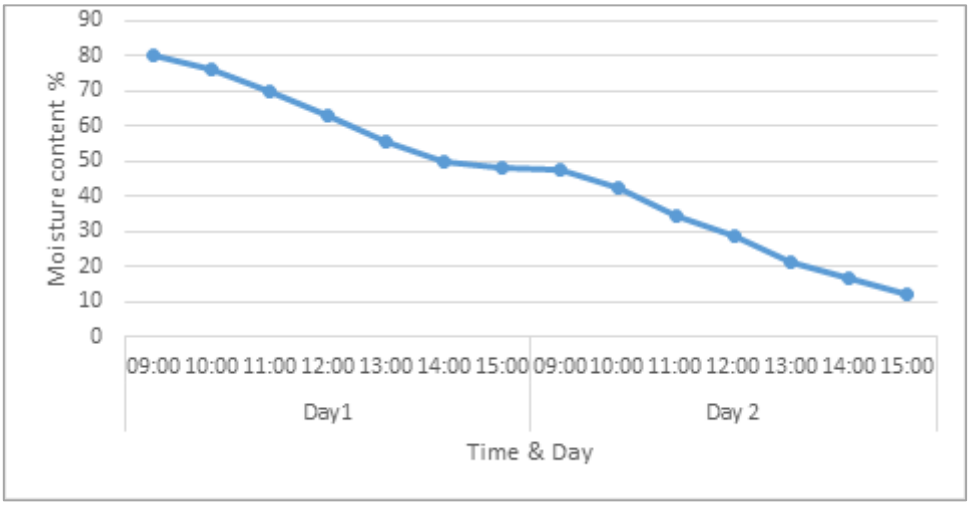


**Figure 3.17. Drying curve during Test 2**

#### 3.4.4.3 *Summary*

The overall performance parameters calculated for the dryer for the first and second test are presented in Table 3.14.

**Table 3.14. Overall testing results calculated after testing**

| | Test 1 | Test 2 |
|---|---|---|
| **Drying time (h)** | 22 | 12 |
| **Drying Rate (kg/h/m$^2$)** | 0.56 | 1.01 |
| **SEC (kWh/ton)** | 655.87 | 363.67 |
| **Efficiency (%)** | 9.6 | 18.08 |

During the first test, synthetic sludge moisture content was reduced from 80% to 6.5% in the space of 4 days with drying times from 5 to 6 hours per day. The first two days did not offer the best weather conditions but managed to achieve an efficiency of almost 20%. Efficiency drastically decreased the next days due to the drying rate lowering as the remaining moisture was more bounded to the solid matrix. The specific energy consumption drastically increased on day 4 due to more power needed to reduce lower moisture content. The more the sludge moisture content is reduced the more difficult it becomes to dry. The overall SEC achieved in the 4 days of test 1 was approximately 655 KW h/ton and overall dryer efficiency of 9.6%. After more than 3 days of testing, specific energy consumption became significantly higher and therefore it must be evaluated the optimal period of drying minimizing energy consumption.

During the second test, synthetic sludge was dried for two days, and sludge was reduced from 80% moisture content to approximately 12% in the space of 12 hours. The dryer achieved 24% efficiency on the first day with a SEC of 231 KW h/ton. This was the lowest SEC achieved in the two sludge tests conducted. After one day of testing, SEC began to rise, and dryer efficiency began to drop drastically. This can be related to a lower mass of moisture in the sludge.

Weather conditions were much better for the second round of tests, causing that the dryer performed significantly better and was able to dry sludge in a much shorter drying time. Weather conditions are then directly proportional to the dryer's performance. Clear skies and high temperatures will promote higher efficiencies and lower SEC.
Three days of testing with good weather is estimated to be enough to dry synthetic sludge of 80% moisture content to very low moisture content. An interesting observation is the high temperatures obtained when the

ventilation system stopped to operate during the load shedding (up to 50°C), during the second day of Test 2. Hence, it could be interesting to explore the use of intermittent ventilation system, alternating periods of operation and pause. During the periods of pause, the heat from the solar thermal energy collection will accumulate within the drier, rising the temperatures and potentially leading to higher drying rates. Before the greenhouse humidity will become too high, the fans will resume their operation to evacuate the evaporated moisture and maintain low levels of relative humidity in the greenhouse.

Note that the wet soil was much easier to handle and dry as compared to faecal sludge. Soil did not stick and clogged the dryer as much as synthetic sludge.

## 3.5 CONCLUSION

The enclosure was completed, and the various subsystems were developed. The linear actuator, guide rails, motors and fans were all procured, installed and tested. Temperature tests in the enclosure were compared to outside temperatures. The greenhouse dryer reached temperatures of 10°C more than that of the outside temperature. Temperatures of 45°C were measured inside the dryer at outside temperatures of less than 30°C. The ventilation fans lower temperatures slightly but allowed removal of moist air and vapour.

Water tests concluded that lower ventilation and circulation rates contribute to higher temperatures, lower humidity, higher water evaporation and lower SEC. Nonetheless, the ventilation and circulation fans are necessary for the good operation, but their intensity must be maintained low. Without ventilation rate, the humidity can build up in the dryer, decreasing the driving force for drying. Without circulation rate, the performance of the greenhouse was considerably lower.

The rake system allowed resulted in less feedstock settling and sticking on the bottom of the drying tray during the tests with wet soil. The rake system allowed a faster drying during the first half and higher efficiency, particularly during the first half of the process. Even though a higher SEC, the use of the rake system will be suitable thanks to its gain of efficiency and improvement of the drying process However, the rake system losses its effectiveness for thin layers of material in the tray.

During the tests with synthetic sludge, the moisture was reduced to less than 15% in less than a week with an efficiency of between 1-30% and overall SEC of between 365-3500 kWh/ton. The high SEC and low efficiency values were calculated when the moisture content was below 20%, reflecting a strong moisture boundness to the solid matrix. Therefore, drying could be stopped before arriving to this level of moisture content, in order to minimise the energy consumption.

The test undertaken during better weather conditions provided much better results (higher drying performance, lower drying time, lower energy consumption). The dryer performance is weather-dependent, wind and clouds negatively affecting the process. The tests have been conducted over the winter period and the dryer was still able to perform efficiently. It could be expected that the results of the dryer will be better during summer.

## 3.6 RECOMMENDATIONS

- A few challenges were encountered when developing the greenhouse dryer prototype. One of the major challenges was installing the PMMA acrylic sheet onto the aluminium frame of the dryer. 3 mm acrylic sheets are very flexible and brittle. The PMMA obtained many cracks and scratches during installation. The recommendations include using thicker acrylic sheets as 3 mm is too brittle and flimsy. Sheets of around 6 mm thickness would be ideal.
- The rake system should also be operated in shorter cycles to reduce power consumption.
- From water testing, it was found that lower fan speeds result in higher temperatures and lower humidity. Therefore, smaller dc fans can be installed instead of ac axial fans. The implementation of dc fans will

make it easier to implement solar photovoltaic energy into the system by installing solar panels and deep-cycle batteries. All the electronic components are capable of operating with a dc configuration except the potentiometer switches. The installation of a solar PV system will ensure less power usage from the grid and power the system during load shedding.

- Temperature sensors experiences interference when the rake system was powered. The motor drivers caused interference as it pulsed power to the stepper motor. Therefore, the electronics from the temperature sensors and rake system drivers should be placed in different boxes.
- Components in the dryer should be painted or sprayed black to achieve higher temperatures reached inside the dryer. Electrical components should be shiny to prevent overheating and seizing of electronics.
- The odour was smelt at the outlet of the dryer during synthetic sludge testing. It would be safer to install filters at the exit when using faecal sludge to ensure no harmful chemicals are released to the outside environment and minimize bad odour around the dryer.

# 4 SCREW CONVEYOR SOLAR DRIER PROTOTYPE

This section is about the presentation of the greenhouse solar drier prototype, including testing plan, the discussion of the obtained results and the main outcomes from the tests. The information from this section was originated from the MSc of Akhil Ramlucken. More details of the results from this Chapter and a deeper level of analysis of the data can be found in the MSc dissertation from Akhil Ramlucken (available from mid-2023 in the Supporting Documents D).

## 4.1 MATERIAL AND METHODS

This Section of the report details the physical device design, and what makes each component unique. Additionally, this section also details the testing methodology and data treatment which was undertaken during the testing of the device.

### 4.1.1 Concept of the technology

In the screw conveyor solar drier prototype, the sludge is dried during its convey through a transparent tube exposed to solar radiation. During this process, the sludge absorbs the solar thermal energy that provides the latent heat for moisture evaporation. An air stream flows inside the transparent tube to enhance the drying process. The air stream can be previously dehumidified and heated before introduction in the drier. Reflectors can be placed next to the transparent tube in order to increase the amount of solar radiation received by the sludge.

The prototype is composed from the following components:

- Drying chamber (DC) composed of an auger inside a transparent tube in acrylic where the faecal sludge is dried.
- A ventilation system (driven by ventilation fans) allowing the circulation of air inside the DC (DC). The air stream is introduced in counter-current with respect to the direction of the sludge flow in order to maximize the heat and mass transfer and enhance the drying process.
- A solar air heater (SAH) to heat the air stream to introduce in the DC (built in-house). The heated air allows to provide additional heat for moisture evaporation and potentially leads to increased drying rates. The relative humidity in the heated air is subsequently lowered, enabling to reach a sludge lower moisture content at the thermodynamic equilibrium and reduce the mass transfer resistance for moisture migration from the sludge to the air, increasing the drying rate.
- An air dehumidifier to lower the relative humidity of the air stream, which is beneficial for the drying process as described above.
- Reflectors to increase the incidence of solar radiation in the sludge, which allows to bring additional solar thermal energy for moisture evaporation.
- Instrumentation to measure the temperature and relative humidity at different locations of the prototype, and the irradiance in the experimentation site.
- An interface system to log the data measurements (temperature and relative humidity) and control the ventilation flowrate.
- An electronic system to log the data from the sensors and to control the ventilation system, and a controller for the auger motor.

The screw conveyor solar sludge drying system is made up of multiple subsystems which function both independently and together. The device may be classified as a hybrid solar thermal device, as it incorporates both direct solar thermal components in the form of the transparent DC, and indirect elements through the SAH system. This may allow for higher performance levels than a solely indirect solar thermal system. Figure

4.1 shows the various subsystems which make up the device, as well as a brief explanation on the function of each component.

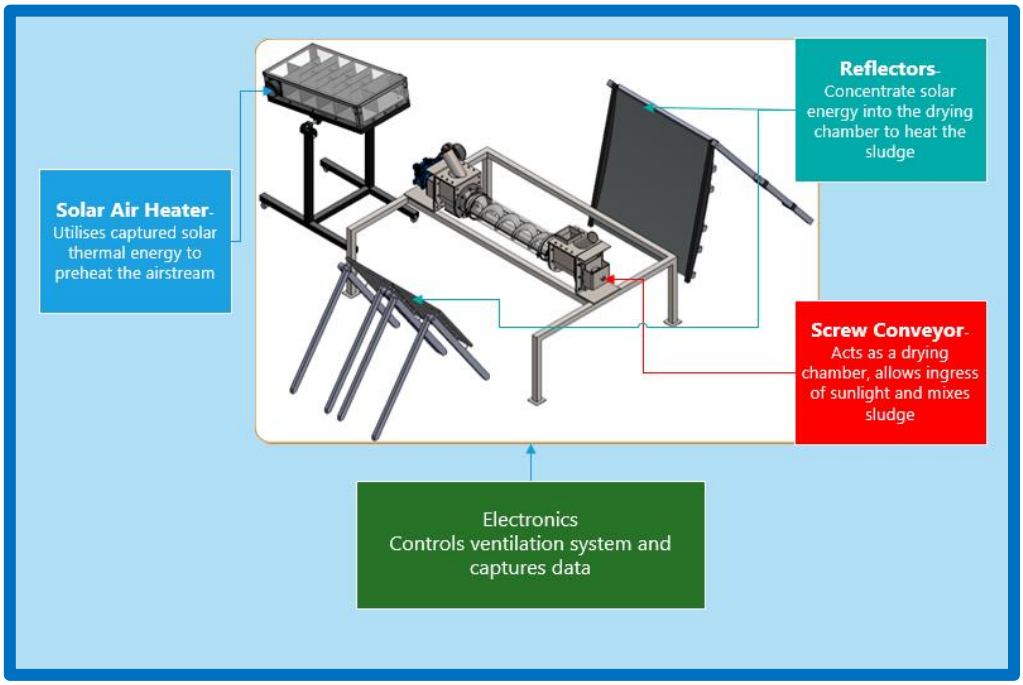


**Figure 4.1. Scheme of the System**

### 4.1.2 Components of the prototype

The sections below explain in greater detail the design characteristics and function of the various subsystems.

#### 4.1.2.1 *Screw Conveyor*

The screw conveyor subsystem was built by a company in Pretoria called *Techflite* according to the specifications required for the device. It is designed with a shaftless auger to limit the amount of sludge getting stuck to the blades. The blades have an outside diameter of 177 mm, an inner diameter of 60 mm, and an overall length of 1,5 m. The motor drive system utilises a 0.37 kW motor from *Motovario*, which drives the screw conveyor through a worm gear reduction drive in order to increase torque significantly. The device was also built with a transparent tube instead of the normal trough, thereby allowing ingress of sunlight directly onto the feedstock being dried within the system. The tube in the prototype consists in a UV resistant acrylic of 1000 mm length and 200 mm diameter. Figure 4.2 shows the screw conveyor set up during an early device test.

**Figure 4.2. Screw Conveyor Subsystem**

The DC utilises a cross flow configuration where the air stream moves in counter-flow with respect to the feedstock convey direction in order to increase the heat and mass transfer as much as possible. Figure 4.3 depicts the representation of the DC during the computation fluid dynamics (CFD) simulation to study the flow within the device.

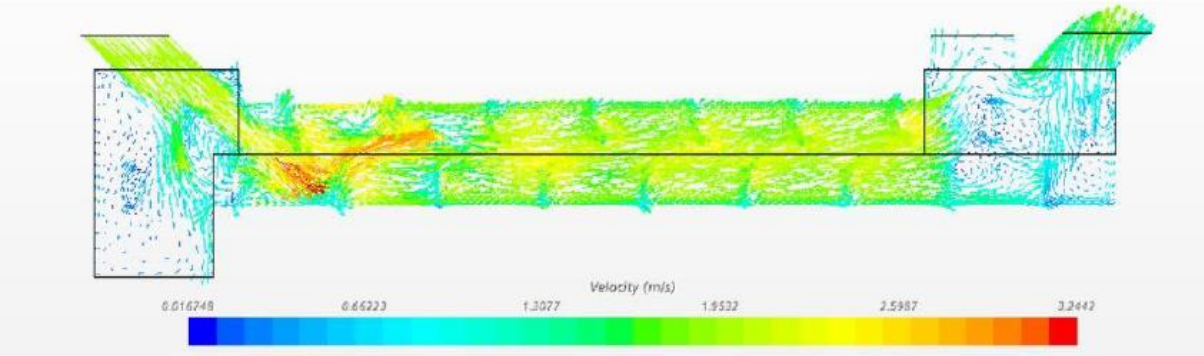


**Figure 4.3. CFD Velocity Plot of Screw Conveyor DC**

#### 4.1.2.2 *Solar Air Heater*

The solar air heater (SAH) was designed in order to preheat the airstream within the dryer, which is expected to result in higher drying rates due to higher thermal energy input for drying. The device includes baffles, as well as flow constrictors in order to both increase the residence time and the turbulence within the flow of the air. Higher turbulences are expected to increase the heat transfer coefficient, thereby enhancing the air stream heating. The effect of the baffles in the flow pattern in the SAH can be observed through CFD simulations in Figure 4.4.

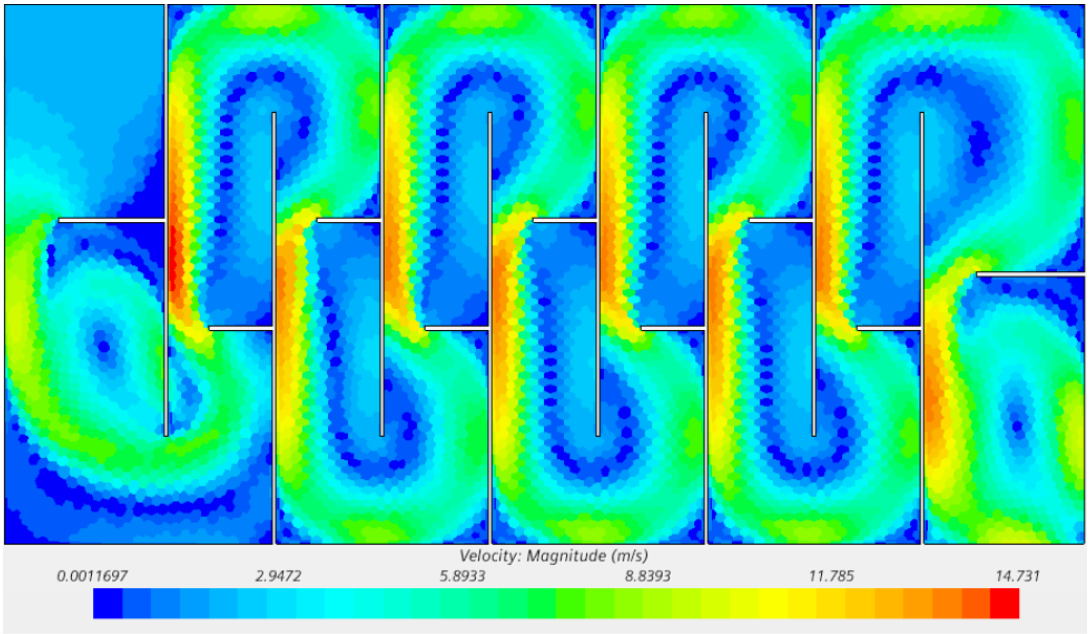


**Figure 4.4. CFD Velocity Plot of SAH Baffle Design**

The absorber plate of the collector is made of 6 mm thick copper plate, which have the mild steel baffles welded to it. The plate dimensions are 1 m by 0.5 m. The absorber plate and baffles were painted in matte black in order to maximise the amount of energy which can be absorbed by the system. The absorber plate utilises a layer of insulation below the plate, in order to reduce losses into the ambient air.

The top and side walls of the device are transparent, constructed from 5 mm acrylic sheets. This was done in order to ensure that as much solar thermal energy as possible was able to enter the system. Figure 4.5 displays a side view of the device, showing the transparent side walls.

**Figure 4.5. Side View of SAH Subsystem**

As can be seen from Figure 4.5, the device sits on a stand which allows for easy angle adjustment of the system throughout the year in order to maximise the amount of energy received by the collector.

The SAH can be coupled to an air dehumidifier, which can be observed in Figure 4.5 (white box). The dehumidifier is an appliance from *Meaco*, consisting in a compressor type dehumidifier which is common. It is rated to remove 10 L of moisture from the air over the course of a day under optimal operating conditions at roughly 80% ambient humidity.

#### 4.1.2.3 *Reflectors*

The reflector subsystem of the device consists of 3 separate reflectors, which work together in order to add additional thermal energy into the system. The reflector subsystem consists of a single large parabolic reflector and two small flat plate collectors. The reflectors are capable of reflecting the solar energy along the length of the DC to add extra heat to the system for drying.

Finding the ideal reflector configuration was done via trial and error. The reflectors were put into various configurations until they were all able to effectively reflect most of their energy onto the DC. The reflectors final configuration cam be seen in Figure 4.6. In this configuration, the shiny parts of the reflectors must be oriented facing North in order to maximise the reflected solar radiation the DC.

**Figure 4.6. Reflector subsystem**

All reflectors utilise a raw aluminium sheet as the reflective surface, with a plastic backing to ensure no damage occurs due to overheating of the reflective surface. The reflectors also utilise a wooden frame, with manually adjustable angles. In general, this subsystem requires the user to set up the reflectors and focus the solar energy upon the DC multiple times a day, as the angle incident of the sun is always changing throughout the day.

#### 4.1.2.4 *Instrumentation, data logging and control system*

The main electronics subsystem serves a dual purpose, in that it allows for the logging of the data from the sensors within the device, as well as individual control of the ventilation fans. The custom solution utilised is largely due to the large cost associated with dedicated data acquisition systems. The electronics system is based upon an Arduino system, and the single microcontroller controls the data logging and fan control at the same time.  Figure 4.7 displays the view of the controller mainboard, as well as the soldering which was done to ensure the correct connections were in place.

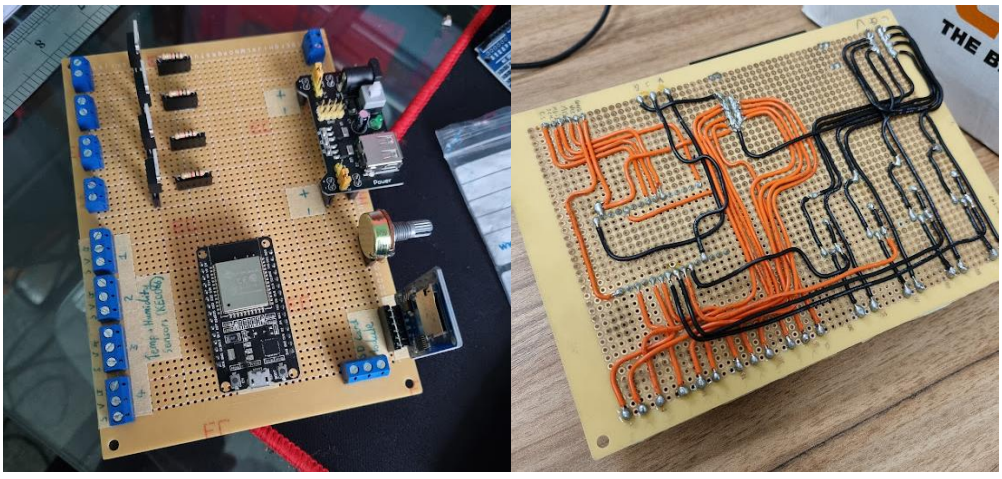

**Figure 4.7. Electronics Mainboard (top view at the left and back view at the right)**

Originally the device would connect to the internet and check the exact date and time from the NTP server, however this was deemed unreliable due to the connection not being reliable, and the device requiring a network connection to function. For this reason, a real time clock module was added to the device, which was powered by a lithium ion button cell, allowing the time data to be kept for a long period of time. The final code flow diagram can be seen in Figure 4.8.

As can be seen in Figure 4.7, there are 2 sets of interface connectors on the board, one with 3 wires, and the other with 2. The 3 wire screw terminals are utilised to connect the temperature and humidity sensors to the device. The sensors utilised are the *DHT22 sensors*, which can determine both temperature and humidity upon a single sensor package. The sensors are capable of accurate temperature readings between -40°C and 80°C, with accurate humidity readings between 0% and 100%. These sensors are also desirable due to the integration with Arduino, which allows for the temperature and humidity data to be accessed with a simple command, instead of sampling the output voltages and mapping to a range of values. Figure 4.9 provides an image of a *DHT22* sensor.

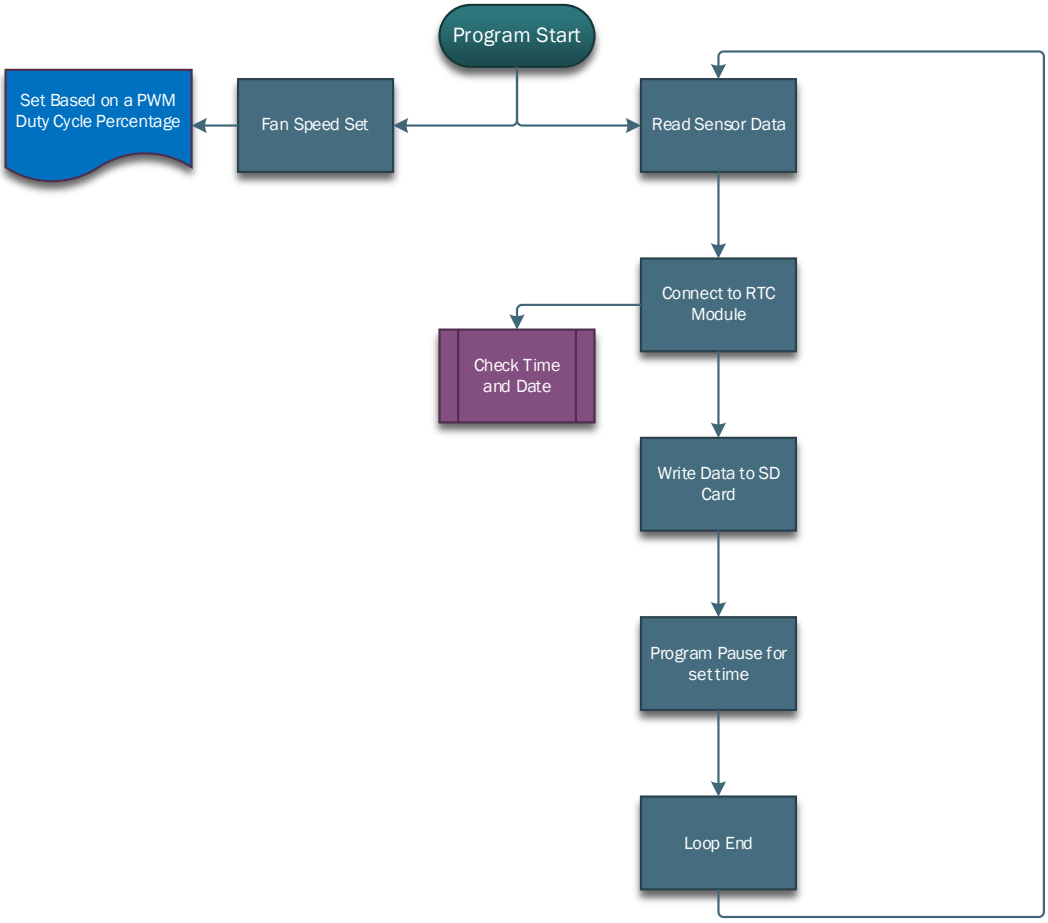


**Figure 4.8. Coding Flow Diagram**

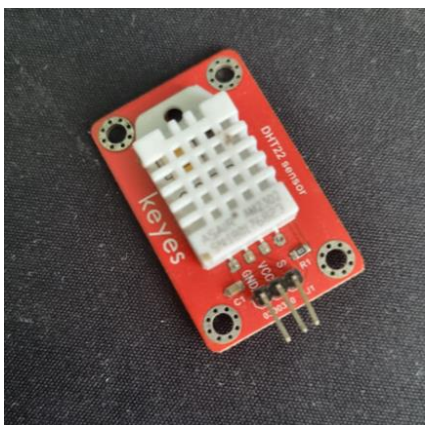


**Figure 4.9. DHT 22 Sensor**

The 2 wire screw terminals are utilised for the airflow inducing fans. The fans utilised are 120 mm, 24v *Sunon* fans. The fans draw at maximum 9.2 W and are capable of a maximum air flowrate of 75 CFM, i.e. 127.4 $m^3$/hour. The calibration data from the fans may be seen in **Error! Reference source not found.**. The placement of both the sensors and fans within the system can be observed in the decomposition diagram in Figure 4.10.

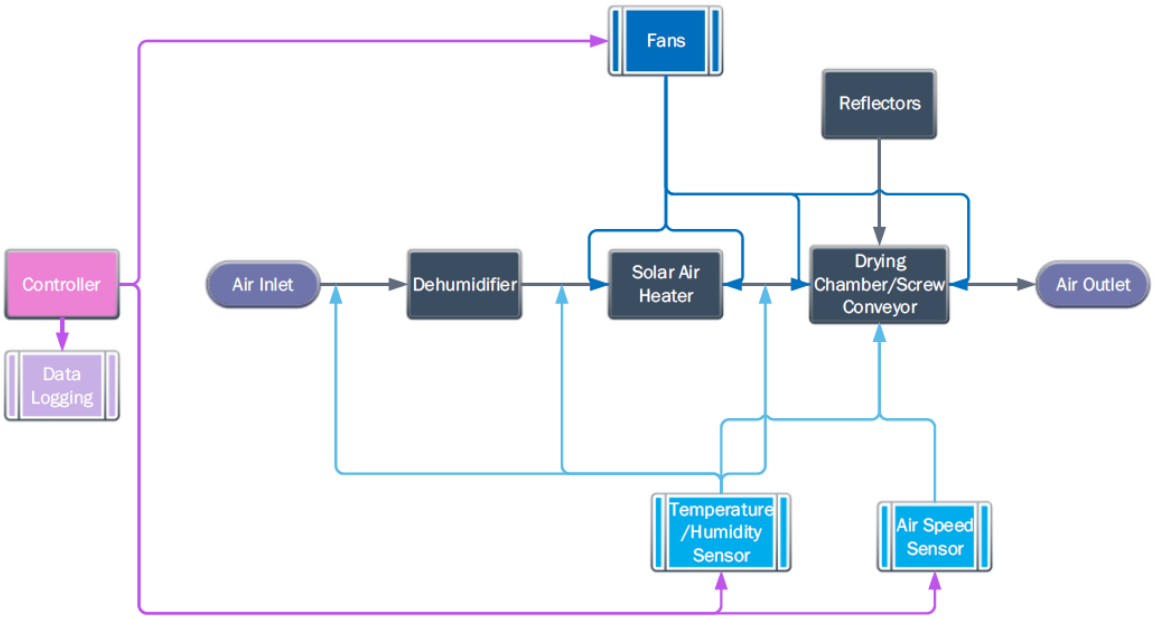


**Figure 4.10. Sensor and fan placement diagram**

The board functions effectively by sampling the data from the sensors every 10 seconds, and then writing the data to a micro-SD card. The data is formatted in a manner where it may easily be read by Microsoft Excel, or Power BI for the generation of graphs and other infographics. Additionally, the device can be connected to a computer in order to monitor the live data from the device, which can be useful to ensure that all the sensors are connected correctly, and to view the exact duty cycle of the fans.

#### 4.1.2.5 *Additional accessories*

In conjunction with the main electronics and data logging system in the system, the following devices were utilised in order to capture additional data which was not integrated into the main board of the device.

- Wattmeter

A *Kill A Watt* online digital wattmeter was utilised in order to determine the power consumption of the device over the course of a testing run. The device can be seen in Figure 4.11.


**Figure 4.11. Digital Wattmeter**

This device functions by being connected in series before the main system load. The wattmeter recorded the amount of power utilised in kWh over the period of operation and displays the current power draw on its main display, accurate to 0.1 W. Additionally, the device measured both the minimum and maximum values of power draw during the recorded testing time.

- Pyranometer

The system utilised a silicon based pyranometer *CMP3* from *Kipp & Zonen* in order to measure the irradiance received by the device during the testing runs. The device was connected to its own data logging system, utilising an Arduino as the microcontroller. The system stored the irradiance data to a Micro SD card, at the same rate as the main system data logger, which allowed for the data to be captured and spliced into the temperature/humidity data easily. The pyranometer device can be seen in Figure 4.12.

**Figure 4.12. Pyranometer**

### 4.1.3 Testing of the prototype

In this section the experiments undertaken, as well as the procedure and parameters measured are detailed. In general, the device testing began with functionality testing of the different components of the prototype and the integrated system. Next, the next round of testing focused on understanding basic drying performance of the device, while also optimising the device configuration using wet soil as feedstock. Lastly the final testing phase aimed to determine the device performance at the optimum operating conditions using synthetic faecal sludge as feedstock, as well as testing the use of additives within the feedstock. The testing of the device was

done on the roof of the Chemical Engineering building at the University of KwaZulu Natal, Howard College campus (Durban, South Africa). Figure 4.13 provides a photograph of the device setup.

The position of the Chemical Engineering building in Durban is indicated in the map below in Figure 4.14. The GPS coordinates of the building are -29.867637552711926, 30.979488232904888. The tests took place in the winter months of 2022, starting on the 12th of July and culminating on the 9th of September. The ambient humidity was generally in the range of 50-60%, however there were days, specifically around rainy days, with values closer to 80%. The ambient temperature was on average around 25°C. The solar irradiance encountered during the tests tended to peak at roughly 750 W/m$^2$, value which started to increase at the end of testing, as the warmer months approached. The SAH tilt was between 25˚ and 30˚ during the testing period, as this angle provided the optimum angle for solar collection during the months of winter. In order to minimise the effect of weather conditions in the variance of the results, the experiments were conducted at sunny conditions low or without cloud coverage.

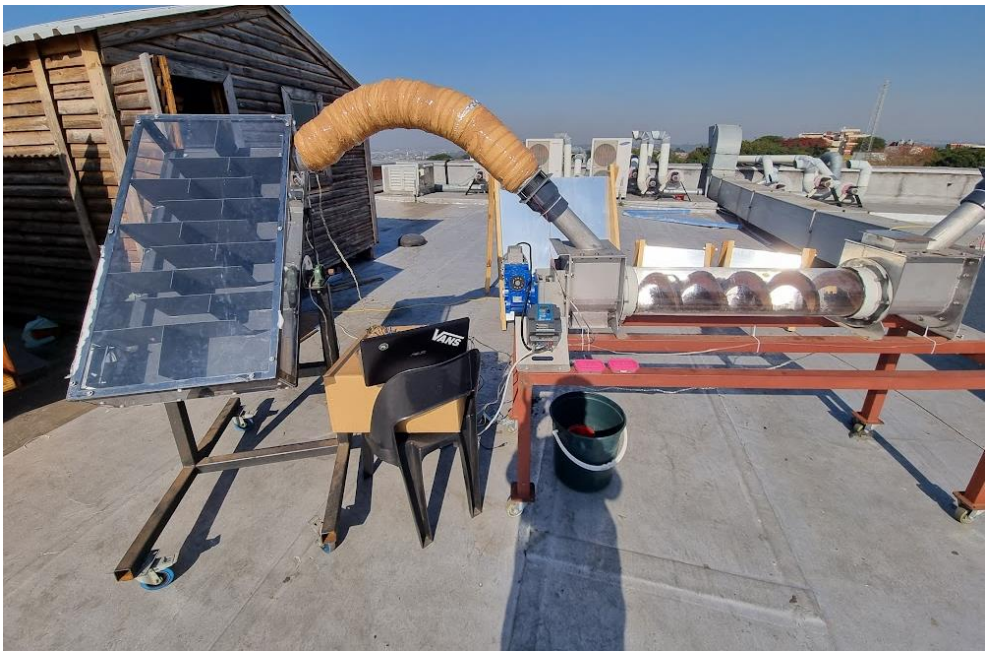

**Figure 4.13. Setup of the screw conveyor solar drier**

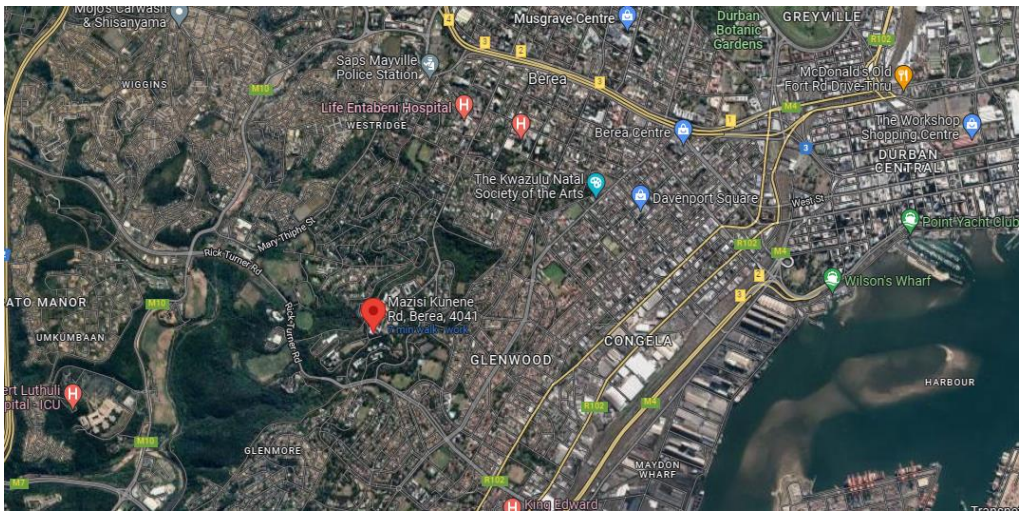


**Figure 4.14. Location of the Chemical Engineering building in Durban**

#### 4.1.3.1 *Compatibility/Functionality Testing*

These tests were undertaken at the beginning of the project. These tests focused to understand how the individual systems functioned by themselves, and when connected. The testing entailed monitoring how the subsystems worked and noting any idiosyncrasies in the way that the individual systems worked that may hinder the functionality of the fully integrated device. Indeed, these tests were undertaken essentially by running a single subsystem for an amount of time and gathering the data from the device's sensors. This allows for the performance of the individual parts of the system to be determined.

Once the sub-systems were confirmed to work, the device subsystems were them connected in various configurations in order to understand how the devices worked together after understanding how they worked alone. The device was tested in its entirety over a range of conditions to monitor the attained temperature and humidity within the system. These tests were undertaken with an empty DC (without feedstock).

#### 4.1.3.2 *Wet soil tests*

A second testing phase was carried in order to determine the optimal device settings and configurations with feedstock, namely wet soil. All tests under this phase were undertaken with 1-hour long test times. The testing first began with individual subsystems being removed from the system, and drying performance assessed. The configurations tested were as follows: (i) tests with the full device; (ii) tests without SAH; (iii) tests without reflectors; (iv) tests without dehumidifier. This process of elimination allowed to identify the key and unnecessary subsystems. Once this set of tests was undertaken, the optimal ventilation settings were searched, by means of undertaking tests at varying ventilation settings (100%, 50%, 25%) and noting which resulted in the best process performance.

This round of testing was undertaken with 1 kg of wetted soil, as this allowed for shorter tests of 1 hour each and allowed for easy cleaning of the DC. The soil was always humidified prior to the testing, generally 400 g of water per kg of dry soil, resulting in a moisture content in the region of 65%. This is lower than the typical faecal sludge moisture content of around 70-80%. However, larger amounts of water in the soil tended to result in a slurry like mixture, which could not be effectively conveyed within the screw conveyor. The unbound moisture would simply flow out the other end of the dryer and bypass the drying entirely.

The device was operated in batch mode for the ease of testing. After placing the wet soil in the feedstock hopper, the auger was run until the material reached the outlet (taking a few minutes for this) and then it was stopped. Thereafter, the tests were undertaken by turning on and off the auger so as to take a sample from the DC every 6 minutes, which allowed for 10 samples per hour. The samples were analysed into a moisture analyser once they were taken, which was able to dry the sample fully, and compute the moisture content. Note that, in real world applications, the device is however expected to operate in continuous mode.

During these tests, the following parameters were measured: temperature, humidity, irradiance, power consumption and moisture content.

#### 4.1.3.3 *Tests with synthetic faecal sludge*

The final testing phase of the system was planned in order to allow for the dryer to be tested with synthetic faecal sludge, utilising the optimised settings found in the previous phase of testing. In the same manner to the wetted soil tests, these synthetic sludge tests will be undertaken in a batch mode, utilising 30 minutes intervals for sample analysis and an overall testing time of 4 hours. The recipe for this sludge may be seen in Appendix C. The recipe is relatively different to standard synthetic sludge recipes as it forgoes the bacterial

component, which generally comes from baking yeast. This would tend to cause issues as the yeast would release carbon dioxide during heating and increase the volume of the sludge to a level that may make difficult the feedstock convey in the screw conveyor DC. The synthetic sludge swelling would not accurately represent the real behaviour of faecal sludge, which will tend to shrink during a drying process. The baseline mixture has a moisture content of 80%.

This phase of testing utilised synthetic sludge at different initial moisture content and varying additives. The dryer was first tested using sludge with 80, 65 and 50% starting moisture content synthetic sludge to determine how well the device functions with each type of sludge. After this, different additives (namely sawdust, activated charcoal and slaked lime) were mixed to the sludge with the main objective of finding which additive can reduce stickiness and improve the drying performance. The additives were all sourced from either the university, or in the case of the slaked lime, the pharmacy. The additives were all added in the ratio of 100 g additive to 4 kg of synthetic sludge.

During these tests, the following parameters were measured: temperature, humidity, irradiance, power consumption and moisture content.

### 4.1.4 Data Treatment

#### 4.1.4.1 *Processing of the raw data*

The raw data captured from the device was in the form of text files, with commas utilised to separate each piece of data. In general, the data collected was treated utilising Python, which removed any null values from the data set and interpolates the data between measurement. Once the data was interpolated, it plotted it to allow for data analysis. The data may be exported from Python as either a CSV or Excel file type and plotted in either Microsoft Excel or Power BI. A more detailed explanation of the data treatment process may be seen in Appendix D. An example of captured is shown in Figure 4.15.

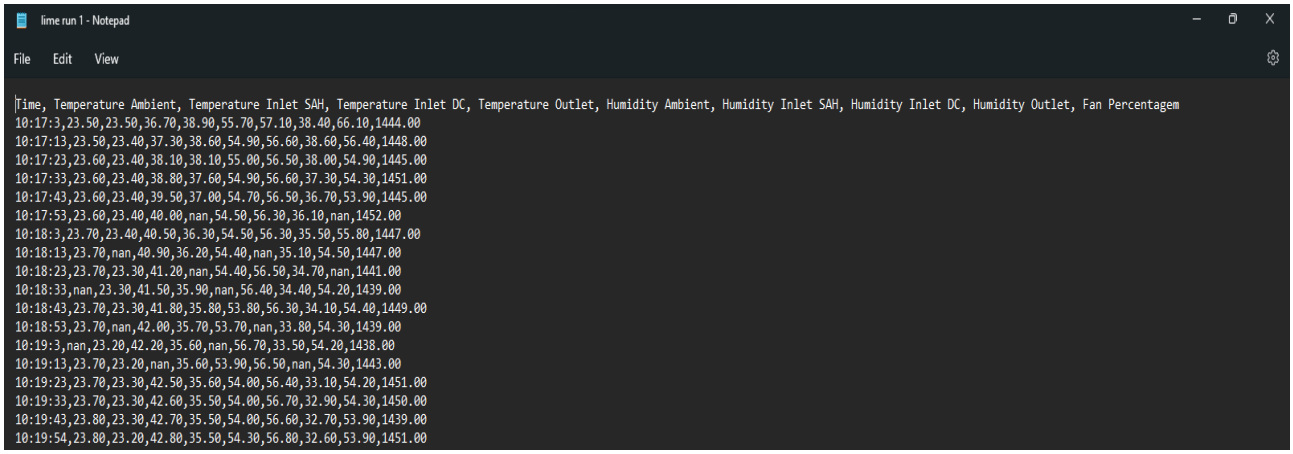


**Figure 4.15. Example of raw data**

#### 4.1.4.2 *Performance parameters calculations*

Once all the data was collected for each run, the information was utilised to calculate certain key performance metrics, which would allow for the tests to be compared to each other and to other drying systems available on literature. The performance parameters are as follows: drying rate, efficiency and specific energy consumption (SEC). The calculations were done using the formulas from the sections below in an excel spreadsheet, as displayed in the example in Figure 4.16.

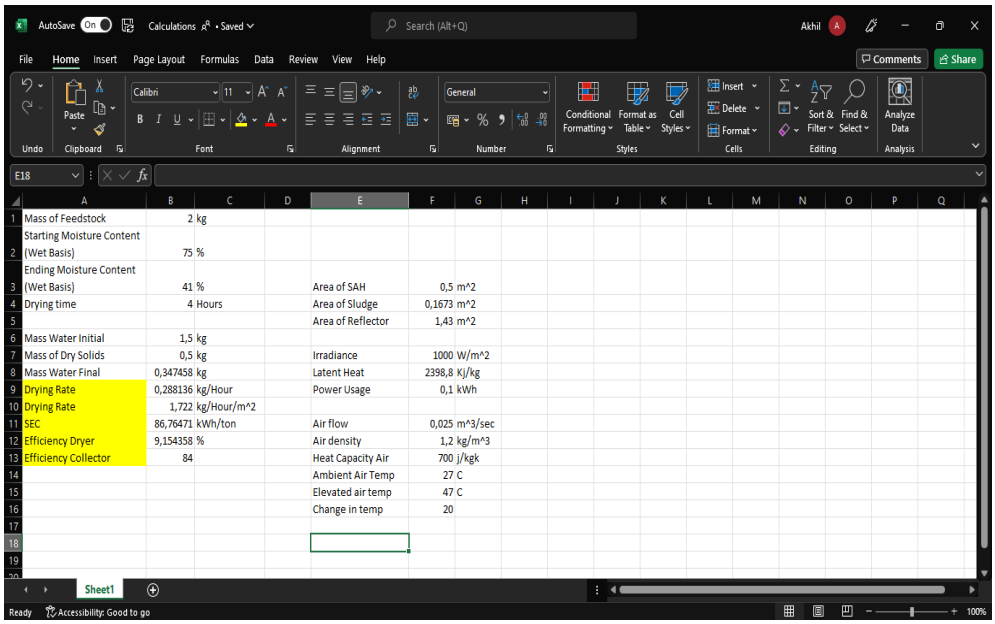


**Figure 4.16. Example of the calculation spreadsheet**

- Drying Rate:

The drying rate of the device results in the amount of moisture liberated from the synthetic sludge per time and unit area. The formula for the drying rate is shown in Equation 4.1.

$$\boldsymbol{DR} = \frac{\Delta \mathbf{m}}{\Delta \mathbf{t} \times \boldsymbol{A_{sludge}}} \qquad \textbf{Equation 4.1}$$

Where,
*DR*: Drying rate (kg/h/m$^2$)
*Δm*: Moisture removal (kg)
$A_{sludge}$: Sludge surface area exposed to solar radiation (m$^2$)

The sludge surface area approximated to the cross-sectional area of the bottom half of the screw conveyor DC. This value corresponds to 0.2 m$^2$. The moisture removal can be defined as displayed in Equation 4.2.

$$\Delta \boldsymbol{m} = (\boldsymbol{Mi} \times \boldsymbol{m}_{\boldsymbol{i}}) - (\boldsymbol{Mf} \times \boldsymbol{m_f}) \qquad \textbf{Equation 4.2}$$

Where,
$m_i$: Initial mass of sample (kg)
$m_f$: Final mass of sample (kg)
$M_i$: Initial moisture content (Wet basis)
$M_f$: Final moisture content (Wet basis)

The final moisture content can be calculated through Equation 4.3.

$$\boldsymbol{m_f} = \frac{\boldsymbol{m_i}(\mathbf{1}-\boldsymbol{M_i})}{\mathbf{1}-\boldsymbol{M_f}} \qquad \textbf{Equation 4.3}$$

- Efficiency:

The efficiency of the device refers to how well the device utilises the solar thermal energy that enters the device. This metric corresponds to the amount of useful output energy in divided by the input energy. There are two calculations undertaken for this project, firstly the one for the SAH efficiency, and second for the total device efficiency.

Equation 4.4 and 4.5 were used to calculate the efficiency of the SAH and full device, respectively.

$$\eta_{collector} = \frac{\dot{m_{air}} \times Cp \times \Delta T_{air}}{I \text{ x } A_{collector}} \quad \textbf{Equation 4.4}$$

$$\eta_{dryer} = \frac{\Delta m_{sludge} \times \Delta H_{drying} \times 3600}{\text{I} \times (A_{sludge} + A_{collector})} \quad \textbf{Equation 4.5}$$

Where,

$\eta_{collector}$: SAH efficiency (-)

$\eta_{dryer}$: Efficiency of the fully integrated solar drying system (-)

$\dot{m_{air}}$: air stream mass flowrate through the system (kg/s)

*Cp*: the constant pressure heat capacity of the air (≈ 1 kJ/kg/°K)

$\Delta T_{air}$: the change in temperature of the air stream between the inlet and outlet of the SAH (˚C).

*I*: average irradiance received by the collector (W/m$^2$)

$\Delta H_{drying}$: heat of drying (≈ 2,260 kJ/kg)

$A_{collector}$: surface area of the SAH exposed to solar radiation (m$^2$)

$A_{reflector}$: surface area of the reflectors (m$^2$)

The irradiance values used for the efficiency calculations corresponded to the global horizontal irradiance values measured by the pyranometer. Note that the pyranometer was not used for the measurement of the tilted irradiance following the SAH inclination. Hence, the SAH efficiency may not be accurate, but rather a rough indication of performance.

The latent heat of pure water vaporization (≈2,260 kJ/kg) was used as an approximation for the heat of drying of faecal sludge. The real value of heat required for faecal sludge drying should be higher than the value of pure water vaporization. However, the calculated efficiency values would allow for comparisons to be drawn between the undertaken tests.

Because of the inaccurate values of the solar irradiance received by the SAH and heat of drying (as explained above), the efficiencies would be likely underestimated and might have to be used with precaution for the comparison of performance with other solar driers.

- Specific Energy Consumption:

The SEC is a metric that describes the performance of the device in comparison to the energy consumed. A lower SEC value is better as it implies that the process is undertaken with lower energy usage and would result in lower operating costs. The formula for the SEC can be seen Equation 4.6.

$$SEC = \frac{E \, x \, 1000}{\Delta m} \quad \textbf{Equation 4.6}$$

Where,

E: electrical energy used by the device during the drying time [kWh]

#### 4.1.4.3 *Statistical analysis*

Two runs at identical operating conditions were done for each experiment in order to ensure that the data collected was reproductible. A statistical analysis was done for the treatment of the data from the duplicates. For this, the average and standard deviation was computed from the data of the duplicate tests for each experimental point. Each graph was then plotted with error bars in order to visually understand the variance in the data. The value utilised for the error bars was the standard deviation of each data point. It has to be noted the dryer functions based upon radiant solar energy, which changes at a day to day based upon factors such as cloud cover, etc. For this reason, even though the duplicate runs were undertaken under at the same operating conditions, there was always a level of unavoidable uncertainty due to the weather conditions that were never identical between two runs (even though the conditions were close most of the time as the tests were performed under sunny conditions).

## 4.2 RESULTS AND DISCUSSION

This section includes some of the data collected during the various testing phases of the device. The entire data may be seen in Appendix E.

### 4.2.1 Compatibility/Functionality Testing

The functionality testing of the device was undertaken in order to determine baseline performance and compatibility between subsystems. These tests were conducted without feedstock.

#### 4.2.1.1 *Dehumidifier Only*

This test was undertaken to understand the manner in which the dehumidifier functions. The temperature and humidity results are displayed in Figure 4.17.

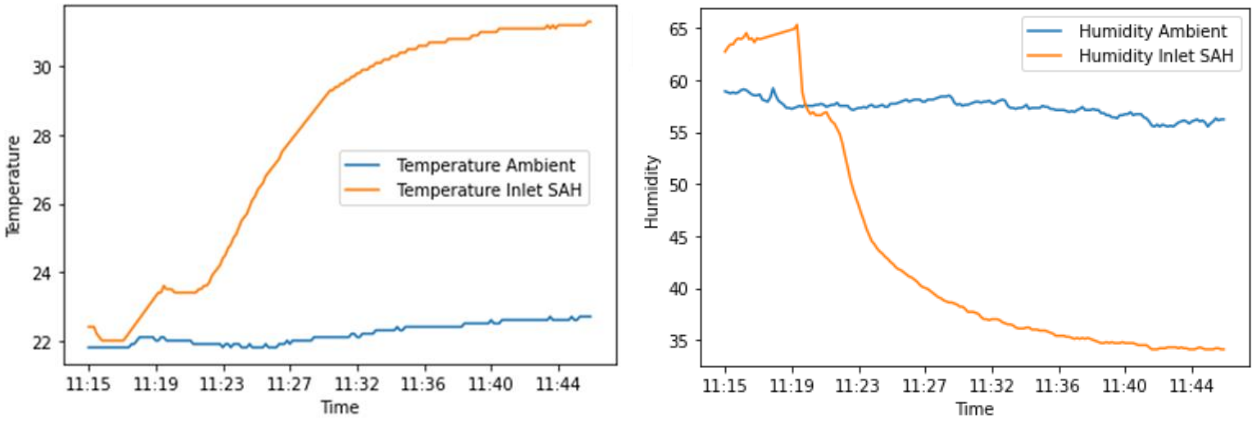


**Figure 4.17. Temperature and relative humidity data during the testing of the dehumidifier**

From Figure 4.17, it is noticeable that the dehumidifier subsystem has a level of ramp up, where over the half hour test conducted, the device was able to gradually reduce the humidity of the airstream. The humidity eventually levelled out, with an ambient value of around 65%, and an outlet value of around 35%. It should also be noted that the outlet air also had an increase in temperature of around 5°C from ambient when the dehumidifier was used. This increase in temperature would contribute to the air humidity drop.

#### 4.2.1.2 *Dehumidifier and SAH*

This test was undertaken utilising the dehumidifier coupled to the SAH subsystems. The temperature and humidity evolution during the tests at the outlet of the dehumidifier and SAH (corresponding to the inlet of the SAH and DC in the legend, respectively), and at the ambient conditions are shown in Figure 4.18.
The results show that together the dehumidifier and the solar air heater are capable to reach elevated temperatures up to 47°C at the steady state. The humidity reduction results were quite good with a minimum humidity value of around 25-27%, which is lower than that of the dehumidifier by itself, and much lower than the 55% ambient humidity. Additionally, it was noticeable that the solar air heater tended to have a high initial temperature (around 55°C), after which the temperature dropped to a point where a pseudo-equilibrium was reached. This tended to suggest that the SAH accumulated heat from the solar radiation prior to operation, which was then released at the beginning of the test until reaching thermal equilibrium.

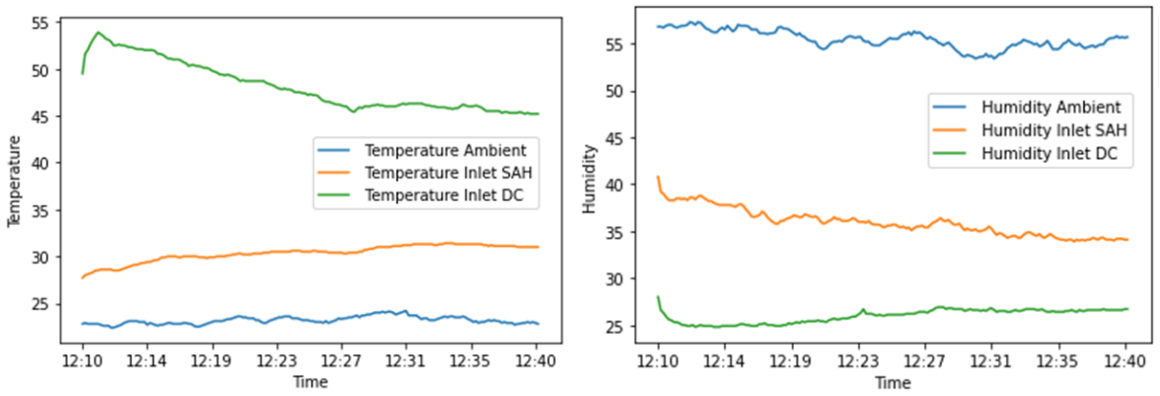


**Figure 4.18. Temperature and relative humidity data during the testing of the dehumidifier and SAH**

Figure 4.18 tends to show that together the dehumidifier and the solar air heater are capable to reach elevated temperatures up to 47°C at the steady state. The humidity reduction results were quite good with a minimum humidity value of around 25-27%, which is lower than that of the dehumidifier by itself, and much lower than the 55% ambient humidity. Additionally, it was noticeable that the solar air heater tended to have a high initial temperature (around 55°C), after which the temperature dropped to a point where a pseudo-equilibrium was reached. This tended to suggest that the SAH accumulated heat from the solar radiation prior to operation, which was then released at the beginning of the test until reaching thermal equilibrium.

#### 4.2.1.3 *Full Device*

This test was undertaken utilising the SAH, dehumidifier and DC. Figure 4.19 presents the temperature and relative humidity results measured at different point from the system (outlet dehumidifier / inlet SAH; outlet SAH / inlet DC; outlet DC) and at the ambient conditions.

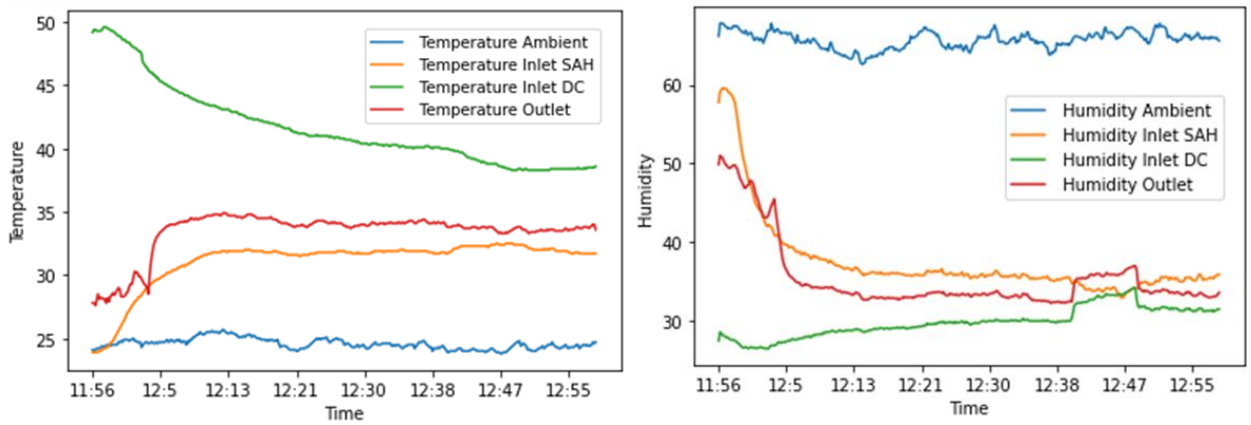


**Figure 4.19. Temperature and relative humidity data during the testing of the fully integrated system**

From Figure 4.19, it is possible to observe a similar trend to Figure 4.18, where the temperature at the SAH outlet (i.e. inlet of the DC) is around 40°C, and the humidity is around 35%. There is a large heat loss within the DC that can be observed by a temperature decrease at the outlet of the DC, which could originate from the airstream transferring energy into the environment through the metal components and acrylic tube. Additionally, these tests were undertaken with no insulation on the flexi piping between the SAH and the DC, which would further allow more heat to be lost during the working fluid flow. Additionally, it was found that a large amount of ambient air entered the system through the sludge inlet hatch (possibly decreasing the air temperature measured at the outlet of the system). For these reasons, the hatch was blocked during the remainder of testing by a piece of cardboard and the pipe between the SAH and DC insulated.

### 4.2.2 Tests with wet soil

The tests with wet soil had two objectives, namely understanding the optimal subsystem configuration in the prototype, and the optimal fan speed for the ventilation system. The first set of tests was undertaken by systematically removing one component of the prototype and measuring the system performance. The second set of tests was done by changing the ventilation rate in order to determine the optimal values.

#### 4.2.2.1 *Tests varying the components configuration in the prototype*

This set of tests was undertaken by methodically removing a single subsystem at a time from the device in order to ascertain the impact this change had to the overall device performance. These tests were undertaken utilising a wetted soil feedstock, 100% fan speed (0.56 $m^3/s$) and 1 hour drying time. Figure 4.20 compares the drying curves achieved by the various permutations of the device, while Figure 4.21 displays the overall drying rates, efficiencies and SEC corresponding to each experimental case.

The overall drying rates varied between 1.5 to 2 $kg/h/m^2$ (Figure 4.21). The results show that the drying rate in the full integrated device was similar than when the reflectors, dehumidifier and SAH were removed. Concerning the drying kinetics, the moisture content decreased with time following the same pattern for the different experimental cases (Figure 4.20).

The efficiency ranged between 60 to 70% (Figure 4.21). Compared to the full integrated system, the efficiency was approximately the same when the SAC and dehumidifier were removed, and slightly higher when the reflectors were removed.

Concerning the SEC, it can be seen that the values very similar between the full device, no reflectors and no SAH test, varying between 400 to 500 kWh/ton (Figure 4.21). The SEC value decreased significantly during the no dehumidifier test up to around 100 kWh/ton. This is due to the fact that the dehumidifier subsystem drawn up to 150 W of power, whereas the remainder of the system would draw closer to 40 W in total. Therefore, when the dehumidifier was removed, the decrease in electricity consumption lowered significantly.

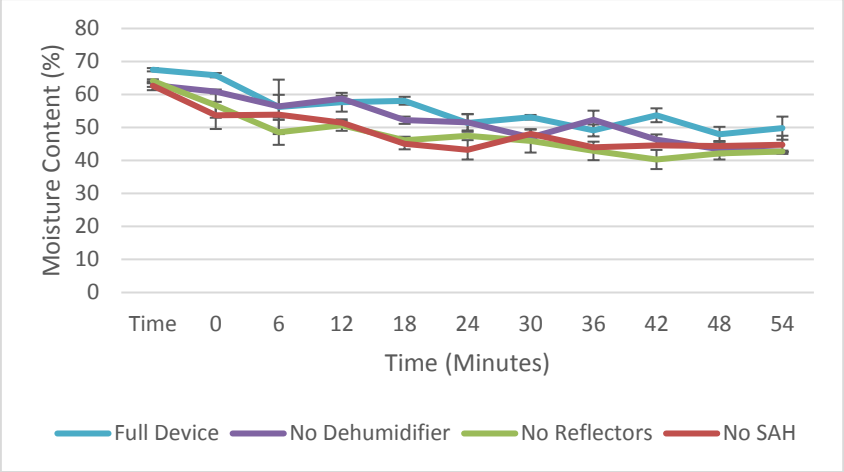


**Figure 4.20. Drying curves at the different components' configuration**


**Figure 4.21. Drying rate, efficiency and SEC at the different components configuration**

A summary of all the data from the varying subsystems test may be seen in Table 4.1. The average irradiance during the tests had small variations (450 to 500 W/m$^2$), showing that tests were done at relatively close solar radiation conditions. It can be noted that the temperature at the DC inlet were similar between the different experimental cases (around 35 to 40°C), expect when the system was run without SAH. In this case, the air temperature was lower and equal to the ambient conditions (~30°C). The temperature tended to decrease from the inlet to the outlet of the DC for the configurations where the SAH was connected, while the humidity increased in all cases. This result reveals that the air stream transferred part of the heat gained in the SAH to the material for its drying and it gained in humidity due to the evaporated moisture.

Overall, the most optimal setup for the device as a compromise between the drying performance and the power consumption would be to utilise the system without the dehumidifier. Indeed, the dehumidifier did not bring any improvement on the drying process while its use increased considerably the energy consumption of the

system. The SAH allowed to get slightly higher temperatures at the DC inlet, which would bring additional heat to the system, but this could not be reflected in an improved drying performance in the testing results. The reflectors did not show to bring any significant improvement either, even though they are supposed to reflect solar radiation towards the DC and thereby increase the collection of solar thermal energy.

**Table 4.1. Summary of the results from the tests varying the components configuration**

| Test | Drying Rate ($kg/hr/m^2$) | SEC (kWh/Ton) | Efficiency (%) | Average irradiance ($W/m^2$) | DC average temperature (°C) | | DC average humidity (%) | |
|---|---|---|---|---|---|---|---|---|
| | | | | | Inlet | Outlet | Inlet | Outlet |
| **Full Device** | 1.75 ± 0.18 | 492 ± 51 | 64 ± 6 | 491 ± 2 | 40 ± 1 | 33 ± 2 | 33 ± 2 | 77 ± 4 |
| **No Reflectors** | 1.81 ± 0.02 | 447 ± 11 | 73 ± 1 | 460 ± 0 | 37 ± 0 | 32 ± 1 | 26 ± 1 | 55 ± 15 |
| **No Dehumidifier** | 1.75 ± 0.05 | 128 ± 18 | 71 ± 4 | 450 ± 41 | 36 ± 2 | 33 ± 1 | 26 ± 2 | 39 ± 2 |
| **No SAH** | 1.62 ± 0.05 | 464 ± 10 | 65 ± 3 | 449 ±11 | 30 ± 0 | 31 ± 0 | 34 ± 1 | 42 ± 0.4 |

#### 4.2.2.2 *Tests varying the ventilation rate*

These tests were undertaken with the full system and the fan speed was varied, with wetted soil as the feedstock and one hour drying time per test. Figure 4.22 shows the drying curves obtained at the different ventilation rates, whereas Figure 4.23 displays the corresponding overall drying rate, efficiency and SEC.

It can be seen that the ventilation rate does not have a considerable effect on the drying kinetics (Figure 4.22) and performance parameters (Figure 4.23).

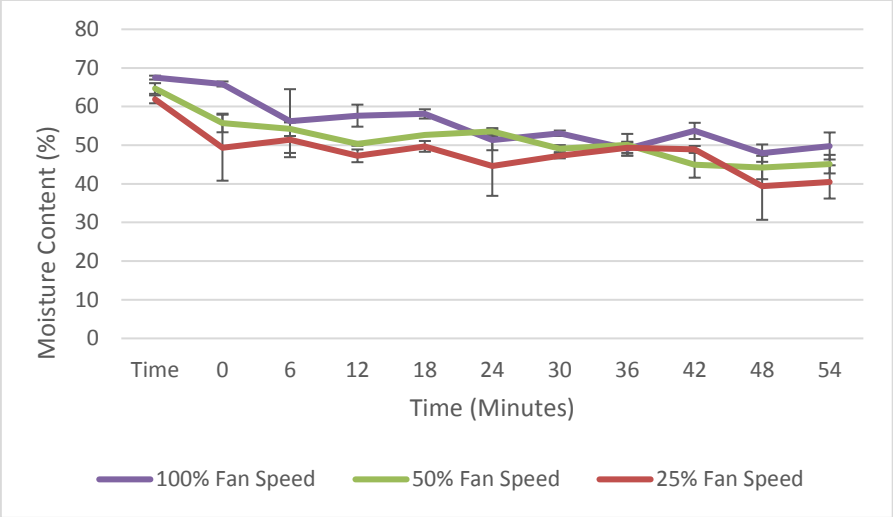


**Figure 4.22. Drying curves at different ventilation rates**

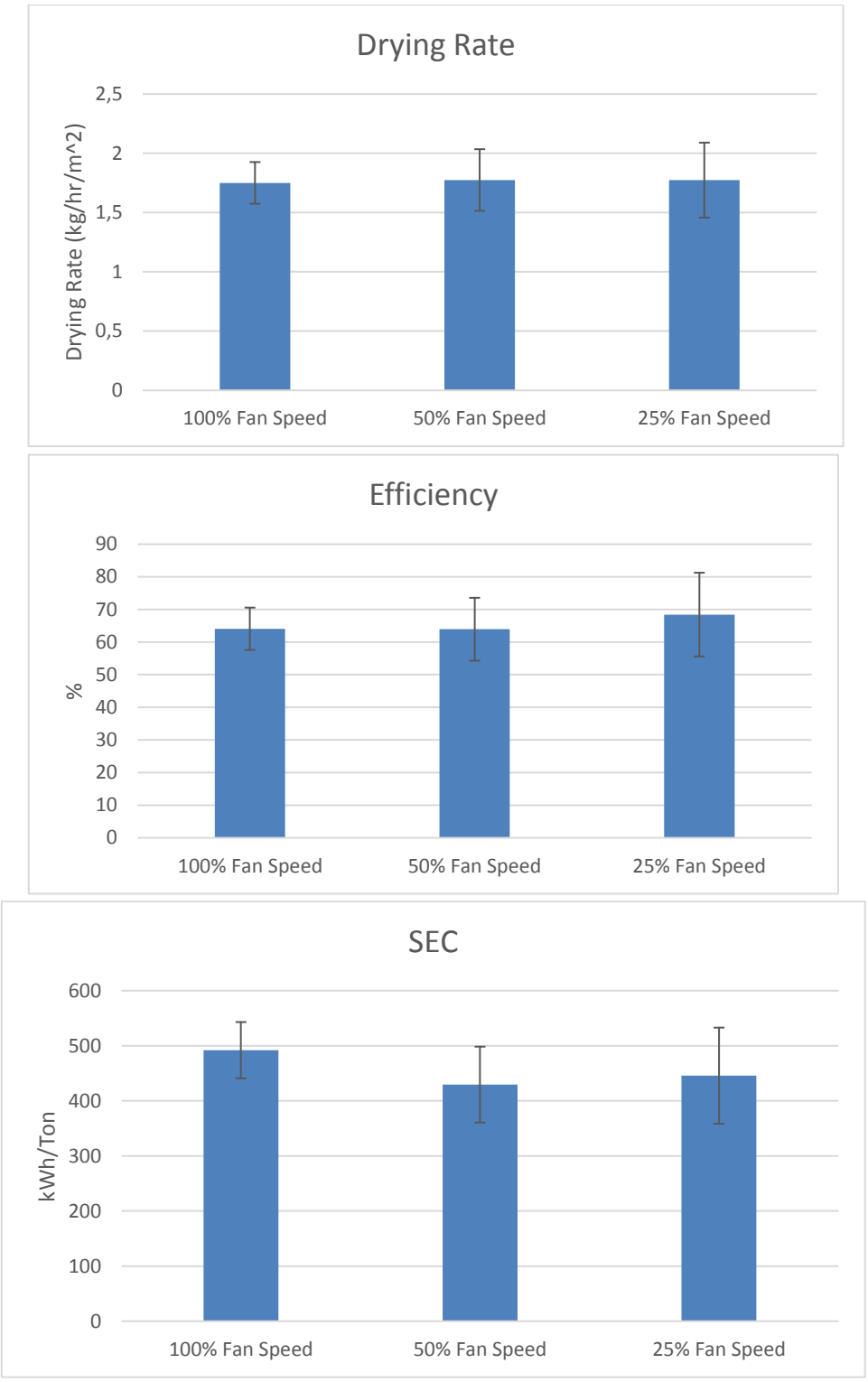


**Figure 4.23. Drying rate, efficiency and SEC at different ventilation rates**

Table 4.2 is a summary of the data collected during this phase of testing. Similar to the previous tests, the temperature in the DC tended to decrease and the humidity to increase from the inlet to the outlet, which could be explained by the air stream ceding part of its sensible heat to the drying process and gaining in humidity from the evaporated moisture. It has to be noted that the air temperature at the inlet of the DC was considerably higher at 25% fan speed. It was suspected that the lower ventilation rate led to a more important heat collection in the SAH due to prolongated contact of the air stream with the solar absorber.

For this series of tests, the solar irradiance conditions were also close between the different experiments (varying between 450 to 500 W/m$^2$).

**Table 4.2. Summary of the results from the tests varying the ventilation rate**

| Test | Drying Rate (kg/hr/m$^2$) | SEC (kWh/Ton) | Efficiency (%) | Average irradiance (W/m$^2$) | DC average temperature (°C) | | DC average humidity (%) | |
|---|---|---|---|---|---|---|---|---|
| | | | | | Inlet | Outlet | Inlet | Outlet |
| **100% Fan Speed** | 1.75 ± 0.18 | 492 ± 51 | 64 ± 6 | 492 ± 2 | 40 ± 1 | 33 ± 2 | 33 ± 2 | 77 ± 4 |
| **50% Fan Speed** | 1.78 ± 0.26 | 430 ± 69 | 64 ± 10 | 497 ± 0 | 38 ± 1 | 33 ± 0 | 30 ± 0 | 43 ± 1 |
| **25% Fan Speed** | 1.77 ± 0.32 | 446 ± 87 | 68 ± 13 | 466 ± 4 | 44 ± 1 | 38 ± 1 | 24 ± 1 | 44 ± 45 |

#### 4.2.2.3 *Discussion*

During the first phase of wet soil tests, the device was tested in order to ascertain the optimal configuration of the system. The SEC values were significantly higher when the dehumidifier system was utilised. Additionally, the dehumidifier reduced the humidity of the air stream in the system, but without it comparable low humidities were obtained, as observed during the functionality tests. Indeed, even with the dehumidifier not being utilised, the SAH subsystem was able to increase the air temperature to a degree that the relative humidity was reduced to levels very similar to when the dehumidifier was used. These results suggest that this subsystem is not substantial for the optimal operation of the integrated system. Besides, this type of dehumidifier (operating by a compressor) tends to function at optimal efficiency and moisture removal at ambient humidity values in excess of 80%, such as what Durban experiences in the summer, meaning that the dehumidifier may be more useful as a subsystem during the summer months, but not in winter that was the period of the tests. Even if the humidifier may be useful in summer, it should be reiterated that this will come with the caveat of far increased power consumption from the system. For the synthetic faecal sludge tests, it was decided that the dehumidifier would not be utilised, as it didn't improve the drying performance but increased the energy consumption.

The use of the SAH subsystem did not lead to a higher drying performance compared to the configuration without it. Nonetheless, it provided a higher temperature at the inlet of the DC. Therefore, the air pre-heating in the SAH could potentially provide supplementary heat for the evaporation of the moisture from the moist material. Even though the higher air temperatures in the DC was not reflected in an improvement of the drying process, it was deemed that the SAH could still bring a positive contribution of the process. Therefore, this subsystem was considered for the next round of tests with synthetic faecal sludge.

When the reflector subsystem was not utilised, the drying rate of the system did not undergo any considerable variation and even the efficiency was slightly higher. This result suggests that the reflectors are not an essential component of the system. Nevertheless, it was decided that the reflectors will be utilised for the next round of tests because it is still assumed that they may bring a positive contribution and they have shown to be not detrimental for the process.

With regards to varying the airflow rates, no considerable effect on the performance of the system was observed. This was different of what was initially expected to happen, as higher airflow rates generally provide higher turbulence leading faster heat and mass transfer, therefore higher drying rates. Nonetheless, the

optimum ventilation rate from the tests range would be 25%, as this would result in less consumed power. Indeed, the system had four ventilation fans of 9.2 W, representing a power consumption of 36.8 W if used at 100% fan speed meaning 9.2 W at 25% fan speed, meaning a power saving of 27.7 W with the ventilation rate at its minimum value. This power consumption saving could be beneficial particularly at long operating times. Moreover, it can be noted that lower ventilation airflow values yielded to higher temperature at the inlet of the DC, in addition to leading to a longer contact time with the moist material. These two factors could result in a higher heat transferred from the pre-heated air stream to the moist material for its drying during the solar drier operation. For practical reasons, a fan speed of 35% was utilised for the next round of tests to avoid issues with regards to starting the fans when powering on the system (as experienced with 25% fan speed).

### 4.2.3 Tests with synthetic faecal sludge

This phase of testing had two goals, namely understanding the effect of the initial moisture content of the feedstock in the system and understanding whether additives may be utilised in order to improve the process by reducing the stickiness and increasing the performance. The tests were undertaken with synthetic faecal sludge at the most optimal conditions, as determined during the wet soil tests (no dehumidifier, low ventilation rate). A fan speed of around 35% was used for this testing phase, as the ventilation system experienced issues of operation at lower fans speeds.

#### 4.2.3.1 *Effect of the Initial Moisture Content*

This phase of testing involved checking the influence of the initial moisture content on the key performance metrics and sludge conveyance through the dryer. This is to understand how the device functions with different moisture contents of sludge, as the dryer would be exposed to many different moisture contents of sludge in the real world.
Figure 4.24 displays the drying curves from the sludge samples at different moisture content and Figure 4.25 presents the performance parameters from each experimental case.

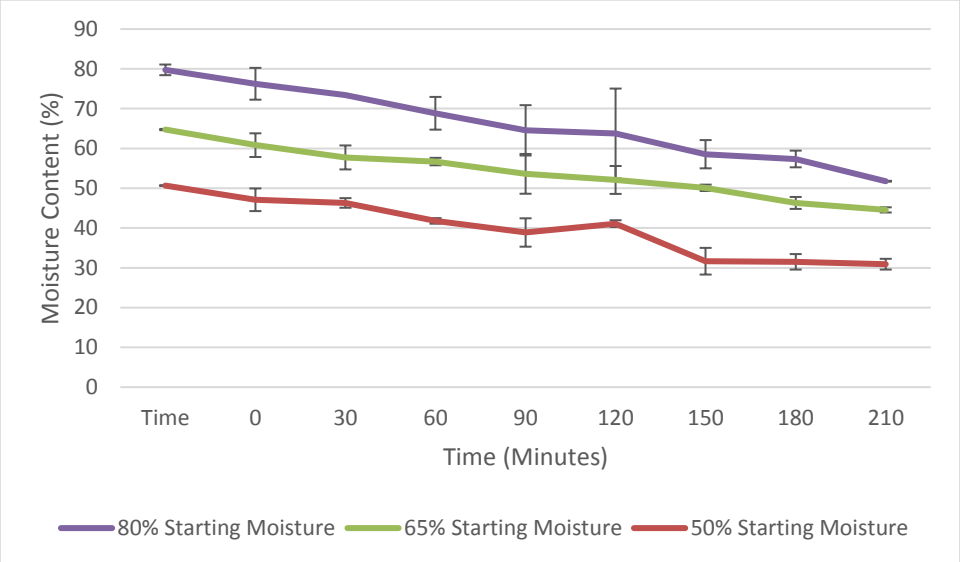


**Figure 4.24. Drying curves at different initial synthetic sludge moisture content**

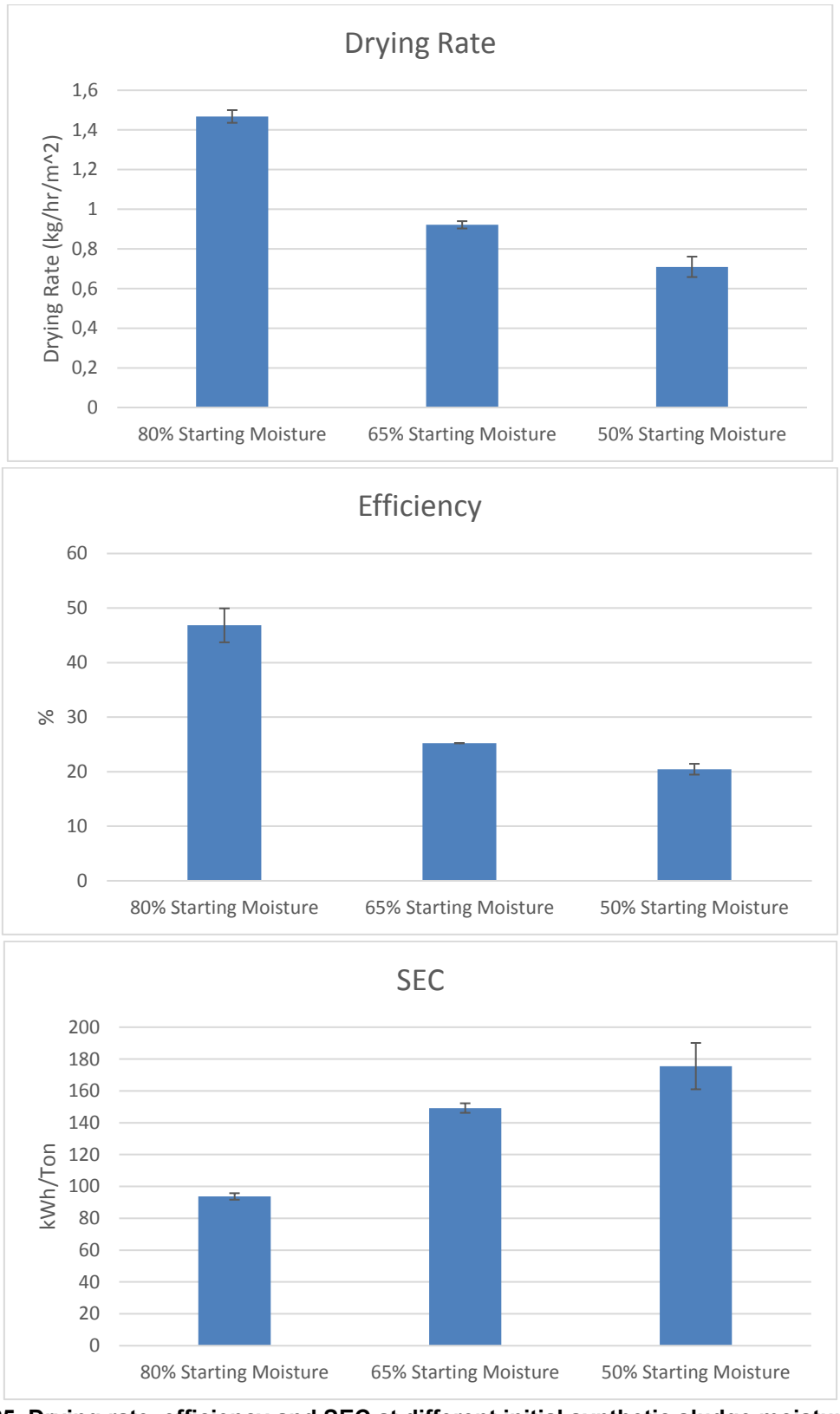


**Figure 4.25. Drying rate, efficiency and SEC at different initial synthetic sludge moisture content**

Figure 4.25 shows that the drying rate of the sludge decreased as the initial moisture content was lower (decrease from 1.4 kg/h/m$^2$ at 80% initial moisture content to 0.7 kg/h/m$^2$ at 50% initial moisture content, representing a decrease of around 50%). This could also be observed in the drying curves (Figure 4.24), as the moisture content decreased during the tests at an increased gradient as the initial moisture content was higher.

The SEC value was significantly increased as the initial moisture content was lower (increase of SEC of a factor 2, i.e. from 90 to 180 kWh/ton, by decreasing the starting moisture content from 80 to 50%). The opposite trend was observed with the efficiencies, namely a decrease of the efficiency from 50% to 20% by reducing the moisture content from 80 to 50%. It can be remarked that the efficiency values for drying synthetic sludge were significantly lower than that of drying wet soil. The main reason for this change may be that the moisture within the sludge was more tightly bound than the moisture within the soil.

The higher moisture content synthetic sludge tended to be extremely sticky during it convey. The high moisture content sludge tended to be conveyed relatively poorly, since the sludge would get stick to the blades of the screw conveyor and the transparent tube of the dryer. A part of the transparent tube would then be covered by sludge as the test began. As the sludge dried, it tended to become much thicker and more rubber like texture. The sludge stuck to the chamber walls would then be pulled off in a layer as it dried. The sludge drying on the blades tended to be an issue with regards to fouling of the dryer, as the sludge stripped off the side walls tended to remain stuck to the blades for a long time. Figure 4.26 gives an example of the sludge sticking to the sides of the DC during the early phases of a drying test with the device.

**Figure 4.26. Synthetic sludge sticking to blades and side walls**

As the initial moisture content was lowered, the sludge was significantly less sticky. The 65% sludge was not very sticky but was also very difficult for the screw conveyor blades to break up and expose the inner layers of the bulk of sludge to the heated airstream as it clumped significantly. As a result, the sludge tended to form a skin at the surface in a much easier manner than the other moisture content sludges. The sludge did not stick to the walls in the same manner as the 80% sludge. This type of sludge is far from ideal, because the consistency of the sludge tends to make the drying rate relatively low due to the skin forming over top and lack of exposure of the sludge from the interior of the bulk material.

The 50% moisture content sludge tended to be the best for conveyance, as the sludge tended to form small pebbles, with the sludge resembling wet beach sand when in the dryer. This sludge tended to convey the best, as the small clumps were able to be agitated, while conveying extremely well. Additionally, the sludge did not tend to stick to the internal walls of the dryer. A photograph of the drying of 50% initial moisture content sludge within the dryer is depicted in Figure 4.27.

**Figure 4.27. Drying of the 50% moisture content sludge**

Table 4.3 summarizes the results obtained during the tests with synthetic faecal sludge at varying starting moisture content. A similar trend was observed with respect to the temperature and humidity evolution inside the DC than for the wet soil tests. There was a slight difference of irradiance between the tests with sludge at 80% moisture content (~ 550 W/m$^2$) and the tests with sludge at 65 and 50% moisture content (~ 650 W/m$^2$). Even though the irradiance was lower in the former case, the temperatures in the DC were similar between the different tests. Therefore, the influence of the irradiance on the results from the tests was minor.

It can be noted that the efficiency of the process was lower for the synthetic faecal sludge than the wet soil. This means that the synthetic faecal sludge was more difficult to dry than the wet soil, probably due to a higher degree of moisture bound to the solid matrix.

**Table 4.3. Summary of the results from the tests varying the initial synthetic sludge moisture content**

| Test | Drying Rate (kg/hr/m$^2$) | SEC (kWh/Ton) | Efficiency (%) | Average irradiance (W/m$^2$) | DC average temperature (°C) | | DC average humidity (%) | |
|---|---|---|---|---|---|---|---|---|
| | | | | | Inlet | Outlet | Inlet | Outlet |
| **80% Starting Moisture** | 1.47 ± 0.03 | 94 ± 2 | 46 ± 3 | 564 ± 49 | 43 ± 2 | 38 ± 3 | 28 ± 1 | 41 ± 4 |
| **65% Starting Moisture** | 0.92 ± 0.02 | 149 ± 3 | 25 ± 0 | 655 ± 13 | 40 ± 1 | 37 ± 3 | 23 ± 2 | 31 ± 1 |
| **50% Starting Moisture** | 0.71 ± 0.05 | 175 ± 15 | 20 ± 1 | 638 ± 2 | 43 ± 2 | 38 ± 3 | 28 ± 1 | 34 ± 1 |

#### 4.2.3.2 *Effect of additives in the sludge*

This phase of testing included testing a variety of additives within the synthetic sludge mixture in order to aid in reducing the stickiness of the sludge and therefore improve the conveyance and reduce fouling of the device mechanics, as well as to identify if these additives can enhance the moisture removal process. Three additives were used for this: slacked lime, charcoal, sawdust. The results from these tests are depicted in Figure 4.28 (drying curves) and Figure 4.29 (performance metrics). Note that the additives slightly decreased the initial moisture content of the synthetic sludge (80% MC).

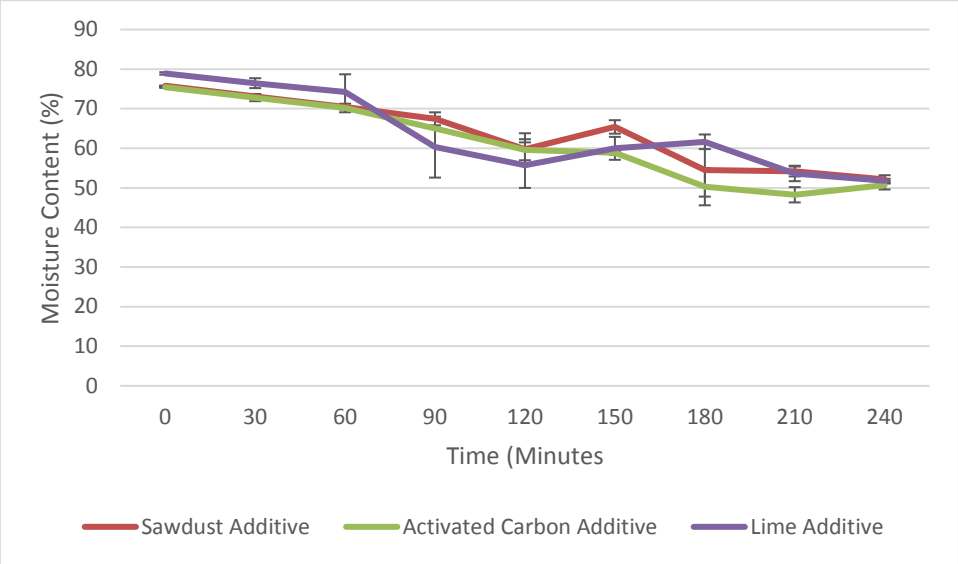


**Figure 4.28. Drying curves of synthetic sludge with different additives**

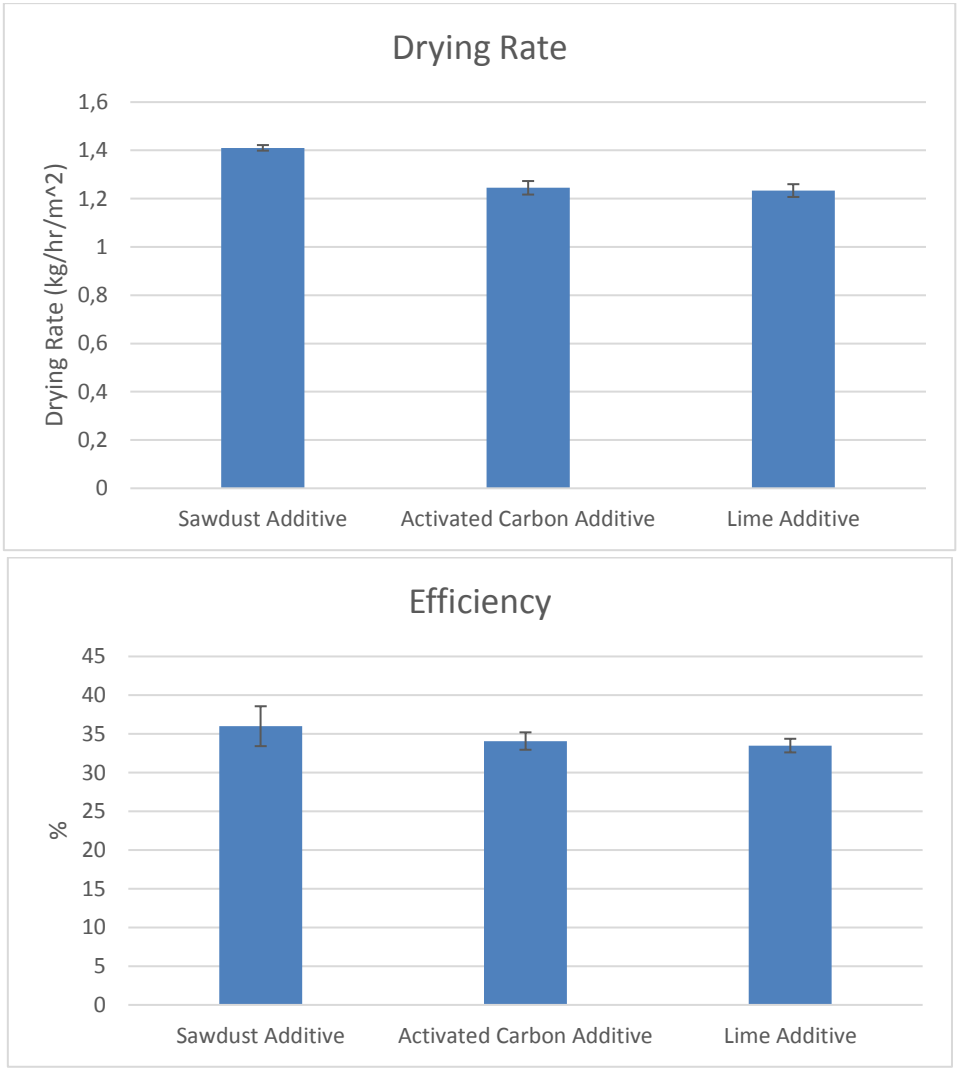

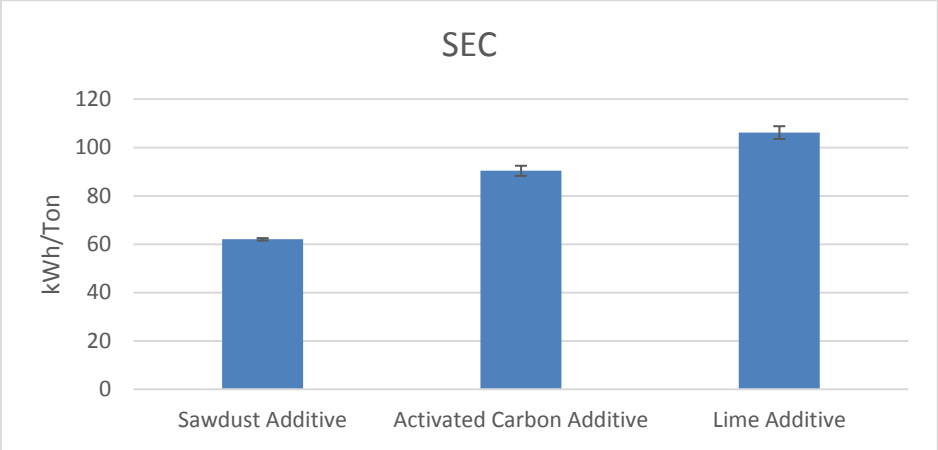


**Figure 4.29. Drying rate, efficiency and SEC of synthetic sludge with different additives**

Table 4.4 presents the results from the solar drying tests using synthetic sludge mixed with sawdust, activated carbon and lime. The higher initial drying rate of the sawdust additive could be explained by the higher average irradiance reeved during that test (~730 W/m$^2$) compared to the tests with the other additives (~650 W/m$^2$). Nonetheless, the air temperature introduced in the DC was approximately the same for the 3 cases (~40°C). Similar to the other tests, the drying of synthetic sludge provoked an air temperature decrease and humidity increase. Compared to the sludge without additive at 80% moisture content, the process was slightly less performant when the sludge was mixed with additives, with slightly less good performance parameters.

**Table 4.4. Summary of the results from the tests varying the synthetic sludge with different additives**

| Test | Drying Rate (kg/hr/m$^2$) | SEC (kWh/Ton) | Efficiency (%) | Average irradiance (W/m$^2$) | DC average temperature (°C) | | DC average humidity (%) | |
|---|---|---|---|---|---|---|---|---|
| | | | | | Inlet | Outlet | Inlet | Outlet |
| **Sawdust Additive** | 1.41 ± 0.01 | 62 ± 1 | 36 ± 3 | 732 ± 47 | 39 ± 1 | 33 ± 2 | 25 ± 2 | 39 ± 2 |
| **Activated Carbon Additive** | 1.25 ± 0.03 | 90 ± 2 | 34 ± 1 | 649 ± 7 | 42 ± 2 | 36 ± 3 | 30 ± 4 | 45 ± 5 |
| **Lime Additive** | 1.23 ± 0.03 | 106 ± 3 | 33 ± 1 | 662 ± 3 | 43 ± 4 | 39 ± 4 | 31 ± 5 | 44 ± 7 |

An important observation made during the testing was the fact that the lime additive tended to provide a superior texture and reduced stickiness to the sludge, which made conveyance easier, and resulted in less fouling of the system. This suggests that the lime additive may be worth utilising in future device tests, however an economic viability analysis is required due to the cost of the additives versus the improvement provided.

#### 4.2.3.3 *Discussion*

Overall, the device was able to handle faecal sludge in a wide range of moisture content. The system exhibited a better performance t with synthetic sludge in the region of 80%, due to the significantly higher drying rate, and the fact that in the long run, the sludge doesn't pose a significant issue with regards to clogging the system if the dryer is periodically cleaned. The 65% starting moisture content sludge was too clumpy, formed a skin which could impede drying performance and did not lead to a good sludge mixing to expose the wet interior of the sludge. The 50% moisture content sludge tended to convey the best, however the lower moisture content

sludge tends to be the hardest to dry, as can be seen by the lower drying rates and higher SEC values for these tests (which could be expected as the material was already quite dry and the remaining moisture was more difficult to remove). It was also noted that sludge with too high moisture content was not a suitable feedstock, as watery sludge cannot be handled by the screw conveyor

as this will flow to the outlet of the dryer very fast after its introduction, not allowing enough time for its drying. The sludge additives tended to not show significant improvement in terms of the overall performance. The sawdust additive tended to result in the highest overall drying rate outside of the original 80% moisture drying test. The texture of the sawdust was very similar to normal sludge, however the dry solids had increased, so the starting moisture content dropped from 80% to ~75%. The activated carbon was envisioned as a method of increasing the efficiency of the absorbance of solar energy by its dark colour. Overall, the efficiency and drying rate of this test was lower than sludge without additive, which means that the use of additive is not a suitable option for the process. Lastly, the lime additive tended to result in a similar texture, however the stickiness was significantly less than the normal 80% moisture content sludge. This additive resulted in a similar drying rate and efficiency to the activated carbon additive, with lower stickiness in the dryer.

Overall, none of the additives outperformed the normal 80% moisture content sludge when being dried. The sawdust and activated carbon additives had no discernible advantages when it came to the conveyance of the synthetic sludge, however the slaked lime additive did have a positive impact upon the characteristics of the sludge. Indeed, the slaked lime additive tended to produce a less sticky sludge, which could still be conveyed effectively by the screw conveyor system. The sludge did still appear to get stuck to the blades but didn't stick as much to the DC walls. The fact that the added dry solids allowed for a slightly lower starting moisture content might be useful, as it means that the sludge is already slightly drier than untreated sludge, however the additives may trap some moisture inside them (as activated carbon). When considering the cost of the additives, it may not be ideal to utilise them, as it could significantly increase running costs, especially since the dryer uses very little energy. It may however be possible to utilise an additive such as the slaked lime, as this is currently used as a treatment in municipal wastewater plants and can be bought in large quantities at an affordable cost.

## 4.3 CONCLUSION

This project suggested the implementation of a system for the solar thermal drying of sludge based on a screw conveyor solar drier, in order to solve the issues of sludge management in municipalities. The device was tested to verify the compatibility with all subsystems which had been designed and built separately, and the performance level of the device was assessed with and without feedstock.

The device was tested using wetted soil as the feedstock in order to find the optimal device configuration and settings. It was found that the dehumidifier subsystem was not necessary as it did not contribute to a better performance and it requires high energy consumption with a SEC value of around 450-500 kWh/ton, whereas the SEC dropped to 80kWh/ton when the dehumidifier was removed. The SAH and dehumidified did not bring any gain in performance, even though they were supposed to bring supplementary thermal heat from solar radiation to the process by pre-heating the air stream before introduction into the DC (for the SAH) and increasing the irradiance received by the system by reflecting the peripheral solar radiation (for the reflectors). Nonetheless, it is still believed that these two sub-systems of the prototype may enhance the performance of the system if their use is further optimised, which is something to tests in future experimental campaigns. It was also found that the air flowrate did not have an effect on the better the drying performance. Nonetheless, lower ventilation rates tended to lead to higher airflow temperatures at the outlet of the SAH, which was suspected to a longer contact time of the air stream with the absorber, and subsequently this increased the heat input in the DC. In addition, the fans operating at lower ventilation rates consumed less electrical power.

Therefore, for long operation periods, it could be expected that a better performance will be observed with lower ventilation rates.

When undertaking the varying starting moisture tests, it was found that the system was able to handle feedstock at different moisture content, thereby at different mechanical and texture properties (from a viscoplastic fluid to a granular solid). Nonetheless, the system is not adapted to deal with high moisture content feedstock with a liquid consistency, since the material will flow quickly to the outlet of the dryer without having enough exposure to the solar energy for its drying.

The system conveyed better the sludge with lower moisture content due to reduced stickiness, but the higher moisture content sludge had significantly higher drying rates likely due to a considerably higher proportion of more loosely bound moisture within that sludge. In fact, the dryer tended to be more efficient with synthetic sludge at a starting moisture content of 80%, compared to 65% or 50% moisture content. Additionally, the SEC values doubled from an initial moisture content of 80% to 50%, showing that drying material with less amount of moisture required more energy probably due to a higher moisture boundness with the solid matrix.

The device was tested with additives; however, these additives did not result in an improved drying performance, but they reduced the initial moisture content due to the added dry solids. The sawdust additive tended to provide the higher drying rate compared to the other additives, but this could be due to a higher irradiance during the tests as the efficiency values were similar. The lime additive did have a positive impact upon the texture and stickiness of the sludge, as the sludge was far less sticky to the various components of the device during the drying process and was therefore easier to handle.

The testing of the screw conveyor solar sludge dryer resulted in a greater understanding of the mechanisms which the dryer utilises to be able to efficiently dry the sludge. The testing was also able to identify the optimal system settings, system configuration and system feedstock. Overall, the device has proved itself as being capable of being able to dry synthetic sludge, however further testing as well as revisions to the hardware will allow for a more complete device to be developed in the future. The drying rates varied between 1 and 2 kg/h/m$^2$, leading to relative high efficiencies ranging from 30 to 70%. The highest efficiencies were found with wet soil as the moisture in this type of material was probably less bound to the solid matrix. The SEC value were lower than industry standard dryers which tend to have SEC values closer to 800-1000kWh/ton of moisture liberated from the feedstock, highlighting that this technology is quite promising as an efficient sludge treatment method.

## 4.4 RECOMMENDATIONS

In general, the operation of the screw conveyor solar sludge dryer allowed for the operator to understand some of the shortcomings of the device. This section will detail some of the possible improvements which could be made to the device, both to improve the general user experience during the device operation, and to improve the performance of the dryer during operation.

### 4.4.1 Material of the screw conveyor transparent walls

During the design phase of the project, the use of acrylic was justified due to the low cost, and ease of workability of the material in comparison to glass. However, this material suffered structural damage during the testing period. This could be seen by the way that the material deformed along the length of the tube, where most of the heat was received during the drying process. Additionally, during the final run of testing, the acrylic tube developed a large crack in it (as observed in Figure 4.30), which can be deduced to be from the internal stresses in the material from the excessive warping.

**Figure 4.30. Cracked acrylic tube**

Another option for the DC tube would be borosilicate glass or quartz glass. Both materials are capable of withstanding large changes in temperature without deforming or cracking. The durability of dryer would significantly drop, as neither material can withstand sharp impacts in the same way that plastics can, and any detritus within the sludge, such as stones could cause the chamber to crack.

Another option is that of a high temperature plastic, such as TPX, which is purportedly up to 90% clear, with temperature resistance up to 200°C. Obtaining a tube of such a material may pose an issue as it is produced by a Japanese company for scientific and medical uses. Another possibility is the use of transparent polycarbonate, this can withstand temperatures of up to 130˚C, while remaining transparent to most light which it is incident to. This is also a thermoplastic, meaning that if the melting point is reached, it will soften and eventually liquify, however it can be reset by cooling, and continue to function with no degradation to the material physical properties. This is the most realistic replacement for acrylic.

### 4.4.2 Choice of motor and gearbox for screw conveyor

The motor which is utilised for the movement of the screw conveyor subsystem is a rotary ac motor, which runs through a worm gear drive gearbox, which allows for a very high reduction ratio and therefore very high torque. This setup is ideal for commercial screw conveyor systems, providing very high torque at normal operating speeds. This setup is an issue for the solar dryer however, as the motor is unable to function at such slow speeds for soft materials as sludge. A heavy-duty stepper motor would function better, as it would possess sufficient torque and have much better slow speed performance. This would allow the system to be operated without the need for intermittent pausing and resuming the screw conveyor, as it was done in this study.

### 4.4.3 Inclusion of a coating on the DC

The system currently operates as a hybrid direct and indirect solar dryer, as the solar collector is utilised to preheat the airstream, while solar radiation is utilised to heat up the bulk of the sludge within the DC. The main issue with this is that the material which is being dried is not always of optimal properties to convert radiant sunlight into thermal energy.

A possible option is to coat the entire transparent DC in the same type of coating utilised for evacuated tube solar collectors. This coating highly efficiently converts solar energy into thermal energy and is also capable of converting infra-red rays into usable thermal energy. Essentially, this coating, or even painting of the chamber would result in much more efficient transformation of irradiance into thermal energy which may be then transferred by conduction to the sludge being dried.

### 4.4.4 Utilisation of a hybrid solar panel for the solar collector

The solar air heater utilises a copper plate as the absorber plate. The technology of photovoltaic cells produces a large amount of thermal energy due to the technology of silicon-based PV cells being only around 30% efficient at best, i.e. 70% of the energy encountered by the cell is generally wasted as heat. For this reason, replacing the copper absorber plate for a PV cell could result in similar drying performance, along with a total or partial reduction in the amount of electricity which is utilised by the system from the grid.

### 4.4.5 Inclusion of a service hatch

The operation of the screw conveyor results in a large amount of dried sludge remaining on the auger blades, especially as the sludge undergoes the sticky phase of drying. This sludge is difficult to remove without actively removing it from the blades. It is quite difficult to clean any part of the dryer without disassembly it, as the clearances from the inlet or outlet ends are too small. A service hatch would allow for the dryer to be superficially cleaned between major cleanings, as well as providing an easier method for procuring samples and readings from the middle of the device during testing.

### 4.4.6 Painting of Screw Conveyor Housing

The ends of the screw conveyor are constructed from bare stainless steel and tend to heat up during testing. Painting the outsides of these chambers black could allow for them to absorb more heat and pre-heat the sludge before it enters the main DC.

# 5 OUTCOMES FROM THE PROJECT

This section describes the outcomes from the project. The main outcome was the development of two solar thermal drying technologies that were specifically designed based on the characteristics of faecal sludge and its behaviour during drying. The first prototype was a greenhouse-type solar drier where the sludge is placed as a bed and is dried by the solar thermal energy harnessed by the system. The second prototype is a screw conveyor solar drier where the sludge is dried with the solar thermal energy received during its convey in a transparent tube.

The second outcome from the project was the creation of knowledge during the development and testing phases of the solar thermal drying technologies. This knowledge was compiled and disseminated through various means (conference, reports, papers).

Finally, the third outcome was the capacity building of students who were involved in this project and acquired new knowledge and learnt skills from the activities undertaken in this project.

## 5.1 DEVELOPMENT OF TWO SOLAR DRYING PROTOTYPES

### 5.1.1 Development of a greenhouse-type solar drier

The greenhouse prototype was developed as part of a MSc research project. The design was done during 2020 after the recruitment of the student, but little work for the building could be done due to the COVID-19 restrictions and its effects (restricted access to campus, slow administrative procedure, material procurement challenging). Most of the prototype was built during 2021 and was completed by mid-2022. The tests were then undertaken for a few months until September. This part of the project was carried out in collaboration with the Solar Thermal Energy Research Group (STERG) from the University of Stellenbosch.

The final product consists in a solar dryer where faecal sludge is placed in a bed and dried using solar thermal energy. The prototype offers an enclosed space where the solar thermal energy can be collected through greenhouse effect and the presence of an absorber wall. It includes a ventilation system and sludge rake system to boost the drying process. The sludge bed stands on a suspended grid, which allows the drying of the sludge from the bottom.

The greenhouse-type solar dryer is composed of the following components:

- A transparent enclosure in acrylic allowing the solar radiation penetration and creating a greenhouse effect by trapping the long-wave infrared radiation emitted by the bodies absorbing the solar thermal energy and protecting the process from the weather elements (in particular the rain from which the sludge can gain moisture) and preventing heat losses.
- A ventilation system (driven by ventilations fans) allowing to renew the air inside the enclosure and evacuate the evaporated moisture to avoid its accumulation, as a wet atmosphere could slow down or stop the drying process, and cause condensation in the walls and remoistening of the sludge.
- An air circulation system (driven by circulation fans) inside the enclosure in order to lead to a more homogeneous distribution of the evaporated moisture inside the volume of the dryer, avoiding the formation of high humidity layer at the surface of the sludge, which will affect negatively the process. Moreover, the circulation system creates movement of air at the surface of the sludge, which should enhance the mass transfer of the evaporated moisture from the sludge to the environment and consequently improve the drying process.
- A support where sludge will be placed as a layer of a given thickness to form a bed. The sludge bed stands on a fine mesh that will be elevated with respect to the ground level to allow air circulation underneath it and the drying of the sludge from the bottom.

- A rake system moving periodically back and forward along the bed to avoid crust formation and mixing the different layers of the sludge bed to lead to a more homogenous drying. The rake system consists in rotating bands with a series of blades orientated in alternate directions.
- A solar collector wall that increases the amount of solar radiation collected by the system. The wall is placed in the solar dryer between the air inlet and the bed. The bottom of the wall presents various holes from which the air stream is introduced to the drying zone. The wall should be placed facing south to collect the solar radiation entering the enclosure whose direction is not oriented to the sludge.
- Instrumentation to measure the temperature and relative humidity at different points inside the dryer, as well as the ambient conditions in the testing site (ambient temperature, ambient relative humidity, solar irradiance).
- An electronic system to log the data from the sensors and the rake system, and controllers for the motors from the ventilation and air circulation systems.

Figure 5.1 shows the drawing of the prototype and the flow patterns inside the dryer (obtained from computation fluid dynamics simulation). It can be seen that the air stream is introduced in the greenhouse from the top section of one of its lateral sides and enters a small volume delimited by the absorber wall. The air stream flows downwards until reaching the holes from the absorber wall, from where it is introduced into the section of the greenhouse where the sludge is placed. There, the air stream flows above and below the suspended sludge bed until exiting the greenhouse. Above the bed, the air stream is mixed in the available volume through the circulation fans before exiting the prototype.
Figure 5.2 depicts photographs from the final greenhouse solar drying prototype.

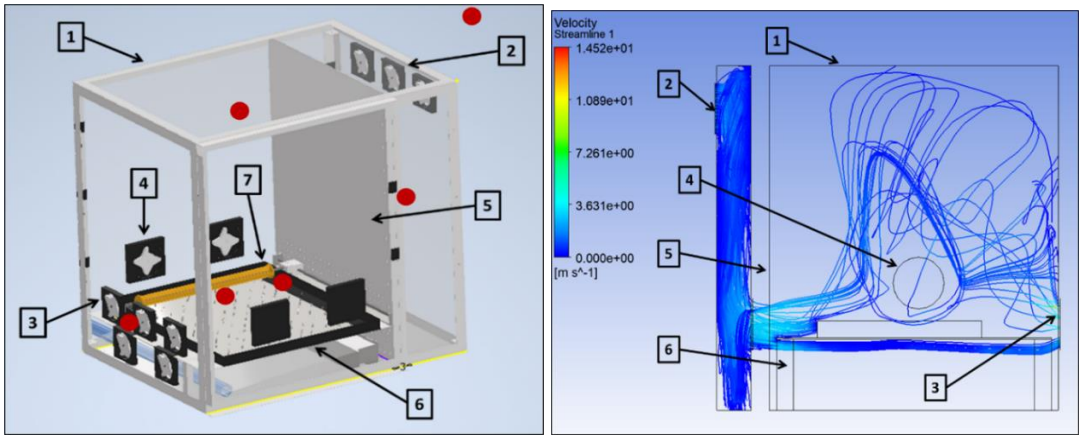


**Figure 5.1. Drawing of the greenhouse solar dryer (left image) and representation of the air flow patterns inside the prototype (right image) {1: enclosure; 2: air inlet; 3: air outlet; 4: circulation fans; 5: absorber wall; 6: sludge bed support; 7: rake system; red points: temperature / relative humidity sensors}**

**Figure 5.2. Photograph of the greenhouse front (at the left) and back (at the right)**

### 5.1.2 Development of a screw conveyer solar drier

The construction of the screw conveyer solar drying prototype started in 2020 through an undergraduate Mechanical Engineering student final year project. However, due to the COVID-19 restrictions and its negative effects on the UKZN administration and supply chain, the prototype could not be completed during this student project, even though this was the target. One of the students from the student project carried out with an MSc to finalize the construction and integration of the screw conveyor solar drier (done in 2021), and its testing (done in 2022). This part of the project was carried out in collaboration with the Mechanical Engineering Department from UKZN.

In the screw conveyor solar drier prototype, the sludge is dried during its convey through a transparent tube exposed to solar radiation. During this process, the sludge absorbs the solar thermal energy that provides the latent heat for moisture evaporation. An air stream flows inside the transparent tube to enhance the drying process. The air stream can be previously dehumidified and heated before introduction in the drier. Reflectors can be placed next to the tube in order to increase the amount of solar radiation received by the sludge.

The prototype is composed from the following components:

- Drying chamber (DC) composed of an auger inside a transparent tube in acrylic where the faecal sludge is dried.
- A ventilation system (driven by ventilation fans) allowing the circulation of air inside the DC. The air stream is introduced in counter-current with respect to the direction of the sludge flow in order to maximize the heat and mass transfer and enhance the drying process.
- A solar air heater (SAH) to heat the air stream to introduce in the DC (built in-house). The heated air allows to provide additional heat for moisture evaporation and potentially leads to increased drying rates. The relative humidity in the heated air is subsequently lowered, enabling to reach a sludge lower moisture content at the thermodynamic equilibrium and reduce the mass transfer resistance for moisture migration from the sludge to the air, increasing the drying rate.
- An air dehumidifier to lower the relative humidity of the air stream, which is beneficial for the drying process as described above.
- Reflectors to increase the incidence of solar radiation in the sludge, which allows to bring additional solar thermal energy for moisture evaporation.
- Instrumentation to measure the temperature and relative humidity at different locations of the prototype, and the irradiance in the experimentation site.
- An interface system to log the data measurements (temperature and relative humidity) and control the ventilation flowrate.
- An electronic system to log the data from the sensors and to control the ventilation system, and a controller for the auger motor.

Figure 5.3 displays the scheme and a photograph the prototype. The air stream enters the system by the dehumidifier and exits by the DC, passing by the solar air heater as an intermediary step.

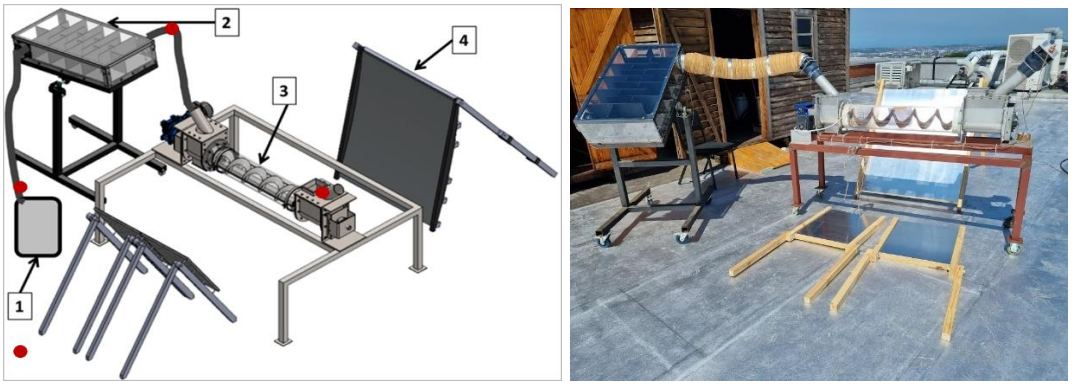


**Figure 5.3. Screw conveyor solar drier schematic representation (at the left) and photograph (at the right) {1: air dehumidifier; 2: SAH; 3: DC; 4: reflector; red points: temperature / relative humidity sensors}**

## 5.2 PERFORMANCE OF THE SOLAR THERMAL DRIERS

Table 5.1 displays the effect of different parameters on the performance of the greenhouse and screw conveyor solar driers. The performance was evaluated through the determination of various metrics, including drying rate, efficiency and specific energy consumption (SEC), during the prototype testing phase.

**Table 5.1. Effect of various parameters in the performance of the prototypes ('+': positive effect; '-': negative effect; 'o': no effect)**

| | | Greenhouse solar drier | | | Screw conveyer solar drier | | |
|---|---|---|---|---|---|---|---|
| | | Drying rate | Efficiency | SEC | Drying rate | Efficiency | SEC |
| **Ventilation** | **Low flowrates** | + | + | + | + | + | + |
| | **High flowrates** | - | - | - | o | o | o |
| **Air circulation** | **Low flowrates** | + | + | + | N.A. | | |
| | **High flowrates** | - | - | - | | | |
| **Rake system** | | + | + | - | N.A. | | |
| **Dehumidifier** | | N.A. | | | o | o | + |
| **Solar air heater** | | | | | o | o | o |
| **Reflectors** | | | | | o | o | o |

For both solar driers, the higher performance was obtained at lower ventilation rates. This result is the opposite to the effect that was initially assumed. The initial assumption considered that high air velocities resulting from high ventilation rates would enhance the mass transfer of moisture, resulting in the drying rate increase. In reality, lower temperature in DC were measured at high ventilation rates, which could explain the lower performance of the driers. Indeed, a high ventilation would not give enough time to the air stream to be heated in system and it even could create a cooling effect, leading to lower temperatures and consequently lower drying rates. Besides, a higher ventilation rate increases the power consumption, in addition to lower drying rates, the overall resulting in higher SEC. Nonetheless, the systems still need a ventilation system to evacuate the evaporated moisture, and avoid its accumulation in the DC, which is negative for the process, but it should be kept at a minimum level. Note that increasing ventilation rate may have a beneficial effect in a range of lower values than those from this study.

In the case of the greenhouse solar drier, the use of the rake system enabled the material to dry faster when it formed a bed of a given thickness. In this case, the positive effect of the rake system on the drying rate could be observed particularly at the first stage of the process. At the last phase, the rake system did not longer cause any improvements, probably because the material had shrunk considerably and broken down into crumbles, making the rake unnecessary at this point. The rake system did not exhibit any effect on the drying rate when low number of samples were placed on the dryer, leading to the formation of thin layer of minimal thickness. Therefore, the rake system will be only effective for important thickness of material. As it could be anticipated, the use of the rake system increased the SEC, but this increase may be worthy by the efficiency gain and dying rate increase, particularly when thick beds will have to be processed (more realistic scenario). During the tests, it was also noticed that the rake system prevented dried material stuck to the support grid. Hence, in despite of the higher SEC, the rake system is a necessary component for the efficient operation of the greenhouse, but its use must be optimised.

Concerning the air circulation system in the greenhouse, it improved considerably the drying process, but the increase of the circulation rate caused a drying rate to decrease and SEC increase. Therefore, similarly to the ventilation, the circulation rate has to be operating during drying for an efficient process but at a low intensity for an optimal operation.

In the case of screw conveyer, the humidifier was identified as not essential component. It lowered the relative humidity of the air stream circulating in the system, but it did not have any effect on the drying rate, and it increased the SEC. Without humidifier, the air humidity was still enough low thanks to temperature increase in the solar air heater. The tests were done in winter, when relative humidity is at the lowest point during the year. Therefore, it could be interesting to test the humidifier in summer, where the ambient humidity is much higher. The SAH and reflectors did not show to provide any improvement in the performance of the system, on the contrary to what was initially expected. Indeed, these components are supposed to bring supplementary thermal heat from solar radiation to the process: the SAH pre-heated the air stream before introduction into the DC and the reflectors increased the irradiance received by the system by reflecting the peripheral solar radiation. Nonetheless, the SAH and reflectors may still enhance the performance of the system if their use is further optimised. This should be tested in future experimental campaigns.

Both prototypes were capable to handle material from viscoelastic consistency (paste-like aspect) to granular solids, but they were not adapted to watery feedstocks. In the greenhouse prototype, the use of a watery feedstock resulted in the drainage of leachate through the grid from the bed support. In the screw conveyor solar drier, the feedstock flowed too quickly through the DC, without having enough exposure to the solar radiation, if it was too liquid.

Table 5.2 summarises the performance metrics of the greenhouse and screw conveyor solar drying prototypes, measured after the tests with wet soil and synthetic faecal sludge at the optimal operating conditions.

**Table 5.2. Summary of the performance parameters measured from the prototypes testing results**

| | Greenhouse solar drier | | Screw conveyer solar drier | |
|---|---|---|---|---|
| | Wet soil tests | Synthetic sludge tests | Wet soil tests | Synthetic sludge tests |
| **Average temperature range (°C)** | 35-45 | | 35-45 | |
| **Peak temperature (°C)** | 50 | | 50 | |
| **Drying rate (kg/h/m$^2$)** | 1-3 | 0.5-1 | 1.5-2.0 | 0.5-1.5 |
| **Efficiency** | 50% | 10-20% | 60-70% | 20-40% |
| **SEC (kWh/ton)** | ~125 | 230-3600 | ~125 | 90-180 |

The performance exhibited by both systems was quite good. The temperatures inside the DC ranged mostly between 35 to 45°C with peaks up to 50°C, representing a temperature difference higher than 10-15°C compared to the ambient conditions. The increase of temperature in the DC allowed to reduce the relative humidity to values lower than 40%, and even lower than 30% in some cases.

The SEC was lower than the typical values from industrial dryers (ranging between 800 to 1000 kWh/ton of evaporated moisture) for most of the cases, and these values can be still decreased with further optimisation of the system. For synthetic faecal sludge tests, it was noted that the SEC increased as the material was dried. The highest SEC value recorded in the greenhouse, superior to the typical SEC from industrial dryers by 3 folds, was obtained when the sludge was dried from 20 to 10% moisture content. Indeed, at this level of moisture content, the moisture is very bounded to the sludge solid matrix, and, in consequence, it is very difficult to remove, requiring an excessive high energy input. Nonetheless, if drying is stopped at 20% moisture content, the SEC is about 700 kWh/ton, which is still lower than industrial dryers.

Therefore, to reduce the energy costs of the process, the process does not have to achieve too low moisture content. The drying could be stopped at a moisture content between 20 to 30%, where the sludge already looks like a granular solid and presents a reduced or null pathogen content.

The screw conveyer solar drier exhibited a better performance than the greenhouse-type solar drier with higher efficiencies and lower SEC. Nevertheless, the screw conveyer prototype faced stickiness problems between the sludge and the tube walls and auger, which may cause serious clogging issues during long operation times and higher feeding rates. Various additives to the sludge were tested to reduce stickiness (lime, activated carbon, sawdust), but none of these solutions successful, even though there was a slight improvement with the lime. Note that the system performed better with sludge without additives than when it was mixed with sawdust, activated carbon or lime.

It can be noticed that wet soil tests tended to yield to higher drying rates and efficiency, and lower SEC than the synthetic faecal sludge tests. This could be explained by a lower binding of moisture with the solid matrix inside the material. In the case of real faecal sludge, it can be hypothesized that the prototype drying performance could be lain between the performance reported with wet soil and synthetic faecal sludge as feedstock. This hypothesis is based on the experimental observations from the preliminary study in a bench-scale solar drier, which demonstrated that real faecal sludge dried considerably faster than synthetic sludge (refer to Chapter 2 from this report).

Considering that a maximum theoretical efficiency can be estimated at around 70-80% (assuming an acrylic transmittance of around 70 to 80% and complete absorbance of the received irradiance by the feedstock), it can be seen that the measured efficiencies were quite good, in particular during the wet soil drying. This result denotes that the prototypes in their current state are fairly enough efficient, and that a low efficiency would be the result of a feedstock difficult to dry rather than a matter related to the system.

## 5.3 PRELIMINARY TECHNO-ECONOMIC ANALYSIS FOR ITS UP-SCALING AND IMPLEMENTATION IN THE FIELD

A preliminary techno-economic analysis was undertaken on the prototypes using the same case study than that from the preliminary study in Chapter 2. In this context, the capital and running costs were calculated considering that the solar driers in their current state would be used to dry the annual production of faecal sludge from ventilated improved pit (VIP) latrines in eThekwini municipality (drying from an initial moisture content of 80% to 20%). Other important parameters were measured, as the required surface for this and the total cost of the sludge treatment.

Table 5.3 presents the results from the techno-economical analysis, which was done based on the performance parameters calculated in this project. The performance parameters values (drying rate and SEC) were selected as roughly the median between the values obtained from the wet soil and synthetic faecal sludge tests (using the values from the overall process until achieving 20% moisture content in the case of the greenhouse). Indeed, it was hypothesized that the behaviour of real faecal sludge during drying will be comprised between the ones from the wet soil and synthetic faecal sludge, based on the previous observation that real sludge dried at a considerably faster rate than synthetic sludge (refer to Chapter 2).

The rest of the hypothesis formulated for the techno-economical analysis are listed here below:

- Total number of VIP latrines: 30,000
- Number of VIP latrines emptied per year (based on 5 years cycle): 6,000 latrines
- VIP sludge per latrine: 2 ton
- VIP sludge production per year: 12,000 ton
- Initial moisture content of sludge: 80%
- Final moisture content of sludge after drying: 20%
- Amount of moisture evaporated per year: 9,000 ton
- Cost of electricity: 2 R / kWh
- Daily operation time of the drier: 7 h
- Days of operation along the year: 310 d (6 days per week)

Because of the high number of approximations and simplifications, the results from this techno-economic analysis must be taken with caution and must be considered as merely rough estimations.

According to the preliminary techno-economic analysis projections, the running costs of the prototype to treat the VIP sludge would be relatively low: around R7 millions per year for the greenhouse and ZAR2 million per year for the screw conveyor solar drier. The cost to treat 1 tonne of VIP sludge would be ZAR600 and ZAR150 for the greenhouse and screw conveyor solar driers, respectively. This means that the sludge from one fully filled VIP latrine would be treated at a cost of ZAR1200 using the greenhouse and R300 using the screw conveyor. These costs can be considerably reduced through the optimization of the prototypes. The surface area required for the prototypes would be also quite low, around 0.4 hectares in total, which is approximately half of the surface are from an official soccer pitch.

Nevertheless, the capital cost calculated from the techno-economical analysis would be excessively high: ZAR400 million and ZAR1,600 million for the greenhouse and screw conveyor, respectively. Considering a payment of the loan to purchase the solar dries in instalments of 10 years, the total cost of treatment including capital costs would be ZAR4,000 and ZAR14,000 for the greenhouse and screw conveyor solar driers, corresponding to ZAR8,000 and ZAR28,000 to treat the sludge from one filled VIP latrine. The high capital costs can be considered normal at the prototype stage, because a drastic decrease of the capital costs can be expected with the improvement of the prototype design where unnecessary pieces of equipment will be identified and with the upscaling of the system leading to a drop of the construction cost. Besides, the tests in this project were done at low feeding rate, explaining the high number of units of prototypes required to treat the faecal sludge, whereas the prototype will operate at much higher feeding rate. Therefore, the high capital costs shouldn’t be taken into serious consideration at this stage and should be considered as an indicator to quantify the future design improvements.

**Table 5.3. Preliminary techno-economic analysis of the solar thermal drying prototypes for their implementation in the field**

| | Greenhouse solar drier | Screw conveyer solar drier |
|---|---|---|
| **Drying rate (kg/h/m$^2$)** | 1.5 | 1.5 |
| **SEC (kWh/ton)** | 400 | 100 |
| **Cost of one unit of prototype (R/unit)*** | 100,000 | 70,000 |
| **Surface area offered in one unit of prototype (m$^2$/unit)** | 1 | 0.2 |
| **Annual energy consumption (kWh/y)** | 2,700,000 | 900,000 |
| **Annual amount of moisture evaporated (kg/y/m$^2$)** | 2,867 | 2,867 |
| **Total required surface area (m$^2$)** | 4,186 | 4,186 |
| **Number of units** | 4,186 | 20,931 |
| **Annual running cost (R/y)** | 7,200,000 | 1,800,000 |
| **Running cost for sludge (R/ton)** | 600 | 150 |
| **Capital cost (R)** | ~400,000,000 | ~1,600,000,000 |
| **Capital cost divided in a period of 10 years instalments to pay the loan (R/y)** | ~40,000,000 | ~160,000,000 |
| **Total cost sludge treatment (R/ton)** | ~4,000 | ~14,000 |

* Breakdown of the prototype development cost in Appendix F

In summary, the screw conveyer presents lower running cost than the greenhouse, but a much higher capital cost and higher overall treatment cost. At the current stage, the prototypes represent promising faecal sludge treatment technologies with relatively low surface are footprint and running costs. It is expected that the future design improvement and operation optimization will decrease the capital and running costs of the prototypes. In the future, tests will have to be undertaken in more realistic conditions (e.g. using faecal sludge as feedstock and higher feeding rates) and more precise information will have to be obtained in order to conduct a more precise techno-economic analysis.

## 5.4 AREA OF IMPROVEMENT AND OPTIMIZATION OF PROTOTYPES

After the testing and analysis of the results, areas for the improvement and optimization of the prototypes were identified as displayed in Table 5.4, which will allow to decrease the capital and running costs of the systems.

**Table 5.4. Major areas of improvement and optimization identified of the prototypes**

| Greenhouse solar drier | Screw conveyer solar drier |
|---|---|
| Decrease the ventilation and circulation fans capacity (too high for the moment) | Decrease the ventilation fans capacity (too high for the moment) |
| Circulation fans at the top instead the sides (as the hottest air accumulates at the top of the greenhouse, above the sludge bed) | Decrease the capacity of the motor driving the auger (too high torque for the moment) |
| Optimization of the ventilation and circulation fans operation (e.g. intermittent operation; to decrease rate as sludge is dried; natural convection) | Change of transparent tube material (use of transparent material more resistant to high temperatures as polycarbonates and glass to limit damage) |
| Optimization of the rake system operation (e.g. to find the optimal operation frequency; | Change of design of DC (e.g. instead using transparent material, use of a glazed metallic |

| | |
|---|---|
| decrease frequency or stop at final stages of drying) | tube painted; build a tube with a hatch for easy of cleaning and maintenance) |
| Operation strategy at night (e.g. to identify the needs of ventilation, air circulation and rake system) | Reduction of stickiness (e.g. additives to sludge to decrease the stickiness; using coating or material reducing adhesion of sludge) |
| - | Improvement of the reflectors (optics and position) |
| | Improvement of the SAH (optimization of operation; combination with PV for electricity generation) |

## 5.5 WRC KNOWLEDGE TREE

The WRC Knowledge Tree elements were addressed in this project, as detailed here below:

- Transformation and Redress: the developed technologies can transform faecal sludge in useful products.
- Sustainable development solutions: the developed technologies are based on solar thermal energy, considered a sustainable source of energy, for the treatment of faecal sludge, a hazardous waste.
- Empowerment of communities: the developed technologies, being relatively simple of operation, could be installed in communities and operated by the after a training.
- Informing policy and decision making: the developed technologies could be included as part of the strategies from municipalities across South Africa for faecal sludge management.
- Human Capital Development in Water and Science sector: involved students for their design, commissioning and testing.
- New products and services for economic development: the developed technologies have the potential to be commercialised.

## 5.6 CAPACITY BUILDING

The list with the details of the students involved in the overall of the project is displayed in Table 5.5.

**Table 5.5. Details of the students involved in the project**

| Name | Gender | Race | Nationality | Degree in course | Affiliation | Year | Task |
|---|---|---|---|---|---|---|---|
| **Léa Guyomarch** | Female | White | French | MScEng | University of Poitiers | 2019 | Solar assessment and preliminary trial in the solar drier from the previous project (K5/2582) |
| **Balakathan Iyer** | Male | Indian | South African | BScEng | UKZN | 2020 | Development of screw conveyor |
| **Thandeka Masango** | Female | African Black | South African | BScEng | UKZN | 2020 | |
| **Akhil Ramlucken** | Male | Indian | South African | MScEng | UKZN | 2020-2022 | Development and testing of screw conveyor |
| **Pareshin Naidoo** | Male | Indian | South African | MScEng | UKZN | 2020-2022 | Development and testing of greenhouse |
| **Santhiran Naidoo** | Male | Indian | South African | BScEng | UKZN | 2021 | Solar drying tests in the solar drier from the previous project (K5/2582) |
| **Leenald Aungunu** | Male | Indian | South African | BScEng | UKZN | 2021 | |
| **Adheesh Ganapathie** | Male | Indian | South African | BScEng | UKZN | 2022 | Support in the testing of the prototypes |
| **Yashlen Pater** | Male | Indian | South African | BScEng | UKZN | 2022 | |
| **Renaldo Soni** | Male | Indian | South African | BScEng | UKZN | 2022 | Installation of electronics in the greenhouse solar-drier |

## 5.7 KNOWLEDGE DISSEMINATION

The knowledge created in this project was disseminated during various conferences and events, including:

- Flash presentation of the PhD student during the UKZN Postgraduate Research and Innovation Symposium (PRIS) 2021.
- Poster presentation for the 22nd International Drying Symposium (IDS) 2022 (25-27 June in Worcester, US), with a paper in the conference proceedings.
- Oral presentation for the 9th International Conference on Engineering for Waste and Biomass Valorisation (WasteEng) 2022 (27-30 June in Copenhagen, Denmark).

- Oral presentation for the 1st International Conference on Sustainable Chemical and Environmental Engineering (SUSTENG) 2022 (31 August to 4 September in Crete, Greece), with a paper in the conference proceedings.
- 2 oral presentations during the WISA 2022 Biennial Conference and Exhibition in Johannesburg, Pretoria (28-30 September in Johannesburg, South Africa).

One or two papers with the outcomes from this investigation are planned in peer-review journals. Two MSc dissertations related to this project are expected to be ready by the beginning or the middle of 2023.
All the material from knowledge dissemination can consulted in the Supporting Documents D.

# 6 WAY FORWARD

Considering Phase 0 as the previous project where the use of solar thermal energy for faecal sludge drying was explored through a bench-scale apparatus (Research ProjecK5/2582) and Phase I as the current project where the solar thermal drying prototypes were developed and the initial testing was conducted to validate the technologies (Research Project K5/2897), Phase II consists in the new project to test, improve and optimize the prototypes towards commercialisation.

Phase II has been secured after obtaining funding from the Royal Academy of Engineering through the 'Transformation Systems through Partnership' grant, in collaboration with Swansea University (Wales, United Kingdom) in 2021. These funds will enable to carry on with the testing of the greenhouse and screw conveyor solar drier and perform modifications for the improvement of the systems. Moreover, Swansea University will perform computational fluid dynamics (CFDs) simulations of the solar thermal systems for their optimization, through student projects.

Another prototype could be included in the project, consisting in the solar thermal dryer developed by Swansea University under the "Reinvent the Toilet Challenge" from the Bill & Melinda Gates Foundation. The testing will be done with real sludge, so the prototypes will have to be moved to the pilot sanitation plant in Newlands-Mashu for health and safety reasons (at UKZN, experiments with sludge are not permitted outside the WASH R&D Centre laboratory, whereas the prototypes need to be tested at the open-air to get exposure to the solar radiation).

At the end of Phase II, it is expected that the solar thermal drying technologies will gain in maturity for their implementation in the field. As final goal, an application to the SASTeP (South Africa Sanitation Technology Platform) program is set to be submitted to the WRC by 2024, following the outcomes from Phase II, to support the commercialisation of the solar thermal technologies (which will correspond to Phase III).
The program of Phase II is summarised in Table 6.1.

**Table 6.1. Program of Phase II**

| **Project milestones** | *Commissioning of the solar thermal dryers in the testing site* | *Testing, improvement and optimization of the solar thermal dryers* | *Development of a market strategy and business case* |
|---|---|---|---|
| **Decision criteria for each milestone** | Commissioning of the solar thermal dryers in the testing site | Validation of the systems improvement and optimization through further testing | Pre-commercialisation strategy fully prepared |
| **Timeline** | November 2022 to March 2023 | March to November 2023 | November 2023 to March 2024 |
| **Activities per milestone** | - Preparation of the logistics to move the prototypes from UKZN to the testing site<br>- Preparation of the logistics to collect the sludge<br>- Transport and installation of the prototypes in the testing site<br>- Preparation of the testing plan<br>- Preparation personnel | - Tests of the prototypes using real sludge<br>- Data analysis<br>- Modifications of the prototypes based on the testing results<br>- Determination of the most optimal operating conditions based on the testing results<br>- Optimization of the systems through computational simulations<br>- Reporting of the results | - Data compilation from the testing campaigns<br>-Techno-economic analysis<br>- Market study in sanitation technologies<br>- Search of industrial partners<br>- Preparation of SASTEP application |

The local partners involved in Phase II are:

- The eThekwini municipality, which can offer the platform to test the technologies with municipal sludges and can involve their staff in the prototype testing (for example, one of the engineers from the municipality is conducting a part-time MSc related to this project);
- Khanyisa Project, which will offer the contractor services required for commissioning of the prototypes (when they will be moved to the Newlands-Mashu pilot plant).
- Mangosuthu University of Technology, which will offer the participation of students from historically disadvantage background in the project.
- EnviroSan, which could be interested in downscaling the solar thermal technologies as back-end treatment systems in a re-engineered toilet.

The collaboration with Swansea University will encompass a series of diverse activities related to this project, such as student exchange and organisation of a workshop for transfer of knowledge.

Other institutions have been approached to support financially Phase II and start the preparation of the commercialisation of the product for the future (Phase III), among which:

- Technology Innovation Agency (through a SEEDS application).
- The Water & Sanitation division from eThekwini municipality that is willing to include financial support to the project in the Memorandum of Understanding with the WASH R&D Centre (discussions in progress).
- DSI and TIA (under initial conversations).
- WRC SASTEP (under initial conversations).

International institutions have shown interest in the prototypes, such as:

- The sanitation social enterprise ‘Sanergy’ (Kenya) that is willing to host the prototypes in a future.
- The sanitation service provider ‘Delvic’ (Senegal) that have demonstrated a similar interest.

- The company ‘Vivunes’ (India), manufacturer of solar thermal drying equipment, which is interested to apply the developed technologies in India.

# 7 APPENDICES

## 7.1 APPENDIX A: TESTING PROCEDURE IN THE GREENHOUSE SOLAR DRIER

### 7.1.1 Testing procedure

#### 7.1.1.1 *Functionality Testing*

The procedure for this phase is carried out as follows:

1) Testing of the various sub systems individually
2) Ensure all sub systems are correctly assembled and working effectively
3) Ensure all electronics are functional and working correctly
4) Connecting electronics to power
5) Calibration of the fans according to the power consumption & fan speeds
6) Record of temperature & humidity at the various points in the dryer
7) Thermal imaging camera to determine temperature of the different surfaces in the dryer
8) Ensure the sub systems are working efficiently without any obstacles or problems occurring
9) Removal of memory card at the end of testing to record temperature and humidity data
10) Disconnect power from the system

#### 7.1.1.2 *Tests with water*

The procedure for the water tests is carried out as follows:

1) Water is poured into crucibles until both crucible and water measure a combined mass of 100 grams
2) Crucibles are placed at assigned positions in the dryer on the drying tray
3) Fans and temperature and humidity control system is connected to power
4) Laptop is used to monitor temperature and humidity system and ensure data is being recorded correctly
5) Ventilation and circulation fans are set accordingly, and ventilation speeds are adjusted on hourly intervals
6) Mass of water and crucibles are measured and recorded on hourly intervals
7) After testing is concluded the dryer electronics are turned off
8) Micro SD card is removed, and data stored on a laptop for evaluation
9) Micro SD card is placed back in electronic boxes
10) Crucibles are removed from the dryer for further testing

#### 7.1.1.3 *Tests with wet soil*

The procedure for this phase is largely similar to the previous phases, and is carried out as follows:

1) Wet soil of determined mass and moisture content is placed on the drying tray in the dryer
2) A 1-gram sample is removed at the beginning of testing and placed in moisture analyser and result is recorded
3) Fans, rake system and temperature & humidity sensors are powered on. Tests are done with and without the rake system in operation so when rake system is not in operation rake system plug is removed
4) Temperature & humidity control system is monitored using a laptop to ensure sensors and control system is working correctly
5) A 1-gram sample of soil is removed every hourly interval to determine the amount of moisture removed from soil.
6) At the end of testing the electronics are turned off and a final sample of soil is removed and placed in the moisture analyser and results recorded.
7) The micro-SD card is removed and stored on laptop
8) The soil is emptied from the drying tray and testing rig cleaned

#### 7.1.1.4 *Tests with synthetic sludge*

The procedure for this phase is largely similar to the previous phases, and is carried out as follows:

1) Synthetic sludge is dropped on the drying tray in the dryer
2) Rake system is positioned to its starting position nearer to the door
3) Electronics was connected and ventilation &circulation fans both set at speed 1
4) 1-gram Samples of synthetic sludge is removed every hour and placed in a moisture analyser and moisture content is recorded
5) Synthetic sludge is left to dry
6) Micro SD card data is extracted at the end of testing
7) At the end of testing sludge is removed from tray
8) Rig is inspected and cleaned

### 7.1.2 Data analysis

#### 7.1.2.1 *Output parameters*

The measured parameters needed to determine moisture removal, dryer efficiency, drying rate and specific energy consumption are as follows:

- Temperature (°C)
- Humidity (%)
- Solar irradiance (I)
- Power consumption (W)
- Mass of drying product (kg)
- Moisture content (%)
- Drying time (hour)

These parameters are measured during drying and are needed to determine the performance parameters of the system, together with the effective area exposed to solar irradiance, the surface area of drying product and latent heat of vaporisation of water to calculate dryer efficiency, drying rate and specific energy consumption.

#### 7.1.2.2 *Data treatment*

Data is stored as text file and is imported into excel where data is labelled. Time, temperature & humidity is recorded for the 6 sensors in and around the greenhouse. The data is treated in excel and graphs are developed. Solar irradiance is recorded on a micro-SD card as an excel file.

## 7.2 APPENDIX B: DATA FROM TESTS IN THE GREENHOUSE SOLAR DRIER

### 7.2.1 Functionality tests

The ventilation system was calibrated by measuring the volumetric flow rate of air for the various speed settings on the fan potentiometer with the use of a vain anemometer. Calibrated ventilation and circulation speeds is shown in Table 7.1.

**Table 7.1. Ventilation and Circulation calibration**

| Circulation fans | | | fan diameter =300 mm |
|---|---|---|---|
| Setting | Speed(m/s) | flow rate ($m^3/s$) | flow rate ($m^3/h$) |
| 1 | 2 | 0.141 | 508.68 |
| 2 | 2.2 | 0.155 | 559.54 |
| 3 | 2.6 | 0.183 | 661.28 |
| 4 | 3 | 0.211 | 763.02 |
| 5 | 4 | 0.282 | 1017.36 |
| 6 | 5 | 0.353 | 1271.70 |
| 7 | 6.5 | 0.459 | 1653.21 |
| 8 | 7.5 | 0.529 | 1907.55 |
| 9 | 7.8 | 0.551 | 1983.85 |
| 10 | 8 | 0.565 | 2034.72 |
| | | | |
| Ventilation fans | | | fan diameter = 204 mm |
| Setting | Speed (m/s) | flow rate ($m^3/s$) | flow rate ($m^3/h$) |
| 1 | 2.5 | 0.081 | 294.01 |
| 2 | 2.9 | 0.094 | 341.05 |
| 3 | 3.15 | 0.102 | 370.46 |
| 4 | 3.6 | 0.117 | 423.38 |
| 5 | 4.6 | 0.150 | 540.99 |
| 6 | 5.5 | 0.179 | 646.83 |
| 7 | 6.24 | 0.203 | 733.86 |
| 8 | 7.1 | 0.231 | 835.00 |
| 9 | 8.15 | 0.266 | 958.49 |
| 10 | 8.6 | 0.280 | 1011.41 |

The power consumption drawn from the various sub-systems is shown in Table 7.2.

**Table 7.2. Power consumption for the various electrical components**

| Circulation and ventilation power consumption for the various circulation and ventilation speeds | | | | | | | | | | | | |
|---|---|---|---|---|---|---|---|---|---|---|---|---|
| | | Ventilation | | | | | | | | | | |
| | | V0 | v1 | v2 | v3 | v4 | v5 | v6 | v7 | v8 | v9 | v10 |
| Circulation | C0 | 0 Watts | 83 | 101 | 120 | 147 | 187 | 210 | 224 | 232 | 240 | 250 |
| | c1 | 96 | 170 | 190 | 210 | 230 | 265 | 290 | 300 | 310 | 320 | 330 |
| | c2 | 118 | 182 | 200 | 220 | 245 | 280 | 310 | 325 | 333 | 340 | 350 |
| | c3 | 138 | 200 | 220 | 240 | 260 | 300 | 330 | 350 | 355 | 360 | 370 |
| | c4 | 165 | 230 | 250 | 270 | 290 | 330 | 350 | 370 | 380 | 390 | 400 |
| | c5 | 198 | 260 | 280 | 300 | 320 | 360 | 380 | 400 | 405 | 415 | 420 |
| | c6 | 220 | 280 | 300 | 320 | 340 | 380 | 405 | 420 | 430 | 440 | 445 |
| | c7 | 240 | 300 | 320 | 340 | 360 | 400 | 425 | 440 | 450 | 460 | 465 |
| | c8 | 260 | 320 | 340 | 360 | 380 | 415 | 440 | 455 | 465 | 470 | 480 |
| | c9 | 280 | 330 | 360 | 380 | 400 | 430 | 460 | 470 | 480 | 485 | 495 |
| | c10 | 300 | 360 | 380 | 400 | 420 | 450 | 485 | 500 | 510 | 515 | 525 |
| 2. Temp Control System – 1 W | | | | | | | | | | | | |
| 3. Rake system – 96 W on start-up & 93 W running | | | | | | | | | | | | |

Table 7.3 shows the temperature difference between the air inside the dryer as compared to the temperature of ambient air outside the dryer and greenhouse dryer temperature tests with ventilation on.

**Table 7.3. Enclosure dry tests**

| Time | Outside Temp(°C) | Enclosure Temp(°C) | Enclosure Temp(°C) – ventilation full | Enclosure Temp(°C) – ventilation half |
|---|---|---|---|---|
| 09:00 | 25.5 | 36.5 | 33.2 | 31.2 |
| 09:30 | 34.4 | 42.9 | 41.2 | 40.2 |
| 10:00 | 34.3 | 43.7 | 38.3 | 37.5 |
| 10:30 | 34.4 | 43.1 | 38.1 | 37.6 |
| 11:00 | 32.2 | 42.9 | 38 | 38.7 |
| 11:30 | 31.3 | 42.4 | 38.5 | 39.6 |
| 12:00 | 30 | 41.4 | 37.6 | 36.8 |

The absorber walls reached temperatures of around 60°C on days when ambient temperatures were less than 30°C. Figure 7.1 shows images of the absorber wall and the thermal imaging was taken.

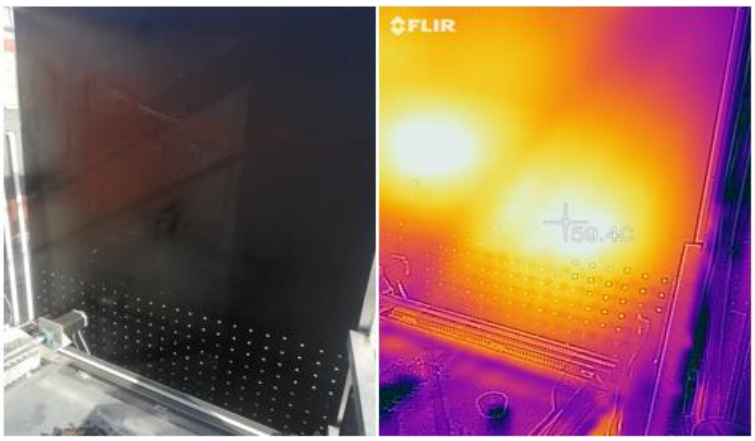


**Figure 7.1. Thermal imaging took using a FLIR 1 camera**

The rake system was working initially with a smaller motor. When the sand was used the motor began to stall. Therefore, the small Nema18 was replaced with a *Nema34* high-torque stepper motor. The rake system is observed to ensure no failure or obstacles affect the rake's operation or components. The system had to be lubricated for the guide rail to travel smoothly.

### 7.2.2 Water tests

Table 7.4 shows the raw data achieved from tests conducted with C3. Temperatures (T) and humidity(H) for the various positions in the dryer are listed separately. Solar irradiance and the mass of water measured every 30-minute interval are also recorded.

**Table 7.4. Temperature and humidity measured during the water tests with C3 at varying ventilation rates (28/07/2022)**

| Ventilation | 28/07/2022 | Collector | | DC elevated | | DC outlet | | DC floor | | DC inlet | | Ambient inlet | | | | |
|---|---|---|---|---|---|---|---|---|---|---|---|---|---|---|---|---|
| | Hour | T1 | H1 | T2 | H2 | T3 | H3 | T4 | H4 | T5 | H5 | T6 | H6 | Solar Irradiance | mass 1 | mass 2 |
| V0 | 09:30 | 30,7 | 49,3 | 38,6 | 33,8 | 34,3 | 43,2 | 27,5 | 45,9 | 32,8 | 43,3 | 31,4 | 43,9 | 383,96 | 100 | 100 |
| V1 | 10:00 | 33,2 | 43,1 | 41,6 | 29,6 | 37,1 | 37,8 | 31,7 | 39,5 | 37,3 | 35,6 | 29,1 | 44,7 | 460,21 | 100 | 100 |
| V1 | 10:30 | 27,2 | 57,1 | 32,9 | 42,3 | 30,8 | 51 | 29,8 | 42,2 | 31,6 | 44,4 | 23,2 | 69,1 | 575,56 | 96 | 98 |
| V4 | 11:00 | 29 | 52,4 | 35,3 | 37,7 | 31,9 | 47,8 | 31 | 40,2 | 32 | 42,8 | 23,4 | 67,8 | 530,59 | 94 | 97 |
| V7 | 11:30 | 26,5 | 58,8 | 32,3 | 41,7 | 29,3 | 54,8 | 28,1 | 44,7 | 29,1 | 48,4 | 22,9 | 71,5 | 540,37 | 92 | 95 |
| V10 | 12:00 | 26,6 | 60,4 | 32,3 | 42,3 | 29,2 | 56,5 | 28,1 | 45,4 | 28,5 | 50,7 | 23,1 | 70,3 | 552,1 | 91 | 94 |
| v1 | 12:30 | 32,4 | 44 | 39,6 | 31,4 | 37,4 | 37,4 | 36,4 | 33,1 | 36,4 | 36 | 25 | 61 | 548,19 | 88 | 92 |
| V4 | 13:00 | 29,8 | 49,3 | 37 | 34,4 | 34,1 | 42,8 | 32,7 | 37,3 | 34 | 38,5 | 24,2 | 64,9 | 534,5 | 86 | 91 |
| V7 | 13:30 | 27,3 | 55,2 | 33,1 | 38,8 | 30,3 | 50,7 | 29,5 | 41,8 | 30,5 | 43,9 | 23,9 | 65,3 | 493,45 | 83 | 89 |
| V10 | 14:00 | 27,7 | 54 | 32,8 | 39,8 | 31,1 | 50 | 29 | 42,1 | 31,1 | 43,9 | 24,3 | 63,3 | 446,52 | 82 | 88 |

Table 7.5 shows the performance data calculated from water tests with circulation speed 3.

**Table 7.5. Performance parameters during the water tests with C3 at varying ventilation rates (28/07/2022)**

| Ventilation speed | Hour | P.C (watts) | ΔM(kg) | DR (kg/h $m^2$) | Dryer eff (%) | SEC (kWh/ton) |
|---|---|---|---|---|---|---|
| V0 | 09:30 | 1 | 0 | 0 | 0 | 0 |
| V1 | 10:00 | 200 | 0 | 0 | 0 | 0 |
| V1 | 10:30 | 200 | 0,003 | 2,527 | 0,212 | 6917 |
| V4 | 11:00 | 260 | 0,0015 | 1,263 | 0,126 | 24500 |
| V7 | 11:30 | 350 | 0,002 | 1,684 | 0,164 | 28000 |
| V10 | 12:00 | 370 | 0,001 | 0,842 | 0,081 | 62500 |
| v1 | 12:30 | 200 | 0,0025 | 2,106 | 0,203 | 8300 |
| V4 | 13:00 | 260 | 0,0015 | 1,263 | 0,125 | 24500 |
| V7 | 13:30 | 350 | 0,0025 | 2,106 | 0,225 | 22400 |
| V10 | 14:00 | 370 | 0,001 | 0,842 | 0,100 | 92500 |

The results from the water tests for the various circulation and ventilation deviations are shown in the tables below.

**Table 7.6. Temperature and humidity measured during the water tests with C10 at varying ventilation rates (02-08-2022)**

| Circulation speed 10 | 02/08/2022 | Collector | | DC elevated | | DC outlet | | DC floor | | DC inlet | | Ambient inlet | | | | |
|---|---|---|---|---|---|---|---|---|---|---|---|---|---|---|---|---|
| Ventilation speed | Hour | T1 | H1 | T2 | H2 | T3 | H3 | T4 | H4 | T5 | H5 | T6 | H6 | Irradiance | mass 1 | mass 2 |
| V1 | 11:30 | 34.5 | 37.9 | 41.6 | 28.7 | 36.6 | 36.1 | 30 | 38.4 | 40.4 | 29.1 | 28.8 | 52.8 | 569.69 | 100 | 100 |
| V1 | 12:00 | 31.9 | 41.7 | 35.2 | 34.9 | 31.5 | 46.6 | 33.6 | 34.2 | 35.3 | 34.3 | 24.5 | 62.2 | 565.75 | 97 | 98 |
| v1 | 12:30 | 31.3 | 43.8 | 34.5 | 36.6 | 30.9 | 48.7 | 33.3 | 35 | 34.2 | 36.2 | 24.1 | 64.9 | 559.92 | 93 | 95 |
| V4 | 13:00 | 27.7 | 52.1 | 33.5 | 38.3 | 32.3 | 46.6 | 31.4 | 37.9 | 32.8 | 39.8 | 23 | 71.5 | 536.46 | 90 | 93 |
| V7 | 13:30 | 25.6 | 61.2 | 30.7 | 45.1 | 28.9 | 57.3 | 28.1 | 43.8 | 28.8 | 48.7 | 22.3 | 75.8 | 499.31 | 88 | 92 |
| V10 | 14:00 | 25.5 | 64.3 | 29.5 | 48.5 | 27.9 | 61.7 | 26.8 | 46 | 27.5 | 52.2 | 21.7 | 79.1 | 440.66 | 87 | 91 |

**Table 7.7. Performance parameters during the water tests with C10 at varying ventilation rates (02-08-2022)**

| Ventilation speed | Hour | P, C (watts) | ΔM(kg) | DR (kg/h $m^2$) | Dryer eff (%) | SEC (Kw h/ton) |
|---|---|---|---|---|---|---|
| V0 | 11:30 | 150 | 0 | 0,00 | 0,00 | 0 |
| V1 | 12:00 | 300 | 0,0025 | 2,11 | 0,20 | 113150 |
| v1 | 12:30 | 300 | 0,0035 | 2,95 | 0,28 | 79989 |
| V4 | 13:00 | 450 | 0,0025 | 2,11 | 0,21 | 107292 |
| V7 | 13:30 | 500 | 0,0015 | 1,27 | 0,13 | 166437 |
| V10 | 14:00 | 525 | 0,001 | 0,84 | 0,10 | 220330 |

**Table 7.8. Temperature and humidity measured during the water tests with C0 and C6 at varying ventilation rates (04-08-2022)**

| No Circulation | | | | | | | | | | | | | | | | |
|---|---|---|---|---|---|---|---|---|---|---|---|---|---|---|---|---|
| Ventilation speed | 04/08/2022 | Collector | | DC elevated | | DC outlet | | DC floor | | DC inlet | | Ambient inlet | | | | |
| | Hour | T1 | H1 | T2 | H2 | T3 | H3 | T4 | H4 | T5 | H5 | T6 | H6 | Solar Irradiance | mass 1 | mass 2 |
| V0 | 09:30 | 30.3 | 39.6 | 36.2 | 39.8 | 33.8 | 30.7 | 32.7 | 38.6 | 33.7 | 43.5 | 27 | 53.2 | 383.96 | 100 | 100 |
| V0 | 10:00 | 31.5 | 30.8 | 39.8 | 33.8 | 36.4 | 33.2 | 35.2 | 34.9 | 37.1 | 36.9 | 24.8 | 58.8 | 395.65 | 100 | 100 |
| V1 | 10:30 | 28.1 | 39.4 | 34.1 | 41.2 | 31.4 | 33.7 | 30.6 | 40.6 | 32 | 43.8 | 23.3 | 58.4 | 491.47 | 99 | 99 |
| V4 | 11:00 | 25.1 | 44.4 | 29.6 | 53.5 | 27.4 | 39.4 | 26.8 | 47.9 | 27.4 | 55.8 | 22.5 | 63.2 | 507.13 | 98 | 98 |
| V7 | 11:30 | 26.4 | 41.3 | 32 | 46.1 | 29.1 | 34.3 | 28 | 45.8 | 28.7 | 53 | 24.3 | 57.5 | 534.5 | 96 | 97 |
| V10 | 12:00 | 32.5 | 34.3 | 35.5 | 40.6 | 33.9 | 31.9 | 31 | 41.3 | 32.3 | 46.7 | 31.9 | 40.6 | 548.19 | 95 | 96 |
| Circulation 6 | | | | | | | | | | | | | | | | |
| Ventilation speed | 04/08/2022 | Collector | | DC elevated | | DC outlet | | DC floor | | DC inlet | | Ambient inlet | | | | |
| | Hour | T1 | H1 | T2 | H2 | T3 | H3 | T4 | H4 | T5 | H5 | T6 | H6 | Solar Irradiance | mass 1 | mass 2 |
| V0 | 12:00 | 32.4 | 53.6 | 36.2 | 39.7 | 34.2 | 50.9 | 31.4 | 69.6 | 33.3 | 44.6 | 27.6 | 56.4 | 533.8 | 100 | 100 |
| V0 | 12:30 | 30.3 | 44.7 | 36.7 | 32.8 | 35.1 | 38.7 | 34.3 | 33.1 | 36.4 | 33.5 | 25.5 | 66.5 | 544.28 | 97 | 98 |
| V1 | 13:00 | 29.9 | 44.1 | 36.1 | 32.7 | 33.6 | 37.2 | 33.8 | 32.9 | 34.5 | 32 | 25.3 | 64.4 | 540.37 | 93 | 95 |
| V4 | 13:30 | 28.5 | 48.3 | 34.3 | 35.9 | 32.1 | 44.3 | 31.1 | 36.9 | 32.3 | 39.1 | 24.9 | 70.2 | 518.86 | 90 | 93 |
| V7 | 14:00 | 28.5 | 51.6 | 32.6 | 39.5 | 31.3 | 50.1 | 29.3 | 41.2 | 31.1 | 43.4 | 25.6 | 77.5 | 502.36 | 87 | 91 |
| V10 | 14:30 | 28.6 | 52.5 | 31.9 | 42 | 29.9 | 54.7 | 28.9 | 41.8 | 29.5 | 46.8 | 23.8 | 81.4 | 480.56 | 85 | 89 |

**Table 7.9. Performance parameters during the water tests with C0 and C6 at varying ventilation rates (04-08-2022)**

| No Circulation (C0) | | | | | |
|---|---|---|---|---|---|
| Ventilation speed | P, C (watts) | ΔM (kg | DR (kg/h $m^2$) | Dryer eff (%) | SEC (Kw h/ton) |
| V0 | 0 | 0 | 0 | 0 | 0 |
| V0 | 1 | 0 | 0 | 0 | 0 |
| V1 | 83 | 0,001 | 0,842105 | 0,0678 | 20750 |
| V4 | 120 | 0,001 | 0,842105 | 0,0657 | 36750 |
| V7 | 224 | 0,0015 | 1,263158 | 0,0935 | 37333,33 |
| V10 | 250 | 0,001 | 0,842105 | 0,0608 | 62500 |
| Circulation 6 (C6) | | | | | |
| Ventilation speed | P, C (watts) | ΔM (kg | DR (kg/h $m^2$) | Dryer eff | SEC (Kw h/ton) |
| V0 | 0 | 0 | 0 | 0 | 0 |
| V0 | 1 | 0,0025 | 2,105263 | 0,1531 | 200 |
| V1 | 280 | 0,0035 | 2,947368 | 0,2159 | 5928,571 |
| V4 | 340 | 0,0025 | 2,105263 | 0,1606 | 14700 |
| V7 | 440 | 0,0025 | 2,105263 | 0,1659 | 22400 |
| V10 | 465 | 0,002 | 1,684211 | 0,1387 | 31250 |

**Table 7.10. Temperature and humidity measured during the water tests with C10 at varying ventilation rates (05-08-2022)**

| Circulation speed 10 | | | | | | | | | | | | | |
|---|---|---|---|---|---|---|---|---|---|---|---|---|---|
| Ventilation speed | 05/08/2022 | Collector | | DC elevated | | DC outlet | | DC floor | | DC inlet | | Ambient inlet | |
| | Hour | T1 | H1 | T2 | H2 | T3 | H3 | T4 | H4 | T5 | H5 | T6 | H6 | Solar Irradiance |
| V0 | 09:30 | 30,2 | 39,8 | 36,1 | 39,9 | 33,8 | 50,9 | 32,6 | 38,7 | 33,7 | 43,6 | 26,8 | 55,8 | 428,56 |
| V1 | 10:00 | 31,5 | 30,9 | 39,8 | 33,8 | 36,4 | 43,2 | 35,2 | 34,9 | 37,1 | 36,9 | 24,8 | 69,1 | 493,45 |
| V1 | 10:30 | 28,1 | 39,7 | 34,2 | 41,2 | 31,4 | 43,8 | 30,6 | 40,8 | 32,1 | 44 | 23,5 | 57,7 | 569,69 |
| V4 | 11:00 | 25,1 | 33,3 | 28,8 | 48,3 | 27,2 | 49,2 | 26,9 | 47,5 | 27,2 | 45,5 | 22,5 | 61,5 | 571,61 |
| V7 | 11:30 | 26,4 | 31,3 | 32 | 46,1 | 29,1 | 44,3 | 28 | 45,8 | 28,7 | 53 | 24,3 | 59,9 | 659 |
| V10 | 12:00 | 32,6 | 33,8 | 35,7 | 40,5 | 33,9 | 40,5 | 31,1 | 40,9 | 33,1 | 44,8 | 31,1 | 51,1 | 686 |

**Table 7.11. Performance parameters during the water tests with C10 at varying ventilation rates (05-08-2022)**

| mass 1 | mass 2 | P, C (watts) | ΔM(kg) | DR (kg/h $m^2$) | Dryer eff | SEC (Kw h/ton) |
|---|---|---|---|---|---|---|
| 100 | 100 | 0 | 0 | 0 | 0 | 0 |
| 99 | 99 | 300 | 0,001 | 0,842105 | 0,000676 | 20750 |
| 95 | 97 | 300 | 0,003 | 2,526316 | 0,001755 | 18333,33333 |
| 94 | 96 | 450 | 0,001 | 0,842105 | 0,000583 | 57500 |
| 92 | 95 | 500 | 0,0015 | 1,263158 | 0,000759 | 40000 |
| 90 | 93 | 525 | 0,002 | 1,684211 | 0,000972 | 32500 |

**Table 7.12. Temperature and humidity measured during the water tests with C0 at varying ventilation rates (27-07-2022)**

| No Circulation | | | | | | | | | | | | | | |
|---|---|---|---|---|---|---|---|---|---|---|---|---|---|---|
| Ventilation speed | 27/07/2022 | Collector | | DC elevated | | DC outlet | | DC floor | | DC inlet | | Ambient inlet | | |
| | Hour | T1 | H1 | T2 | H2 | T3 | H3 | T4 | H4 | T5 | H5 | T6 | H6 | Solar Irradiance |
| v1 | 10:00 | 26,3 | 34,7 | 36,6 | 25,9 | 28,8 | 32,9 | 24,6 | 33,9 | 29,3 | 29,6 | 21,3 | 40,4 | 403,51 |
| V1 | 10:30 | 27,5 | 34,5 | 39,5 | 24,6 | 30,7 | 31,3 | 26,5 | 32,9 | 31,6 | 28 | 22,3 | 41,2 | 350,73 |
| V4 | 11:00 | 28,3 | 33 | 38,7 | 24,5 | 30,8 | 30,9 | 28,1 | 31 | 31,5 | 27,8 | 22,8 | 40,1 | 518,86 |
| V7 | 11:30 | 27,2 | 33 | 34,7 | 25,7 | 28,9 | 31,9 | 28,1 | 30,2 | 29,3 | 28,5 | 23,5 | 37,6 | 544,28 |
| V10 | 12:00 | 26,8 | 33,4 | 34,1 | 26,3 | 28,7 | 32,3 | 28 | 30,3 | 28,5 | 29,2 | 23 | 38,6 | 563,83 |
| v1 | 12:30 | 30 | 31,5 | 37,8 | 25,6 | 32,7 | 30,5 | 29,9 | 30,1 | 32,4 | 28 | 24,1 | 39,1 | 552,1 |
| V4 | 13:00 | 24,6 | 37,6 | 27,3 | 32,2 | 25,8 | 36,9 | 25,7 | 33,1 | 25,9 | 32,6 | 21,8 | 42,3 | 530,59 |

**Table 7.13. Performance parameters during the water tests with C0 at varying ventilation rates (27-07-2022)**

| mass 1 | mass 2 | P.C (watts) | ΔM(kg) | DR (kg/h $m^2$) | Dryer eff | SEC (Kw h/ton) |
|---|---|---|---|---|---|---|
| 0,1 | 0,1 | 83 | 0,000 | 0 | 0 | 0 |
| 0,096 | 0,098 | 83 | 0,003 | 2,526714744 | 0,26135964 | 6916,666667 |
| 0,096 | 0,098 | 147 | 0,000 | 0 | 0 | 0 |
| 0,095 | 0,097 | 224 | 0,001 | 0,842238248 | 0,056139405 | 56000 |
| 0,094 | 0,096 | 250 | 0,001 | 0,842238248 | 0,054192852 | 62500 |
| 0,092 | 0,094 | 83 | 0,002 | 1,684476496 | 0,110688482 | 10375 |
| 0,092 | 0,094 | 147 | 0,000 | 0 | 0 | 0 |

### 7.2.3 Soil tests

Soil tests were conducted between the period 10th August 2022 to the 17th August 2022. Two mass quantities were used for the soil testing. These quantities are 1.4 Kg and 15 Kg wet soil at approximately 70 percent moisture content. Soil tests were conducted to observe mixing effect and determine dryer efficiency and performance. The most important quantities to observe is the temperature, humidity, moisture content and power consumption. Water tests were conducted with a set circulation and ventilation speed. Ventilation and circulation speeds were set at speed 1 on the potentiometers. From water tests it was observed lower fan speeds achieved higher temperatures and humidity. Two different mass of soil were conducted during soil tests. These two masses are 1.4 kg and 15 kg. The soil tests temperatures, humidity, solar irradiance and moisture content for the various days of testing is shown in the Tables below.

**Table 7.14. Testing data of 1.4 kg soil dried with the rake system not in operation (10/08/2022)**

| No rake operating 1.4 kg of wet soil | | | | | | | | | | | | | | |
|---|---|---|---|---|---|---|---|---|---|---|---|---|---|---|
| 10/08/2022 | Collector | | DC elevated | | DC outlet | | DC floor | | DC inlet | | Ambient inlet | | | |
| Hour | T1 | H1 | T2 | H2 | T3 | H3 | T4 | H4 | T5 | H5 | T6 | H6 | Solar Irradiance | MC(%) |
| 10:00 | 41.4 | 27.5 | 40.5 | 31.3 | 36 | 37.1 | 34.7 | 42.2 | 36.3 | 33.4 | 25.4 | 43.5 | 552.1 | 60 |
| 11:00 | 43 | 26.9 | 43.3 | 29.6 | 38.4 | 34.5 | 37.3 | 39.1 | 39.7 | 29.9 | 27.3 | 42.1 | 628.34 | 54 |
| 12:00 | 43.9 | 27.1 | 46.5 | 28.4 | 40.7 | 32.6 | 39.3 | 37.1 | 42.8 | 28.1 | 27.5 | 42.8 | 681.13 | 38 |
| 13:00 | 43.5 | 26.9 | 46.5 | 28.2 | 40.8 | 32.4 | 39.4 | 37 | 43 | 28 | 27.6 | 43 | 663.53 | 32 |
| 14:00 | 40.2 | 30.1 | 47.3 | 28.8 | 40.3 | 35.2 | 38.9 | 38.9 | 43.5 | 29.1 | 26.7 | 47.1 | 563.83 | 26 |
| 15:00 | 35.6 | 37.1 | 43.6 | 31.4 | 35.2 | 43.1 | 35.9 | 43.4 | 40 | 31.7 | 26 | 50.7 | 417.4 | 22 |

**Table 7.15:Performanc calculations for hourly intervals (10/08/2022)**

| P,C (watts) | ΔM(%) | ΔM(KG) | DR (kg/h $m^2$) | Dryer eff | SEC (Kw h/ton) |
|---|---|---|---|---|---|
| 170 | 0 | 0 | 0 | 0 | 0 |
| 170 | 6 | 0,0840 | 0,7 | 2,228 | 2023,809 |
| 170 | 16 | 0,2105 | 1,754 | 5,152 | 807,370 |
| 170 | 6 | 0,0663 | 0,552 | 1,665 | 2563,081 |
| 170 | 6 | 0,0623 | 0,519 | 1,842 | 2726,682 |
| 170 | 4 | 0,0390 | 0,325 | 1,560 | 4351,089 |

**Table 7.16: Overall performance calculations**

| Quantity | rake | Unit |
|---|---|---|
| Mwi | 0,81 | Kg |
| Ms | 0,59 | Kg |
| Mwf | 0,17 | Kg |
| | | |
| Drying Rate | 0,13 | kg/Hour |
| Drying Rate | 1,07 | kg/Hour/m^2 |
| SEC | 2494,41 | KW h/ton |
| Efficiency | 4,41 | % |

**Table 7.17. Testing data of 1.4 kg soil dried with the rake system in operation (11/08/2022)**

rake operating 1,4 kg of wet soil

| 11/08/2022 | Collector | | DC elevated | | DC outlet | | DC floor | | DC inlet | | Ambient inlet | | | |
|---|---|---|---|---|---|---|---|---|---|---|---|---|---|---|
| Hour | T1 | H1 | T2 | H2 | T3 | H3 | T4 | H4 | T5 | H5 | T6 | H6 | Solar Irradiance | MC (%) |
| 10:00 | 40,2 | 27,5 | 40,5 | 31,3 | 36 | 37,1 | 34,7 | 39,8 | 36,3 | 33,4 | 25,4 | 43,5 | 634,21 | 65 |
| 11:00 | 40,6 | 31,6 | 41,4 | 35,3 | 36,9 | 37 | 35,7 | 39,7 | 37,5 | 36,3 | 25,7 | 50,7 | 677,21 | 55 |
| 12:00 | 41,4 | 31,4 | 43,2 | 33,8 | 38,4 | 44,6 | 37,2 | 47,4 | 39,1 | 34,6 | 26,2 | 51,1 | 747,6 | 45 |
| 13:00 | 39,1 | 35,2 | 43,4 | 33,9 | 38,2 | 45,3 | 37,1 | 47,3 | 39,8 | 34 | 25,7 | 53,5 | 731,2 | 42 |
| 14:00 | 37,4 | 37,3 | 43,7 | 33,5 | 37,9 | 46 | 36,1 | 48,4 | 38,5 | 35,6 | 25,4 | 54,7 | 628,34 | 33 |
| 15:00 | 32,5 | 45,5 | 39,1 | 37,5 | 33,8 | 54 | 32,7 | 53,5 | 34,8 | 41,4 | 24,2 | 57,3 | 468,03 | 21 |

**Table 7.18. Calculated performance parameters for 1.4 kg soil dried (11/08/2022)**

| P, C (watts) | ΔM (%) | ΔM(KG) | DR (kg/h $m^2$) | Dryer eff | SEC (Kw h/ton) |
|---|---|---|---|---|---|
| 235 | 0 | 0 | 0 | 0 | 0 |
| 235 | 10 | 0,140 | 1,17 | 3,45 | 1678,57 |
| 235 | 10 | 0,126 | 1,05 | 2,81 | 1865,08 |
| 235 | 3 | 0,034 | 0,28 | 0,78 | 6907,70 |
| 235 | 9 | 0,099 | 0,82 | 2,63 | 2373,78 |
| 235 | 12 | 0,120 | 1,00 | 4,28 | 1956,41 |

**Table 7.19. Overall performance parameters for 1.4 kg soil (11/08/2022)**

| Quantity | No rake | Rake | Unit |
|---|---|---|---|
| Mwi | 0,91 | 0,91 | Kg |
| Ms | 0,49 | 0,49 | Kg |
| Mwf | 0,74 | 0,13 | Kg |
| | | | |
| Drying Rate | 0,15 | 0,16 | kg/Hour |
| | | | kg/Hour/ |
| Drying Rate | 1,29 | 1,30 | m^2 |
| SEC | 608,93 | 2956,31 | KW h/ton |
| Efficiency | 5,55 | 5,93 | % |

**Table 7.20.Testing data for 15 kg sample of soil dried without the use of rake system (12-08-2022)**

| No rake operating 15kg kg of wet soil | | | | | | | | | | | | | | |
|---|---|---|---|---|---|---|---|---|---|---|---|---|---|---|
| 12/08/2022 | Collector | | DC elevated | | DC outlet | | DC floor | | DC inlet | | Ambient inlet | | | |
| Hour | T1 | H1 | T2 | H2 | T3 | H3 | T4 | H4 | T5 | H5 | T6 | H6 | Solar Irradiance | MC(%) |
| 10:00 | 42.3 | 27.3 | 40 | 34.1 | 36 | 35.9 | 34.7 | 36.43 | 39.1 | 31.8 | 28.2 | 39.3 | 569.69 | 70 |
| 11:00 | 43.4 | 27.5 | 42 | 35.5 | 37 | 39.3 | 36.2 | 38.8 | 40.1 | 32.7 | 29.5 | 40.3 | 702.63 | 48 |
| 12:00 | 46.1 | 24.5 | 46.8 | 29.1 | 41.1 | 29.5 | 39.9 | 29.5 | 42.6 | 27.9 | 32.3 | 33 | 735.87 | 35 |
| 13:00 | 45.1 | 23.3 | 49.9 | 25.6 | 43.3 | 29.6 | 41.5 | 27.5 | 45 | 24.1 | 32.8 | 32.5 | 745.55 | 28 |
| 14:00 | 38.2 | 26.6 | 42.5 | 26.8 | 38.2 | 30.9 | 36.8 | 30.3 | 38.9 | 25.8 | 30 | 32.3 | 516.91 | 24 |
| 15:00 | 34.8 | 41 | 39.6 | 37.3 | 33.7 | 42.8 | 33.7 | 45.2 | 35.2 | 41.1 | 24.7 | 58.2 | 445.34 | 19 |

**Table 7.21. Performance parameters for 15 kg soil tests without the rake system operating (12/08/2022)**

| Time | P. C (watts) | ΔM (%) | ΔM(KG) | DR (kg/h $m^2$) | Dryer eff | SEC (Kw h/ton) |
|---|---|---|---|---|---|---|
| 10:00 | 0 | 0 | 0 | 0 | 0 | 0 |
| 11:00 | 170 | 22 | 3.30 | 5.16 | 78.27 | 51.52 |
| 12:00 | 170 | 13 | 1.52 | 2.38 | 34.44 | 111.77 |
| 13:00 | 170 | 7 | 0.71 | 1.11 | 15.92 | 238.59 |
| 14:00 | 170 | 4 | 0.38 | 0.59 | 12.20 | 448.95 |
| 15:00 | 170 | 5 | 0.45 | 0.71 | 17.01 | 374.13 |

**Table 7.22. Overall performance calculations for 15 kg wet soil test without the use of the rake system**

| Quantity | Amount | Unit |
|---|---|---|
| Mwi | 10,50 | Kg |
| Ms | 4,50 | Kg |
| Mwf | 1,06 | Kg |
| | | |
| Drying Rate | 1,89 | kg/Hour |
| Drying Rate | 2,95 | kg/Hour/m^2 |
| SEC | 424,84 | KW h/ton |
| Efficiency | 50,83 | % |

**Table 7.23. Testing data for 15kg of wet soil with the rake system in operation (17/08/2022)**

| rake operating 15 kg of wet soil | | | | | | | | | | | | | | |
|---|---|---|---|---|---|---|---|---|---|---|---|---|---|---|
| 17/08/2022 | Collector | | DC elevated | | DC outlet | | DC floor | | DC inlet | | Ambient inlet | | | |
| Hour | T1 | H1 | T2 | H2 | T3 | H3 | T4 | H4 | T5 | H5 | T6 | H6 | Solar Irradiance | MC(%) |
| 10:00 | 38.6 | 22.6 | 38.6 | 25.2 | 34.9 | 29.3 | 35.7 | 31.2 | 37 | 23.6 | 26.5 | 47.8 | 677.2 | 70 |
| 11:00 | 39 | 22.1 | 38.9 | 26.2 | 35.1 | 31 | 34.5 | 33.4 | 37.5 | 23.6 | 29.2 | 44.7 | 675.26 | 36 |
| 12:00 | 40.8 | 21.4 | 41.2 | 24.2 | 37.2 | 27.9 | 36.5 | 30.8 | 38.9 | 22.3 | 30.5 | 44.2 | 591.2 | 28 |
| 13:00 | 40.5 | 24.8 | 43.4 | 26.7 | 39 | 31.8 | 38.3 | 34.7 | 40.5 | 25 | 31.8 | 48.4 | 401.56 | 25 |
| 14:00 | 38.5 | 28.5 | 43.7 | 28.3 | 39.4 | 33.9 | 39 | 37.5 | 41.5 | 27.5 | 31.6 | 53.3 | 542.32 | 22 |
| 15:00 | 36.8 | 28.1 | 41.1 | 27.4 | 37.2 | 32.6 | 36.2 | 35.4 | 38.3 | 27 | 31 | 50.9 | 321.4 | 18 |

**Table 7.24. Calculated performance data for 15 kg wet soil with the use of the rake system(17/08/2022)**

| Hour | MC (%) | ΔM (%) | ΔM(KG) | DR (kg/h $m^2$) | Dryer eff | SEC (Kw h/ton) |
|---|---|---|---|---|---|---|
| 10:00 | 70 | 0 | 0.00 | 0.00 | 0.00 | 0 |
| 11:00 | 36 | 34 | 5.10 | 7.97 | 125.88 | 46.08 |
| 12:00 | 28 | 8 | 0.79 | 0.78 | 22.33 | 470.00 |
| 13:00 | 25 | 3 | 0.27 | 0.25 | 11.34 | 1468.75 |
| 14:00 | 22 | 3 | 0.27 | 0.23 | 8.15 | 1591.15 |
| 15:00 | 18 | 4 | 0.34 | 0.28 | 17.78 | 1304.74 |

**Table 7.25. Performance data calculated from 15 kg wet soil test with the use of rake system) (17/08/2022)**

| Quantity | Amount | Unit |
|---|---|---|
| Drying time | 5 | hours |
| Solar irradiance | 582 | $W/m^2$ |
| Avg Power | 238 | W |
| Mwi | 10.5 | Kg |
| Ms | 4.5 | Kg |
| Mwf | 0.988 | Kg |
| Drying Rate | 1.90 | kg/Hour |
| Drying Rate | 2.97 | $kg/Hour/m^2$ |
| SEC | 123.54 | Kwh/ton |
| Efficiency | 72.95 | % |

### 7.2.4 Synthetic sludge

Testing for the first day of testing was stopped at 2 PM due to cloud cover and roof becoming very windy. Temperatures struggled to surpass 40°C but good amounts of sunshine were observed throughout the day. The testing data recorded for the different days of synthetic sludge drying tests is shown in the tables below.

**Table 7.26. Day1 (05/09/2022) testing data for synthetic sludge**

| 05/09/2022 | Collector | | DC elevated | | DC outlet | | DC floor | | DC inlet | | Ambient inlet | | | |
|---|---|---|---|---|---|---|---|---|---|---|---|---|---|---|
| Hour | T1 | H1 | T2 | H2 | T3 | H3 | T4 | H4 | T5 | H5 | T6 | H6 | Solar Irradiance | MC (%) |
| 09:00 | 25.8 | 31.2 | 26.9 | 30 | 24.6 | 39.1 | 23.1 | 40.9 | 25.8 | 29 | 16.1 | 40.9 | 560 | 80.3 |
| 10:00 | 34 | 46.7 | 33 | 50.8 | 30.8 | 40.6 | 29.6 | 47.6 | 35 | 43.5 | 23.2 | 56.4 | 647 | 75.9 |
| 11:00 | 37.3 | 42.9 | 36.9 | 43.4 | 32 | 43.4 | 32.7 | 49.4 | 38.5 | 38.3 | 23.5 | 57.9 | 743 | 73.5 |
| 12:00 | 36.3 | 43.5 | 38.6 | 41.9 | 32.6 | 42.5 | 33.6 | 46.4 | 37.7 | 40.2 | 24.2 | 57.1 | 761 | 71.9 |
| 13:00 | 34.1 | 51.7 | 36.1 | 47.6 | 31.6 | 41.9 | 32.2 | 43.4 | 35 | 43.6 | 24.1 | 58.2 | 700 | 71.5 |
| 14:00 | 32.7 | 55.2 | 37.1 | 45.3 | 33 | 37.1 | 32.3 | 32.2 | 38 | 40.3 | 23.9 | 58.8 | 567 | 69.4 |

**Table 7.27: Calculated performance parameters for day 1 of testing (05/09/2022)**

| Hour | MC (%) | P, C (watts) | ΔM (%) | ΔMdb (KG) | DR (kg/h) | Dryer eff | SEC (Kw h/ton) |
|---|---|---|---|---|---|---|---|
| 09:00 | 80.32 | 0 | 4.081300813 | 0 | 0 | 0 | 0 |
| 10:00 | 75.913 | 235 | 3.151617055 | 0.0620869 | 1.831477 | 53.61435475 | 128.31 |
| 11:00 | 73.52 | 235 | 2.776435045 | 0.0546958 | 0.739109 | 18.84097234 | 317.95 |
| 12:00 | 71.909 | 235 | 2.55985903 | 0.0504292 | 0.426655 | 10.61880935 | 550.80 |
| 13:00 | 71.5 | 235 | 2.50877193 | 0.0494228 | 0.100642 | 2.723098361 | 2335.02 |
| 14:00 | 69.36 | 235 | 2.263707572 | 0.044595 | 0.482777 | 16.10574354 | 486.77 |

**Table 7.28: Day 2 (06/09/2022) testing data for synthetic sludge**

| 06/09/2022 | Collector | | DC elevated | | DC outlet | | DC floor | | DC inlet | | Ambient inlet | | | |
|---|---|---|---|---|---|---|---|---|---|---|---|---|---|---|
| Hour | T1 | H1 | T2 | H2 | T3 | H3 | T4 | H4 | T5 | H5 | T6 | H6 | Solar Irradiance | MC (%) |
| 09:00 | 37 | 38,4 | 35,1 | 43,8 | 30 | 35,2 | 26,4 | 48,2 | 30,4 | 52,5 | 25,9 | 45,8 | 194,33 | 69,36 |
| 10:00 | 30,8 | 48,1 | 31,6 | 54,4 | 29 | 35,4 | 29,2 | 43,3 | 31,6 | 48,8 | 22,5 | 56,3 | 360,5 | 68,1 |
| 11:00 | 27,9 | 53,2 | 27,3 | 51,4 | 25,1 | 52,2 | 25,9 | 56,1 | 29,5 | 50,1 | 21,9 | 59 | 448,48 | 66,68 |
| 12:00 | 36,8 | 39,7 | 39,6 | 39,3 | 34,5 | 35,7 | 34 | 36,1 | 36,9 | 35,3 | 24,1 | 50,8 | 643,98 | 63,52 |
| 13:00 | 32,7 | 42,4 | 32,7 | 42,7 | 28,3 | 39 | 29 | 44 | 35,1 | 35,9 | 24,6 | 48,4 | 426,96 | 59,189 |
| 14:00 | 25 | 48,4 | 25,8 | 49 | 25,1 | 48,2 | 25 | 50,6 | 27,9 | 47,9 | 21,4 | 57 | 112,12 | 57,827 |

**Table 7.29: Calculated performance parameters for day 2 of testing (06/09/2022)**

| Hour | MC (%) | P, C (watts) | ΔM (%) | ΔMdb (KG) | DR (kg/h) | Dryer eff | SEC (Kw h/ton) |
|---|---|---|---|---|---|---|---|
| 09:00 | 69.36 | 0 | 2.26 | 0 | 0 | 0 | 0 |
| 10:00 | 68.1 | 235 | 2.13 | 0.042 | 0.254 | 13.342 | 925.36 |
| 11:00 | 66.68 | 235 | 2.00 | 0.039 | 0.263 | 11.115 | 892.91 |
| 12:00 | 63.52 | 235 | 1.74 | 0.034 | 0.512 | 15.063 | 458.85 |
| 13:00 | 59.189 | 235 | 1.45 | 0.029 | 0.573 | 25.423 | 410.06 |
| 14:00 | 57.827 | 235 | 1.37 | 0.027 | 0.156 | 26.335 | 1507.43 |

**Table 7.30. Day 3 (07/09/2022) testing data for synthetic sludge**

| 07/09/2022 | Collector | | DC elevated | | DC outlet | | DC floor | | DC inlet | | Ambient inlet | | | |
|---|---|---|---|---|---|---|---|---|---|---|---|---|---|---|
| Hour | T1 | H1 | T2 | H2 | T3 | H3 | T4 | H4 | T5 | H5 | T6 | H6 | Solar Irradiance | MC (%) |
| 09:00 | 28.8 | 40 | 27.3 | 42.8 | 25.1 | 43 | 24.1 | 49.2 | 24.9 | 48.8 | 24.5 | 50.1 | 237.3 | 55.23 |
| 10:00 | 30 | 43.5 | 30.8 | 47.1 | 28.4 | 44.4 | 28.8 | 41 | 32.1 | 46.7 | 22.4 | 54.7 | 747.6 | 51.45 |
| 11:00 | 37.3 | 42.5 | 38.4 | 41.7 | 34.7 | 34.8 | 34 | 35.4 | 39.5 | 35.2 | 24 | 54.2 | 790.61 | 38.838 |
| 12:00 | 38.2 | 39.5 | 41.3 | 36.7 | 37 | 35 | 37.5 | 31.4 | 41.7 | 32.8 | 24.6 | 52.9 | 810.16 | 37.858 |
| 13:00 | 35.9 | 43 | 40.7 | 36.1 | 36.4 | 43.4 | 34.9 | 42.5 | 39.5 | 32.8 | 25.2 | 52.4 | 763.24 | 28.697 |
| 14:00 | 34.4 | 47.2 | 39.5 | 37.7 | 35.5 | 44.9 | 34.4 | 42.7 | 37.5 | 33.8 | 24.3 | 55.8 | 626.39 | 22.876 |
| 15:00 | 31.5 | 45.2 | 37.9 | 39.2 | 34 | 47 | 32.8 | 45.4 | 35.3 | 41.4 | 24 | 56.4 | 489.52 | 19.602 |

**Table 7.31.Calculated performance parameters for day 3 of testing (07/09/2022)**

| Hour | MC (%) | P, C (watts) | ΔM (%) | ΔMdb (KG) | DR (kg/h) | Dryer eff | SEC (Kw h/ton) |
|---|---|---|---|---|---|---|---|
| 09:00 | 55.23 | 0.00 | 1.23 | 0.00 | 0.00 | 0.00 | 0.00 |
| 10:00 | 51.45 | 235.00 | 1.06 | 0.02 | 0.34 | 8.67 | 686.48 |
| 11:00 | 38.84 | 235.00 | 0.64 | 0.01 | 0.84 | 20.04 | 280.86 |
| 12:00 | 37.86 | 235.00 | 0.61 | 0.01 | 0.05 | 1.19 | 4626.39 |
| 13:00 | 28.70 | 235.00 | 0.40 | 0.01 | 0.41 | 10.11 | 576.97 |
| 14:00 | 22.88 | 235.00 | 0.30 | 0.01 | 0.21 | 6.31 | 1126.94 |
| 15:00 | 19.60 | 235.00 | 0.24 | 0.00 | 0.10 | 4.02 | 3530.02 |

**Table 7.32. Day 4 (08/09/2022) testing data for synthetic sludge**

| 08/09/2022 | Collector | | DC elevated | | DC outlet | | DC floor | | DC inlet | | Ambient inlet | | | |
|---|---|---|---|---|---|---|---|---|---|---|---|---|---|---|
| Hour | T1 | H1 | T2 | H2 | T3 | H3 | T4 | H4 | T5 | H5 | T6 | H6 | Solar Irradiance | MC (%) |
| 09:00 | 32,4 | 51,4 | 33,7 | 46 | 31,1 | 51 | 28,9 | 51,5 | 31,7 | 49,5 | 22,4 | 56,6 | 518,32 | 18,823 |
| 10:00 | 36,5 | 42,5 | 37,9 | 39,3 | 35,3 | 47,2 | 36,7 | 39,8 | 35,5 | 43,6 | 24,2 | 52,7 | 747,6 | 12,86 |
| 11:00 | 41 | 34,2 | 41,8 | 34,8 | 38,5 | 46,7 | 36,7 | 35,3 | 39,9 | 31,6 | 26,2 | 50,7 | 920,35 | 10,601 |
| 12:00 | 41 | 34,8 | 44,7 | 31,6 | 40,7 | 41,3 | 41,5 | 38,3 | 43,9 | 29,2 | 26,9 | 48,6 | 984,3 | 8,13 |
| 13:00 | 40,4 | 35,5 | 44,9 | 31,8 | 40,6 | 41,4 | 40,4 | 38,3 | 40,3 | 30,7 | 26,8 | 49,7 | 895,35 | 6,869 |
| 14:00 | 38,6 | 40,8 | 45,7 | 32,6 | 41,1 | 42,4 | 39 | 40,2 | 41,3 | 30,5 | 28 | 51 | 823,42 | 6,83 |
| 15:00 | 34,6 | 51,5 | 41,1 | 37,4 | 34,8 | 46,1 | 34,6 | 47,7 | 41,4 | 34,7 | 27,4 | 54 | 695,68 | 6,518 |

**Table 7.33. Calculated performance parameters for day 4 of testing (08/09/2022)**

| Hour | MC (%) | P, C (watts) | ΔM (%) | ΔMdb (KG) | DR (kg/h) | Dryer eff | SEC (Kw h/ton) |
|---|---|---|---|---|---|---|---|
| 09:00 | 18.823 | 0 | 0.23 | 0.0000 | 0.00 | 0.00 | 0.00 |
| 10:00 | 12.86 | 235 | 0.15 | 0.0029 | 0.17 | 4.19 | 1421.91 |
| 11:00 | 10.601 | 235 | 0.12 | 0.0023 | 0.06 | 1.18 | 4113.73 |
| 12:00 | 8.13 | 235 | 0.09 | 0.0017 | 0.06 | 1.14 | 3964.93 |
| 13:00 | 6.869 | 235 | 0.07 | 0.0015 | 0.03 | 0.61 | 8093.84 |
| 14:00 | 6.83 | 235 | 0.07 | 0.0014 | 0.00 | 0.02 | 265403.96 |
| 15:00 | 6.518 | 235 | 0.07 | 0.0014 | 0.01 | 0.19 | 52032.08 |

**Table 7.34. Day 1 of duplicate synthetic sludge testing data (14-09-2022)**

| 14/09/2022 | Collector | | DC elevated | | DC outlet | | DC floor | | DC inlet | | Ambient inlet | | | |
|---|---|---|---|---|---|---|---|---|---|---|---|---|---|---|
| Hour | T1 | H1 | T2 | H2 | T3 | H3 | T4 | H4 | T5 | H5 | T6 | H6 | Solar Irradiance | MC (%) |
| 09:00 | 32.8 | 57.3 | 32.2 | 54.6 | 29.5 | 56.4 | 27.3 | 57.9 | 30.1 | 58.9 | 22.8 | 58.3 | 579.47 | 80.046 |
| 10:00 | 38.1 | 42 | 37.3 | 47.1 | 33.8 | 47.6 | 36.8 | 43.6 | 41.3 | 36.8 | 24.7 | 54.4 | 745.65 | 76.459 |
| 11:00 | 40.5 | 39.2 | 35.5 | 45.1 | 31.3 | 47.3 | 33.1 | 47.8 | 41.6 | 35.1 | 25.7 | 54.6 | 855.13 | 70.065 |
| 12:00 | 40.7 | 38 | 41 | 42.4 | 36.7 | 49.8 | 40.6 | 46.7 | 44.6 | 32.4 | 25.6 | 54.7 | 872.72 | 62.76 |
| 13:00 | 37.7 | 43.4 | 41.7 | 44.6 | 36.9 | 49.4 | 36 | 43.5 | 44.7 | 34.4 | 26.6 | 54.9 | 784.75 | 55.843 |
| 14:00 | 34.8 | 47.9 | 39.2 | 43.8 | 35.9 | 50.5 | 34.8 | 46 | 43 | 35.1 | 25.6 | 56.6 | 661.58 | 50.082 |
| 15:00 | 32.7 | 56.7 | 40.2 | 43 | 33.5 | 48.2 | 32.9 | 50.8 | 36.8 | 40.1 | 25.4 | 58.2 | 123.94 | 48.038 |

**Table 7.35. Calculated performance parameters for day 1 of duplicate testing (14/09/2022)**

| Hour | MC (%) | P, C (watts) | ΔM (%) | ΔMdb (KG) | DR (kg/h) | Dryer eff | SEC (Kw h/ton) |
|---|---|---|---|---|---|---|---|
| 09:00 | 80.046 | 0 | 4.01 | 0.000 | 0.00 | 0.00 | 0 |
| 10:00 | 76.459 | 235 | 3.25 | 0.064 | 1.50 | 38.21 | 156.22 |
| 11:00 | 70.065 | 235 | 2.34 | 0.046 | 1.79 | 39.59 | 131.47 |
| 12:00 | 62.76 | 235 | 1.69 | 0.033 | 1.29 | 28.02 | 182.04 |
| 13:00 | 55.843 | 235 | 1.26 | 0.025 | 0.83 | 20.00 | 283.59 |
| 14:00 | 50.082 | 235 | 1.00 | 0.020 | 0.51 | 14.74 | 456.42 |
| 15:00 | 48.038 | 235 | 0.92 | 0.018 | 0.16 | 23.72 | 2365.29 |

**Table 7.36. Day 2 synthetic sludge duplicate testing data (15-09-2022)**

| 15/09/2022 | Collector | | DC elevated | | DC outlet | | DC floor | | DC inlet | | Ambient inlet | | | |
|---|---|---|---|---|---|---|---|---|---|---|---|---|---|---|
| Hour | T1 | H1 | T2 | H2 | T3 | H3 | T4 | H4 | T5 | H5 | T6 | H6 | Solar Irradiance | MC (%) |
| 09:00 | 34.3 | 55.4 | 33.7 | 54.8 | 31.3 | 55.1 | 29.4 | 56.2 | 31.2 | 57.8 | 24.9 | 55.1 | 616.61 | 47.851 |
| 10:00 | 40.7 | 39.4 | 40.3 | 42.7 | 37.1 | 45.7 | 38.8 | 44.9 | 39.2 | 38.9 | 27.3 | 51.8 | 757.38 | 42.32 |
| 11:00 | 43.2 | 36.8 | 42.1 | 40.3 | 38.1 | 43.1 | 37.7 | 48.3 | 42.8 | 33.1 | 28.2 | 51.2 | 837.53 | 34.655 |
| 12:00 | 43.4 | 35.4 | 45.6 | 36.5 | 41.3 | 35.1 | 44.9 | 35.4 | 45.7 | 30.1 | 29.5 | 48 | 833.62 | 28.422 |
| 13:00 | 52.4 | 29.3 | 55 | 30.3 | 46.5 | 36.1 | 41.8 | 34.2 | 55.4 | 26.2 | 41.5 | 31 | 794.65 | 20.995 |
| 14:00 | 50.1 | 30.1 | 52 | 30.3 | 44.4 | 35.1 | 40 | 34.7 | 54.3 | 26.7 | 40.6 | 33.4 | 608.79 | 16.573 |
| 15:00 | 36.3 | 43.5 | 43.9 | 36.5 | 38 | 34.5 | 43 | 32.5 | 43 | 32.5 | 28.9 | 50.4 | 405.47 | 12.276 |

**Table 7.37. Calculated performance parameters for day 2 of duplicate testing (15/09/2022)**

| Hour | MC (%) | P, C (watts) | ΔM (%) | ΔMdb (KG) | DR (kg/h) | Dryer eff | SEC (Kw h/ton) |
|---|---|---|---|---|---|---|---|
| 09:00 | 47.851 | 0 | 0.92 | 0.000 | 0.00 | 0.00 | 0 |
| 10:00 | 42.32 | 235 | 0.73 | 0.014 | 0.36 | 9.06 | 648.74 |
| 11:00 | 34.655 | 235 | 0.53 | 0.010 | 0.40 | 9.06 | 586.58 |
| 12:00 | 28.422 | 235 | 0.40 | 0.008 | 0.26 | 5.96 | 895.15 |
| 13:00 | 20.995 | 235 | 0.27 | 0.005 | 0.26 | 6.17 | 908.29 |
| 14:00 | 16.573 | 235 | 0.20 | 0.004 | 0.13 | 4.11 | 1778.05 |
| 15:00 | 12.276 | 235 | 0.14 | 0.003 | 0.12 | 5.40 | 3174.54 |

## 7.3 APPENDIX C: SYNTHETIC FAECAL SLUDGE PROCEDURE PREPARATION

### 7.3.1 Recipe for Synthetic Sludge

The original sludge recipe was adapted from a past final year mechanical engineering project which produced a greenhouse type dryer. The original recipe may be seen in the table below.

**Table 7.38. Original Synthetic Sludge Recipe (80% Moisture Content)**

| Ingredients | Amount (For 4kg Batch) [g] |
|---|---|
| **Water** | 2692.56 |
| **Psyllium Husk** | 144.38 |
| **Peanut Oil** | 229.38 |
| **Miso Paste** | 144.38 |
| **Probiotics** | 1 Capsule |
| **Ground Vegetables** | 26.036 |
| **Cellulose Paste** | 50.416 |
| **Polyethylene Glycol** | 144.38 |
| **Calcium Phosphate** | 144.38 |

This recipe was used as the basis for the recipe utilised during this testing of the screw conveyor sludge dryer system. The recipe was modified in a few ways in order to both eliminate unnecessary items, and to allow for a cheaper mixture. The probiotics were removed, as the elimination of pathogens was not a focus of this stage of this prototype's development, for this reason a biological component within the synthetic sludge was not needed. Additionally peanut oil was substituted with sunflower oil, due to the substantially lower cost, and much wider availability while possessing very similar composition. Lastly, cellulose paste was unable to be sourced at the university, so a cellulose powder was utilised in its stead. The updated recipe may be seen in the table below, the substitutions made did not have any discernible impact on moisture content, as the samples tested possessed moisture content values of 80% (Table 7.39).

**Table 7.39 Modified Synthetic Sludge Recipe (80% Moisture Content)**

| Ingredients | Amount (For 4kg Batch) [g] |
|---|---|
| **Water** | 2692.56 |
| **Psyllium Husk** | 144.38 |
| **Sunflower Oil** | 229.38 |
| **Miso Paste** | 144.38 |
| **Ground Vegetables** | 26.036 |
| **Cellulose Powder** | 50.416 |
| **Polyethylene Glycol** | 144.38 |
| **Calcium Phosphate** | 144.38 |

The modified recipe devised for the project was then further modified in order to yield varying moisture contents within the sludge for more in-depth testing of the dryer capabilities. Shown below is the ingredients list for synthetic sludge with 65% starting moisture content.

**Table 7.40. Modified Synthetic Sludge Recipe (80% Moisture Content)**

| Ingredients | Amount (For 4kg Batch) [g] |
|---|---|
| **Water** | 2416 |
| **Psyllium Husk** | 303.32 |
| **Sunflower Oil** | 210.08 |
| **Miso Paste** | 303.32 |
| **Ground Vegetables** | 54.69 |
| **Cellulose Powder** | 105.92 |
| **Polyethylene Glycol** | 303.32 |
| **Calcium Phosphate** | 303.32 |

Similarly, shown below is the ingredients list for synthetic sludge with a starting moisture content of 50%.

**Table 7.41. Modified Synthetic Sludge Recipe (50% Moisture Content)**

| Ingredients | Amount (For 4kg Batch) [g] |
|---|---|
| **Water** | 1799.14 |
| **Psyllium Husk** | 432.93 |
| **Sunflower Oil** | 239.89 |
| **Miso Paste** | 432.93 |
| **Ground Vegetables** | 78.07 |
| **Cellulose Powder** | 151.18 |
| **Polyethylene Glycol** | 432.93 |
| **Calcium Phosphate** | 432.93 |

### 7.3.2 Mixing of synthetic sludge

The mixing of the synthetic sludge is a relatively basic process, but it must be done effectively in order to have a homogenous mixture in terms of both texture and moisture content. This is important as having repeatability in terms of the feedstock ensures that the only parameters being tested on the device is the variable in question when comparing to previous and control data.

The mixing of the sludge is undertaken in the following steps:

1. Utilise appropriate PPE according to the HIRA of the substance. In general, gloves, safety boots, safety goggles and a lab coat should be used during the mixing procedure to ensure no raw chemicals contact the mixer
2. Gather all of the required chemicals, and ensure there is sufficient amount of all to mix a batch
3. Grind the dried vegetables into a fine powder, and measure out the desired amount
4. Add the dry ingredients to the mixing container (Calcium phosphate, Cellulose powder, Psyllium husk, Ground vegetables), and incorporate them fully by mixing with a stirring rod, being careful to not eject powder into the air
5. Measure out and add the miso paste to the dry ingredients and mix thoroughly to incorporate the miso paste into the powder.
6. Measure and add both the oil and the polyethylene glycol to the mixture. Mix by hand until a thick paste forms
7. Measure and add the water to the mixture. If hand mixing this may be easier to undertake by adding small amounts of water at a time and gradually mixing. The sludge may be hand mixed for moisture contents of around 80%, for lower values, an electric stirrer or paint stirrer should be utilised to ensure adequate mixing of the ingredients.
8. The mixture should be mixed continuously until it is felt to thicken, this indicates that the psyllium husk has begun to hydrate
9. Once the sludge has been properly mixed, and it has become suitably thick (~10 minutes of mixing), it should be covered, and stored within a refrigerator or cold room for at least 4 hours prior to usage to allow the husk to fully hydrate.

10. The sludge should be used within 2 weeks from date of mixing, as there is potential for mould growth within the mixture

## 7.4 APPENDIX D: DETAILED TESTING AND DATA ANALYSIS PROCEDURES FOR THE TESTS IN THE SCREW CONVEYOR SOLAR DRIER

### 7.4.1 Testing Procedure

#### 7.4.1.1 *Functionality Testing*

The procedure for this phase is carried out as follows:

11) Assemble the drying system according to the test being conducted
12) Connect all sensors to the electronics mainboard
13) Connect all airflow inducing fans to the mainboard
14) Ensure Micro SD card is inserted to the SD card module to ensure data is recorded, this step must be completed before turning the electronics on.
15) Check integrity of data from the sensors by connecting the mainboard to a computer and utilising the serial monitor function of the Arduino IDE. It is normal to see some null data values intermittently, however if a particular sensor is continuously showing no data, the connections and sensor integrity should be verified.
16) Start recording of data
17) The device should be run for long enough for sufficient data to be recorded for the test.
18) Once the drying test is complete, the device should be powered down, after which all electrical connections may be disconnected, and the individual subsystems stowed in the sheds. It should be noted that the solar collector and drying chamber may require some time to cool down before handling.
19) The micro-SD card may then be removed, and the days data processed.

#### 7.4.1.2 *Tests with wet soil*

The procedure for this phase is largely like the previous phases, and is carried out as follows:

11) Assemble the drying system according to the test being conducted
12) Connect all sensors to the electronics mainboard
13) Connect all airflow inducing fans to the mainboard
14) Ensure Micro SD card is inserted to the SD card module to ensure data is recorded, this step must be completed before turning the electronics on.
15) Check integrity of data from the sensors by connecting the mainboard to a computer and utilising the serial monitor function of the Arduino IDE. It is normal to see some null data values intermittently, however if a particular sensor is continuously showing no data, the connections and sensor integrity should be verified.
16) Ensure that the fans are set to the correct speed by noting the value within the serial monitor and ensure that it corresponds to the test being conducted.
17) Measure out 2kg of soil, and add 400g of water to allow for a moisture content of ~65%
18) Set up a container to catch any stray material from the dryer outlet
19) Start recording of data
20) Run the screw conveyor at the desired speed. All tests undertaken in this phase has a residence time of 1 hour, meaning the conveyor had to be run intermittently as the maximum residence time afforded when running the conveyor continuously is 10 minutes at most.
21) Samples should be taken from the outlet side of the dryer, in 6-minute intervals, allowing for 10 total samples per run.
22) Samples taken can be processed with little rush, however the samples must be stored in airtight containers to ensure that there is no moisture loss which may skew results.
23) Once the drying test is complete, the device should be powered down, after which all electrical connections may be disconnected, and the individual subsystems stowed in the sheds. It should be noted that the solar collector and drying chamber may require some time to cool down before handling.
24) The micro-SD card may then be removed, and the days data processed.

#### 7.4.1.3 *Tests with synthetic sludge*

The procedure for this phase is largely similar to the previous phases, and is carried out as follows:

9) Assemble the drying system, this differs to preliminary testing in that the dehumidifier subsystem was omitted. Additionally, the solar collector and drying chamber should be set up at least 20-30 minutes before the start of testing to allow for warmup of the systems, this is especially true of the solar collector due to the very high thermal mass of the absorber plate.
10) Connect all sensors to the electronics mainboard
11) Connect all airflow inducing fans to the mainboard
12) Ensure Micro SD card is inserted to the SD card module to ensure data is recorded, this step must be completed before turning the electronics on.
13) Check integrity of data from the sensors by connecting the mainboard to a computer and utilising the serial monitor function of the Arduino IDE. It is normal to see some null data values intermittently, however if a particular sensor is continuously showing no data, the connections and sensor integrity should be verified.
14) Measure out 2kg of synthetic sludge and load it into the drying chamber through the inlet hatch. When additives are utilised, these additives may be mixed into the sludge measured out. The sludge should be mixed very thoroughly as the texture does not allow for easy mixing.
15) Set up a container to catch any stray material from the dryer outlet
16) Start recording of data
17) Run the screw conveyor at the desired speed. All tests undertaken in this phase has a residence time of 4 hours, meaning the conveyor had to be run intermittently as the maximum residence time afforded when running the conveyor continuously is 10 minutes at most.
18) Samples should be taken from the outlet side of the dryer, in 30-minute intervals.
19) Samples taken must be processed in the moisture analyser within 2 days to ensure that there is no contamination of the samples through mould growth.
20) Once the drying test is complete, the device should be powered down, after which all electrical connections may be disconnected, and the individual subsystems stowed in the sheds.
21) The micro-SD card may then be removed, and the days data processed.

### 7.4.2 Data Treatment Procedure

The raw data from the device testing tends to have some null values due to interference within the system. The null values are intermittent, and since the data is sampled every 10 seconds, it is easy to interpolate the values utilising software.

The data is interpolated utilising the Pandas data analysis suite within Python. Shown in Figure 7.2 is an example of the untreated data, and in Figure 7.3 below it is an image of the data after it has been interpolated.

| | Time | Temperature Ambient | Temperature Inlet SAH | Temperature Inlet DC | Temperature Outlet | Humidity Ambient | Humidity Inlet SAH | Humidity Inlet DC | Humidity Outlet | Fan Percentagem |
|---|---|---|---|---|---|---|---|---|---|---|
| 0 | 10:40:49 | 22.9 | 21.0 | 42.5 | 33.0 | 99.9 | 99.9 | 47.7 | 80.5 | 4095.0 |
| 1 | 10:40:59 | 22.8 | 20.9 | 42.3 | 32.5 | 99.9 | 99.9 | 48.8 | 80.6 | 4095.0 |
| 2 | 10:41:9 | 22.8 | NaN | 46.4 | 30.2 | 99.9 | NaN | 47.6 | 76.6 | 4095.0 |
| 3 | 10:41:19 | 22.8 | 20.9 | 47.9 | NaN | 99.9 | 99.9 | 46.1 | NaN | 4095.0 |
| 4 | 10:41:29 | 22.7 | 20.9 | 48.7 | 29.8 | 99.9 | 99.9 | 44.8 | 79.5 | 4095.0 |
| ... | ... | ... | ... | ... | ... | ... | ... | ... | ... | ... |
| 494 | 12:18:1 | 23.1 | 32.1 | 37.5 | 36.1 | 99.9 | 32.4 | 31.8 | 59.6 | 4095.0 |
| 495 | 12:18:11 | 23.1 | 32.1 | NaN | 36.1 | 99.9 | 32.6 | NaN | 58.1 | 4095.0 |
| 496 | 12:18:21 | 23.1 | 32.0 | 37.5 | 36.1 | 99.9 | 32.4 | 31.8 | 58.9 | 4095.0 |
| 497 | 12:18:31 | 23.1 | 32.0 | 37.5 | 36.1 | 99.9 | 32.5 | 31.8 | 56.6 | 4095.0 |
| 498 | 12:18:41 | 23.2 | 31.9 | 37.5 | 36.1 | 99.9 | 32.6 | 31.8 | 56.2 | 4095.0 |

**Figure 7.2. Example of Untreated Testing Data**

| | Time | Temperature Ambient | Temperature Inlet SAH | Temperature Inlet DC | Temperature Outlet | Humidity Ambient | Humidity Inlet SAH | Humidity Inlet DC | Humidity Outlet | Fan Percentagem |
|---|---|---|---|---|---|---|---|---|---|---|
| 0 | 10:40:49 | 22.9 | 21.0 | 42.5 | 33.0 | 99.9 | 99.9 | 47.7 | 80.50 | 4095.0 |
| 1 | 10:40:59 | 22.8 | 20.9 | 42.3 | 32.5 | 99.9 | 99.9 | 48.8 | 80.60 | 4095.0 |
| 2 | 10:41:9 | 22.8 | 20.9 | 46.4 | 30.2 | 99.9 | 99.9 | 47.6 | 76.60 | 4095.0 |
| 3 | 10:41:19 | 22.8 | 20.9 | 47.9 | 30.0 | 99.9 | 99.9 | 46.1 | 78.05 | 4095.0 |
| 4 | 10:41:29 | 22.7 | 20.9 | 48.7 | 29.8 | 99.9 | 99.9 | 44.8 | 79.50 | 4095.0 |
| ... | ... | ... | ... | ... | ... | ... | ... | ... | ... | ... |
| 494 | 12:18:1 | 23.1 | 32.1 | 37.5 | 36.1 | 99.9 | 32.4 | 31.8 | 59.60 | 4095.0 |
| 495 | 12:18:11 | 23.1 | 32.1 | 37.5 | 36.1 | 99.9 | 32.6 | 31.8 | 58.10 | 4095.0 |
| 496 | 12:18:21 | 23.1 | 32.0 | 37.5 | 36.1 | 99.9 | 32.4 | 31.8 | 58.90 | 4095.0 |
| 497 | 12:18:31 | 23.1 | 32.0 | 37.5 | 36.1 | 99.9 | 32.5 | 31.8 | 56.60 | 4095.0 |
| 498 | 12:18:41 | 23.2 | 31.9 | 37.5 | 36.1 | 99.9 | 32.6 | 31.8 | 56.20 | 4095.0 |

**Figure 7.3. Example of Treated Testing Data**

As can be seen in Figure 7.2, the data originally had multiple NaN, or “Not a Number” values, which were then interpolated in Figure 7.3. Interpolation simply means that the missing data is approximated based upon the data surrounding the missing value. The interpolation technique utilised for this data treatment is known as linear interpolation, and only works effectively when the data samples are all fairly evenly spaced, which the data in this project is. Additionally, the interpolation is capable of interpolating in both directions, meaning that missing values at the start or end of the dataset can be interpolated effectively.

Once the data is interpolated, the dataframe may be utilised to generate some basic graphs, which can be used to ensure that the basic data looks fine, and that the sensors are functioning as intended. If the data shows anomalies, such as humidity values which are far too high, it is understood that the sensor needs to be replaced. Shown in Figure 7.4 below is an example of the data exhibiting anomalies in that some of the humidity data is always at 100%, this is obviously untrue, as the relative humidity in Durban during winter tends to be closer to between 50-60%.

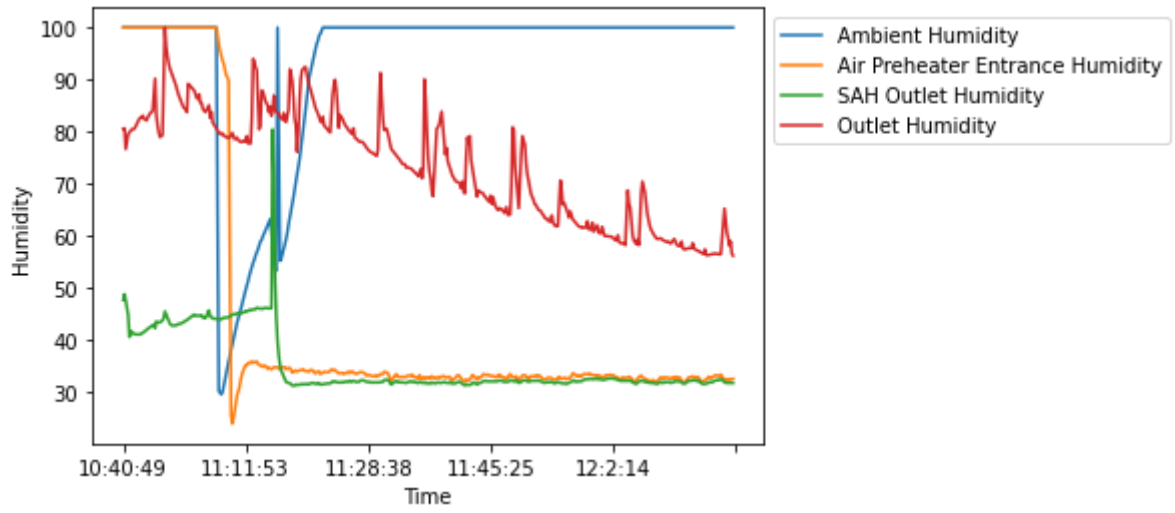


**Figure 7.4. Humidity Data Showing Malfunctioning Sensor**

It is clear from the above graph that the ambient humidity sensor has ailed, as it constantly reports at 100% ambient humidity. This tends to occur when the humidity part of the sensor has been waterlogged, and the easiest way to remedy the situation is to purchase new sensors. During the course of this project the suite of sensors were replaced only once, when the sensors displayed the anomalies described in the above paragraphs.

Once the data has been deemed acceptable, there is additional Python code which exports the dataframe as a Microsoft Excel spreadsheet, which makes the data easier to view and construct more visually attractive graphics. The graphs from the treated data were generated utilising Microsoft Power BI, which is a data

visualisation suite, which allows for the average of the data over each unit time to be plotted, which results in a much smoother and easy to understand graph. Shown below is an example of a graph which was generated utilising Power BI.

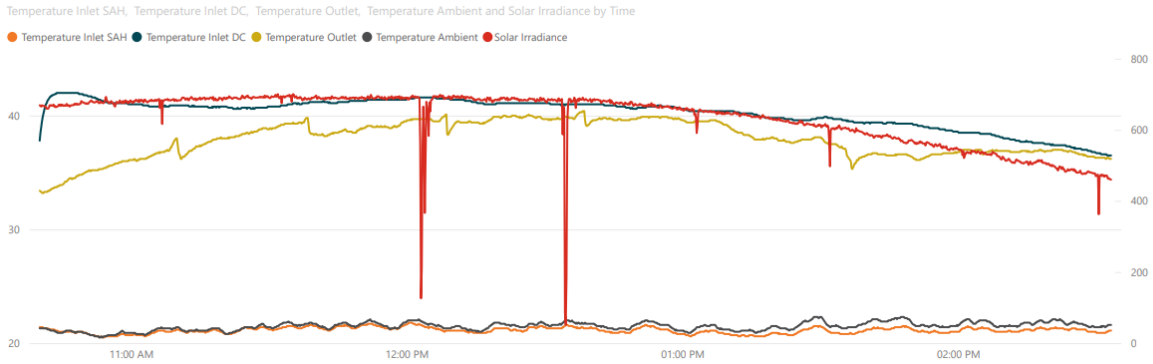


**Figure 7.5. Example of Power BI Visual**

## 7.5 APPENDIX E: DATA FROM THE SCREW CONVEYOR SOLAR DRYING TESTS

### 7.5.1 Calibration of the ventilation fans

The ventilation data was calibrated utilising an anemometer (Table 7.42). The fans were started at a particular percentage of the overall duty cycle, and the air flow was measured by the anemometer. The data was then plotted, which resulted in the plot in Figure 7.6.

**Table 7.42. Raw Calibration Data for Ventilation Fans**

| Pot Reading | Fan Perc. (%) | Velocity (m/s) | Volumetric Flow (m^3/s) |
|---|---|---|---|
| **368** | 8,986568987 | 1,23 | 0,013910972 |
| **645** | 15,75091575 | 1,7 | 0,019226547 |
| **816** | 19,92673993 | 1,7 | 0,019226547 |
| **915** | 22,34432234 | 1,85 | 0,020923007 |
| **1088** | 26,56898657 | 1,9 | 0,021488494 |
| **1248** | 30,47619048 | 2,17 | 0,024542122 |
| **1450** | 35,40903541 | 2,35 | 0,026577874 |
| **1705** | 41,63614164 | 2,76 | 0,031214865 |
| **1911** | 46,66666667 | 3 | 0,033929201 |
| **2109** | 51,5018315 | 3,3 | 0,037322121 |
| **2339** | 57,11843712 | 3,5 | 0,039584067 |
| **2559** | 62,49084249 | 3,8 | 0,042976988 |
| **2807** | 68,54700855 | 4,09 | 0,04625681 |
| **3135** | 76,55677656 | 4,25 | 0,048066368 |
| **3471** | 84,76190476 | 4,45 | 0,050328314 |
| **3807** | 92,96703297 | 4,7 | 0,053155748 |
| **3959** | 96,67887668 | 4,9 | 0,055417694 |
| **4095** | 100 | 5 | 0,056548668 |

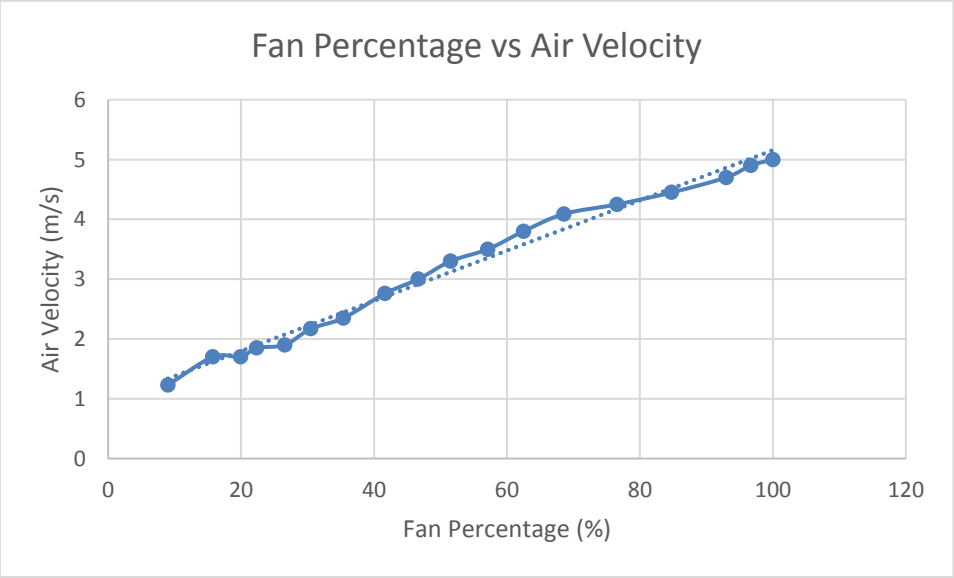


**Figure 7.6. Fan Percentage Vs Air Velocity Graph**

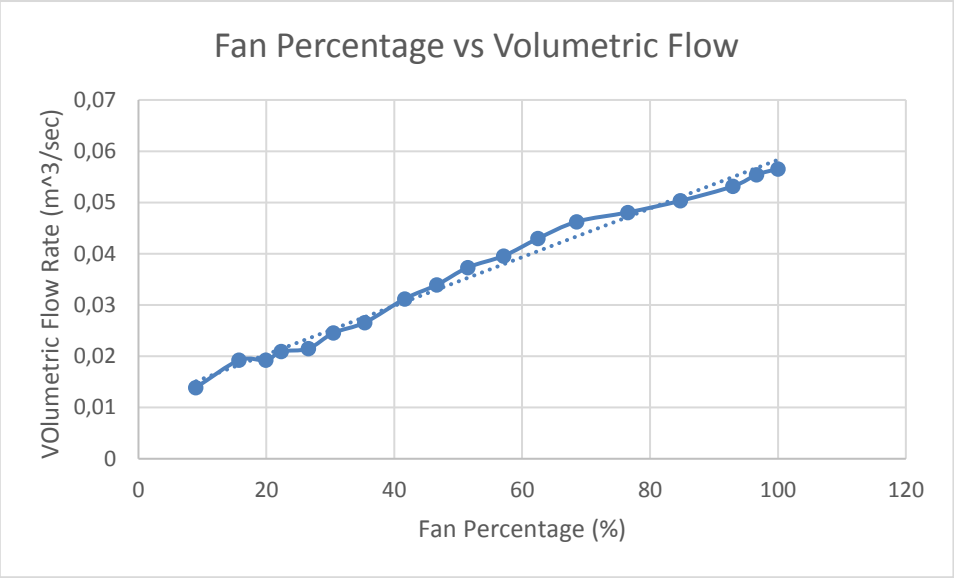


**Figure 7.7. Fan Percentage Vs Volumetric Air Flow Graph**

### 7.5.2 Residence Time Calibration

The residence time of the device was calibrated by running the conveyor at a specific speed, and timing how long it took an item to be conveyed through the drying chamber. The data was recorded in Table 7.43 and plotted in Figure 7.8.

**Table 7.43. Residence Time Calibration Data**

| VFD Reading | Residence Time |
|---|---|
| **50** | 0:00:48 |
| **45,07** | 0:00:50 |
| **40,16** | 0:00:55 |
| **35,13** | 0:01:03 |
| **30,1** | 0:01:17 |
| **25,09** | 0:01:32 |
| **20,13** | 0:01:45 |
| **15** | 0:02:25 |
| **10,11** | 0:03:22 |
| **5,1** | 0:07:15 |
| **4,09** | 0:10:10 |
| **3,07** | 0:17:36 |
| **2** | did not run |
| **1** | did not run |

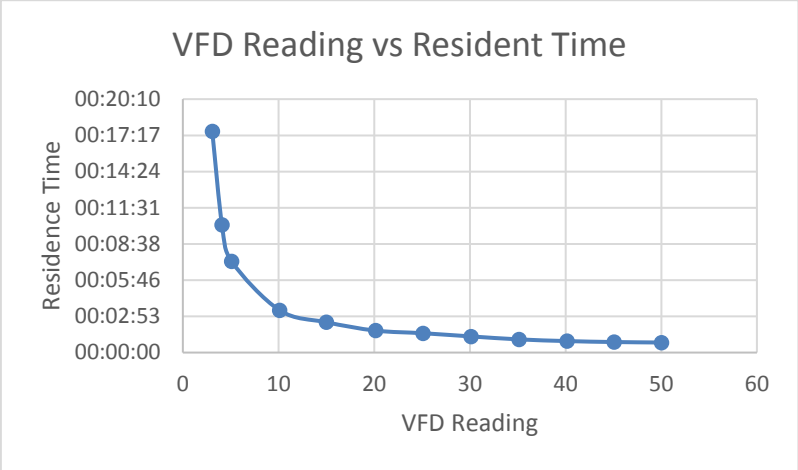


**Figure 7.8. Residence Time Calibration Plot**

### 7.5.3 Temperature and relative humidity data

#### 7.5.3.1 *Functionality tests*

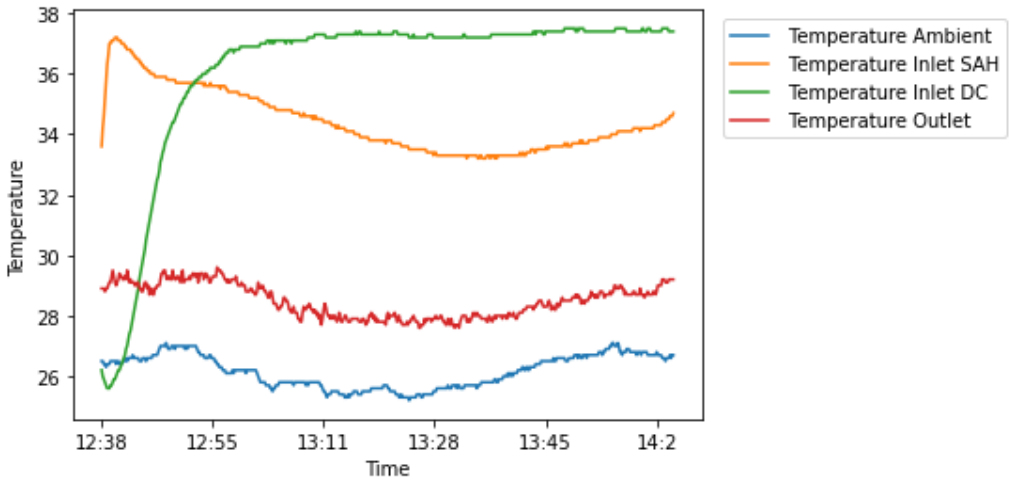


**Figure 7.9. Full Device Functionality Test 1 Temperature Vs Time**

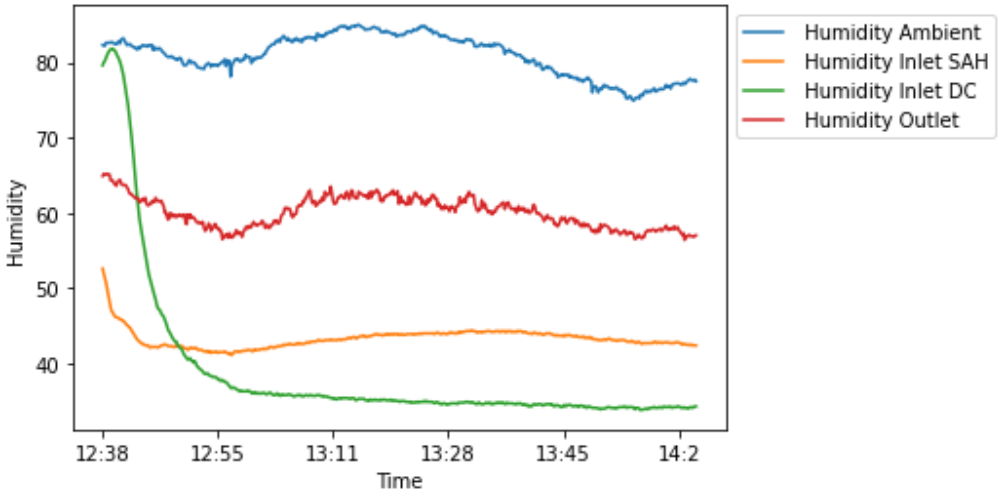


**Figure 7.10. Full Device Functionality Test 1 Humidity Vs Time**

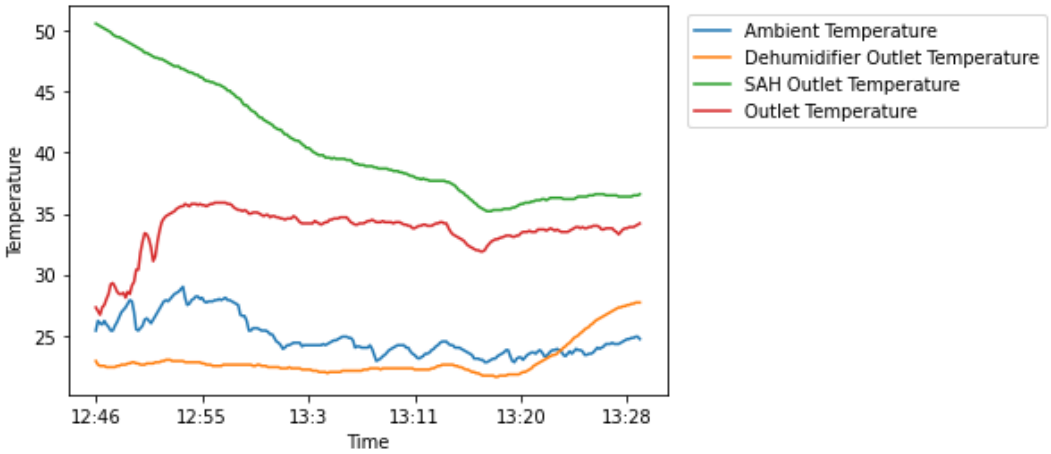


**Figure 7.11. Full Device Functionality Test 2 Humidity Vs Time**

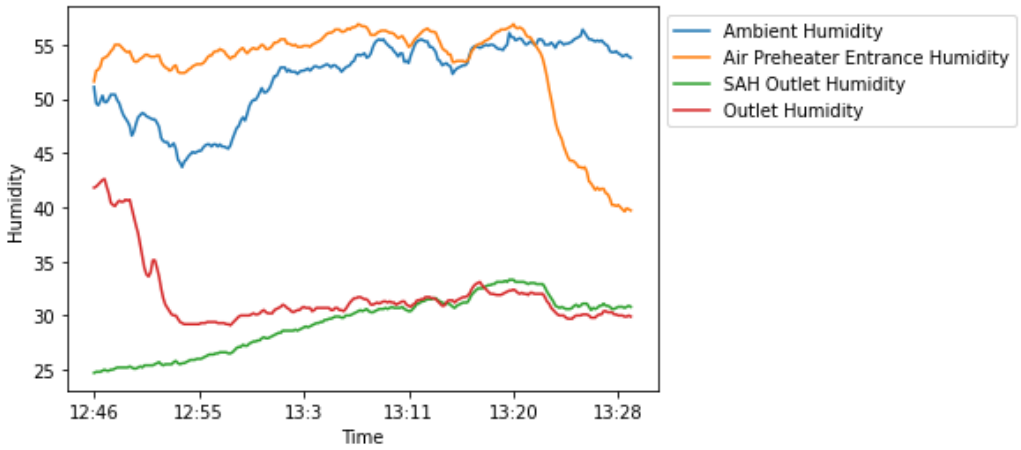


**Figure 7.12. Full Device Functionality Test 2 Humidity Vs Time**

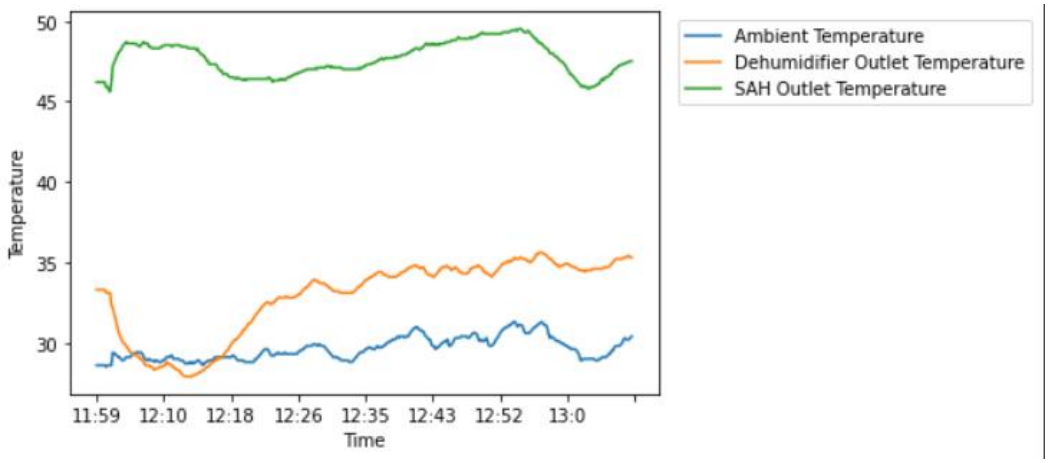


**Figure 7.13. SAH & Dehumidifier Functionality Test 1 Temperature Vs Time**

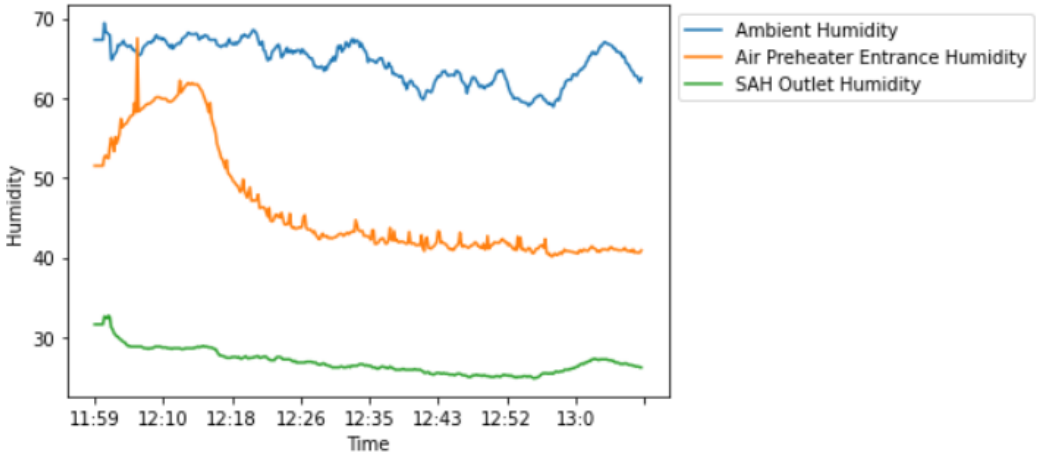


**Figure 7.14. Dehumidifier and SAH Functionality Test 1 Humidity Vs Time**

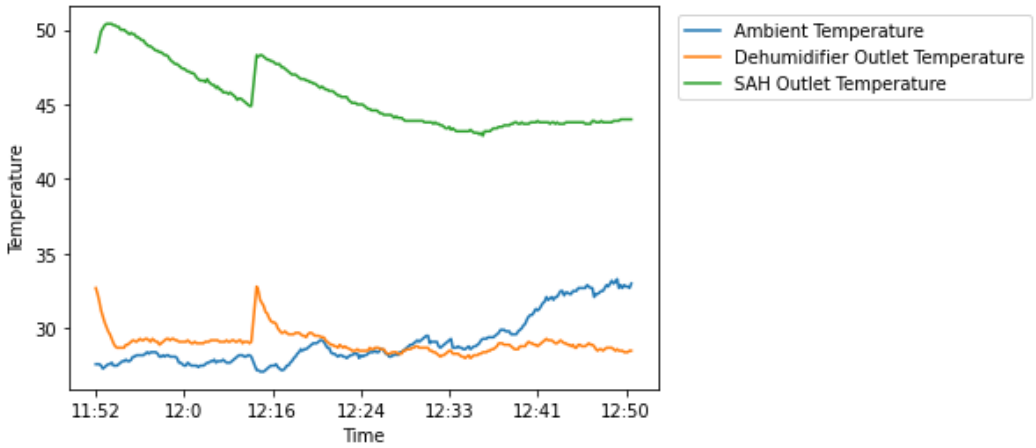


**Figure 7.15. Dehumidifier and SAH Functionality Test 2 Temperature Vs Time**

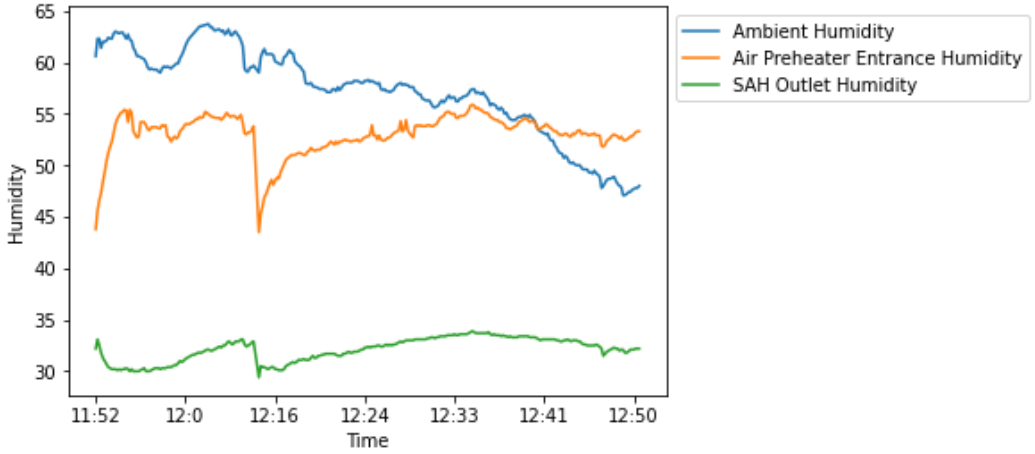


**Figure 7.16. Dehumidifier and SAH Functionality Test 2 Humidity Vs Time**

### 7.5.3.2 *Wet soil tests*

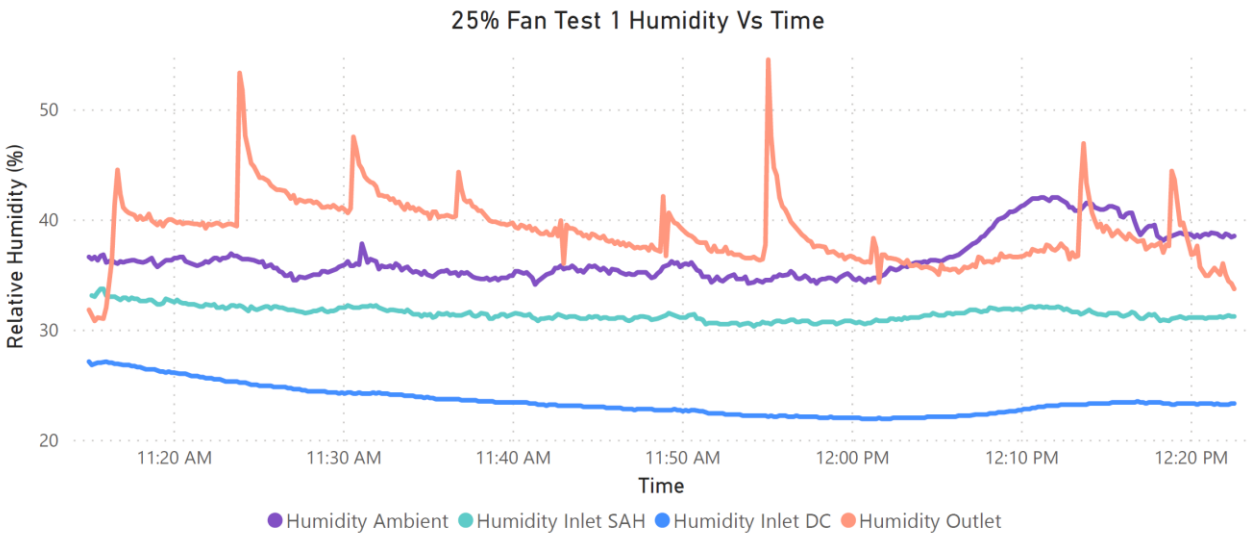


**Figure 7.17. 25% Fan Speed Test 1 Humidity Vs Time**

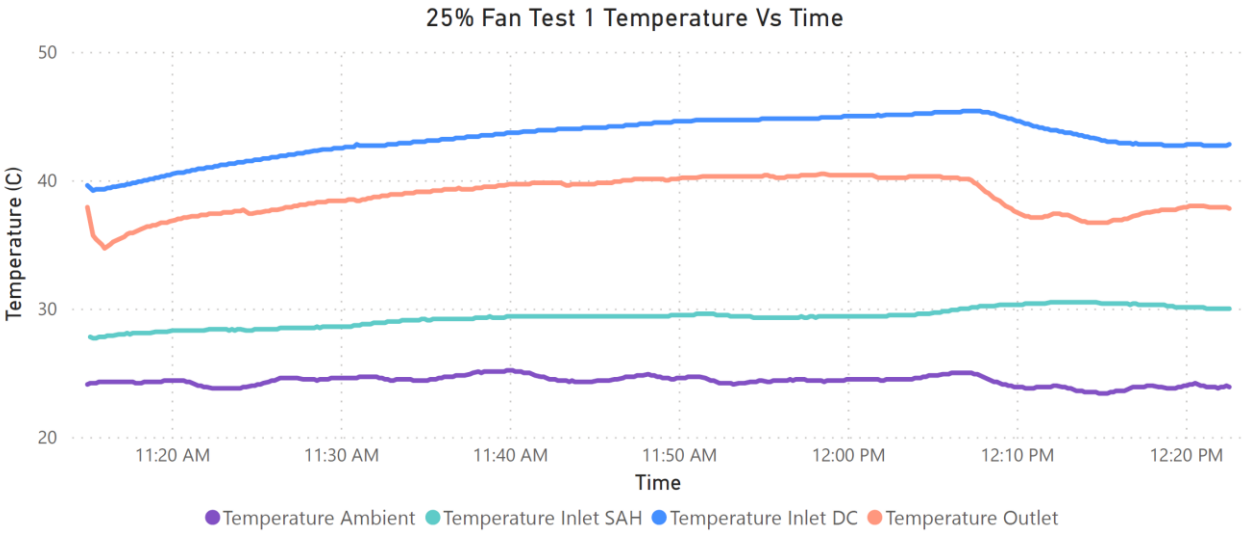


**Figure 7.18. 25% Fan Speed Test 1 Temp Vs Time**

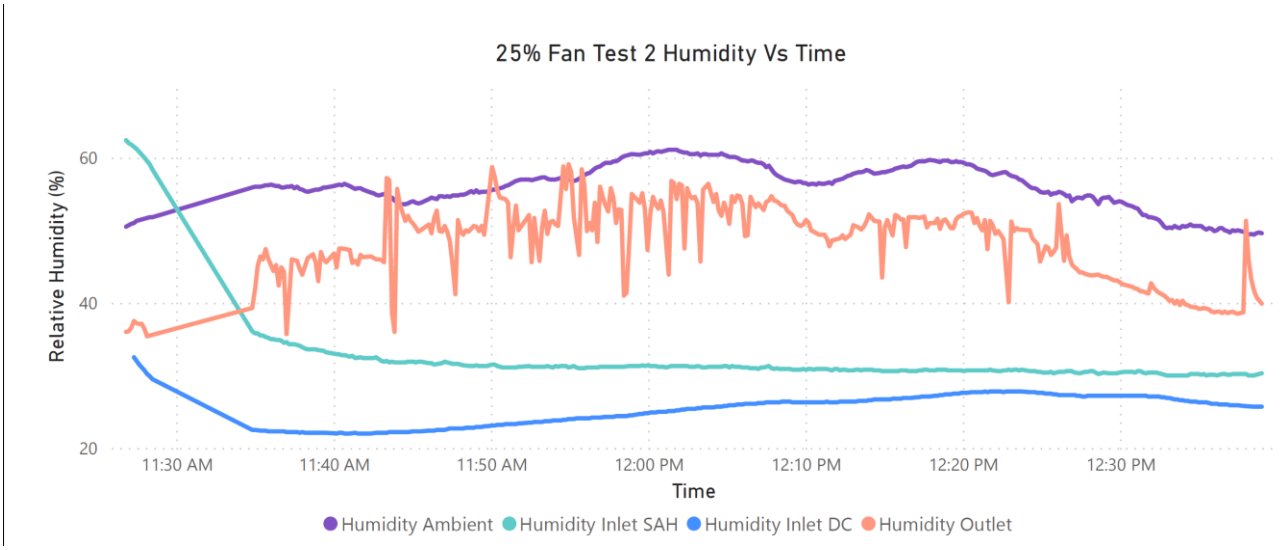


**Figure 7.19. 25% Fan Speed Test 2 Humidity Vs Time**

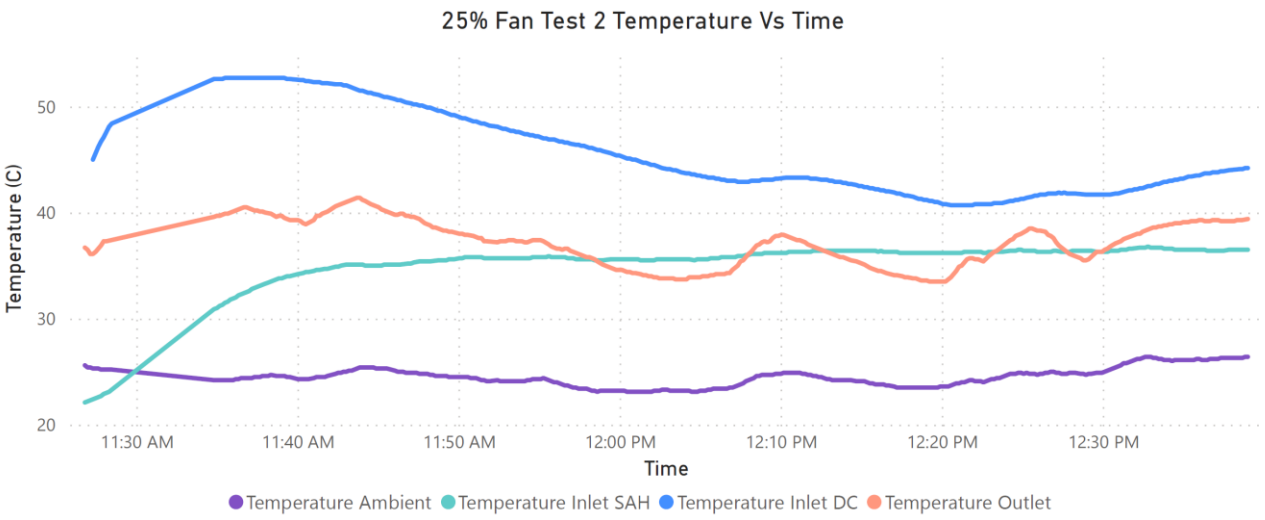


**Figure 7.20. 25% Fan Speed Test 2 Temp Vs Time**

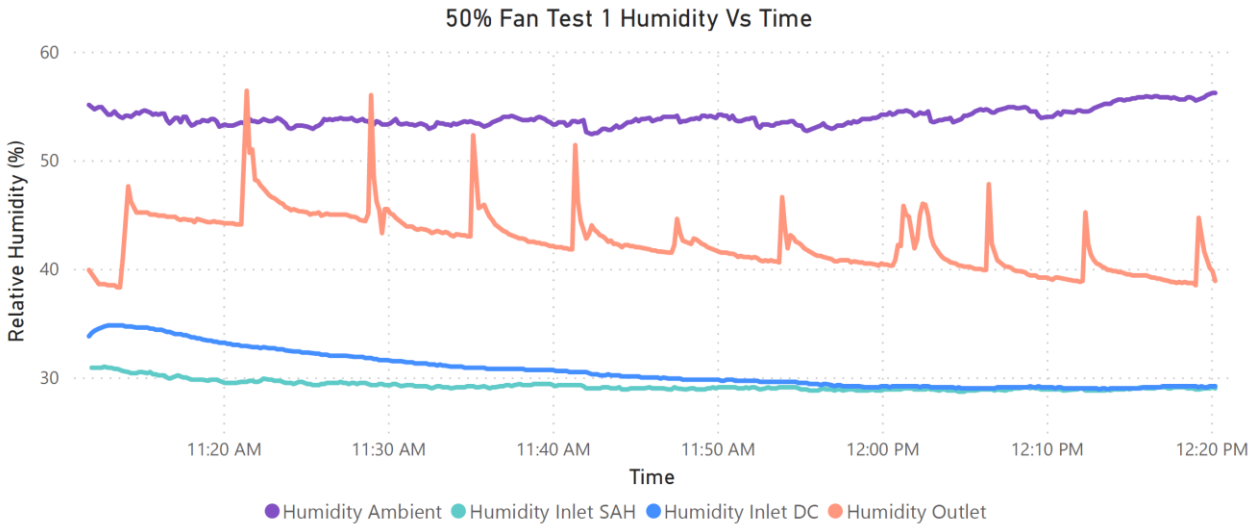


**Figure 7.21. 50% Fan Speed Test 1 Humidity Vs Time**

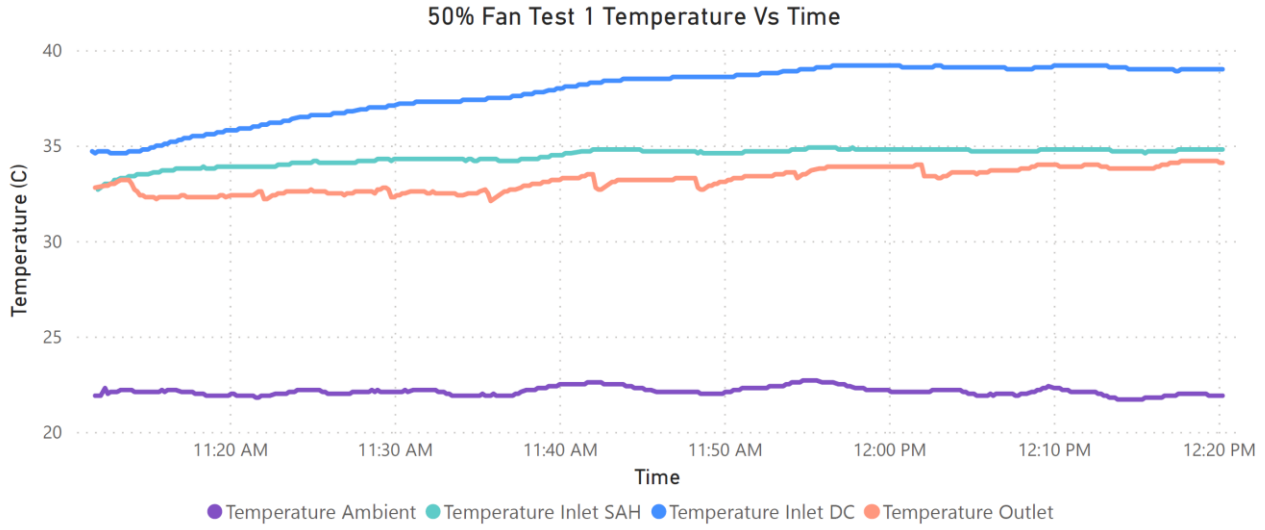


**Figure 7.22. 50% Fan Speed Test 1 Temp Vs Time**

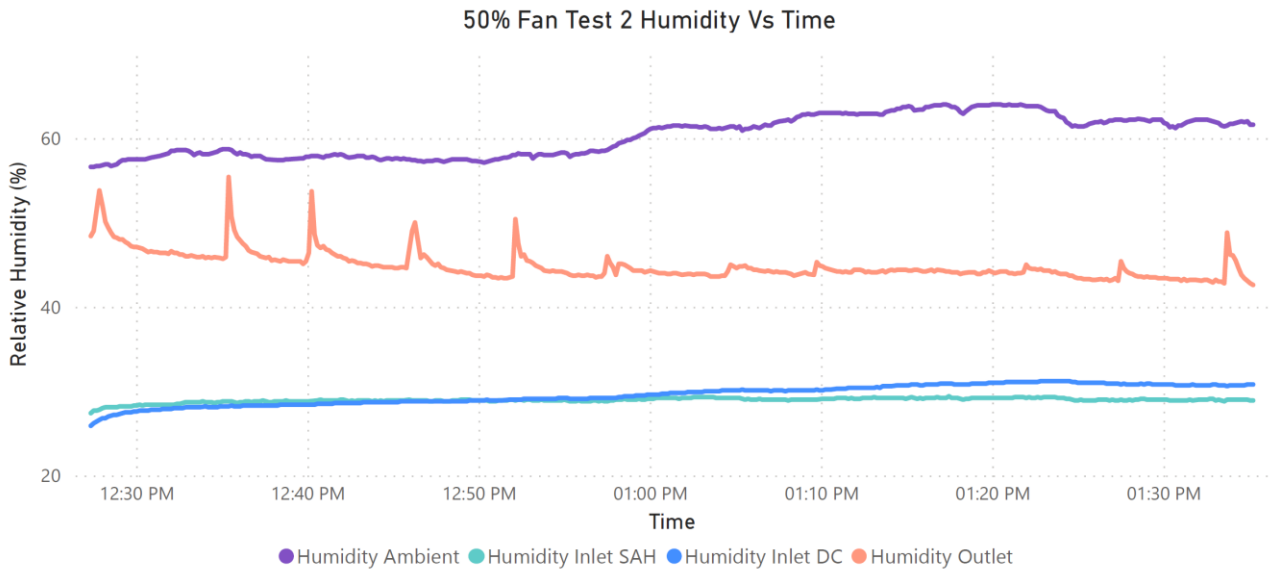


**Figure 7.23. 50% Fan Speed Test 2 Humidity Vs Time**

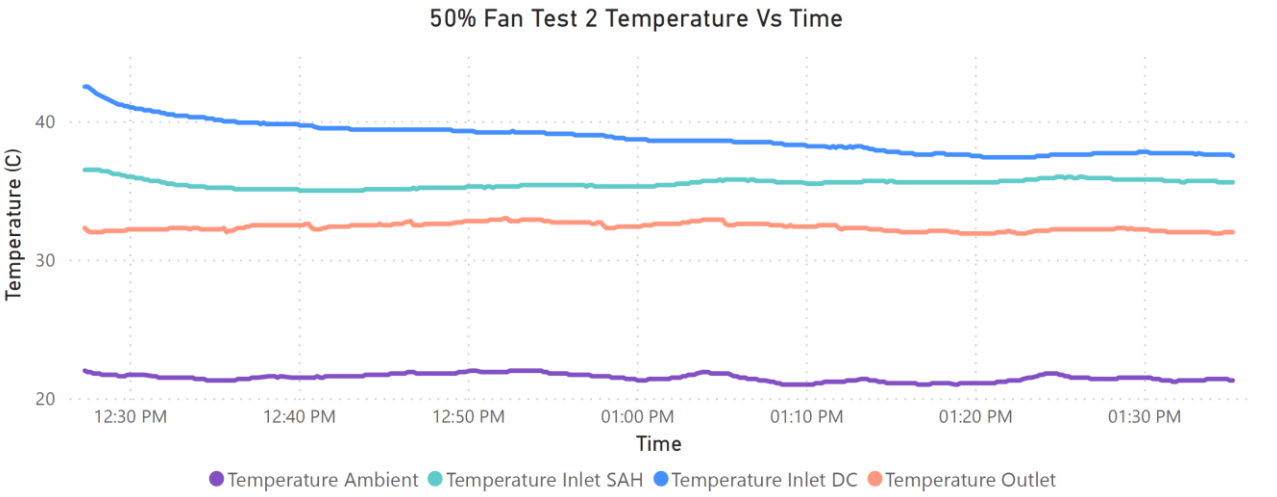


**Figure 7.24. 50% Fan Speed Test 2 Temp Vs Time**

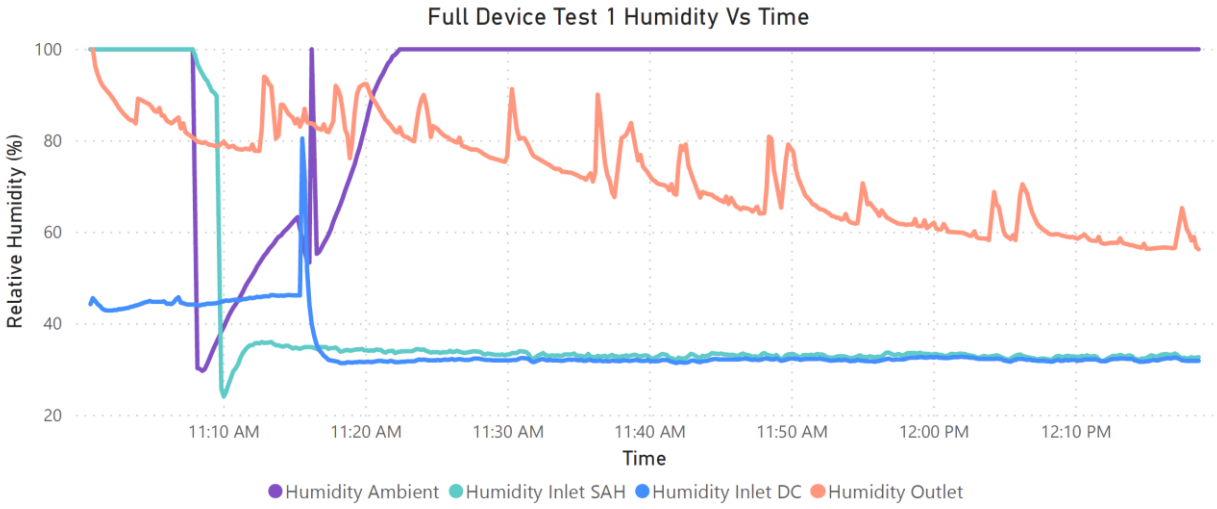


**Figure 7.25. Full Device Test 1 Humidity Vs Time**

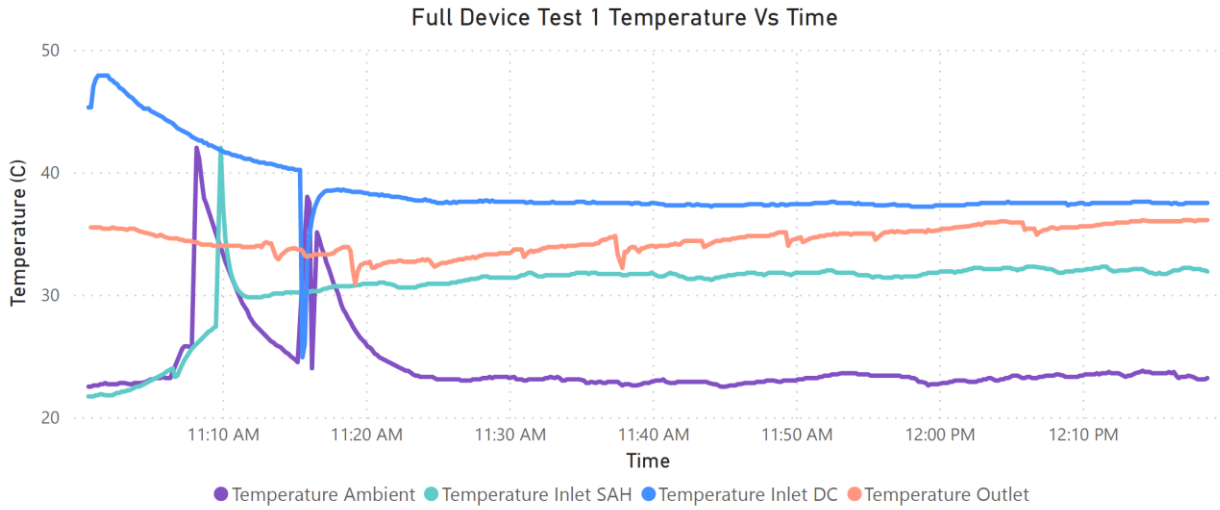


**Figure 7.26. 50% Fan Speed Test 1 Temp Vs Time**

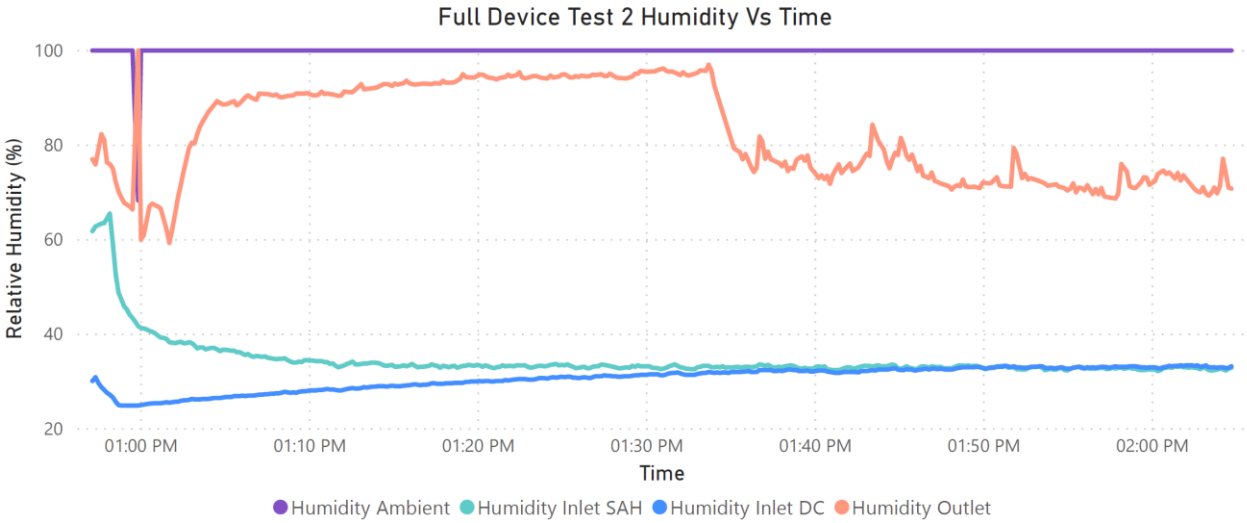


**Figure 7.27. 50% Fan Speed Test 2 Humidity Vs Time**

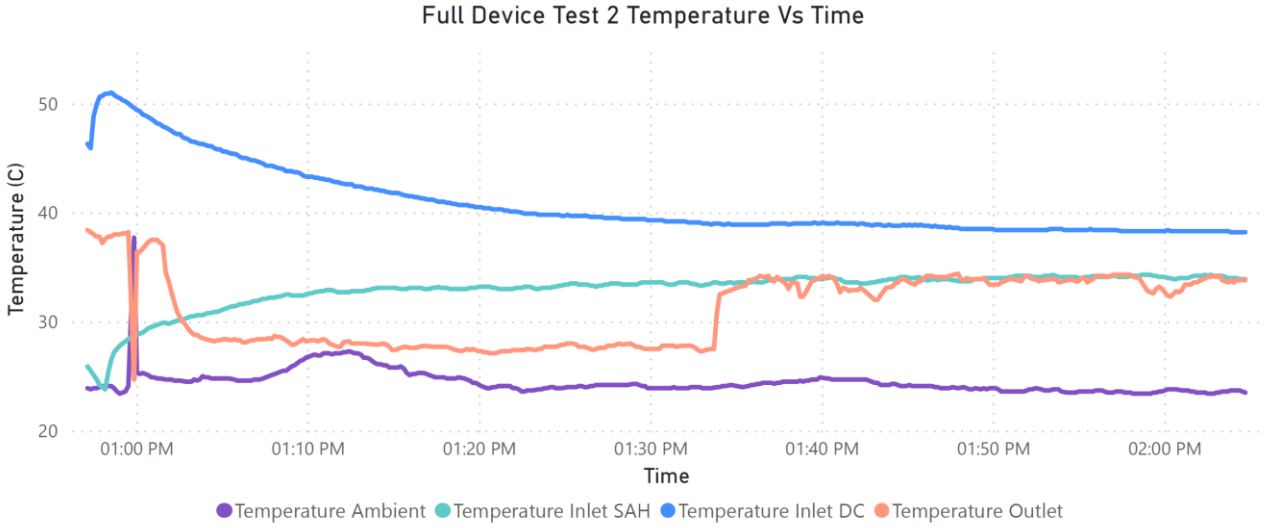


**Figure 7.28. 50% Fan Speed Test 2 Temp Vs Time**

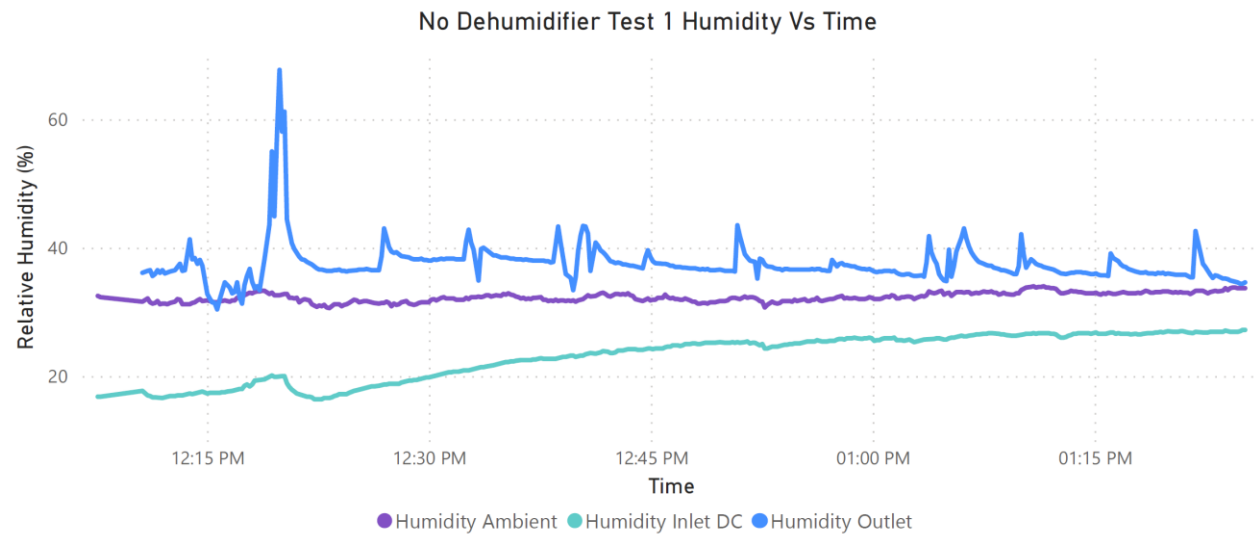


**Figure 7.29. No Dehumidifier Test 1 Humidity Vs Time**

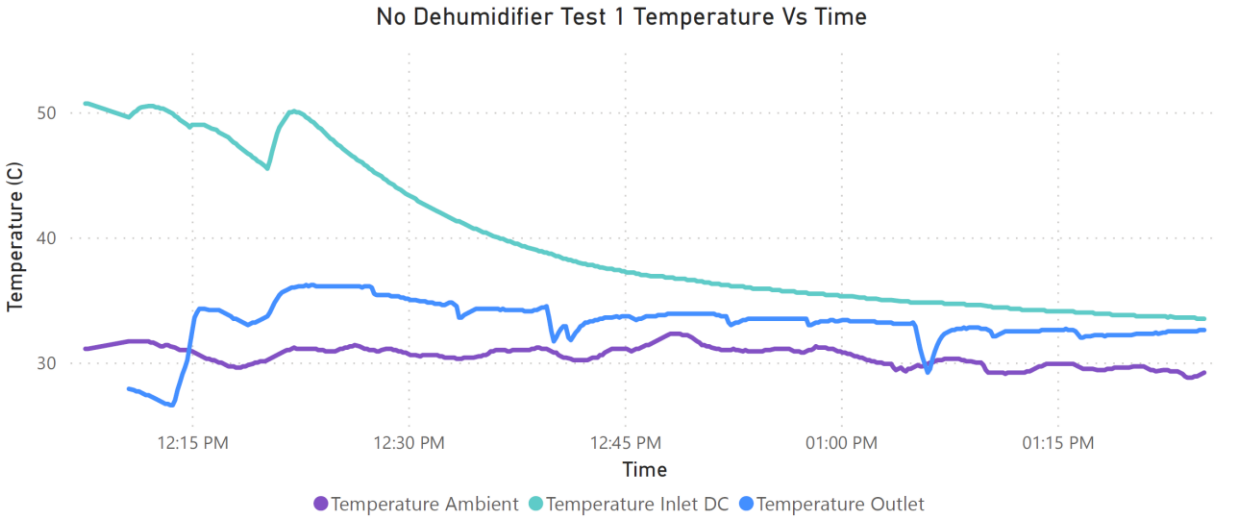


**Figure 7.30. No Dehumidifier Test 1 Temp Vs Time**

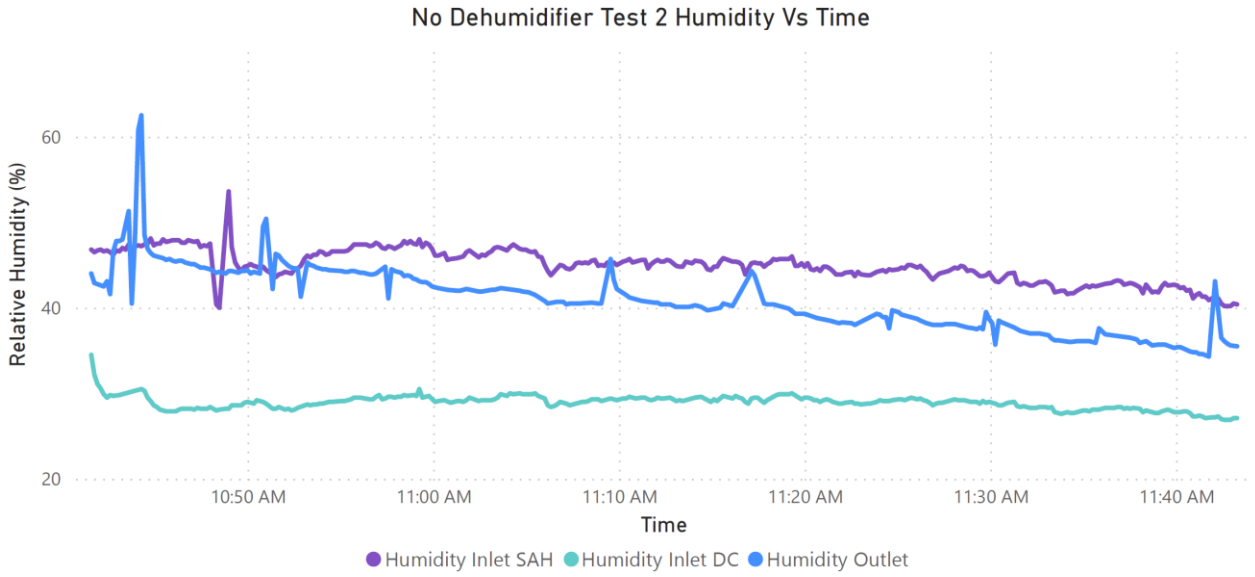


**Figure 7.31. No Dehumidifier Test 2 Humidity Vs Time**

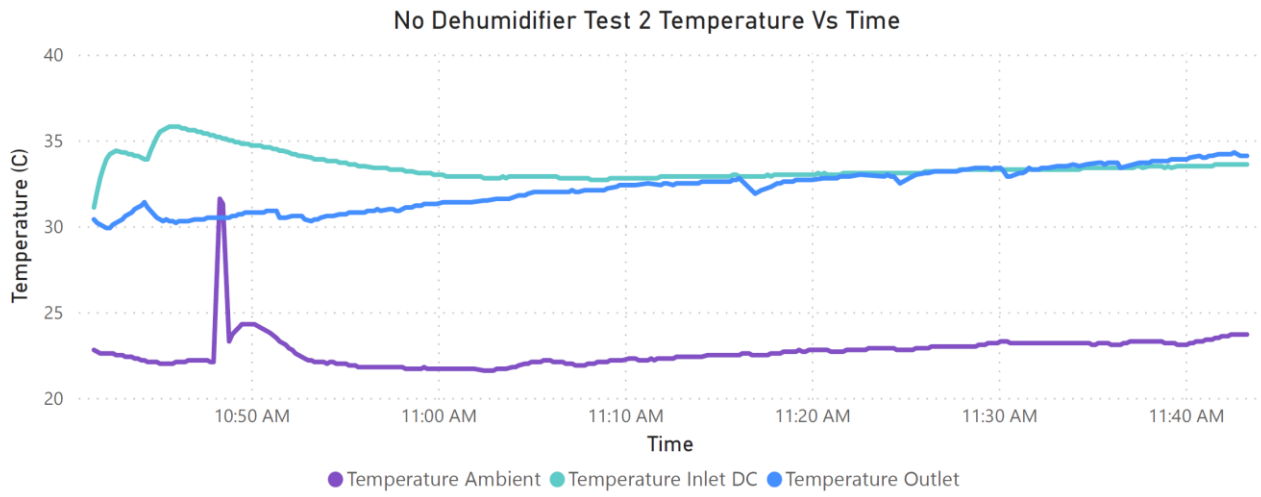


**Figure 7.32. No Dehumidifier Test 2 Temp Vs Time**

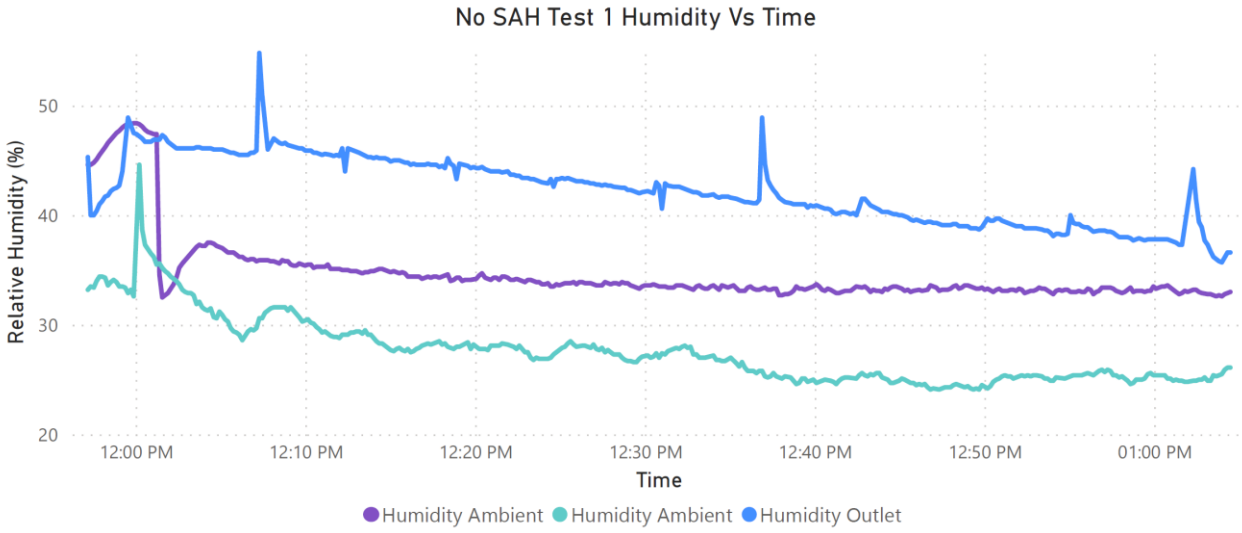


**Figure 7.33. No SAH Test 1 Humidity Vs Time**

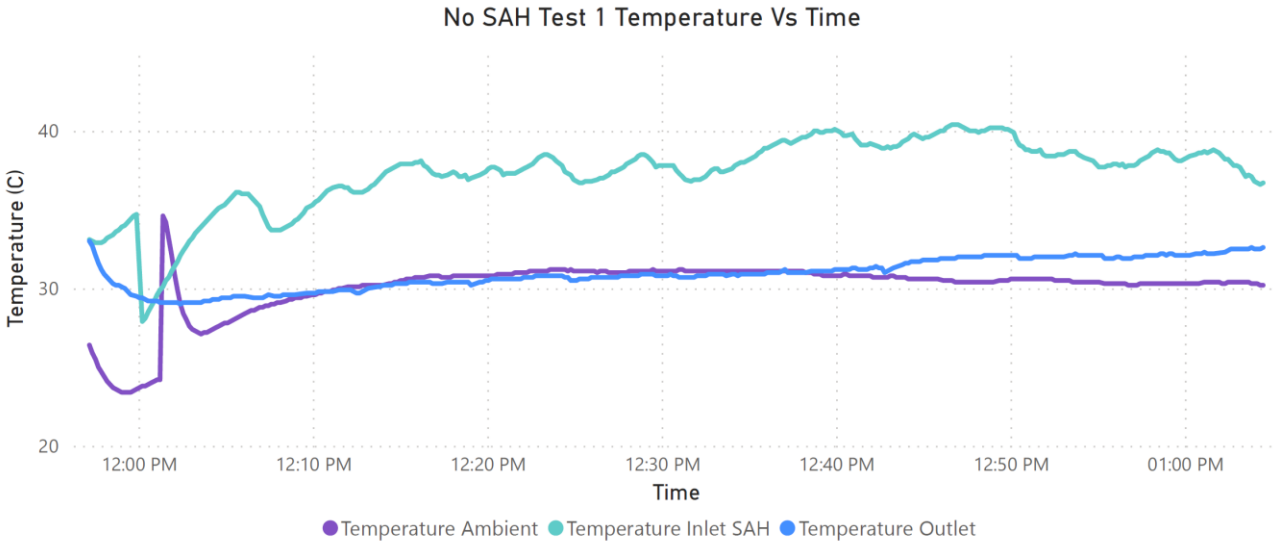


**Figure 7.34. No SAH Test 1 Temp Vs Time**

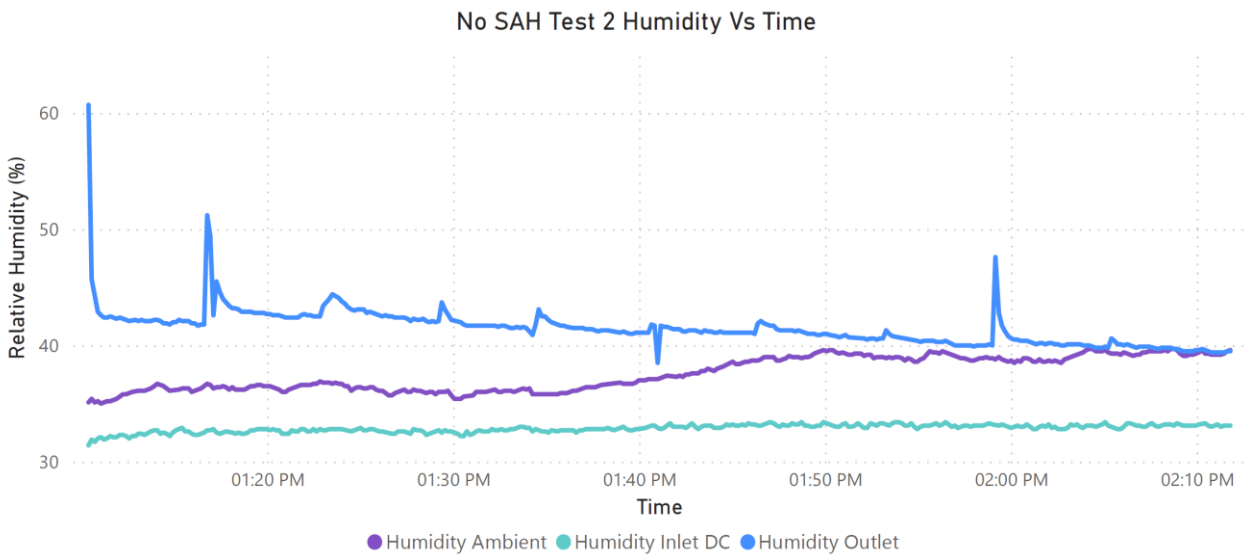


**Figure 7.35. No SAH Test 2 Humidity Vs Time**

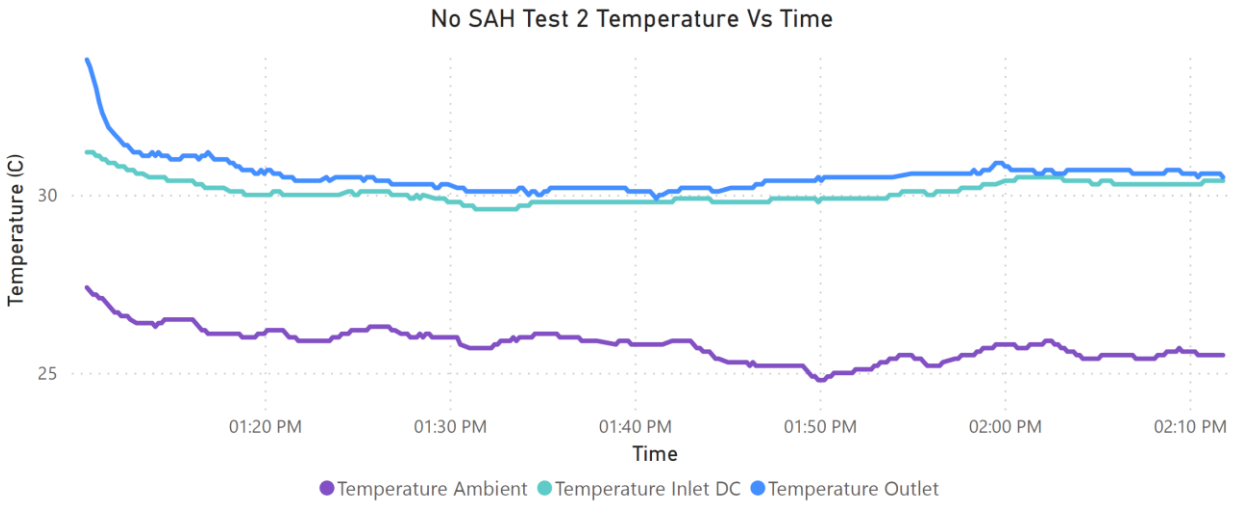


**Figure 7.36. No SAH Test 2 Temp Vs Time**

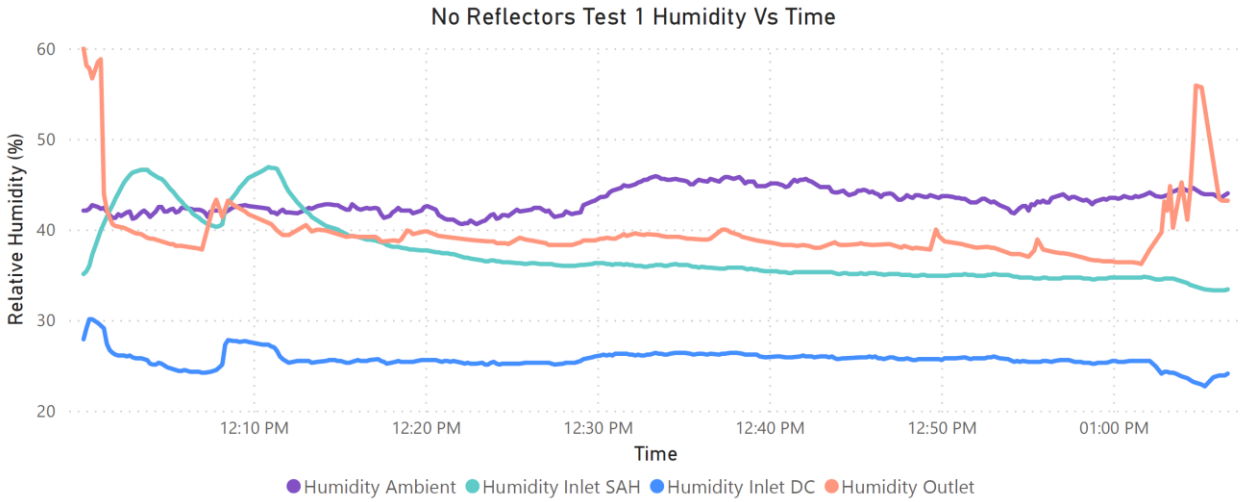


**Figure 7.37. No Reflectors Test 1 Humidity Vs Time**

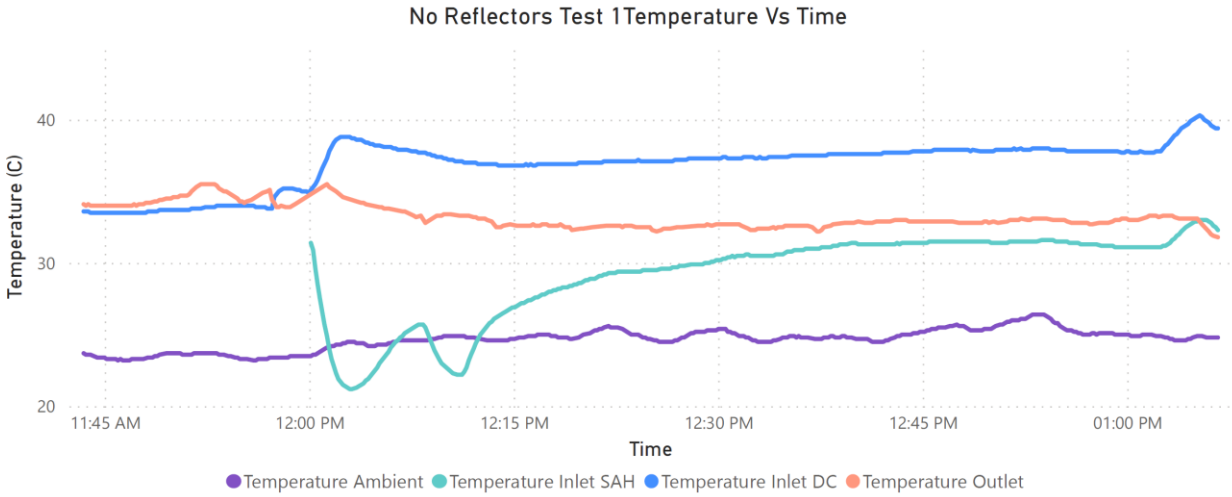


**Figure 7.38. No Reflectors Test 1 Temp Vs Time**

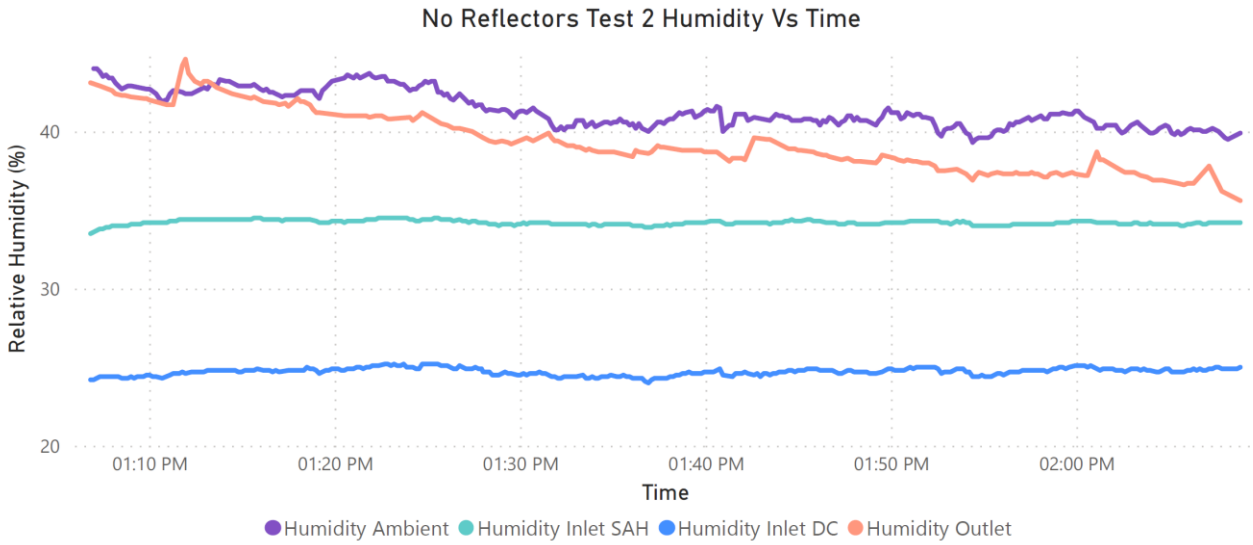


**Figure 7.39. No Reflectors Test 2 Humidity Vs Time**

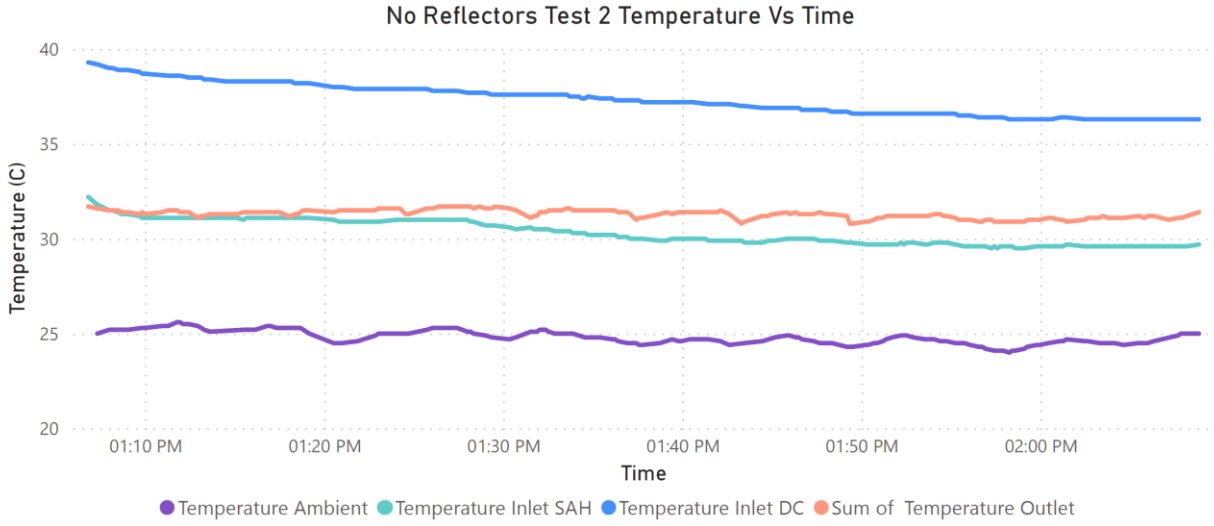


**Figure 7.40. No Reflectors Test 2 Temp Vs Time**

### 7.5.3.3 *Synthetic faecal sludge tests*

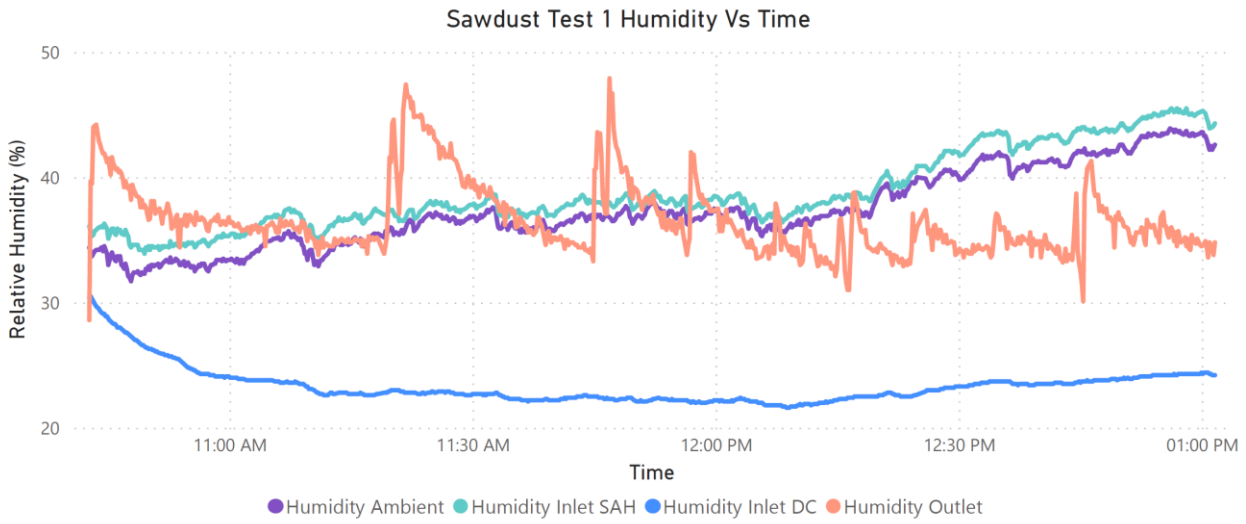


**Figure 7.41. Sawdust Additive Test 1 Humidity Vs Time**

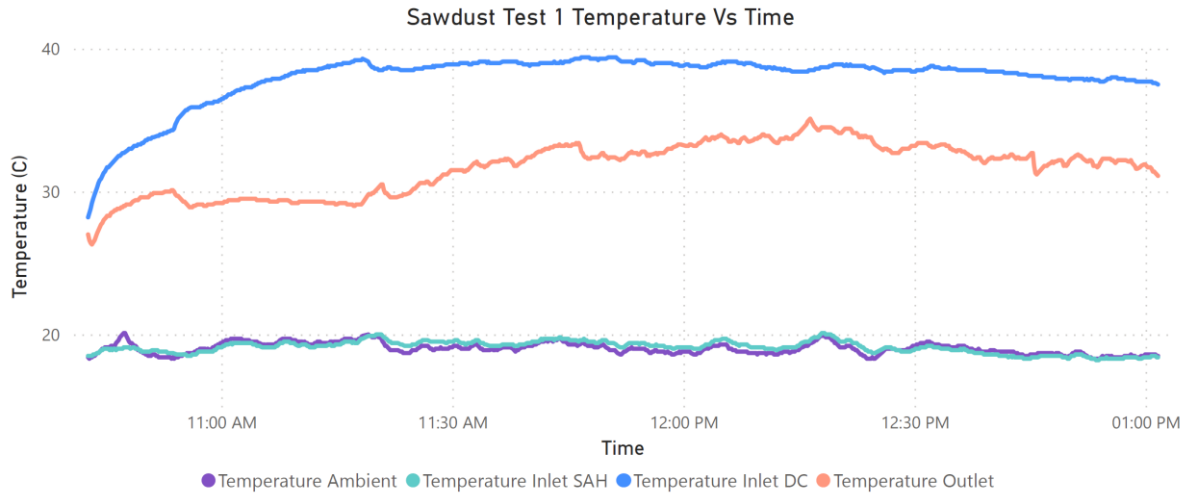


**Figure 7.42. Sawdust Additive Test 1 Temp Vs Time**

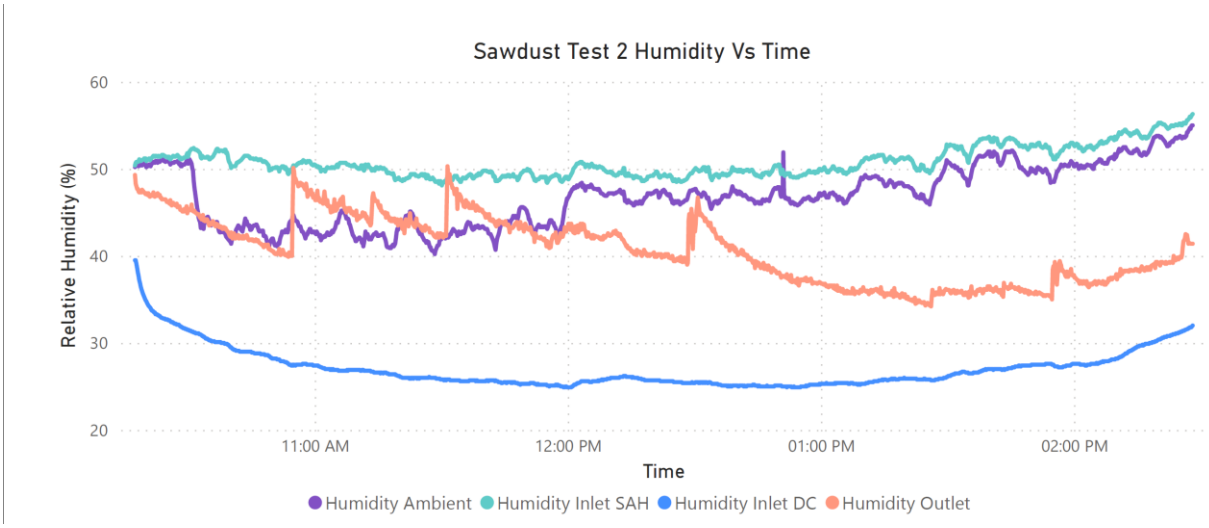


**Figure 7.43. Sawdust Additive Test 2 Humidity Vs Time**

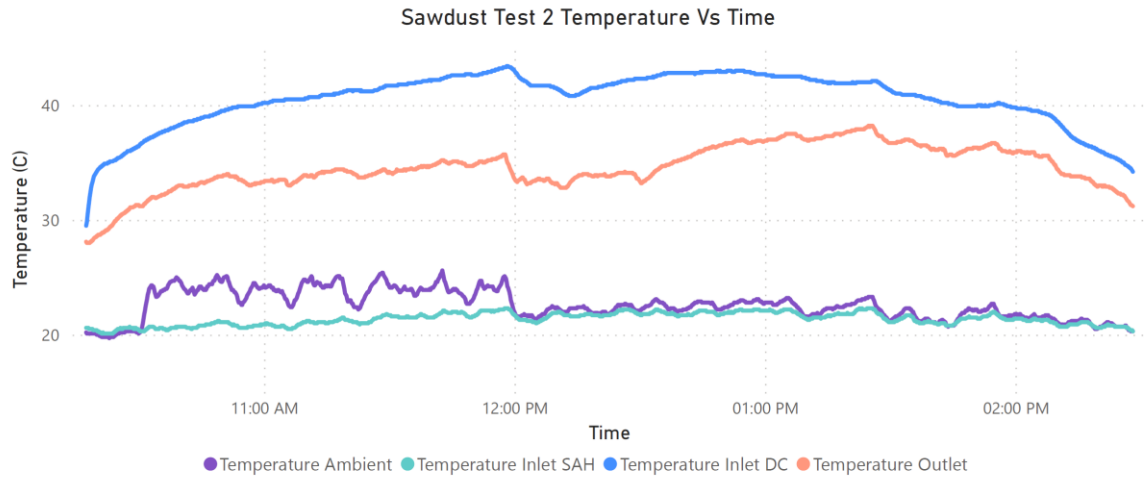


**Figure 7.44. Sawdust Additive Test 2 Temp Vs Time**

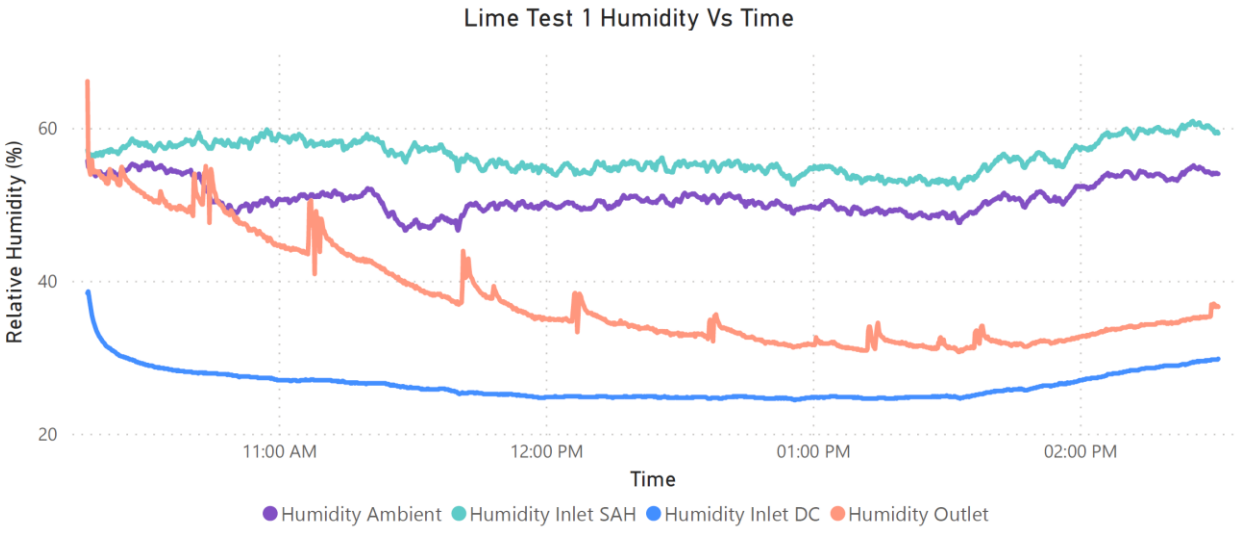


**Figure 7.45. Lime Additive Test 1 Humidity Vs Time**

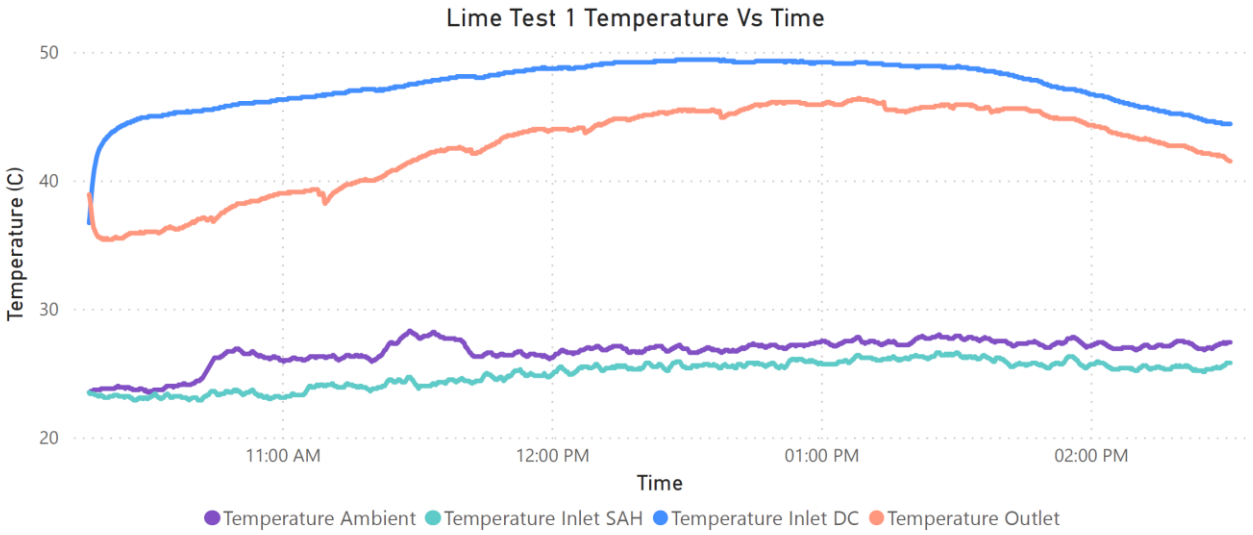


**Figure 7.46. Lime Additive Test 1 Temp Vs Time**

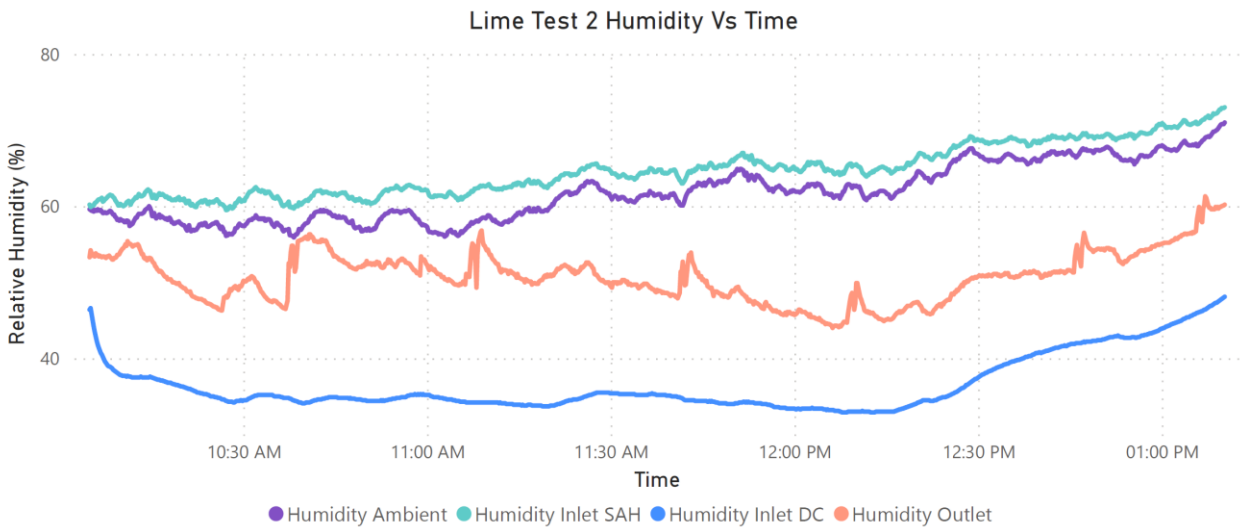


**Figure 7.47. Lime Additive Test 2 Humidity Vs Time**

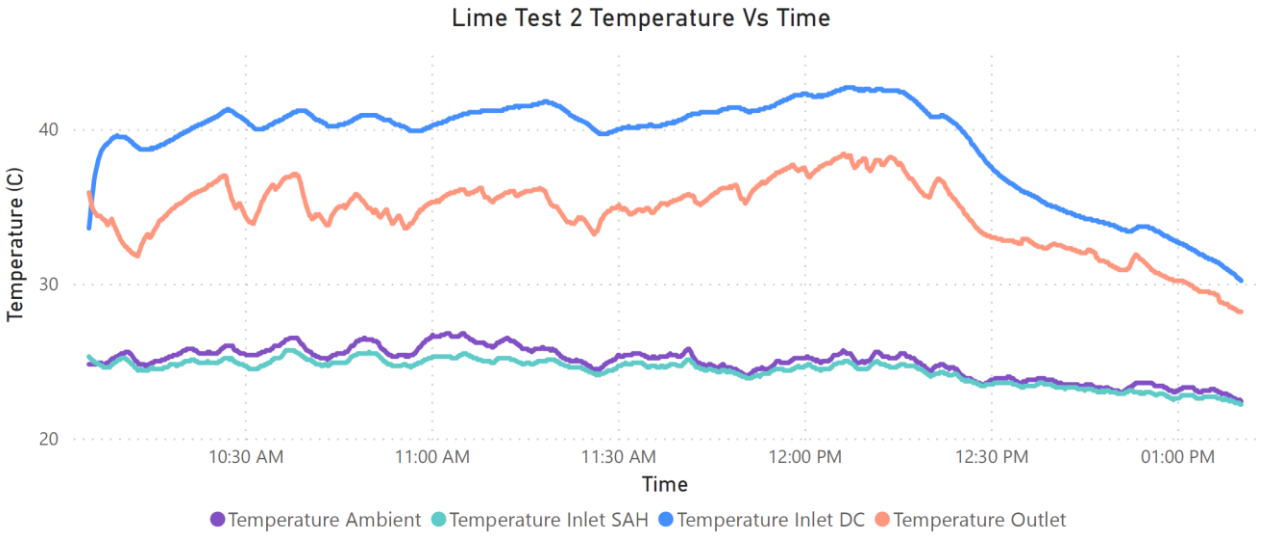


**Figure 7.48. Lime Additive Test 2 Temp Vs Time**

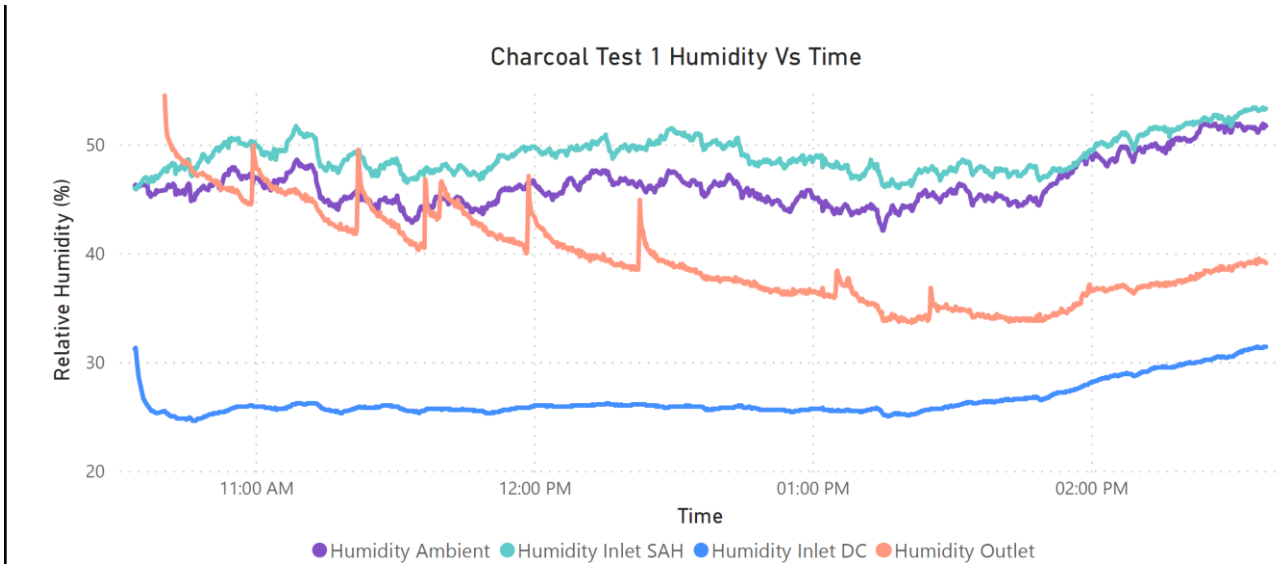


**Figure 7.49. Charcoal Additive Test 1 Humidity Vs Time**

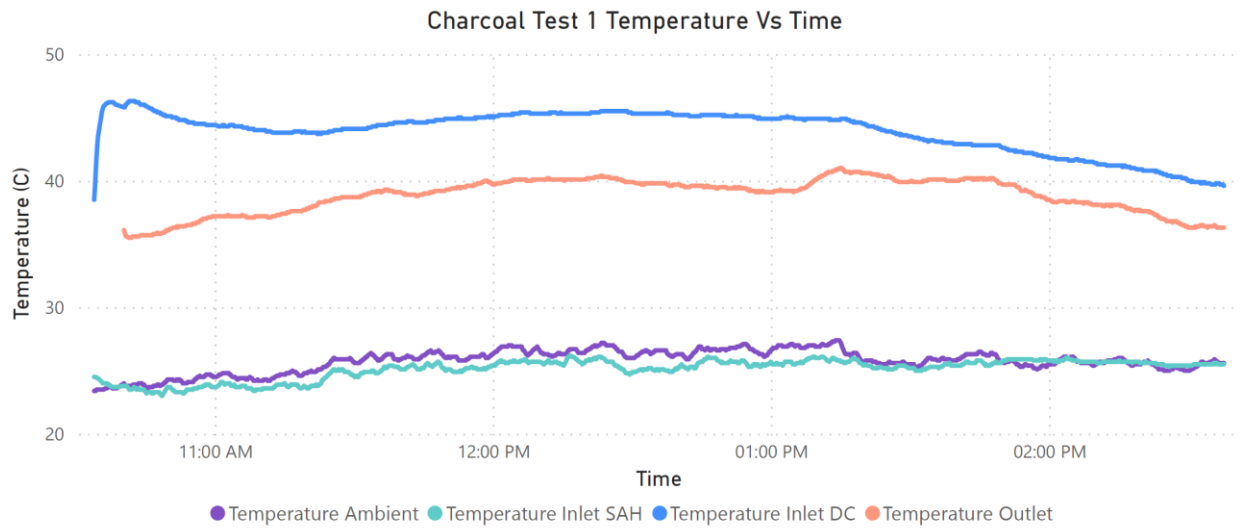


**Figure 7.50. Charcoal Additive Test 1 Temp Vs Time**

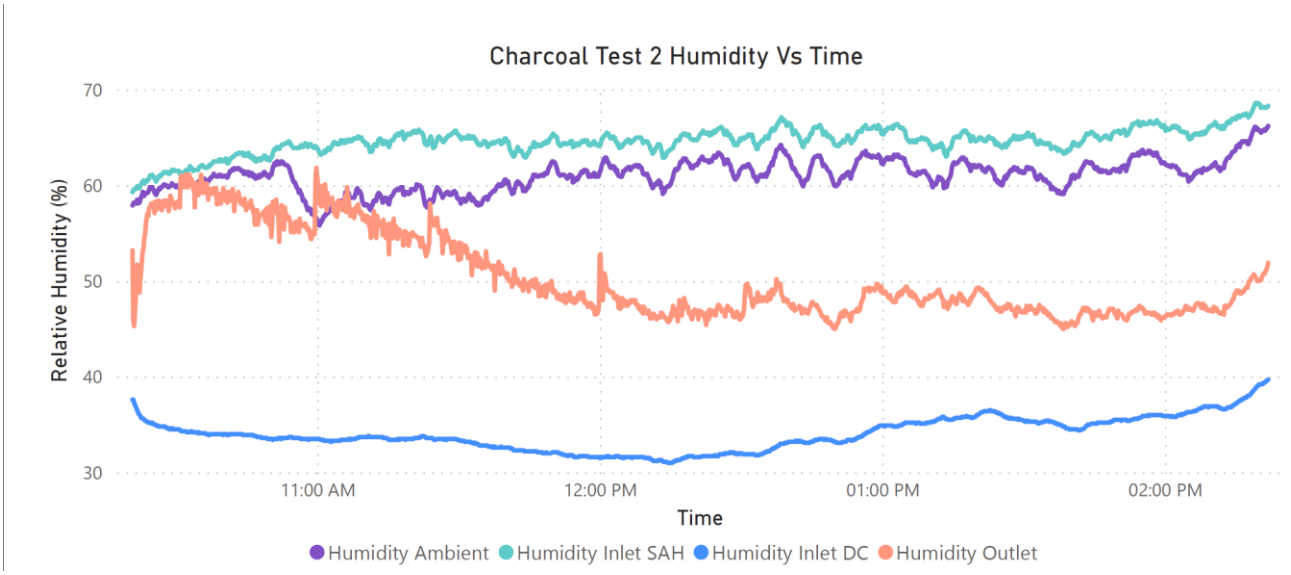


**Figure 7.51. Charcoal Additive Test 2 Humidity Vs Time**

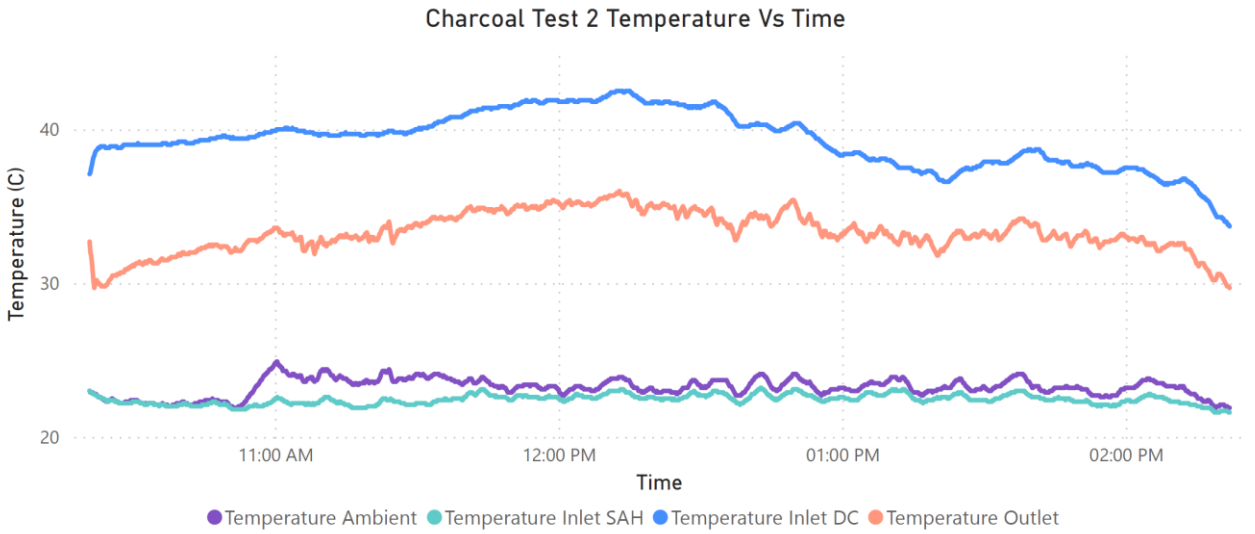


**Figure 7.52. Charcoal Additive Test 2 Temp Vs Time**

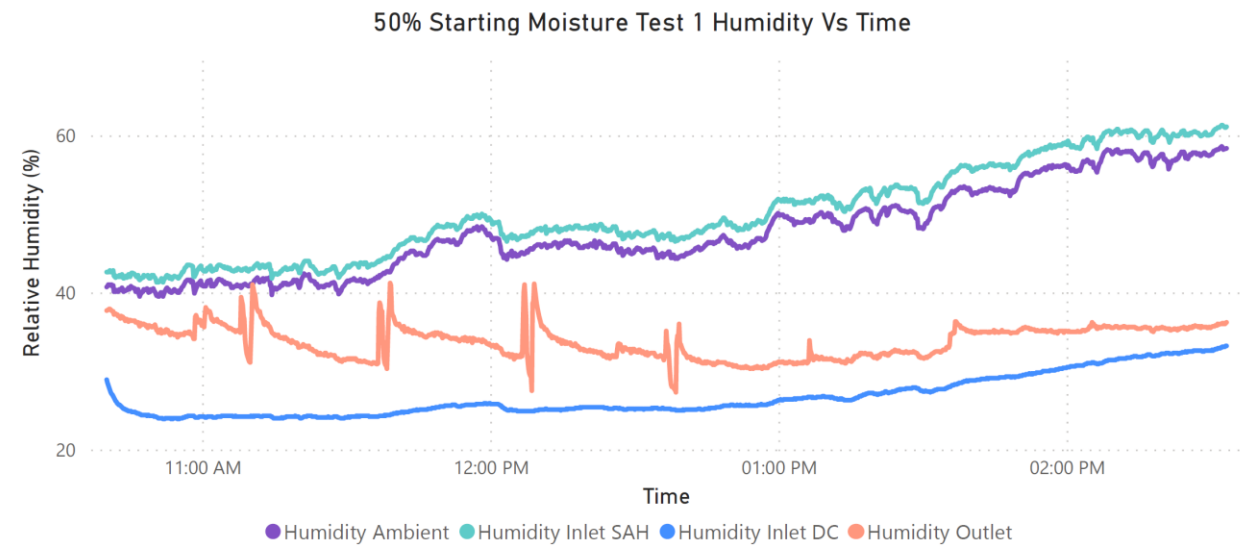


**Figure 7.53. 50% Starting Moisture Test 1 Humidity Vs Time**

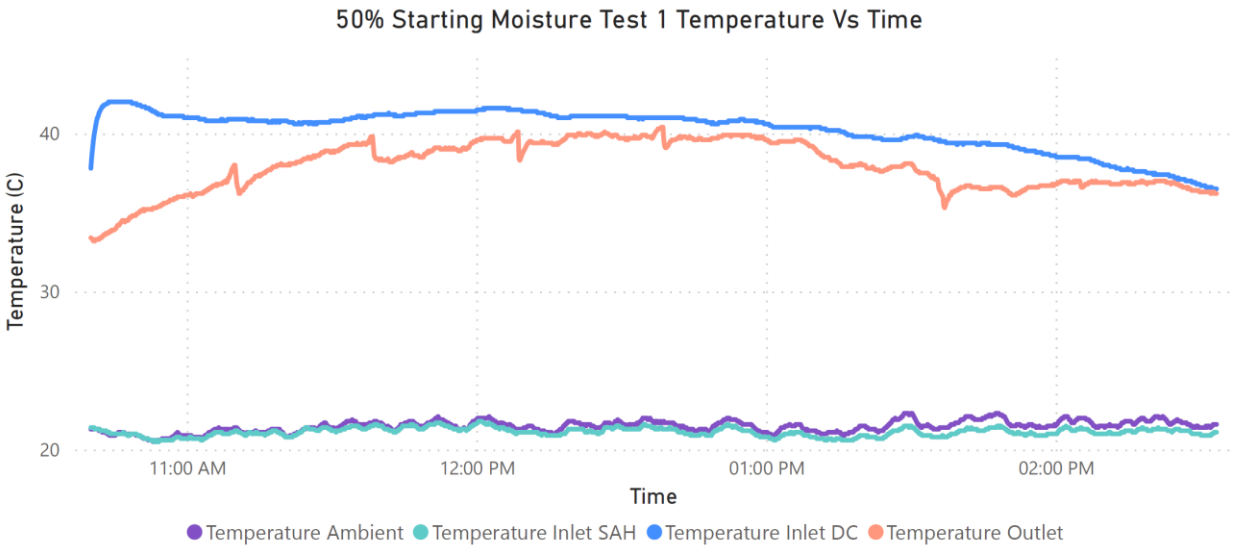


**Figure 7.54. 50% Starting Moisture Test 1 Temp Vs Time**

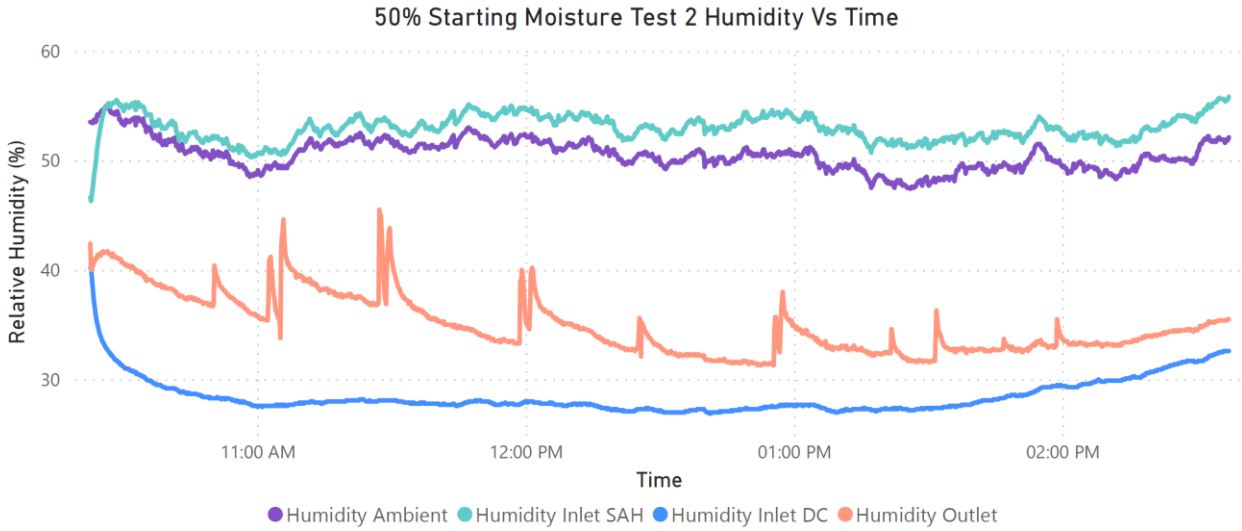


**Figure 7.55. 50% Starting Moisture Test 2 Humidity Vs Time**

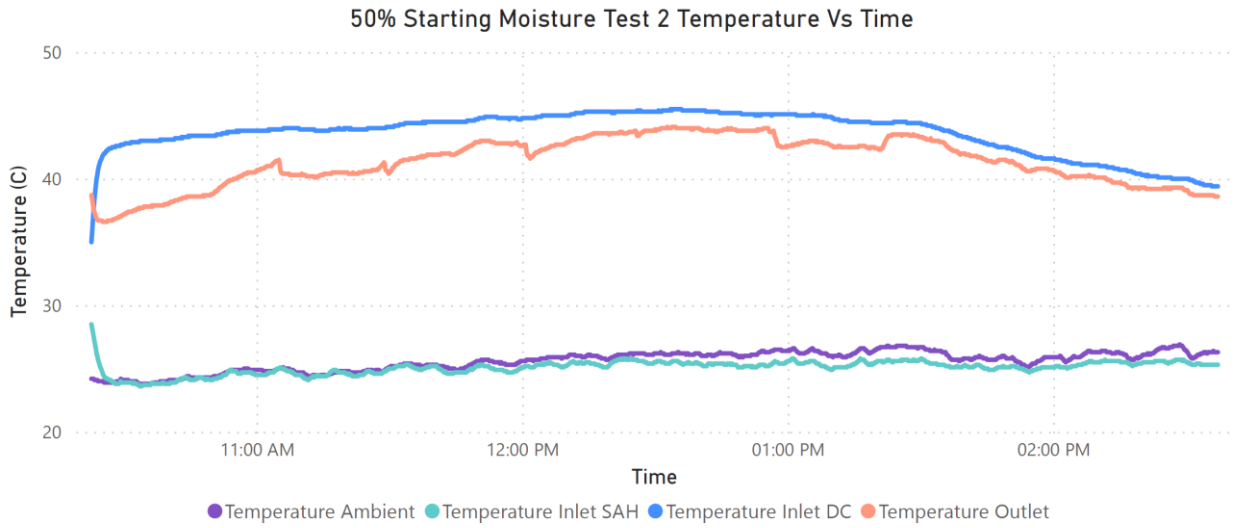


**Figure 7.56. 50% Starting Moisture Test 1 Temp Vs Time**

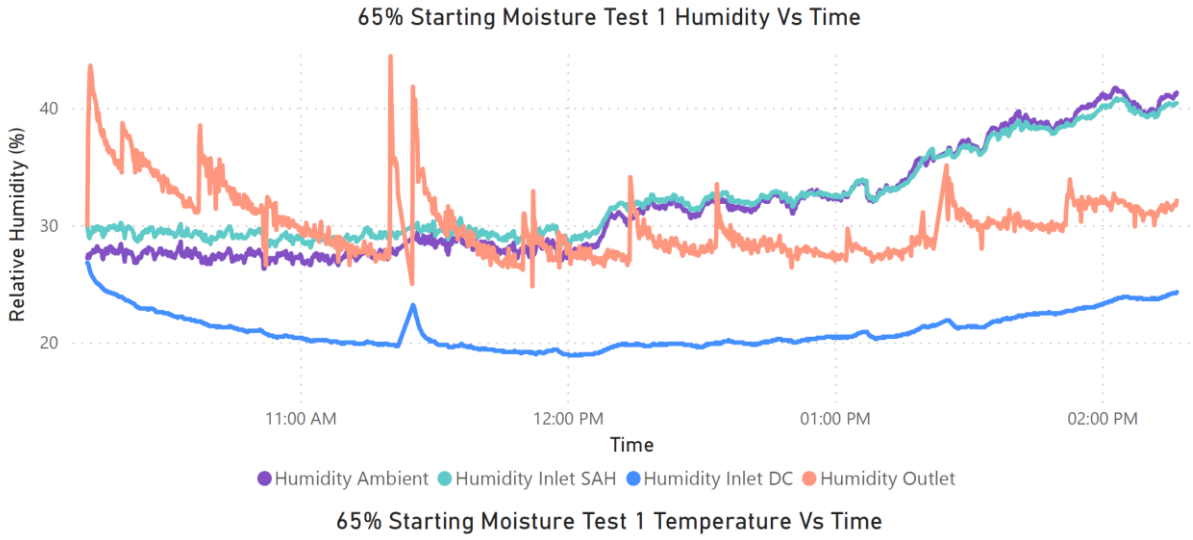


65% Starting Moisture Test 1 Temperature Vs Time

**Figure 7.57. 65% Starting Moisture Test 1 Humidity Vs Time**

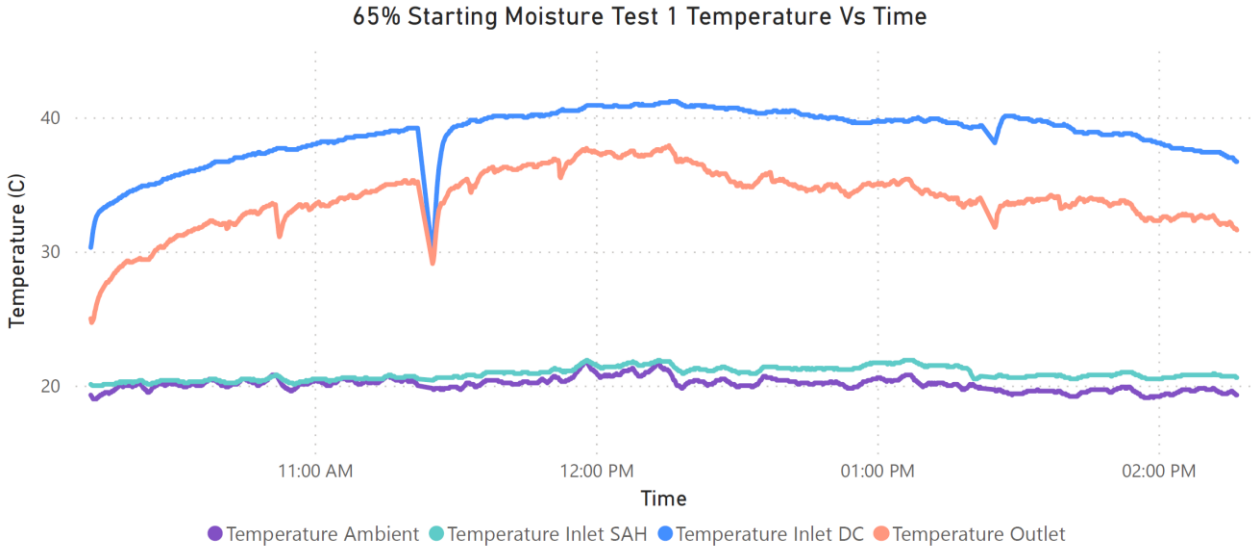


**Figure 7.58. 65% Starting Moisture Test 1 Temp Vs Time**

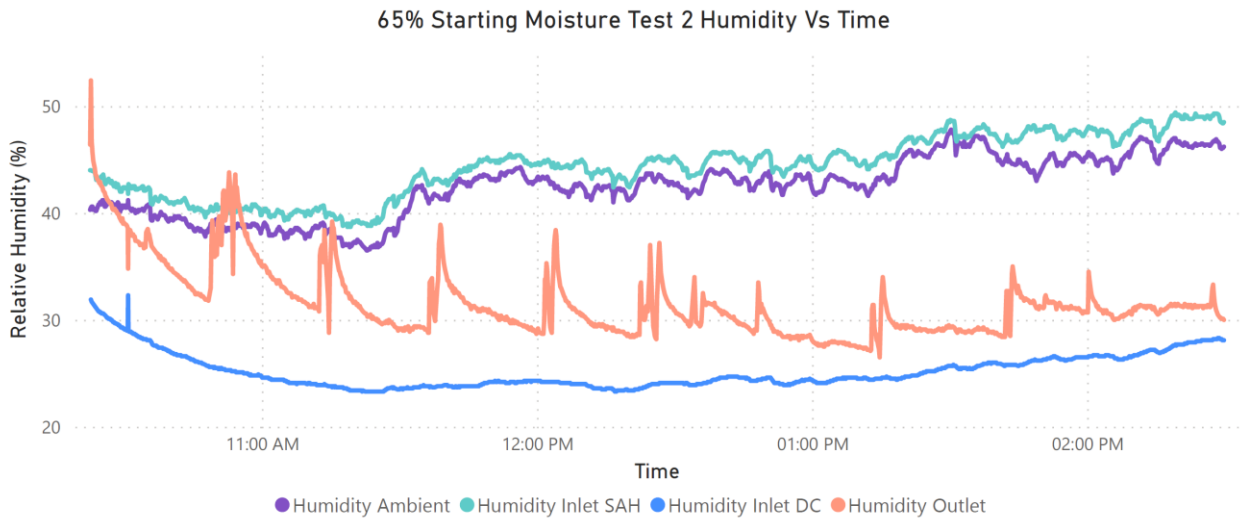


**Figure 7.59. 65% Starting Moisture Test 2 Humidity Vs Time**

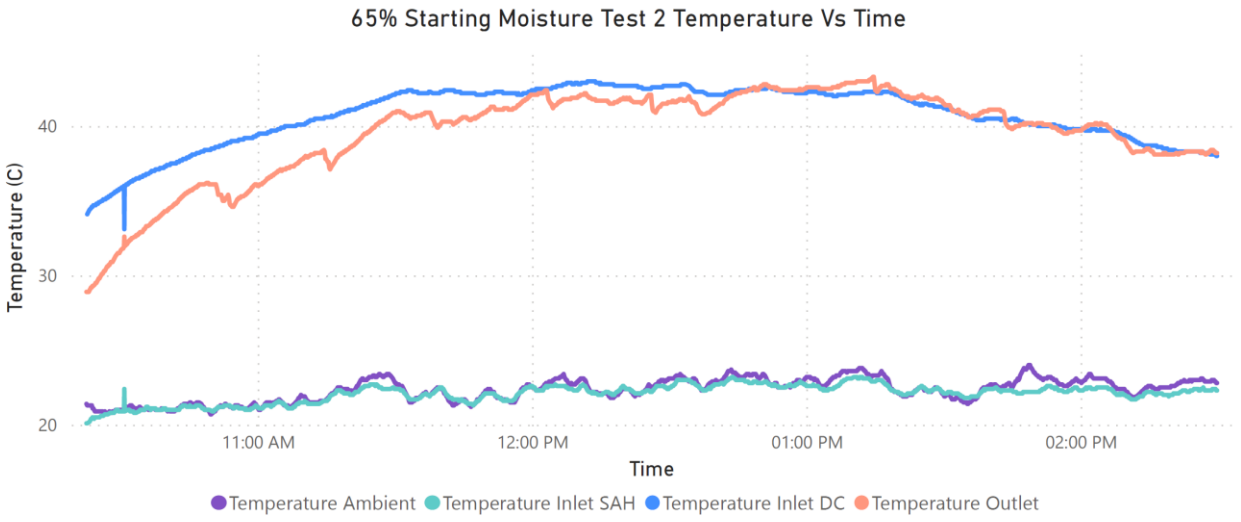


**Figure 7.60. 65% Starting Moisture Test 2 Temp Vs Time**

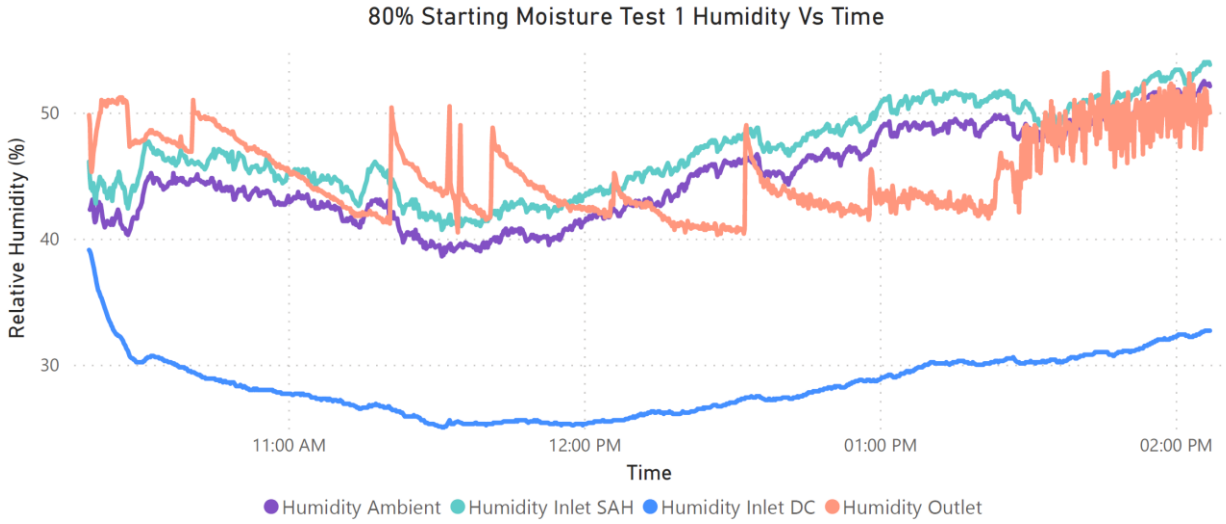


**Figure 7.61. 80% Starting Moisture Test 1 Humidity Vs Time**

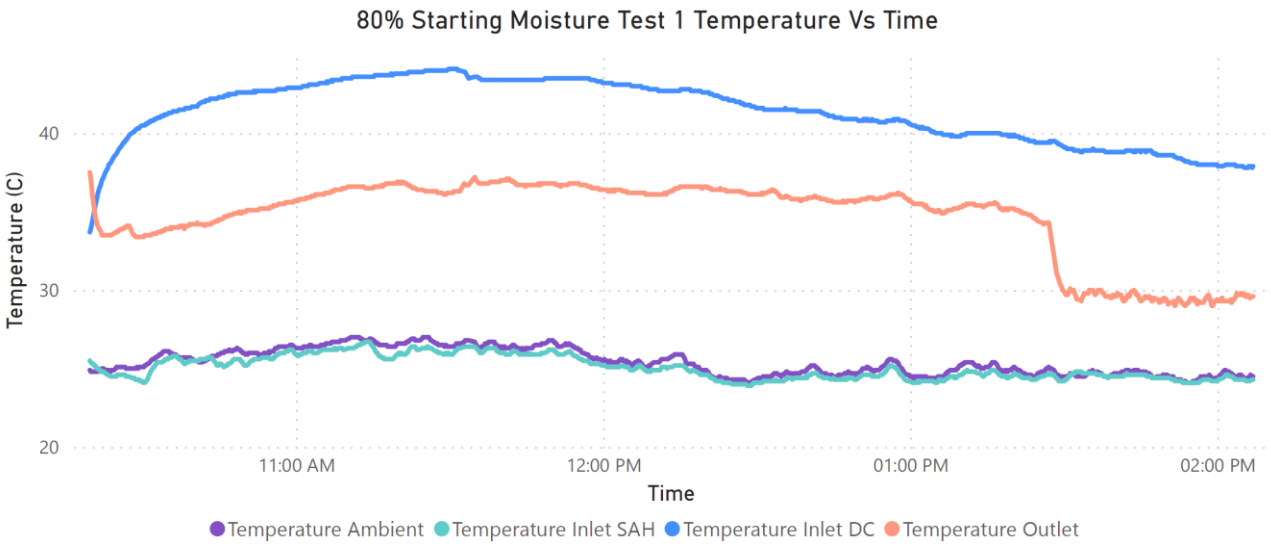


**Figure 7.62. 80% Starting Moisture Test 1 Temp Vs Time**

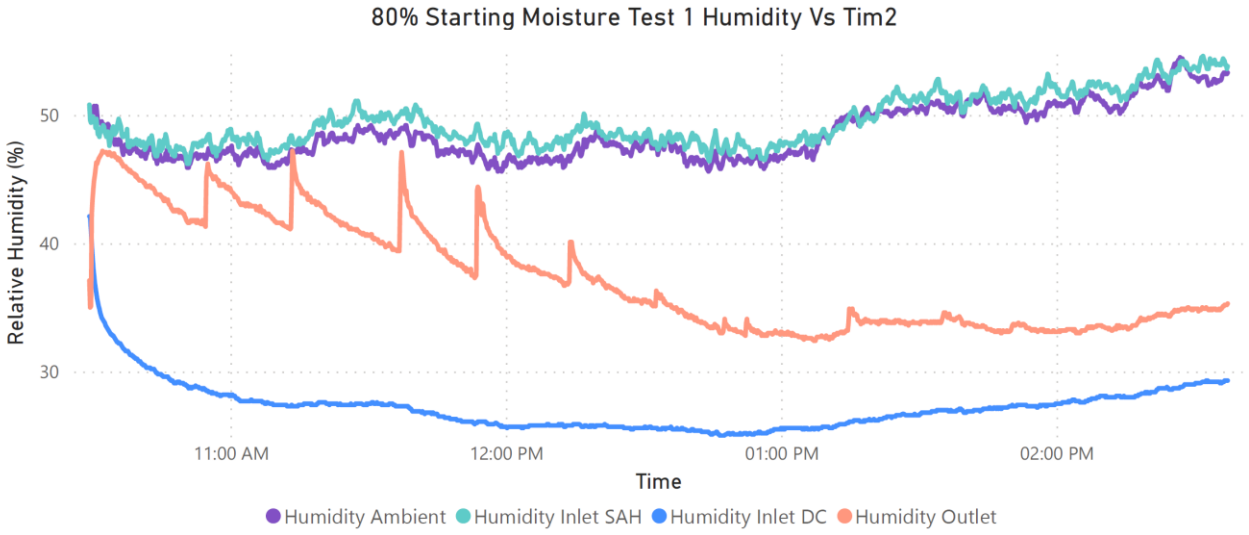


**Figure 7.63. 80% Starting Moisture Test 2 Humidity Vs Time**

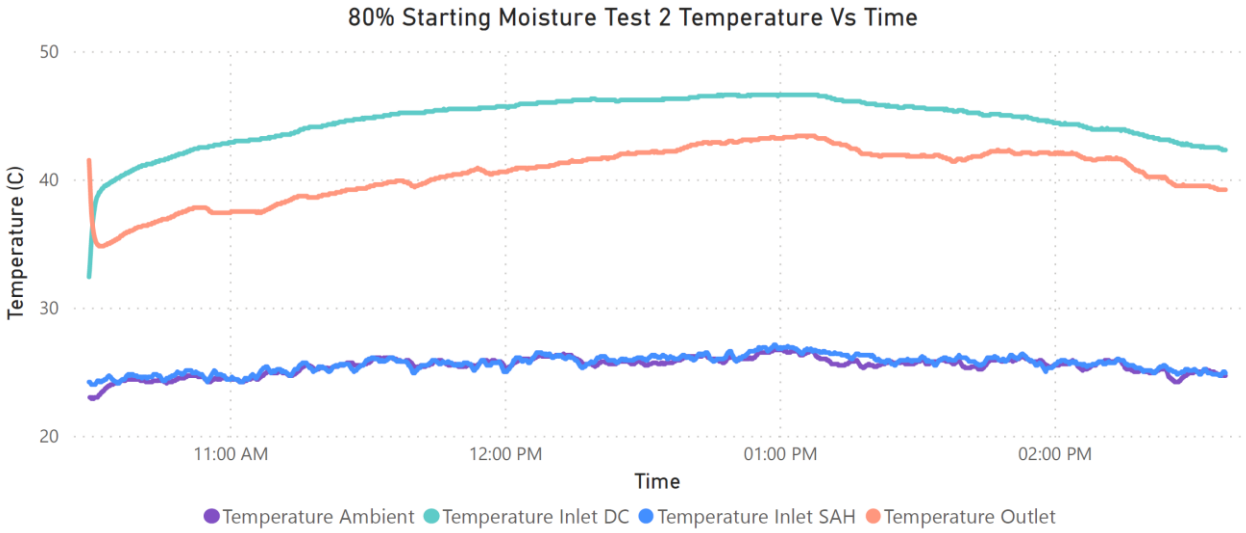


**Figure 7.64. 80% Starting Moisture Test 2 Temp Vs Time**

7.5.3.4 *Summary*

**Table 7.44. Summary of Temperature and Humidity Data Across All Tests**

| Test | Run | Temperature Ambient | Temperature Inlet SAH | Temperature Inlet DC | Temperature Outlet | Humidity Ambient | Humidity Inlet SAH | Humidity Inlet DC | Humidity Outlet | Average Drying Chamber Temperature | Average Drying Chamber Humidity |
|---|---|---|---|---|---|---|---|---|---|---|---|
| **Full Device** | 1 | 24,46 | 32,98 | 40,84 | 31,27 | 99,81 | 34,26 | 30,53 | 81,86 | 36,06 | 56,20 |
| **Full Device** | 2 | 24,30 | 30,58 | 38,60 | 34,40 | 92,73 | 40,90 | 34,73 | 73,09 | 36,50 | 53,91 |
| **No Reflectors** | 1 | 24,80 | 30,33 | 37,31 | 31,14 | 41,31 | 34,20 | 24,72 | 70,12 | 34,23 | 47,42 |
| **No Reflectors** | 2 | 24,65 | 29,03 | 36,86 | 33,39 | 42,81 | 37,19 | 26,72 | 39,57 | 35,12 | 33,15 |
| **No Dehumidifier** | 1 | | 22,23 | 33,17 | 32,14 | | 44,56 | 28,76 | 41,00 | 32,65 | 34,88 |
| **No Dehumidifier** | 2 | | 30,47 | 37,87 | 33,54 | | 32,34 | 24,00 | 37,52 | 35,70 | 30,76 |
| **No SAH** | 1 | 25,79 | | 30,09 | 30,57 | 37,60 | | 32,85 | 41,50 | 30,33 | 37,18 |
| **No SAH** | 2 | 37,27 | | 30,02 | 30,92 | 27,63 | | 34,79 | 42,22 | 30,47 | 38,50 |
| **50% Fan** | 1 | 21,49 | 35,52 | 38,80 | 32,36 | 60,29 | 28,94 | 29,60 | 44,87 | 35,58 | 37,24 |
| **50% Fan** | 2 | 22,13 | 34,22 | 37,67 | 32,97 | 53,95 | 29,16 | 30,56 | 42,41 | 35,32 | 36,48 |
| **25% Fan** | 1 | 24,47 | 35,68 | 45,45 | 37,16 | 56,30 | 31,25 | 25,17 | 48,47 | 41,31 | 36,82 |
| **25% Fan** | 2 | 24,36 | 29,32 | 43,33 | 38,77 | 36,55 | 31,47 | 23,51 | 38,96 | 41,05 | 31,24 |
| **80% MC** | 1 | 25,45 | 25,63 | 44,60 | 40,55 | 48,60 | 49,57 | 27,26 | 37,32 | 42,58 | 32,29 |
| **80% MC** | 2 | 25,35 | 24,86 | 41,31 | 34,46 | 44,85 | 46,89 | 28,43 | 45,06 | 37,89 | 36,75 |
| **65% MC** | 1 | 22,21 | 21,97 | 40,65 | 39,58 | 42,41 | 44,25 | 25,16 | 31,56 | 40,12 | 28,36 |
| **65% MC** | 2 | 19,95 | 20,73 | 38,61 | 33,94 | 31,57 | 32,20 | 20,96 | 30,06 | 36,28 | 25,51 |
| **50% MC** | 1 | 25,59 | 25,07 | 43,61 | 41,36 | 50,54 | 52,95 | 28,46 | 34,98 | 42,49 | 31,72 |
| **50% MC** | 2 | 21,47 | 21,12 | 40,23 | 37,93 | 47,73 | 49,99 | 26,68 | 33,77 | 39,08 | 30,23 |
| **Sawdust Additive** | 1 | 22,57 | 21,37 | 40,52 | 34,58 | 46,92 | 50,77 | 27,05 | 40,72 | 37,55 | 33,88 |
| **Sawdust Additive** | 2 | 18,76 | 18,92 | 37,62 | 31,45 | 37,19 | 38,70 | 23,24 | 36,47 | 34,53 | 29,86 |

| | | | | | | | | | | | |
|---|---|---|---|---|---|---|---|---|---|---|---|
| **Activated Carbon Additive** | 1 | 23,22 | 22,44 | 39,35 | 33,32 | 60,99 | 64,60 | 33,97 | 50,47 | 36,34 | 42,22 |
| **Activated Carbon Additive** | 2 | 25,72 | 25,06 | 43,84 | 38,85 | 46,31 | 49,01 | 26,47 | 39,42 | 41,35 | 32,95 |
| **Lime Additive** | 1 | 24,91 | 24,37 | 39,20 | 34,51 | 61,79 | 64,64 | 36,54 | 50,88 | 36,85 | 43,71 |
| **Lime Additive** | 2 | 26,69 | 24,95 | 47,46 | 42,80 | 50,84 | 56,25 | 26,34 | 37,52 | 45,13 | 31,93 |

### 7.5.4 Drying curves

#### 7.5.4.1 *Wet soil tests*

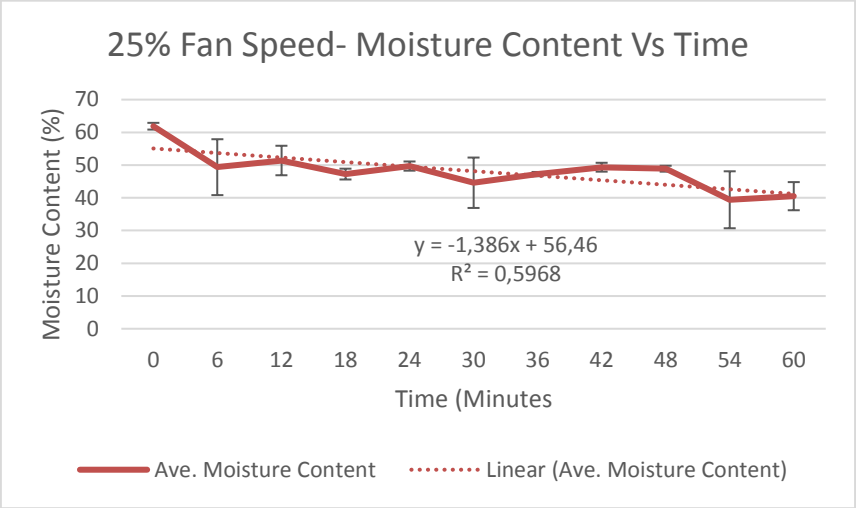


**Figure 7.65. 25% Fan Speed Moisture Content Vs Time**

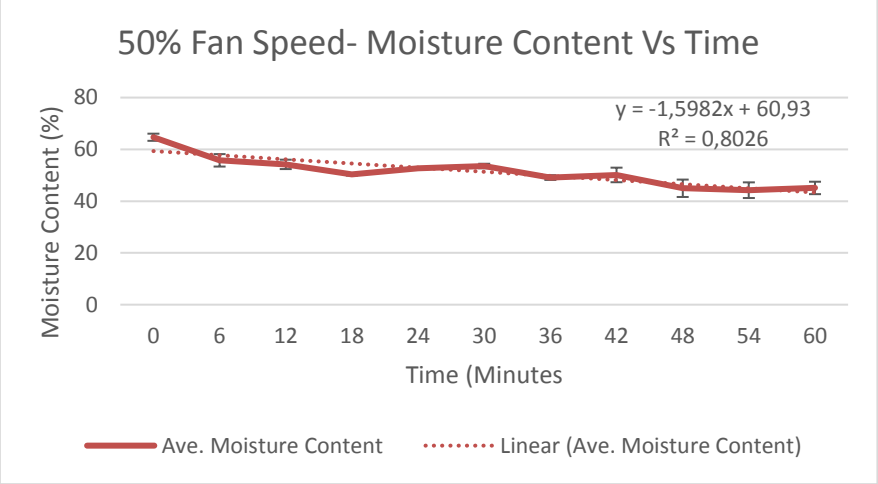


**Figure 7.66. 50% Fan Speed Moisture Content Vs Time**

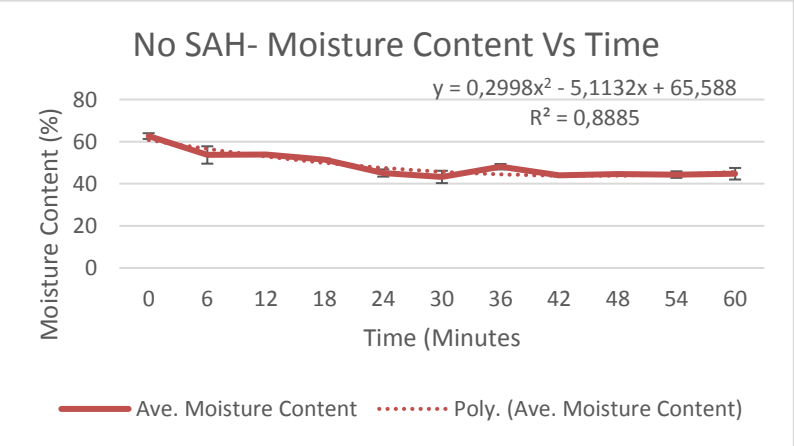


**Figure 7.67. No SAH Moisture Content Vs Time**

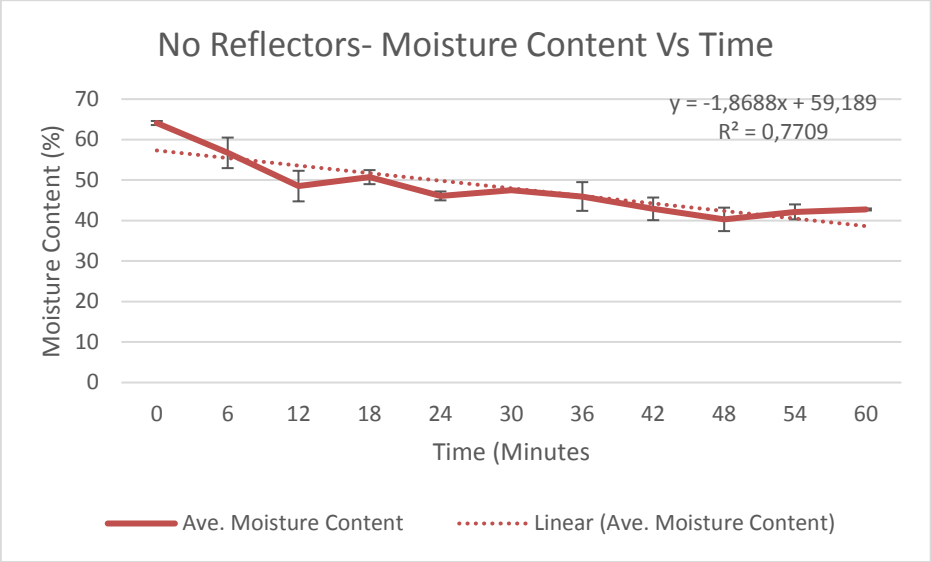


**Figure 7.68. No Reflectors Moisture Content Vs Time**

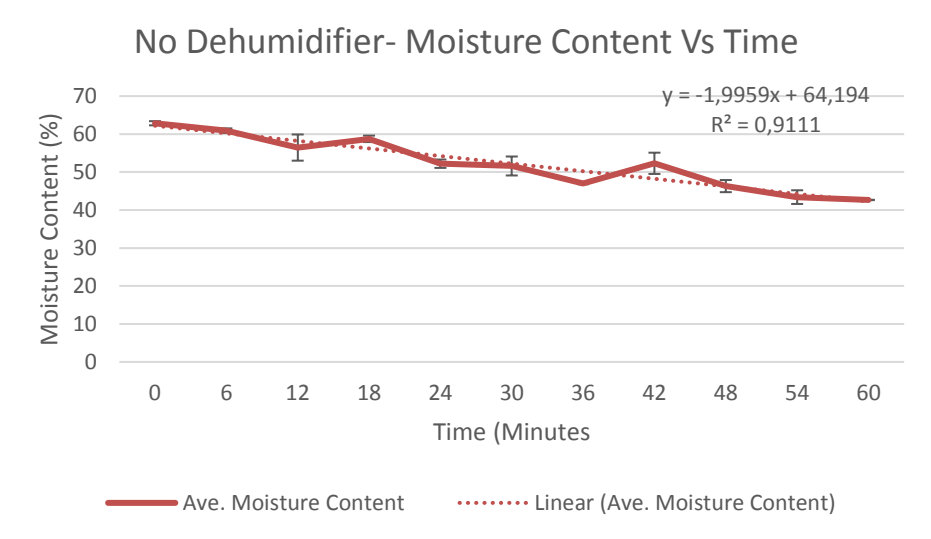


**Figure 7.69. No Dehumidifier Moisture Content Vs Time**

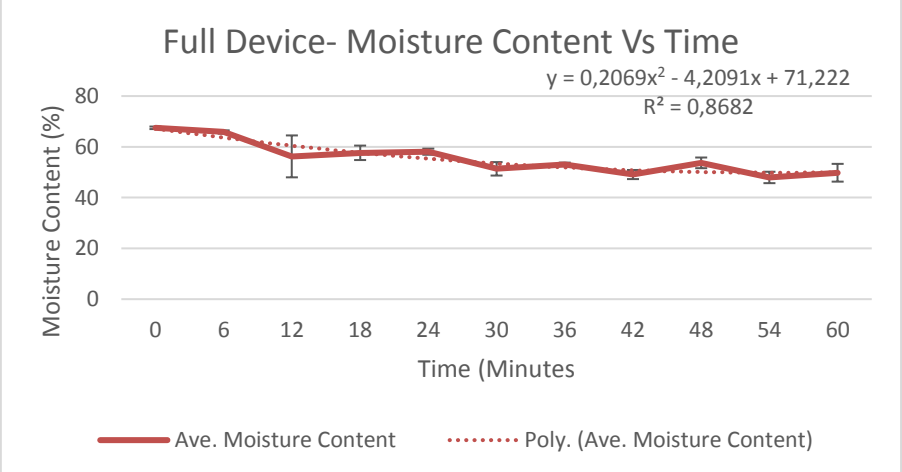


**Figure 7.70. Full Device Moisture Content Vs Time**

### 7.5.4.2 *Synthetic sludge tests*

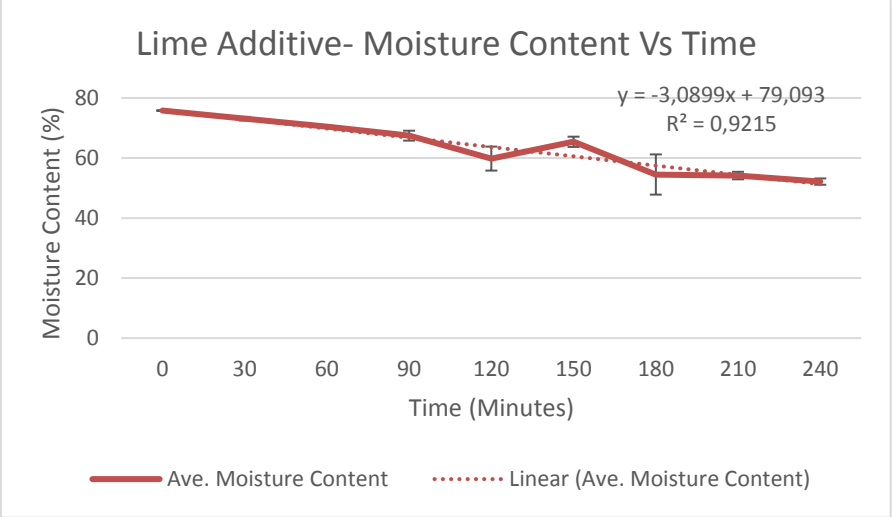


**Figure 7.71. Lime Additive Moisture Content Vs Time**

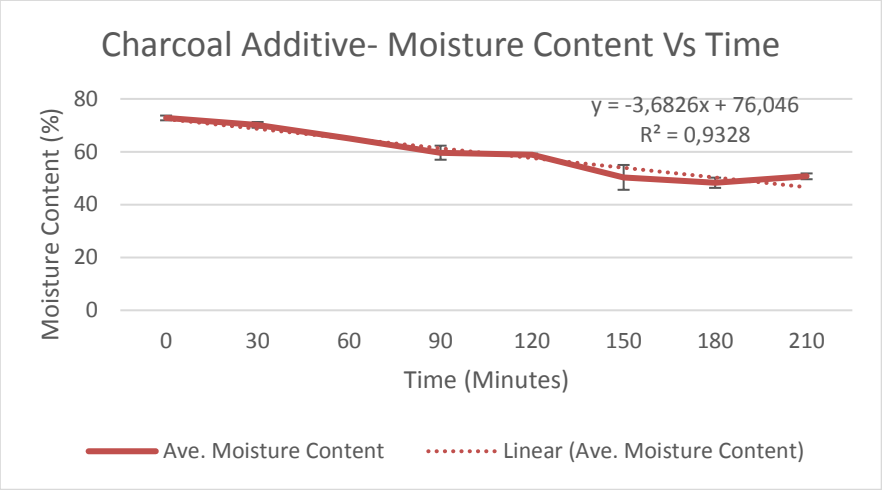


**Figure 7.72. Charcoal Additive Moisture Content Vs Time**

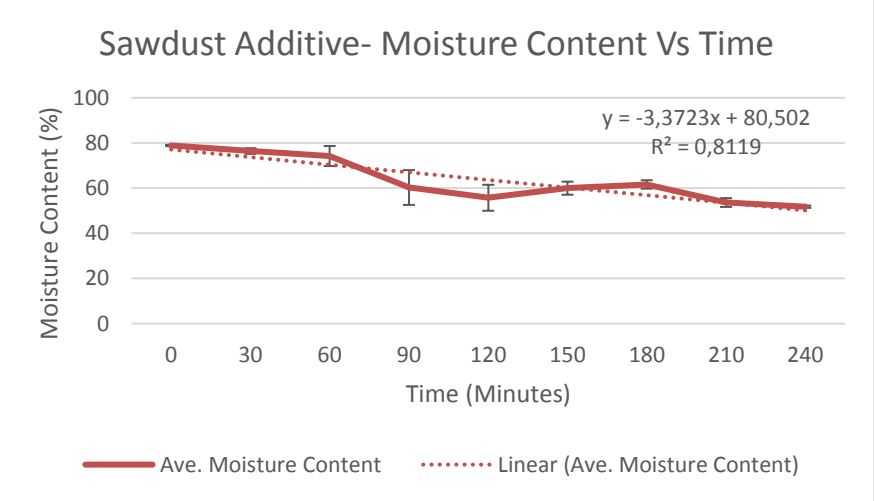


**Figure 7.73. Sawdust Additive Moisture Content Vs Time**

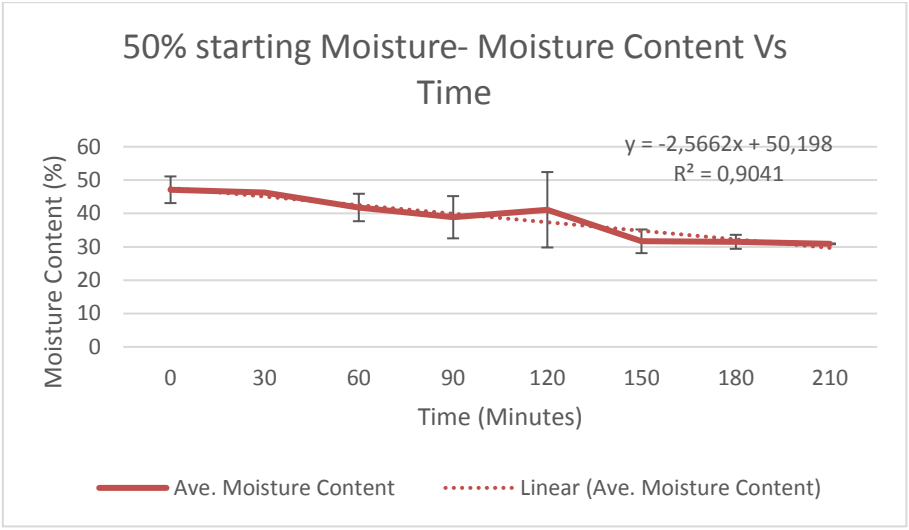


**Figure 7.74. 50% Starting Moisture- Moisture Content Vs Time**

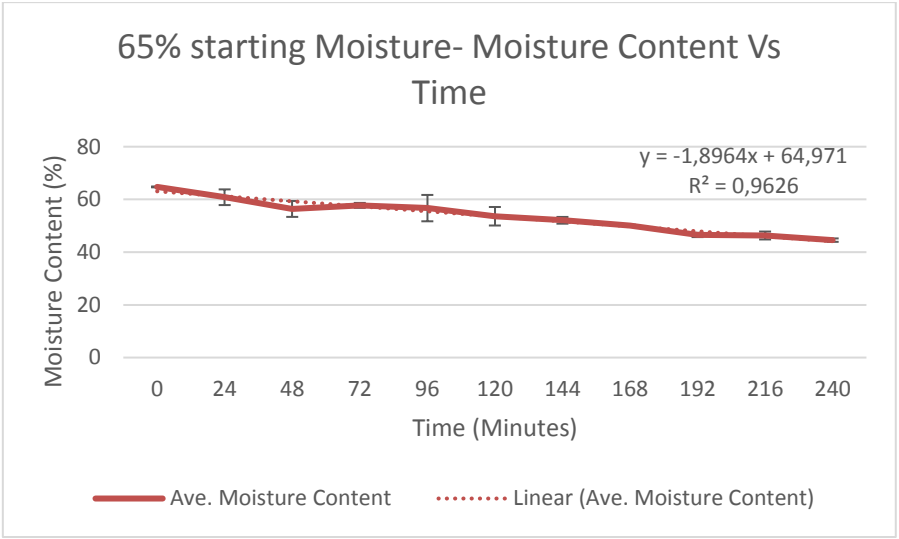


**Figure 7.75. 65% Starting Moisture- Moisture Content Vs Time**

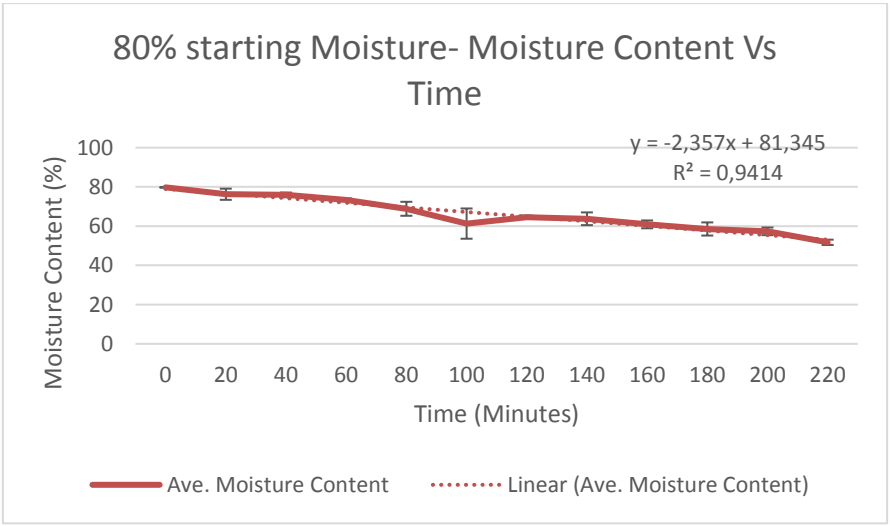


**Figure 7.76. 80% Starting Moisture- Moisture Content Vs Time**

### 7.5.5 Drying Rate Vs Moisture Content Graphs

#### 7.5.5.1 *Wet soils tests*

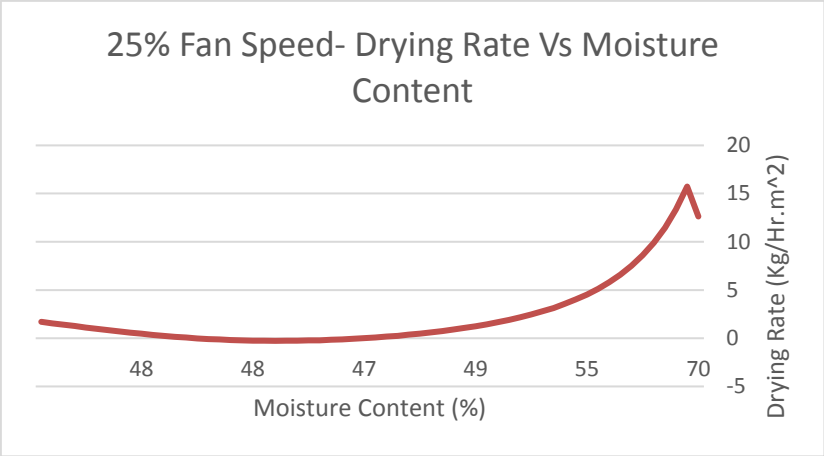


**Figure 7.77. 25% Fan Speed Drying Rate Vs Moisture Content**

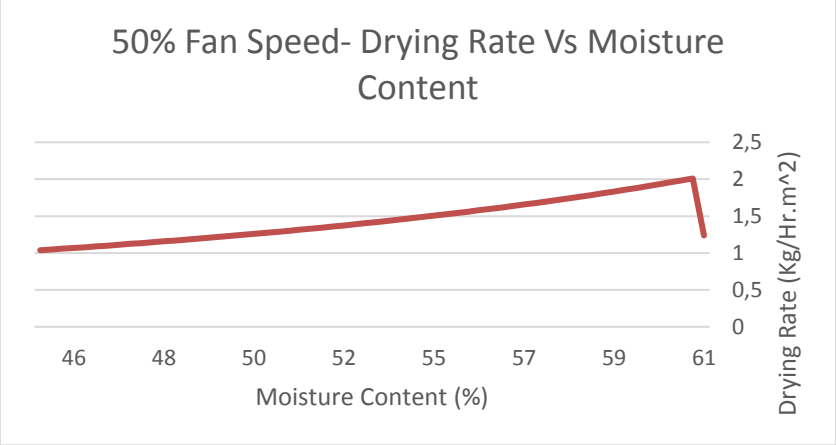


**Figure 7.78. 50% Fan Speed Drying Rate Vs Moisture Content**

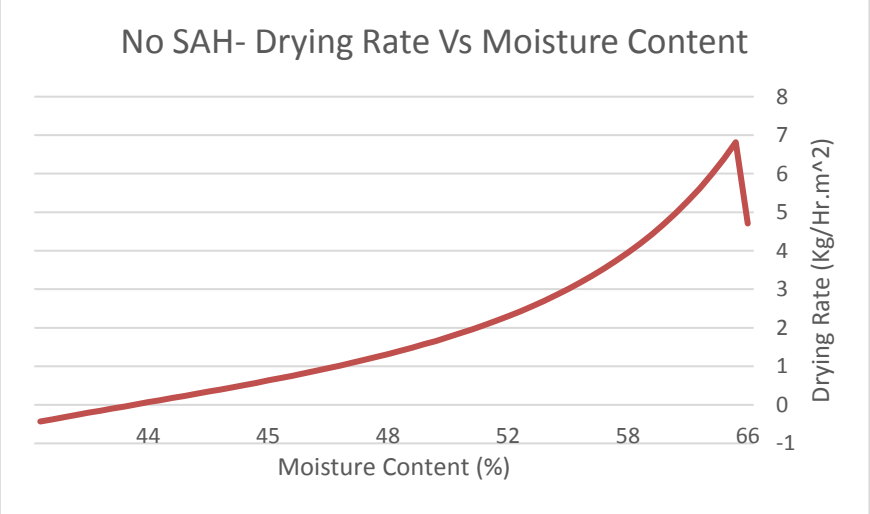


**Figure 7.79. No SAH Drying Rate Vs Moisture Content**

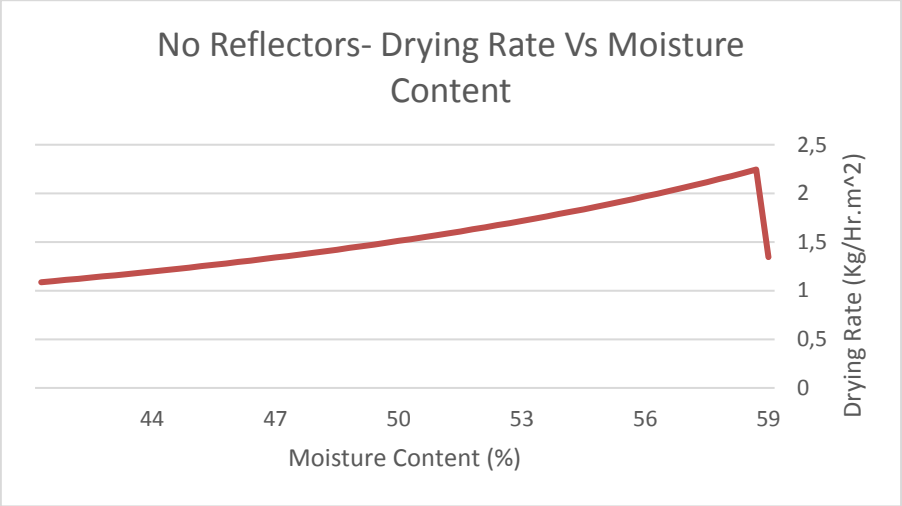


**Figure 7.80. No Reflectors Drying Rate Vs Moisture Content**

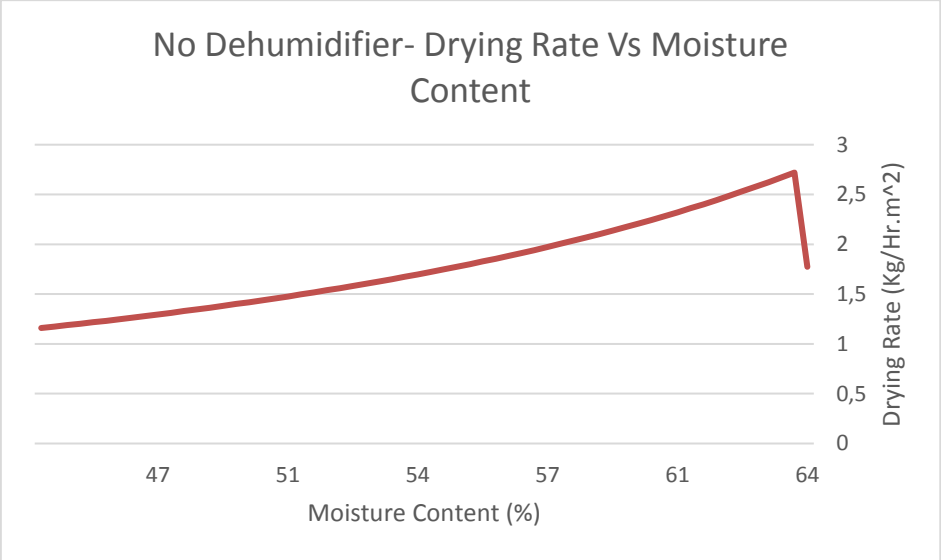


**Figure 7.81. No Dehumidifier Drying Rate Vs Moisture Content**

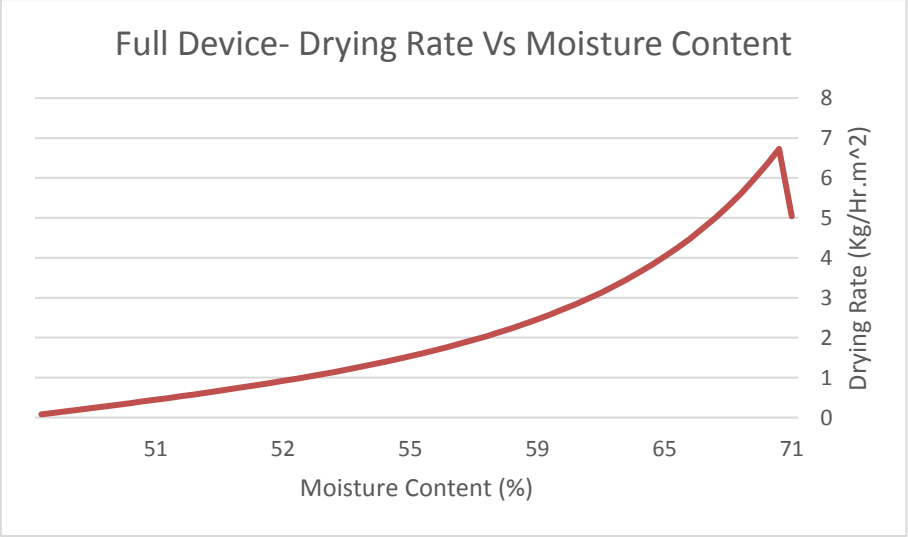


**Figure 7.82. Full Device Drying Rate Vs Moisture Content**

7.5.5.2 *Synthetic sludge tests*

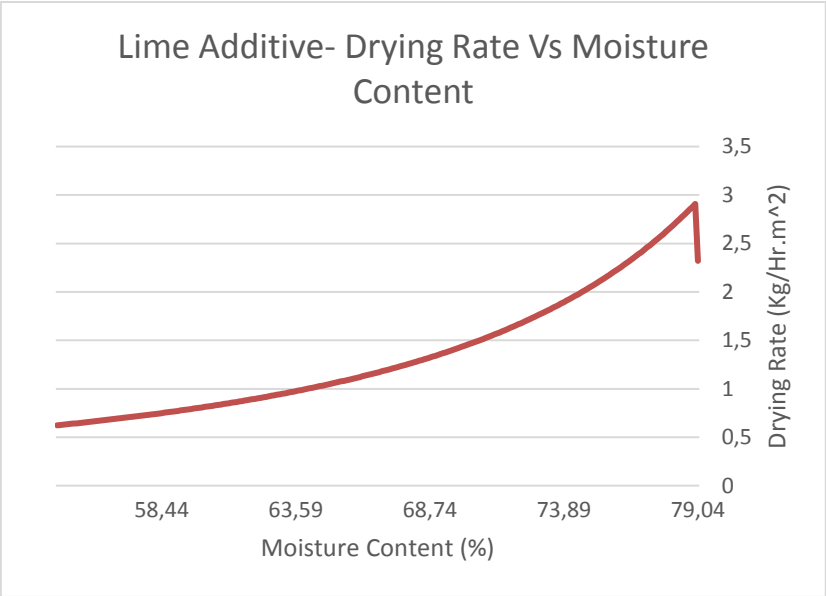


**Figure 7.83. Lime Additive Drying Rate Vs Moisture Content**

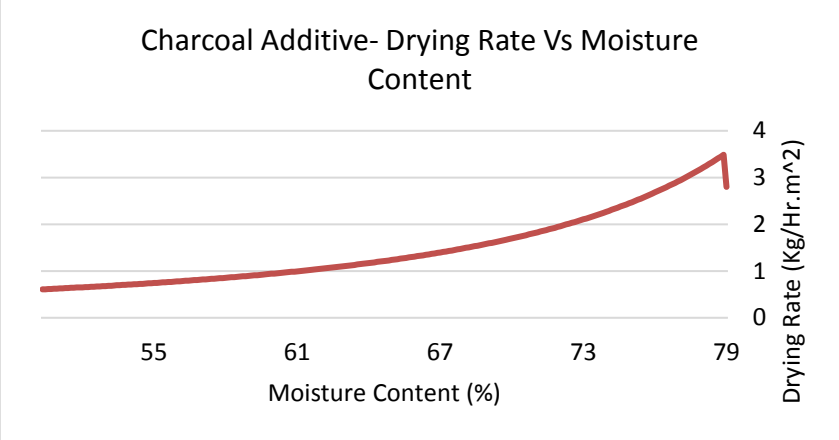


**Figure 7.84. Charcoal Additive Drying Rate Vs Moisture Content**

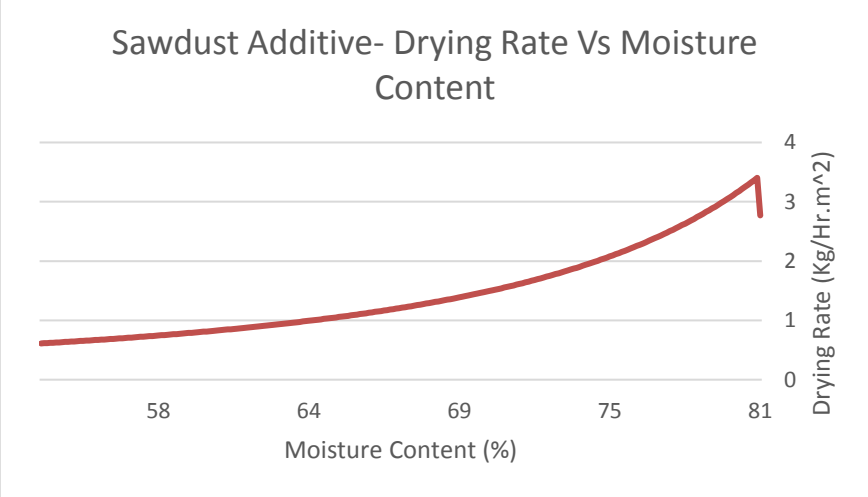


**Figure 7.85. Sawdust Additive Drying Rate Vs Moisture Content**

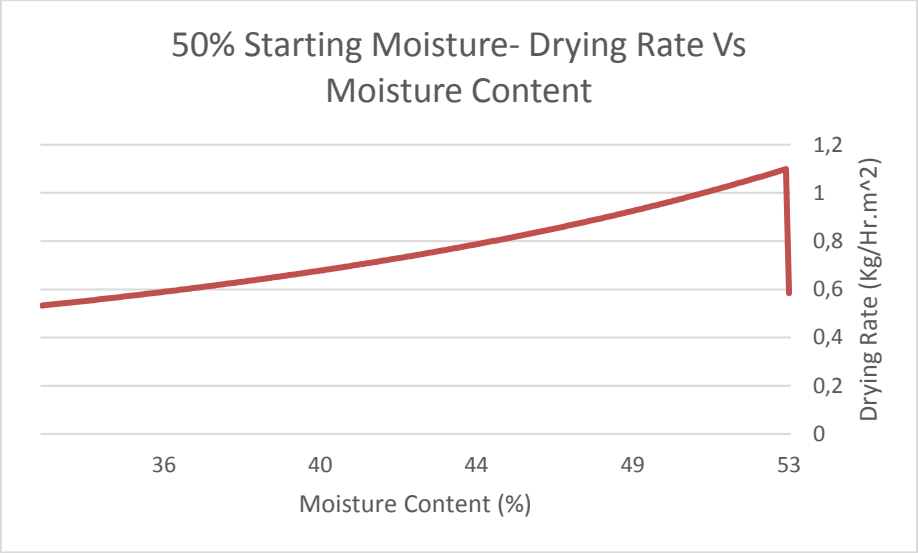


**Figure 7.86. 50% Starting Moisture Drying Rate Vs Moisture Content**

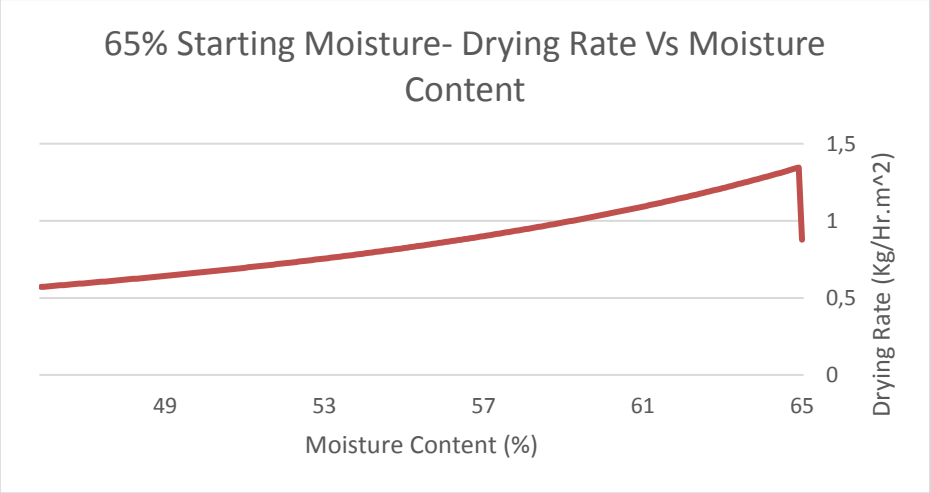


**Figure 7.87. 65% Starting Moisture Drying Rate Vs Moisture Content**

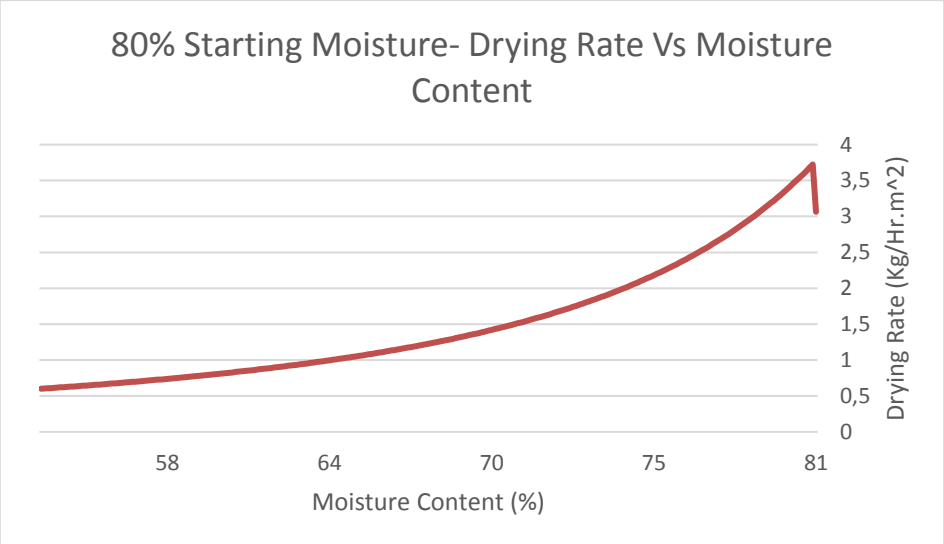


**Figure 7.88. 80% Starting Moisture Drying Rate Vs Moisture Content**

### 7.5.6 Performance parameters

**Table 7.45. Summary of Performance Metric Data Across All Tests**

| Test | Run Number | Drying Rate (kg/hr/m^2) | SEC (kWh/Ton) | Efficiency Overall (%) | Irradiance Ave |
|---|---|---|---|---|---|
| **Full Device** | 1 | 1,574 | 540,07 | 57,61 | 490 |
| **Full Device** | 2 | 1,927 | 443,61 | 70,12 | 493 |
| **No Reflectors** | 1 | 1,895 | 435,41 | 73,85 | 460 |
| **No Reflectors** | 2 | 1,835 | 457,82 | 71,54 | 460 |
| **No Dehumidifier** | 1 | 1,82 | 110,38 | 66,32 | 490 |
| **No Dehumidifier** | 2 | 1,71 | 146,17 | 75 | 409 |
| **No SAH** | 1 | 1,57 | 474,1 | 61,27 | 460 |
| **No SAH** | 2 | 1,664 | 453,78 | 68,13 | 438 |
| **50% Fan** | 1 | 2,033 | 361,5 | 73,37 | 497 |
| **50% Fan** | 2 | 1,505 | 498,41 | 54,306 | 497 |
| **25% Fan** | 1 | 2,092 | 358,42 | 81,23 | 462 |
| **25% Fan** | 2 | 1,46 | 511,11 | 56,11 | 469 |
| **80% MC** | 1 | 1,436 | 95,74 | 49,94 | 515 |
| **80% MC** | 2 | 1,49 | 83,78 | 43,72 | 612 |
| **65% MC** | 1 | 0,884 | 155,52 | 24,7 | 642 |
| **65% MC** | 2 | 0,936 | 133,57 | 25,12 | 668 |
| **50% MC** | 1 | 0,761 | 161 | 21,45 | 636 |
| **50% MC** | 2 | 0,669 | 186,82 | 18,78 | 639 |
| **Sawdust Additive** | 1 | 1,37 | 63,47 | 31,73 | 779 |
| **Sawdust Additive** | 2 | 1,43 | 87,2 | 37,53 | 685 |

| | | | | | |
|---|---|---|---|---|---|
| **Activated Carbon Additive** | 1 | 1,21 | 92,45 | 33,32 | 655 |
| **Activated Carbon Additive** | 2 | 1,29 | 87,23 | 36,03 | 642 |
| **Lime Additive** | 1 | 1,26 | 108,8 | 34,37 | 659 |
| **Lime Additive** | 2 | 1,2 | 103,53 | 32,61 | 664 |

## 7.6 APPENDIX F: CONSTRUCTION COST OF THE SOLAR THERMAL DRYING PROTOTYPES

### 7.6.1 Greenhouse solar drier

**Table 7.46. Construction cost from the greenhouse solar drier**

| Enclosure material | dimensions | Quantities | |
|---|---|---|---|
| PMMA (Acrylic) | 3m*2m*3mm | 5 | R5755 |
| Aluminium square hollow tubing | 38mm x 38 mm1m length | 1 | R95 |
| Angle iron | 1mx 15mm x15 mm | 8 | R2,000 |
| Hinges | Stainless steel | 4 | R600 |
| Floor Aluminium sheet | 3m x 2m x 3mm thick sheet | 1 | R1500 |
| Ventilation | | | |
| 70W AC Axial Plate Fan | 205mm x 205 mm | 4 | R10000 |
| 60 W Ac axial fan | 180 mm x 180 mm | 8 | R1500 |
| Speed control switch | 220 V, 5A | 1 | R 2000 |
| Rake system | | | |
| 1000 mm Stroke Linear Actuator | Electric (150 N axial force) | 1 | R25,000 |
| Stainless steel hollow tube | 20mm x 1 m | 1 | R450 |
| Stepper motors | 12 V,110 rpm | 1 | R850 |
| Linear guide rail | 1.5 m length | 1 | R5000 |
| Guide carriage | To fit guide rail | 1 | R2500 |
| Drying tray | | | |
| Steel Fine wire mesh | 1mm holes (4 x 500 mm x 500 mm) | 1 | R1500 |
| Angle iron | 1mx 15mm x15 mm | 6 | R1500 |
| Absorber wall | | | |
| Aluminium sheet | 3m x 2m x 3mm thick sheet | 1 | R1500 |
| Paint | | 1 | R300 |
| Drainage system | | | |
| Aluminium sheet 0.7mm thick | 2m x 2m x 0.5 mm thick | 1 | R300 |
| ball valve | tap | 1 | R80 |
| Circulation fans | | | |
| 420 W axial circulation plate fan | 350 mm x 350 mm | 4 | R18500 |
| Speed control switch | 220 V, 5A | 1 | R 2000 |
| Instrumentation | | 1 | |
| RS PRO Solar power meter | 10 w/$m^2$ Resolution | 1 | R8,000 |
| Temperature Probe | 20-105 degrees C | 1 | R3,000 |
| Moisture Meter | | 1 | R5,000 |
| control logic unit | | 1 | R2,500 |
| | | | |
| Total | | | R101 130 |

### 7.6.2 screw conveyor solar drier

**Table 7.47. Construction cost from the greenhouse solar drier**

| Item | Price |
|---|---|
| Screw Conveyor | R 50 158.00 |
| Reflectors | R 3 876.00 |
| SAH | R 8 663.00 |
| Electronics | R 2 507.00 |
| Dehumidifier | R 5 500.00 |
| Total | R70 704.00 |

# SUPPORTING DOCUMENTS

Supporting Document A: Final report from the WRC project K5/2858

Supporting Document B: MSc dissertation from Martin Mawejje about the study of solar thermal drying using the experimental rig developed during the project K5/2858

Supporting Documents C:  Deliverables from this project

Supporting Documents D: Knowledge dissemination material